

Understanding and Minimizing Density Functional Failures Using Dispersion Corrections

THÈSE N° 5535 (2012)

PRÉSENTÉE LE 23 OCTOBRE 2012

À LA FACULTÉ DES SCIENCES DE BASE

LABORATOIRE DE DESIGN MOLÉCULAIRE COMPUTATIONNEL

PROGRAMME DOCTORAL EN CHIMIE ET GÉNIE CHIMIQUE

ÉCOLE POLYTECHNIQUE FÉDÉRALE DE LAUSANNE

POUR L'OBTENTION DU GRADE DE DOCTEUR ÈS SCIENCES

PAR

Stephan Niklaus STEINMANN

acceptée sur proposition du jury:

Prof. J. Zhu, président du jury
Prof. A.-C. Corminboeuf, directrice de thèse
Dr I. Tavernelli, rapporteur
Dr A. Tkatchenko, rapporteur
Dr T. A. Wesolowski, rapporteur



ÉCOLE POLYTECHNIQUE
FÉDÉRALE DE LAUSANNE

Suisse
2012

To Schrödinger's cat

Il n'est pas de destin qui ne se surmonte par le mépris.
— Albert Camus, *Le mythe de Sisyphe*

But it ain't about how hard ya hit.
It's about how hard you can get it and keep moving forward.
— Rocky Balboa

Acknowledgements

First and foremost, my advisor Prof. Clémence Corminboeuf has fostered my scientific curiosity and provided the framework of the four years I spent happily pursuing the doctoral studies here in Lausanne. I am immensely grateful to her for having accepted me in her group and for believing more in me than I ever did myself. In particular, I have profited tremendously from her constant availability to share her opinion and to discuss various chemical questions. If this thesis is written well, it is because of all the great help and advices Clémence has given me.

The members of the “Laboratory for Computational Molecular Design” have never failed to support me. Since my early days, I admire Matthew Wodrich’s love for alkanes and Fabrice Avaltroni’s passion for Bash-scripting and Daniel Jana’s remarkable aptitude to make beautiful pictures. The three have really got me started in the lab and never complained when I wasted their time by asking stupid questions. Only few months after I started, Jérôme Gonthier joined the lab and became essentially my “brother in arms”: every day we have discussed our research and shared our enthusiasm about the latest articles or conferences; furthermore, I am very grateful for his corrections of the French abstract. Tanya Todorova has brought many joyful moments to our lunch breaks: she transforms even the most insignificant event into a funny story! I will leave the LCMD wondering: does Laëtita Bomble complain more or less than me? In any case, I enjoyed the discussion with her, even though I rarely agreed with her; after all: where is the discussion if everyone shares the same opinion? I warmly welcome Riccardo Petraglia, who carries on the flame of dispersion corrections. Taking care of students has provided me welcome excuses to take a break, as Matthieu Mottet has pointed out.

In addition to my four brothers, the friends in Basel have also been very supportive. In particular, Franziska Hofmann has kept me motivated and while Andrin Bürgin has regularly reminded me how strange the world I am living in is, Jörg Duschmalé shared my passion for the beauty of exactly this world, where doing science is more imperative than earning money. My deepest gratitude goes to my parents, who have never questioned any of my decisions and let me pursue my way between books, chemistry and the computer.

More direct contributions to this thesis have been made by Gabor Csonka, who has brought our attention to the Tang and Toennies damping function, further discussions about damping functions with Alexandre Tkatchenko, Zhengting Gan and Jing Kong from Q-Chem Inc. who provided their source code and Stan Gisbergen and Pier Philipsen from SCM who helped with the implementation in ADF. I am also very grateful to Tomasz Wesolowski, Alexandre Tkatchenko and Ivano Tavernelli for having accepted to be on my jury. Finally, the Swiss NSF Grant 200021_121577/1, and EPFL are respectfully acknowledged for their financial support.

Abstract

This thesis introduces original formalisms to achieve an accurate description of dispersion interactions within the framework of density functional theory. The presented research focuses on two specific objectives related to density functional approximations: (1) the development and implementation of dispersion corrections that dramatically reduce the failures for both inter- and intramolecular interaction energies and (2) the identification of the key factors at the origin of the errors in thermochemistry.

Kohn-Sham density functional theory has become the preferred methodology for modeling the energy and structural properties of large molecules, yet common semilocal and hybrid approximations are affected by well-known deficiencies as illustrated by both the delocalization error and their inability to accurately describe omnipresent long-range (van der Waals) interactions.

After proposing an improved variant of “classical” atom pairwise dispersion correction, we formulate an efficient dispersion correction that is dependent upon the electron density. In contrast to the schemes that are typically applied, these dispersion coefficients reflect the charge-distribution within a molecule. Additionally, the use of density overlaps allows for distinguishing of non-bonded regions from bonded atom pairs, which eliminates the correction at covalent distances. A clear advantage of the proposed dDsC scheme is its ability to improve the performance of a variety of standard density functionals for both hydrocarbon reaction energies and typical weak interaction energies simultaneously. The density dependence also offers advantages for highly polarized and charged systems.

Interaction energies of ground-state charge-transfer complexes and π -dimer radical cations are illustrative examples for which the delocalization error partially counterbalances the missing dispersion. We demonstrate, however, that, in practical situations, dispersion energy corrections are mandatory. Following van der Waals interactions, (long-range) “exact” exchange has been identified as the second most important ingredient for obtaining robust results. The versatile methodology devised herein reveals the “true” performance of standard approximations and promises many fruitful applications from metal-organic catalysis to organic-electronics.

Keywords: density functional theory, van der Waals interactions, London dispersion, dispersion correction, hydrocarbon, charge-transfer complex, charge-carrier

Résumé

Cette thèse introduit des formulations originales pour obtenir une description précise des interactions de dispersion dans le cadre de la théorie de la fonctionnelle de la densité basée sur le formalisme Kohn-Sham (KS-DFT). La recherche présentée ici se concentre sur deux objectifs spécifiques : 1) le développement et l'implémentation de corrections qui réduisent considérablement les erreurs des fonctionnelles de la densité pour les interactions de dispersion inter- et intramoléculaires ; 2) l'identification des principales origines des erreurs des fonctionnelles standard.

La DFT s'est imposée comme la méthode de choix pour la modélisation de l'énergie et des propriétés structurales de molécules de grande taille. Néanmoins, les approximations semi-locales et hybrides entraînent des défaillances bien connues, par exemple l'erreur de délocalisation et leur incapacité à décrire fidèlement les interactions omniprésentes de longue portée (van der Waals).

Ayant proposé une version améliorée d'une correction interatomique « classique » pour la dispersion, nous formulons ensuite une correction efficace qui dépend de la densité. À la différence de l'approche typiquement utilisée, nos coefficients de dispersion reflètent la distribution de la charge électronique. De plus, le recouvrement des densités atomique permet de distinguer les contacts non-liants des liaisons chimiques, éliminant ainsi la correction dans les distances covalentes. L'avantage incontestable de l'approche proposée, dDsC, réside dans sa capacité d'améliorer conjointement les énergies de réaction d'hydrocarbures et les interactions faibles pour une grande sélection de fonctionnelles standard. De plus, les systèmes chargés ou fortement polarisés bénéficient grandement de la dépendance de la densité.

Des complexes de transfert de charge et des cations radicalaires de dimères π sont étudiés en tant qu'exemples illustratifs de la compensation partielle entre le manque de dispersion et l'erreur de délocalisation. Nous démontrons qu'en pratique les corrections de dispersion sont indispensables. Une fois les interactions de van der Waals prises en compte, l'échange « exact » (à longue portée) est l'ingrédient le plus important pour obtenir des résultats robustes.

La méthodologie polyvalente présentée ici révèle la « vraie » performance des fonctionnelles standard et laisse entrevoir des applications dans des domaines aussi divers que la catalyse organométallique et l'électronique organique.

Mots-clés : théorie de fonctionnelle de la densité, interactions de van der Waals, dispersion de London, correction de dispersion, hydrocarbure, complexe de transfert de charge, porteur de charge.

Contents

Acknowledgements	v
Abstract	vii
Résumé	ix
Table of Contents	xi
1 Introduction	1
2 Theoretical Background	5
2.1 Dispersion Interactions	5
2.2 Density Functional Theory	8
2.2.1 Principles	9
2.2.2 Failures	13
3 Unified Inter- and Intramolecular Dispersion Correction Formula for Generalized Gradient Approximation Density Functional Theory	21
3.1 Introduction	21
3.2 Computational Methods	23
3.3 Results and Discussion	28
3.4 Conclusions	33
4 A System-Dependent Density-Based Dispersion Correction	35
4.1 Introduction	35
4.2 Theory	36
4.2.1 Dispersion Coefficients	37
4.2.2 Atomic Partitioning Weights	38
4.2.3 The Damping	39
4.3 Determination of the Adjustable Parameters	41
4.4 Test Sets	42
4.5 Computational Methods	43
4.6 Results and Discussion	43
4.6.1 Classical Hirshfeld Partitioning and C ₆ -Only Dispersion Corrections	45
4.6.2 Interaction Energy Profiles	47
4.7 Conclusions	49

5	Overcoming Systematic DFT Errors for Hydrocarbon Reaction Energies	51
5.1	Introduction	51
5.2	Computational Methods	53
5.2.1	Test Sets	53
5.2.2	Functionals	54
5.3	Results and Discussions	56
5.3.1	General Performance	56
5.3.2	Detailed Analysis of the Functional Performance	59
5.4	Conclusions	64
6	A Generalized Gradient Approximation Exchange Hole Model for Dispersion Coefficients	65
6.1	Introduction	65
6.2	The Exchange Hole Model	66
6.3	Atomic Partitioning	67
6.4	Results	68
6.5	Conclusion	70
7	Comprehensive Benchmarking of a Density-Dependent Dispersion Correction	71
7.1	Introduction	71
7.2	Theory	72
7.3	Determination of the Adjustable Parameters	75
7.4	Test Sets	76
7.5	Computational Methods	76
7.6	Results and Discussion	78
7.7	Conclusions	84
8	Why are the Interaction Energies of Charge-Transfer Complexes Challenging for DFT?	87
8.1	Introduction	87
8.2	Theoretical Background, Methods, and Computational Details	90
8.2.1	Benchmark Values	94
8.3	Results and Discussion	94
8.3.1	General Trends	94
8.3.2	Relationship between the Nature of Binding Energies and DFT Performance	97
8.3.3	The Energy Decomposition	99
8.3.4	The Particular Case of M06-2X	101
8.3.5	A Prototype Organic Charge-Transfer Complex	102
8.4	Conclusions	104
9	Exploring the Limits of DFT for Interaction Energies of Molecular Precursors to Organic Electronics	107
9.1	Introduction	107
9.2	Methods and Computational Details	108
9.2.1	Construction of the test set	108
9.2.2	Benchmark Computations	109
9.2.3	Symmetry Adapted Perturbation Theory	110

9.2.4	Density Functionals Tested	111
9.3	Results and Discussion	112
9.3.1	The Test Sets	112
9.3.2	Performance of Standard Wave Function Methods	118
9.3.3	Performance of Density Functional Approximations	118
9.3.4	Interaction Energy Profiles	121
9.3.5	Basis Set Dependence	124
9.4	Conclusions	124
10	General Conclusions and Outlook	127
	Bibliography	131
	Glossary	153
	Curriculum Vitae	157

1 Introduction

Computational chemistry provides a great deal of information about the properties of molecules and the mechanism that describe chemical reactions. Moreover, computations also represent a practical tool both for identifying and validating design principles, leading to improved drugs, more efficient catalysts and fine-tuned self-assembled nanostructures for organic electronics.¹⁻⁶ A myriad of chemical phenomena involve non-covalent interactions, which govern a variety of molecular architectures. Typical examples of systems dominated by dispersion interactions include lipid-bilayers, π - π stacking of DNA base pairs⁷ and the arrangement of non-polar amino acid side chains.⁸ Similarly, supramolecular chemistry critically depends on these ubiquitous attractive forces,⁹ which are also responsible for condensed phases of non-polar organic molecules (e.g., liquid and crystalline benzene).

Density functional theory¹⁰ is in principle exact, however, in practical applications only approximations to the exact, unknown, density functional are available. From the computational perspective, Kohn-Sham density functional theory¹¹ is a powerful framework for many aspects of electronic structure theory. Note that throughout this thesis we will use the acronym DFT for both, the exact theory and the methodology, where approximations are inevitable. Due to its excellent ratio of performance to computational cost, DFT has become the preferred methodology for modeling the energy and structural properties of large molecules containing more than a handful of atoms.⁴⁻⁶ Alternatively, the more realistic description of chemical reactions in solution is generally achieved by combining a simplified treatment of the solvent with a DFT based time evolution of the reactants.^{3,12}

Unfortunately, approximations to DFT have some serious drawbacks: standard density functionalsⁱ neglect long-range dispersion interactions¹³⁻²³ and overly stabilize electron delocalized structures (i.e., delocalization error).²⁴⁻³⁰ These two shortcomings are best illustrated by the typical underbinding of supramolecular assemblies (neglect of dispersion)³¹ and the overbinding of charge-transfer complexes (overstabilization of electron delocalization).^{32,33} To make matters more complicated, these two deficiencies are rooted in unrelated approximations and have opposite signs. Given the ubiquitous nature of weak interactions in chemistry,

ⁱ“standard” refers to the most widely used semilocal (hybrid) density functional approximations developed without special consideration of weak interactions.

developing an accurate, yet efficient, *a posteriori* corrective energy termⁱⁱ yields the main results of this thesis. The development is complemented by analyzing and understanding the interplay between the delocalization error and (missing) dispersion interactions in relevant chemical systems, with the broad goal of devising and identifying efficient methods that are sufficiently robust to overcome both inadequacies.

The physical origin and description of dispersion interactions is discussed in **Chapter 2**, followed by an introduction to density functional theory and the general principles of standard approximations. Two major shortcomings³⁴ of these approaches are relevant to this thesis and therefore explained in detail: the delocalization (or self-interaction) error^{24–29} and the neglect of dispersion.^{13–23} The delocalization error leads to spurious fractional charges in dissociating charged complexes²⁶ and affects geometries and energetics of hydrocarbons.^{35,36} The most promising approach to overcome this failure, i.e., exploiting long-range “exact” exchange, is presented.²⁸ The primary focus of this work concerns the inability of standard approximations to accurately describe dispersion interactions. The attractive concept of atom pairwise dispersion corrections (C_6/R^6 , damped at short internuclear distances, R)^{37–39} is introduced and alternative approaches are briefly reviewed.

The field of dispersion corrections to density functionals has evolved considerably in recent years. Since the beginning of this Ph. D. thesis (end of 2008), a plethora of new schemes have been published.^{40–61} To facilitate the presentation of the work accomplished during this thesis, one adopts a chronological order.

Reactions involving seemingly simple hydrocarbons were among the first unexpected, serious failures of standard density functional approximations.^{62–71} As a result, the last decade experienced a revived interest in developing fundamentally improved density functionals. Corminboeuf and coworkers were the first to realize that a dispersion correction has the potential to remove systematic errors associated with alkane thermochemistry.⁷² However, their dispersion correction is specifically tailored to alkanes and tends to overbind intermolecular complexes such as the benzene dimer. By building more physics into the model, **Chapter 3** presents a dispersion correction, dD10, which overcomes the lack of robustness and performs well for both hydrocarbons and intermolecular complexes. dD10 falls in the category of “classical” dispersion corrections, in the sense that the parameters are fixed for each element and do not depend on the chemical environment. However, dD10 goes beyond the standard approximation by improving the description of medium-range nonbonded interactions (e.g., 1,3 C···C or 1,5 H···H) through higher-order terms (i.e., beyond C_6/R^6) and relying on the Tang and Toennies damping function⁷³ which has a strong physical background. This chapter is published in the *Journal of Chemical Theory and Computation*.⁷⁴

Building on the success of dD10, **Chapter 4** introduces a more general dispersion correction, which depends on the density of the molecule, while preserving the appealing simplicity

ⁱⁱ All the developed dispersion corrections are applied post-SCF, i.e., they do not influence the electron density, but only the energies. See page 2.2.2 for more details.

of a sum over atom pairs, in contrast to more complex fully nonlocal functionals. The density dependence is incorporated in the dispersion coefficients (C_6 , C_8 and C_{10}) through the nonempirical exchange hole dipole moment (XDM) formalism of Becke and Johnson.^{75–80} In addition, the Tang and Toennies damping function⁷³ is adapted to account for ionic and covalent bonding regimes. The resulting scheme, called dDXDM, is tested on a broad set of systems for which dispersion interactions are prevalent. The results presented in this chapter are also published in *Journal of Chemical Theory and Computation*.⁸¹

With the previously developed accurate dispersion correction at hand, **Chapter 5** aims at understanding deficiencies in standard density functionals for hydrocarbon chemistry. The analysis is based on bond separation energies^{82–84} for alkanes, which are seriously underestimated by standard density functionals and therefore highly challenging.^{69,70,72} These failures are correlated with errors in the repulsive regime, i.e., with the performance for the compressed methane dimer.³⁶ Additional information is gathered from typical systems for intramolecular dispersion in hydrocarbon chemistry, best exemplified by paracyclophanes or the photo-dimer of anthracene.⁸⁵ The origin of the error can be traced to a combination of over-repulsiveness and missing dispersion, in both the medium and long-range. Many modern methods improve over standard functionals, but are not as successful as the density-dependent dispersion correction dDXDM, designed to handle hydrocarbon chemistry. The analysis presented in this chapter is published in the *Theoretical Chemistry Accounts*.⁸⁶

The highly encouraging performance of dDXDM, motivated the elaboration of a simplified variant of Becke and Johnson’s exchange hole dipole moment (XDM): the XDM formalism is nonempirical, but associated with an intricate dependence on the electron density and its derivatives.^{75–80} As a result, the method has not been widely implemented, and is available only in Becke’s in-house code as well as in one commercial program.⁸⁷ **Chapter 6** demonstrates that accurate dispersion coefficients (C_6) are obtained with only two semi-empirical parameters. The scheme is simple to implement, relying only on the electron density and its first derivative. This development is presented in *The Journal of Chemical Physics*.⁸⁸

Chapter 7 presents the final version of the dispersion correction developed in this thesis: aiming at improved general thermochemistry with standard density functionals, the simplified dispersion coefficients are incorporated in a well balanced density-dependent dispersion correction called dDsC. Due to the carefully designed damping function, the leading C_6 term provides essentially the same accuracy as obtained when higher-order terms are included. The scheme is validated by extensive benchmarking on diverse reaction energies, including not only hydrocarbons and weak intermolecular complexes, but also alkali metal and water clusters. Geometry optimizations of tricky molecules, such as C_2Br_6 or [2.2]paracyclophane confirm that dDsC is broadly applicable to “real” chemical situations. The results presented in this chapter are published in the *Journal of Chemical Theory and Computation*⁸⁹ and the dDsC correction is available in widely used quantum chemistry codes.

The interplay between two fundamental failures (missing dispersion and delocalization error)

of standard DFT approximations is investigated in **Chapter 8** using illustrative charge-transfer complexes. Based on high-level *ab initio* data, energy decomposition analysis and the effect of dDsC, it is demonstrated that the failure to describe accurately the binding energy in the ground state is not only due to the missing long-range exchange as generally assumed, but also to the neglect of weak interactions. The realization that the charge-transfer interaction itself accounts only for a minor fraction of the binding energy is key to understanding the importance of applying a dispersion correction to standard DFT, even for charge-transfer complexes. The role of the actual charge-transfer is to enable the monomers to approach each other more closely, rather than to provide binding, which is dominated by dispersion interactions. These findings are also published in the *Journal of Chemical Theory and Computation*.⁹⁰

Introducing a benchmark database of π -dimer radical cations (e.g., (thiophene)₂^{•+}), **Chapter 9** explores the limit of applicability of dispersion corrected standard functionals: in comparison to charge-transfer complexes, the delocalization error is more pronounced, while dispersion still plays a significant role. Hence, the description of the interaction energy is tricky even around the equilibrium distance. The analysis further reveals that achieving the correct dissociation behavior requires a drastically reduced delocalization error and an accurate modeling of dispersion interactions. This chapter will be published in the *Journal of Chemical Theory and Computation*.

Finally, **Chapter 10** concludes this thesis putting emphasis on the crucial role that dispersion energy corrections play to broaden the applicability of standard methods and understand their failures. Perspectives on the few remaining limitations of current dispersion corrections are also presented.

2 Theoretical Background

This chapter introduces the theoretical background most relevant to this thesis. The first section gives a historical overview for the origin of dispersion and summarizes the physical description of the phenomenon. All the development and analysis presented in the following chapters are based on Kohn-Sham density functional theory,^{10,11} which is introduced in the second section. Note that post-Hartree-Fock (e.g., Møller-Plesset perturbation⁹¹ and coupled-cluster theory⁹²) supermolecular approaches and symmetry adapted perturbation theory⁹³ (SAPT) computations that serve as benchmark data throughout this work are not discussed. Density functional approximations suffer from two major drawbacks, i.e., the delocalization (or self-interaction) error and the neglect of dispersion interactions, which are particularly relevant to the present context. The origin of the two errors is explained extensively and perspectives on how to reduce the consequent failures are also presented.

2.1 Dispersion Interactions

Understanding the origin of dispersion interactions relies upon two important related physical phenomena that were reported in the earlier scientific literature: optical dispersion and van der Waals' equation of state.

In the second half of the 17th century, Newton demonstrated that white light passing through a glass prism gets split into the spectral colors. The underlying frequency dependent propagation of electromagnetic radiation is known as (optical) dispersion. This phenomenon is successfully explained by a collection of Drude oscillators, i.e., electrons behave as (coupled) harmonic oscillators. Non-equilibrium positions correspond to induced dipole moments arising from the interaction with an electric field. The dispersion theory was established before the advent of quantum mechanics, but adjustments to account for the quantum nature of electrons were minor.⁹⁴

The second piece of classical physics pertinent to dispersion is van der Waals' equation for

non-ideal gases⁹⁵

$$\left(p + \frac{a_{\text{vdW}} N^2}{V^2}\right) \left(\frac{V}{N} - b_{\text{vdW}}\right) = k_B T \quad (2.1)$$

where p is the pressure, N the number of particles in volume V , k_B Boltzmann's constant and T the absolute temperature. a_{vdW} and b_{vdW} are the (empirical) parameters, characterizing attractive and repulsive forces between the particles, respectively. According to classical physics, rare-gas atoms should not attract each other, as they do not possess any electrostatic multipole moments and do not benefit from gravitation, which is completely negligible at the atomic level. Nevertheless, the rationalization of the properties of rare gases requires a weak attractive force ($a_{\text{vdW}} > 0$).

The physical origin of the weak attractive term in van der Waals' equation remained a mystery until the early days of quantum mechanics: London realized that applying perturbation theory to the interaction between any two atoms gives rise to weak interactions at second order.⁹⁶ The mathematical description is reminiscent of what could be expected from an interaction with a "virtual radiation", i.e., from the interacting (Drude) oscillators of the classical dispersion theory. Soon afterwards,⁹⁷ London introduced the term "dispersion interactions" and demonstrated that they are responsible for the major contribution to the attractive van der Waals force.ⁱ

Exploiting classical dispersion theory, the phenomenon is easily rationalized as the interaction between oscillators with frequencies corresponding to optically allowed electronic excitations.⁹⁸ In this terminology, dispersion arises from a spontaneous dipole moment (emanating from zero-point motions of electrons, i.e., non-equilibrium positions of the oscillators) on one monomer, inducing a dipole moment on the second monomer. For two non-overlapping atoms or molecules A and B in their ground state, the second order dispersion interaction is given by

$$E_{\text{disp}}^{(2)} = -\frac{2}{3} \frac{1}{R^6} \sum_{n_A, n_B} \frac{\mu_{n_A}^2 \mu_{n_B}^2}{\Delta E_{n_A} + \Delta E_{n_B}} \quad (2.2)$$

where n_A and n_B are the (virtual, allowed) excited states of molecule A and B , respectively, ΔE_{n_A} and ΔE_{n_B} are the corresponding excitation energies and μ_{n_A} and μ_{n_B} the associated transition dipole moments. The three significant characteristics of equation 2.2 are:

- Dispersion interactions between molecules in the excited states are potentially repulsive, as some terms in the denominator become negative.
- Species featuring low-lying excited states (i.e., colored or charge-transfer complexes) benefit from strong dispersion interactions due to their smaller contribution in the denominator.
- Valid for dimers, the "peculiarity of additivity"⁹⁸ is obtained when eq 2 is generalized to oligomers in a pairwise manner. Corrections for trimers^{99,100} are obtained at 3rd

ⁱSome authors like to distinguish London dispersion from van der Waals interaction, considering that vdW includes all non-covalent interactions, not only London dispersion. Herein, we will use (London) dispersion and van der Waals interactions interchangeably.

order perturbation theory and many-body terms have to be considered in general. Drude oscillators or the somewhat more general coupled plasmon model,^{101–105} conveniently approximate the many-body terms, which become especially important for very anisotropic systems, such as two molecular chains.¹⁰⁶

Charge density response functions $\chi(\mathbf{r}, \mathbf{r}'; i\omega)$, are the main ingredient of the generalized Casimir Polder formula,^{107,108} which describe dispersion as well as equation 2.2

$$E_{\text{disp}}^{(2)} = \int_0^\infty d\omega \int \int \int \int d\mathbf{r} d\mathbf{r}' d\mathbf{s} d\mathbf{s}' \chi_A(\mathbf{r}, \mathbf{r}'; i\omega) \frac{1}{|\mathbf{r}' - \mathbf{s}|} \chi_B(\mathbf{s}, \mathbf{s}'; i\omega) \frac{1}{|\mathbf{s}' - \mathbf{r}|} \quad (2.3)$$

where \mathbf{r} and \mathbf{r}' refer to subsystem A , while \mathbf{s} and \mathbf{s}' are the space variables in subsystem B . This formulation is widely used to derive approximations.^{109–112}

Equation 2.2 depicts the dipole-dipole interaction, whereas equation 2.3 illustrates more clearly the coupled charge fluctuations. Furthermore, according to the original work of Casimir and Polder,¹¹³ the inclusion of “retardation” effects, i.e., corrections for the finite speed of light, is more transparent in eq 2.3 than in eq 2.2. Retardation effects, which are only prevalent on the nanolength scale, modify the $1/R^6$ asymptotic form into $1/R^7$. The pairwise $1/R^6$ asymptote implies some locality within a system, i.e., the electron fluctuations are occurring on the length scale of an atom, which is a very good approximation in insulators. However, when the band gap is close to zero such as in semi-conductors and metals, the electron fluctuations (induced dipoles) are delocalized over lengths scales much larger than an atom. Dobson and coworkers,^{105,114–116} emphasized that these delocalized fluctuations lead to deviations from the standard $1/R^6$ form.^{116,117} Graphitic systems and graphene are typical examples of organic materials that do not follow the atom pairwise $1/R^6$ form.¹¹⁴

The dispersion energy beyond second order is best defined as a special case of the exact expression for the correlation energy given by the adiabatic connection fluctuation-dissipation theorem formalism to DFT (see page 11 for some more details).

Note, that all post-HF methods (i.e., MP2 and higher) include automatically energy terms that are of the form of equation 2.2 or 2.3 and therefore account for long-range dispersion. However, the accuracy can vary significantly and has motivated correction schemes for MP2.^{112,118–121}

The static picture, i.e., without invoking fluctuating dipoles/charge densities (see Figure 2.1), provides an alternative view on the origin of the attractive force arising from dispersion interactions: the correlated motion induces a small deformation of the monomer electron density and an accumulation of excess density between the nuclei. The attractive force is then explained in terms of the (classical) electrostatic interaction between the nucleus with its distorted electron density.¹²² The main advantage of the static depiction is that the effect of dispersion interactions can be visualized in real-space, which is somewhat more intuitive. The evaluation of the weak dispersion forces according to the Hellmann-Feynman theorem, i.e., based on the electrostatic interaction, requires an exceptional degree of (numerical) accuracy when computing electron densities,^{23,123} which might rationalize the general observation that in the DFT context, self-consistent treatment of dispersion is not needed for accurate interaction energies (*vide infra*). Nevertheless, the visualization of the electron density rearrangement can

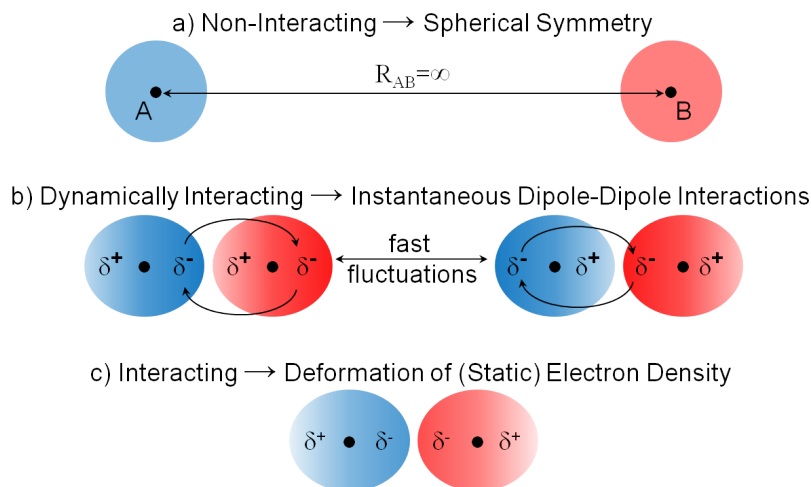


Figure 2.1: Schematic view on how two atoms without any electrical monopoles interact through dispersion: a) At infinite separation, there is no interaction and the spherical symmetry is preserved. b) When the electrons interact, they are correlated and the instantaneous dipole moment in system *A* induces a dipole moment in system *B*. c) In the time independent picture, the correlated motion of electrons leads to a slightly polarized electron density.

serve as a validation of existing approximate schemes or as a source of inspiration for devising new approximations.

In summary, there exists a weak attractive interaction (i.e., dispersion) between any two (ground state) atoms or molecules. Accounting for London dispersion requires the description of the correlated motion of two electrons that is inherently challenging. However, the effort is worthwhile: understanding and modeling van der Waals interactions is of utmost importance for describing various phenomena, including π - π stacking and condensed phases of neutral organic molecules. Not to mention that dispersion allows geckos to crawl up walls,¹²⁴ French fries to be crispy¹²⁵ and crime scenes^{126,127} to be resolved through fingerprints!

2.2 Density Functional Theory

Electronic structure theory aims at approximating the solution to Schrödinger's equation for atoms, molecules and solids as accurately as possible, given the system size and computational resources.

In the time-independent Schrödinger equation, the wave function Ψ is an eigenfunction of the Hamiltonian \hat{H} , with E being the associated eigenvalue, identified as the energy.

$$\hat{H}\Psi = E\Psi \quad (2.4)$$

Throughout this thesis, the Born-Oppenheimer approximation is applied, i.e., Schrödinger's equation is solved for electrons in the (fixed) field of point-charges representing the nuclei,

which corresponds to the following Hamiltonian

$$\hat{H} = -\frac{1}{2} \sum_{i=1}^N \nabla_i^2 - \sum_{i=1}^N \sum_{A=1}^{N_{\text{at}}} \frac{Z_A}{|\mathbf{r}_i - \mathbf{r}_A|} + \sum_{i=1}^N \sum_{j>i}^N \frac{1}{|\mathbf{r}_i - \mathbf{r}_j|} \quad (2.5)$$

where N is the number of electrons, ∇^2 is the Laplacian and index A runs over all atoms N_{at} with the nuclear charge Z_A .

Restricting the maximal complexity of the wave functions to a level that is computationally manageable leads to the traditional approximate solutions of Schrödinger's equation such as Hartree-Fock or multi-configurational self-consistent field (MCSCF). In contrast, density functional approximations avoid the explicit construction of a wave function and rather modify the Hamiltonian, making an exact solution computationally tractable. In addition to the modest computational cost, approximate DFT has two key advantages: (i) The ease of application to solids and condensed phase in general, i.e., DFT is not only used for atoms and molecules but also readily applied to surface chemistry and solid state physics. (ii) Excited states are as readily obtained as ground states. As neither of these features is exploited in this thesis, they will not be discussed further.

2.2.1 Principles

The main idea of density functional theory is that the complexity of the wave function $\Psi(\mathbf{x})$, depending on $4N$ variables (each of the N electrons has 3 spatial and 1 spin coordinate), is higher than needed for fully describing the system. The appealing ansatz of DFT is to develop a theory that does not require explicitly the complicated wave function but only the much simpler electron density

$$\rho(\mathbf{r}) = \int \cdots \int |\Psi(\mathbf{x}_1, \mathbf{x}_2, \dots, \mathbf{x}_N)|^2 ds_1 d\mathbf{x}_2 \dots d\mathbf{x}_N \quad (2.6)$$

which depends only on 3 variables (x , y and z in real space). If equations depending on $\rho(\mathbf{r})$ could describe the system equally well as the wave function, one would achieve an enormous computational speedup. The early days of quantum mechanics already witnessed the development of density functionals based on the homogeneous electron gas. Thomas¹²⁸ and Fermi¹²⁹ explored a functional for the kinetic energy in 1927, whereas Dirac's exchange functional¹³⁰ from 1930 is still in use, although often referred to as Slater's functional.¹³¹ Unfortunately, the Thomas-Fermi-Dirac functional is of no value for chemistry:¹³² molecules are not bound!

Modern DFT is based on the Hohenberg-Kohn theorems,¹⁰ which (i) assure that the electron density determines the ground state of a system completely and (ii) that a variational principle holds: the energy of the ground state density is the global minimum. Hence, on a formal level the wave function is not needed. As Levy remembers,¹³³ Bright Wilson trivialized the Hohenberg-Kohn existence theorem: according to Kato's cusp condition,^{134,135} the cusps of an electron density determine the charge (identity) of the nuclei. Additionally, the number

Chapter 2. Theoretical Background

of electrons is obtained by simple integration. The two pieces together are enough to specify the molecular Hamiltonian and thus all properties unambiguously, but without leading to any practical consequences. A more constructive formulation is Levy's constrained search,¹³⁶ bridging the gap between DFT and wave functions.

$$E_0 = \min_{\rho \rightarrow N} \left(\min_{\Psi \rightarrow \rho} \langle \Psi | \hat{T} + \hat{V}_{ne} + \hat{V}_{ee} | \Psi \rangle \right) \quad (2.7)$$

where \hat{T} is the kinetic energy operator, \hat{V}_{ne} the electron-nuclei and \hat{V}_{ee} electron-electron interactions, respectively. Levy's formalism opens the possibility to explore properties of the exact functional and hence goes further than the existence theorems of Hohenberg and Kohn. One year after the Hohenberg-Kohn theorems, Kohn and Sham introduced a more practical formalism.¹¹ In KS-DFT, the electronic energy is expressed in terms of a non-interacting model system, representing the exact density by a single Slater determinant

$$E[\rho] = T_s[\rho] + V_{ne}[\rho] + J[\rho] + E_{xc}[\rho] \quad (2.8)$$

The kinetic energy of a single Slater determinant, $T_s[\rho]$, is known exactly as an implicit density functional: the Slater determinant ψ built from the occupied orbitals $\phi_i(\mathbf{r})$ corresponds to the exact density and minimizes the kinetic energy.

$$T_s[\rho] = \min_{\psi \rightarrow \rho} \left(-\frac{1}{2} \sum_i^N \int \phi_i(\mathbf{r}) |\nabla^2| \phi_i(\mathbf{r}) d\mathbf{r} \right) \quad (2.9)$$

where N is the number of electrons and ∇^2 is the Laplacian. According to the virial theorem,¹³⁷ the kinetic energy accounts for half of the potential energy. Therefore, a relatively small error (e.g., 10%) in the kinetic energy has serious consequences. In fact, the inaccurate treatment of the kinetic energy as an explicit functional of the electron density (e.g., the Thomas-Fermi model) entails disastrous results for the energy of molecules and limits the practical usefulness of Hohenberg-Kohn DFT. Conversely, $T_s[\rho]$ is the main reason for the success of KS-DFT, since only a small correction term to the kinetic energy needs to be approximated as an explicit density functional.

$V_{ne}[\rho]$ and $J[\rho]$ are straightforward integrals accounting for the classical electrostatic electron-nuclei attraction and the electron-electron repulsion, respectively

$$V_{ne}[\rho] = - \int \rho(\mathbf{r}) \sum_{A=1}^{N_{at}} \frac{Z_A}{|\mathbf{r} - \mathbf{r}_A|} d\mathbf{r} \quad J[\rho] = \frac{1}{2} \int \int \frac{\rho(\mathbf{r})\rho(\mathbf{r}')}{|\mathbf{r} - \mathbf{r}'|} d\mathbf{r} d\mathbf{r}' \quad (2.10)$$

where index A runs over all atoms N_{at} with the nuclear charge Z_A .

The only quantity not known explicitly is the exchange-correlation functional $E_{xc}[\rho]$ which incorporates all the intricate many-body physics of the real quantum mechanical (QM) problem and can be formally re-expressed as

$$E_{xc}[\rho] = (T[\rho] - T_s[\rho]) + (V_{ee}[\rho] - J[\rho]) \quad (2.11)$$

where the first term is the correction for the kinetic energy difference between the single determinant and the true kinetic energy $T[\rho]$. The second term is the difference between the QM interelectronic interaction V_{ee} and its classical analogue J .

Hartree-Fock (HF) can be seen as a special case of a DFT functional: correlation is completely neglected, but exchange is treated “exactly”, i.e., by the formula for a single Slater determinant

$$E_x^{HF} = -\frac{1}{2} \sum_{i,j}^N \int \int \phi_i^*(\mathbf{r}_1) \phi_j(\mathbf{r}_1) \frac{1}{|\mathbf{r}_1 - \mathbf{r}_2|} \phi_i(\mathbf{r}_2) \phi_j^*(\mathbf{r}_2) d\mathbf{r}_1 d\mathbf{r}_2 \quad (2.12)$$

However, correlation is very important for chemical and physical phenomena and needs to be taken into account.

The adiabatic connection fluctuation-dissipation theorem approach to DFT provides exact expressions for the correlation energy^{138–140}

$$E_c = -\frac{1}{2} \int_0^1 d\lambda \int_0^\infty \frac{d\omega}{\pi} \text{Im} \int d\mathbf{r} d\mathbf{r}' \frac{1}{|\mathbf{r} - \mathbf{r}'|} [\chi_\lambda(\mathbf{r}, \mathbf{r}', \omega) - \chi_0(\mathbf{r}, \mathbf{r}', \omega)] \quad (2.13)$$

where the integral over λ is the coupling strength integration of the interelectronic interaction $\frac{\lambda}{|\mathbf{r} - \mathbf{r}'|}$ from a non-interacting ($\lambda = 0$) to the fully interacting ($\lambda = 1$) system, while keeping the ground-state density ρ fixed at its true ($\lambda = 1$) value. χ_0 and χ_λ are the non-interacting and λ scaled interacting (frequency ω dependent) density – density response functions to perturbations to the external potential $e^{-i\omega t} \delta V_{\text{ext}}(\mathbf{r})$ and satisfy

$$\delta \rho(\mathbf{r}, t) = e^{-i\omega t} \int \chi_\lambda(\mathbf{r}, \mathbf{r}', \omega) \delta V_{\text{ext}}(\mathbf{r}') d\mathbf{r}' \quad (2.14)$$

Alternatively, χ_λ can be defined as

$$\chi_\lambda(\mathbf{r}, \mathbf{r}', \omega) = \chi_0(\mathbf{r}, \mathbf{r}', \omega) + \int d\mathbf{r}_1 d\mathbf{r}_2 \chi_0(\mathbf{r}, \mathbf{r}_1, \omega) \left[\frac{1}{|\mathbf{r} - \mathbf{r}'|} + f_\lambda^{xc}(\mathbf{r}, \mathbf{r}', \omega) \right] \chi_\lambda(\mathbf{r}_2, \mathbf{r}', \omega) \quad (2.15)$$

where the exchange-correlation kernel is given by

$$f_\lambda^{xc}(\mathbf{r}, \mathbf{r}', \omega) = \frac{\delta^2 E_{xc}^\lambda[\rho]}{\delta \rho(\mathbf{r}) \delta \rho(\mathbf{r}')} \quad (2.16)$$

Equation 2.13 is the starting point not only for deriving van der Waals density functionals¹⁴¹ but also for the random phase approximation (RPA) in the DFT context, where $f_\lambda^{xc}(\mathbf{r}, \mathbf{r}', \omega) = 0$ is employed.¹⁴² Restricting χ to responses to dipole perturbations, an exact expression for the dispersion energy is obtained that, in contrast to eq 2.2, includes all many-body effects.¹⁴³ Note that charge – density response functions can also be exploited to define the exact electronic energy of a system, without invoking any non-interacting reference system or a coupling strength integration.¹⁴⁴

Since E_{xc} has to be approximated, the success of DFT is driven by the ongoing quest for improved exchange-correlation functionals. In contrast to wave function based electronic

Chapter 2. Theoretical Background

structure theory, the complexity of the many-body nature of Coulomb interactions in DFT is incorporated in the functional itself. In other words, once the universal functional (or a good approximation for it) is known, the actual computations are done in a one-particle formalism, which is considerably less demanding than the determination of the correlated wave function. If this comparable simplicity of DFT has to be sacrificed for an accurate description of challenging systems, the main advantage of the formalism is lost.

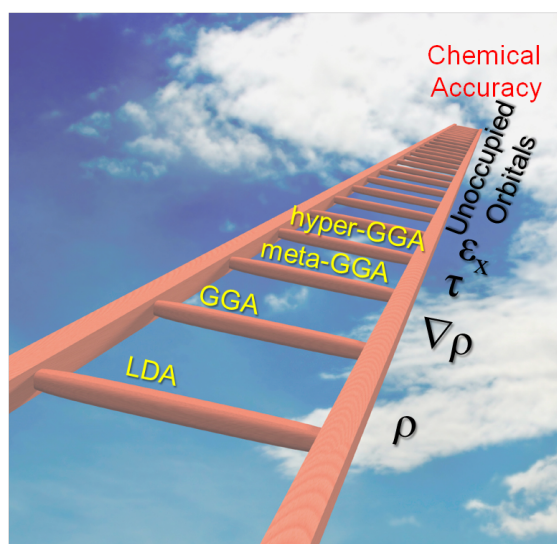


Figure 2.2: Jacob's ladder of density functional approximations toward chemical accuracy. First rung functionals depend on the local density, second rung on the density and its gradient, third rung on the kinetic energy density τ , fourth rung functionals depend non-locally on the occupied orbitals, while the fifth rung introduces dependence on the unoccupied orbitals.

Common Density Functional Approximations

Density functional approximations E_{xc} are usually formulated as a combination of an exchange functional E_x and a correlation functional E_c . This splitting into two components has many formal advantages (especially since many properties of “exact” exchange are known from Hartree-Fock), but is also associated with “artificial” difficulties¹⁴⁵ and, as a result, has been partially abandoned lately.¹⁴⁶

The common ingredient for density functionals is the electron density $\rho(\mathbf{r})$ itself, giving the local (spin) density L(S)DA approximation. LSDA exchange is uniquely defined analytically,^{130,131} whereas several slightly different parameterizations are available for the correlation functional, mostly relying on highly accurate Quantum Monte Carlo simulations,¹⁴⁷ but also on low- and high-density asymptotic limits.¹⁴⁸ SVWN5¹⁴⁹ and SPW92¹⁵⁰ are the LSDA functionals used routinely.

In the generalized gradient approximation (GGA),¹⁵¹ the variations of the electron density are accounted for by including a dependence on the density gradient $\nabla\rho(\mathbf{r})$. There exists a large diversity of GGA functionals in the literature given that the flexibility of GGAs is too limited to simultaneously satisfy all constraints relevant for solids and molecules.^{152,153} BLYP^{154,155} and PBE¹⁵⁶ are the most widely applied GGA functionals in chemistry and physics.

Meta-GGA functionals depend also on the kinetic energy density $\tau(\mathbf{r}) = \sum_i^N |\nabla \psi_i(\mathbf{r})|^2$ which contains similar information¹⁵⁷ as the Laplacian of the electron density $\nabla^2 \rho(\mathbf{r})$ that is hardly incorporated. Popular examples of $\tau(\mathbf{r})$ -dependent functionals are TPSS¹⁵⁸ and M06-L,¹⁵⁹ the most important example of a Laplacian dependent functional is the BR89¹⁶⁰ exchange functional.

GGA and meta-GGA functionals are called semilocal functionals, as they depend on local information and the infinitesimal close vicinity. Beyond the semilocal approximations, hybrid (or hyper-)GGA functionals, exemplified by the famous B3LYP functional,^{161,162} include a fraction of (nonlocal) Hartree-Fock exchange (eq 2.12). Similarly, double hybrid functionals (e.g., B2PLYP¹⁶³) include a fraction of many-body second order perturbation theory correlation energy.^{163,164}

There is no systematic route for improving density functionals except through the costly coupling of many-body wave function approaches with DFT in “*ab initio* DFT”.^{165–167} Nevertheless, the continuous improvement when going from LDA to double hybrid functionals corresponds to Perdew’s dream,¹⁶⁸ represented by the Jacob’s ladder climbing from the world of LDA to the heaven of chemical accuracy (Figure 2.2).

2.2.2 Failures

Approximations currently available suffer from three serious short-comings:³⁴

- The delocalization error^{24,26–29} causes erroneous dissociation curves of odd electron bonds (e.g., H_2^+) and produces fractionally charged instead of neutral atoms upon dissociating alkali halides or hydrides.^{25,27,169,170}
- The attractive long-range London dispersion is missing.¹⁴
- The static correlation error (deviation from a constant energy for fractional spins) affects singlet-triplet gaps and occurs typically in transition metal compounds,^{171–173} π -conjugated molecules^{174–176} and stretched covalent bonds.^{177–180}

The static correlation error is not relevant to the present thesis, and therefore not discussed further. The following two subsections are devoted to the first two failures, i.e., delocalization error and neglect of dispersion.

Delocalization or Self-Interaction Error

One electron does not interact with itself. Despite its simplicity, this statement is not as trivial as it seems in the context of approximate methods. The origin of the problem is the classical Hartree energy J of eq 2.8: a classical charge density has a non-zero Coulomb energy.

In wave function methods, the Hartree term of a single electron is identically canceled by the exchange interaction

$$E_x^{HF} = -\frac{1}{2} \int \int \frac{\phi^*(\mathbf{r})\phi(\mathbf{r})\phi^*(\mathbf{r}')\phi(\mathbf{r}')}{|\mathbf{r} - \mathbf{r}'|} d\mathbf{r}d\mathbf{r}' = -J = -\frac{1}{2} \int \int \frac{\rho(\mathbf{r})\rho(\mathbf{r}')}{|\mathbf{r} - \mathbf{r}'|} d\mathbf{r}d\mathbf{r}' \quad (2.17)$$

Therefore, Hartree-Fock is exact for all one-electron systems and wave function methods are one-electron self-interaction free, assuming zero correlation energy for one electron. However, for density functionals, where exchange and correlation are approximated, self-interaction is a serious issue. In fact, already in 1934, a long time before the advent of “modern” density functional theory, Fermi and Amaldi proposed an approximation to remove the self-interaction.¹⁸¹ Slater noted later that molecules such as NaCl dissociate into non-integer charged fragments as a consequence of self-interaction energy terms,¹⁶⁹ nevertheless he seems not to have realized the unphysical nature of the fractional charges.²⁵

Self-interaction in modern density functionals is extensively discussed since Perdew and Zunger’s seminal work.²⁴ They proposed to remove the self-interaction error orbital by orbital. Not only is the Perdew-Zunger self-interaction correction (PZ-SIC) computationally intensive, but the energy is not invariant with respect to orbital localization. Furthermore, PZ-SIC has an equivocal impact on the results: electron affinities,²⁴ challenging reaction barriers¹⁸² and chemical shifts¹⁸³ are improved, but most thermochemistry benchmarks are dramatically deteriorated.¹⁸⁴

Assigning a zero energy contribution to one-electron densities avoids self-correlation (e.g., LYP,¹⁵⁵ B95¹⁸⁵ and TPSS¹⁵⁸ correlation functionals). However, the exchange has to cancel the Hartree term exactly and thus is more challenging. So far, only functionals relying on 100% “exact” exchange (MCY2,¹⁸⁶ B05¹⁸⁷ and PTST¹⁸⁸) are free from one electron self-interaction error (1-SIE) without an explicit SIC. Unfortunately, in many-electron systems, even 1-SIE free functionals behave very similarly to standard approximations.^{28,29,189,190} This recurrent deficiency has been coined many-electron self-interaction error (N-SIE).^{28,29} The formal condition for being N-SIE free is not well known. “Delocalization error” is an alternate terminology,^{30,36} which emphasizes the physical consequence of the problem: electron densities are too delocalized, causing the erroneous stabilization of fractionally charged atoms and molecules,^{30,36} unbound electrons in certain anions^{191,192} and an overstabilization of conjugated geometries with respect to non-conjugated ones.³⁵

The most promising approach to reduce delocalization errors is probably the use of long-range corrected exchange functionals, which treat the long-range electron-electron interaction by “exact” exchange.²⁸ Savin and coworkers developed the range-separation to rigorously combine DFT ideas with multi-determinantal wave function techniques.^{193,194} As a byproduct, the long-range correction (LC) scheme for LDA exchange was obtained. The idea is to split the electron repulsion operator $\frac{1}{r_{12}}$ into two ranges (long and short) with the most common choice being an Ewald-style partition based on the error function

$$\frac{1}{r_{12}} = \underbrace{\frac{\text{erfc}(\mu r_{12})}{r_{12}}}_{\text{SR}} + \underbrace{\frac{\text{erf}(\mu r_{12})}{r_{12}}}_{\text{LR}} \quad (2.18)$$

where the μ parameter is generally selected empirically and controls the definition of the two ranges. The physical motivation for the LC scheme is the incorrectly decaying potential of standard DFT functionals: the xc potential $v_{xc} = \frac{\delta E_{xc}[\rho]}{\delta \rho}$ of semilocal functionals decays exponentially along with the density, violating the exact $-1/r$ asymptotic form.^{195,196} Applying

the range-separation and introducing HF-exchange for the long-range restores the correct asymptote.

LC functionals reduce the delocalization error considerably, but the choice of range-separation parameter remains inconvenient.^{197–200} The determination of μ is possible according to first principles, i.e., μ is tuned to reproduce the vertical ionization energy and electron affinity by the HOMO and LUMO energies, respectively. This choice leads to a consistent improvement for excitation energies and other properties.^{199–203} However, tuning the functional for each molecule specifically is not only cumbersome, but also precludes the computation of reaction energies: if the functional changes from reactants to products, the energies are not comparable, i.e., range-tuning breaks size-consistency. Variants based on local range-separated hybrids²⁰⁴ are size-consistent, but not broadly explored because of their computational complexity.

In summary, self-interaction errors are nearly omnipresent within approximate density functionals. Even though long-range corrected exchange functionals offer many advantages and minimize the failures considerably, more development is needed to solve the problem rigorously.

Dispersion Interactions

The ubiquitous nature of dispersion interactions, which are neglected at the semilocal (hybrid) density functional level,^{13,14,19,23,105,116} has stimulated intense research during the last decade. The literature is too vast for providing a detailed survey on the available methods or on all the issues resulting from the neglect of van der Waals interactions. The discussion of specific errors is postponed to the following chapters, as well as all the aspects directly relevant to the particular dispersion corrections developed within this thesis. This section provides an overview of the available approaches and emphasizes the scheme diversity.

Long-range dispersion interactions are undeniably missing at the semilocal (hybrid) density functional level. However, around the equilibrium distance, many intermolecular complexes are characterized by an appreciable nonbonded density overlap and density functionals can recover “dispersion like” interactions. The extent to which dispersion is accurately described depends dramatically on the precise definition of the functional. Wesolowski et al. have nicely demonstrated that the energy density associated with the high gradient, low electron density regime determines the accuracy of GGA functionals.²⁰⁵ First principles information about the corresponding large reduced density gradient ($s = \frac{|\nabla\rho|}{2 \cdot (3\pi^2)^{1/3} \cdot \rho^{4/3}}$) is contradicting: the enhancement factor (by which Dirac’s exchange is multiplied) is divergent if a GGA is built to satisfy the correct asymptotic $-1/R$ exchange energy density, the main achievement of Becke’s 1988 functional.¹⁵⁴ However, only modest asymptotic values ensure the global Lieb-Oxford bound,^{206,207} which gives a lower limit to the total energy and is an essential input in nonempirical functionals such as PBE. The conflicting first principles arguments motivate to seek empirical functionals that exploit maximally the information of nonbonded densities. The success of the empirical approach was, at first, relatively modest, e.g., X3LYP²⁰⁸ binds rare gas dimers, but does not describe π - π stacking well.³¹ The design of more flexible

functionals^{209,210} and the expansion from GGAs to meta-GGAs^{211–213} has resulted in the development of M06-2X,²¹⁴ one of the most accurate hybrid meta-GGA functional for weak interactions. Nevertheless, in order to account for long-range dispersion interactions, either nonlocal correlation functionals or dispersion corrections are mandatory.

Dependence on Virtual Orbitals Dispersion interactions are incorporated in all post-HF methods. Therefore, borrowing ideas from wave function theory overcomes the limitations of semilocal approximations. However, in most practical schemes the dependence on the virtual orbitals is not included self-consistently, i.e., they are done “post-KS”, in analogy to post-HF methods. Therefore, these methods can be considered energy corrections, rather than improved exchange-correlation functionals. Nevertheless, self-consistency can be achieved, e.g., through the optimized effective potential (OEP) approach.^{215,216}

The simplest variants are double hybrid functionals, which include a percentage of many-body second order perturbation theory correlation energy.^{163,164} Similar to hybrid functionals,²¹⁷ double hybrid functionals can be rationalized from first principles.^{218–220} Depending on the formulation and the parameters, the percentage is high enough to account for weak long-range interactions.^{221–223} However, in most functionals the percentage is rather small (e.g., 27% MBPT2 in B2PLYP¹⁶³) and an additional dispersion correction is recommended.^{85,224–226} In analogy with (global) hybrid functionals, long-range corrected correlation functionals introduce the wave function correlation only at long interelectronic distance, a concept that has been paired with PT2²²⁷ and more accurate methods, such as CCSD(T).²²⁸ The simplest approximation to the exact eq 2.13, i.e., setting the exchange-correlation kernel (eq 2.16) to zero, is the increasingly popular, although computationally expensive, RPA. There are many formulations of RPA and we refer to ref 142 for a review. It is sufficient to say that the appealing features are the inclusion of many-body effects, the applicability to the solid state and to zero band-gap systems, (e.g., metals or strongly correlated materials), for which PT2, included in double hybrids, diverges.

The major disadvantage of the dependence on virtual orbitals is the computational expense and the (re-)introduction of the basis set dependence inherent to post-HF methods.^{229–231} The reduced basis set dependence of standard density functionals is rooted in its very different description of correlation: in wave function methods, correlation effects are described as excitations into virtual orbitals whereas in DFT correlation is directly based on the density. The virtual space, describing the full flexibility of electrons, is much more complex than the (few) occupied orbitals. For example, the cusp condition (related to the probability of finding two electrons of opposite spin at the same point in space) is approximately included at the LDA level,^{140,232} but reproducing a cusp with atom centered Gaussian basis sets is a considerable task.^{233,234}

van der Waals Density Functionals and Dispersion Corrections The van der Waals density functionals are fully nonlocal and independent from virtual orbitals.^{47,48,53,141} Roughly, these nonlocal functionals model dispersion based on coupled local oscillators having a frequency

determined by the local density and its gradient. The coupling responsible for dispersion interactions is introduced through a double integration. The chosen form ensures the standard $-C_6/R^6$ asymptote, but does not account for more intricate many-body effects. Four main flavors have been developed: vdW-DF04¹⁴¹ and vdW-DF10⁵³ from Langreth’s group, and the somewhat more heuristic VV09⁴⁷ and VV10⁴⁸ functionals from Vydrov and van Voorhis. The double numerical integration is, in general, rather expensive, but reformulations involving Fourier transforms²³⁵ or use of coarse grids²³⁶ now make their evaluation routinely feasible. The local response for dispersion (LRD) formalism of Sato and Nakai^{45,46} combines VV09 with a dramatic simplification: the double numerical integral is avoided by expressing the van der Waals interaction as an atom pairwise sum, which leads to the general form of typical dispersion corrections

$$E_{\text{disp}} = - \sum_{i=1}^{N_{\text{at}}} \sum_{j>i}^{N_{\text{at}}} f_d(R_{ij}) \frac{C_6^{ij}}{R_{ij}^6} \quad (2.19)$$

where N_{at} is the number of atoms in the system, R_{ij} is the internuclear distance between atom i and j and C_6^{ij} is the associated dispersion coefficient. $f_d(R_{ij})$ is a damping function, accounting for the physical damping arising from to density overlap and removing the unphysical divergence for zero internuclear distance. The form and role of the damping function is discussed after the next paragraph that gives an overview on atom pairwise dispersion corrections.

Atom pairwise dispersion corrections (eq 2.19) have a long history and were developed originally for Hartree-Fock.^{37,237–239} After an hesitant exploration of such corrections in the context of density functional approximations,^{22,240} the breakthrough was stimulated by the improvement of semi-empirical methods²⁴¹ and the systematic study of weak interactions of hydrocarbon dimers by Wu and Yang.³⁸ The most popular dispersion correction to date was developed by Grimme in 2006,³⁹ providing for the first time a set of parameters for most elements of the Periodic Table and parameterizations for several popular density functionals. The acronym DFT-D has been firmly established ever since. Many reparameterizations of DFT-D are available, most of them concentrating on intermolecular complexes around equilibrium, few including non-equilibrium geometries explicitly in the training set. In addition to the training set, the obvious differences between the approaches are related to the damping function $f_d(R_{ij})$ and the dispersion coefficients C_6 . We refer to these methods as “classical” dispersion corrections, if the C_6 coefficients and van der Waals radii (R_0) or other parameters for the damping function are tabulated *a priori*. C_6 and R_0 parameters can be freely fitted, derived from experimental data or computed for atoms or reference compounds. In Grimme’s latest dispersion correction (dubbed D3)⁴² the C_6 coefficients are determined by interpolation between a fixed number of reference values. Therefore, even though geometry dependent through fractional coordination numbers, we consider D3 a “classical” dispersion correction. Beyond the “classical” schemes the choice is more limited. The most prevalent variants of atom pairwise, density-dependent dispersion corrections are Becke and Johnson’s exchange hole dipole moment (XDM) formalism,^{75–80} Tkatchenko and Scheffler’s vdW-TS method⁴⁴ and

Sato and Nakai's local response for dispersion (LRD).^{45,46} XDM requires tabulated free atomic polarizabilities and vdW-TS relies on free atomic C_6 coefficients and vdW-radii. Only LRD does not depend on any atomic reference data and has, through its VV09 roots,⁴⁷ probably the strongest physical background. Our most successful scheme (i.e., dDsC),⁸⁹ exploits an XDM formalism and will be detailed in Chapter 7. Note that all density-dependent dispersion corrections should be implemented self-consistently, i.e., their contribution to the Fock matrix should be included. However, both the LRD²⁴² and the XDM⁸⁷ formalism turned out to influence the SCF solution only to a negligible extent, which is also in line with experiences for the van der Waals density functionals.^{243–245} Therefore, all our dispersion corrections are applied as pure *a posteriori* energy corrections, i.e., the electron density with/without dispersion correction is identical.

Most atom pairwise dispersion correction are based on isotropic C_6 coefficients. However, in general dispersion interactions are anisotropic and the anisotropy has a nontrivial influence on thermodynamic averages.²⁴⁶ The importance of anisotropy for small intermolecular complexes has recently been investigated by Krishtal et al.²⁴⁷ However, since no damping function has been included, the extent to which an (anisotropic) damping function could lead to sufficient accuracy remains somewhat unclear. On the other hand, the LRD dispersion correction is anisotropic, but the damping function is isotropic.^{45,46}

Due to the atom pairwise approximation many-body effects between atomic centers are completely missing.ⁱⁱ Including many-body effects at the level of dispersion corrections to density functional approximations is in its infancy. Promising approaches are being actively developed and tested for molecules and condensed phases mainly by Tkatchenko, Scheffler and coworkers.^{248,249} These many-body effects are expected to become more important with increasing system size, increased electron delocalization and a closing band gap

Since Yang's pioneering work,³⁸ the damping function $f_d(R_{ij})$ has been a central element in the development of dispersion corrections. Most damping functions $f_d(R_{ij})$ reduce to zero for $R_{ij} = 0$. However, Koide demonstrated that the proper asymptote is a constant: two hydrogen atoms at zero internuclear distance, i.e., a helium atom, have a dispersion energy of 8.7 mhartree,²⁵⁰ which is equal to about 20% of the total correlation energy of helium. In the framework of a dispersion correction to density functionals, the rationale behind damping to zero is rather simple: the correlation functional describes electron correlation in atoms and covalent bonds. Some functionals, e.g., LYP¹⁵⁵ are explicitly fitted to reproduce the correlation energy of helium and therefore formally adding a dispersion correction for these situations is certainly not more justified than letting the correction go to zero. The disadvantage of $f_d(0) = 0$ is that repulsive gradients are obtained at short internuclear distances, possibly entailing suboptimal performance for geometry optimizations of non-bonded contacts in close proximity.^{43,54} Since the decomposition of correlation in density functionals is not clear-cut, the damping function is intrinsically empirical in nature. Thus, a flexible damping function is required to adapt the dispersion correction to a given functional and to minimize double counting effects as much as possible. Overall, the diversity in the literature reflects rather personal preferences and experiences than fundamental understanding.

ⁱⁱNote that current versions of the van der Waals density functionals neglect many-body effects as well.¹¹⁶

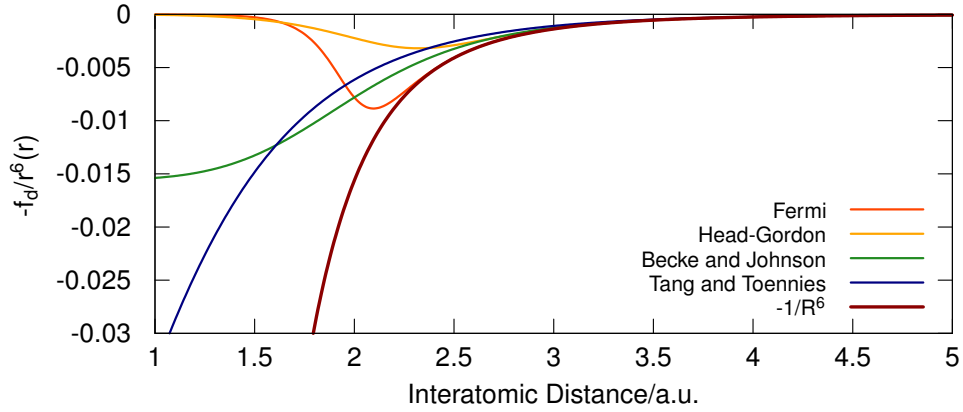


Figure 2.3: The effect of four different damping functions on the pure $-1/R^6$ dependence of dispersion interactions. For the Fermi damping function (eq 2.20) the steepness $d = 23$, Head-Gordon's function (eq 2.21) is used with $a = 6$ and $q = 12$, Tang and Toennies (eq 2.23) with $b = 3.0$, while all other parameters are set to unity, except for R_0 , which is 2.0 a.u. (note, that Tang and Toennies function does not depend on R_0 at all).

The four most widely used damping functions, applied to $-1/R^6$, are compared in Figure 2.3:

1. The Fermi damping has dominated the field^{38,39,44,251}

$$f_F(R) = -\frac{1}{1 + e^{-d(R/R_0-1)}} \frac{1}{R^6} \quad (2.20)$$

where d determines the steepness of the switching function and R_0 is the vdW distance.

2. Head-Gordon's power law,²⁵² which has been adopted in the "D3" correction⁴²

$$f_{HG}(R) = -\frac{1}{1 + a(R/R_0)^{-q}} \frac{1}{R^6} \quad (2.21)$$

where a and q are positive parameters to adjust the damping function to a given functional. Note that the Fermi damping and the power-law can be combined in one "universal" damping function that is more flexible than the standard variants.²⁵³

3. The rational damping function of Becke and Johnson⁷⁹ is given by

$$f_{BJ}(R) = -\frac{1}{R^6 + R_0^6} \quad (2.22)$$

$f_{BJ}(R)$ has the unique feature that it goes to a constant for vanishing internuclear distance, reducing the corresponding gradient to zero.^{43,54,58,79}

4. Tang and Toennies' damping function⁷³ plays a central role in this thesis

$$f_{TT}(R) = -\left(1 - \exp(-b \cdot R) \sum_{k=0}^6 \frac{(b \cdot R)^k}{k!}\right) \frac{1}{R^6} \quad (2.23)$$

where b is a fitted parameter.

Chapter 2. Theoretical Background

Dispersion corrected atom centered potentials (DCACP) are a completely different approach introduced by R  thlisberger and coworkers^{254–256} for plane waves and extended to Gaussian basis sets by DiLabio’s group.^{55,56,257,258} The central idea is to add an atom centered nonlocal potential that accounts approximately for dispersion effects, just like pseudopotentials account for core electrons in plane wave codes^{259,260} or effective core potentials (ECPs) can include scalar relativistic effects for Gaussian basis sets.^{261,262} DCACPs have two main advantages compared to “classical” dispersion corrections: (i) The dispersion correction is system dependent through the electron density, with $\rho(\mathbf{r})$ being modified by the added potential. (ii) DCACPs are easy to “implement”: plane wave codes automatically come with support for pseudopotentials and most Gaussian basis set based codes handle ECPs. The drawback is twofold: first, the empirical nature of the potentials necessitates careful fitting of parameters for each element to achieve a reasonably transferable scheme and second the interaction energy does not necessarily follow the proper $(1/R^6)$ asymptote, even though the formalism in principle supports the correct form.²⁶³

In summary, dispersion interactions can be introduced into the framework of density functional approximations at various computational costs and degree of theoretical sophistications. For the time being, it is not yet clear which approach has the best performance to cost ratio. One might argue that the inexpensive “classical” dispersion corrections generally provide reliable results. However, in highly polarized situations the “classical” scheme is inaccurate: even Grimme’s latest (system dependent) dispersion correction⁴² needs “special adjustments” for ionic crystals²⁶⁴ and fluorine seems to be somewhat problematic as well.²⁶⁵ As illustrated in the rest of this thesis, we predict a bright future to physically motivated density-dependent schemes.

3 Unified Inter- and Intramolecular Dispersion Correction Formula for Generalized Gradient Approximation Density Functional Theory

3.1 Introduction

This chapter proposes a simple and efficient, *a posteriori*, double-damped attractive weak interaction energy correction formula for nonempirical generalized gradient approximations^{151,156,266–268} (GGAs) of the Kohn-Sham density functional theory (DFT).¹¹ GGA functionals might provide a reasonable description of the weak interactions arising from nonbonded density overlap but cannot describe the long-range part of the van der Waals (vdW) interaction that acts between nonoverlapped densities. As proposed earlier,^{37–39,237–239,269} a properly constructed damped attractive energy correction summed over all atom pairs in the system efficiently remedies this deficiency of GGA^{38,39,269} (and also the hybrid GGA and meta-GGA) functionals at a negligible computational cost. Such a correction must be convergent with respect to the internuclear separation, R_{ij} and must properly follow the $\sim R^{-6}$ decay of the dispersion interaction at large R_{ij} . At shorter internuclear separations the $\sim R^{-8}$ and $\sim R^{-10}$ terms might also have non-negligible contribution to the interaction energy. In this chapter, we further develop the idea of a general interatomic dispersion corrected GGA functional as suggested by Grimme^{39,269} and show the benefits of using a double-damping as well as higher-order dispersion terms for such corrections. In our formulation, the inter- and intramolecular dispersion corrections are treated jointly in a single formula as opposed to two separate parametrizations (i.e., PBE-inter or PBE-intra)^{72,270} containing only $\sim R^{-6}$ terms. Inter- and intramolecular van der Waals interactions are responsible for many energetic and structural phenomena such as the heats of sublimation of hydrocarbons, the crystal packing of organic molecules, host-guest chemistry, the orientation of molecules on surfaces, the stacking of nucleic acids in DNA,⁷ and protein folding⁸ as well as the properties of polar and

apolar solvents.

It is known that the Hartree-Fock (HF) method cannot describe these weak interactions, arising from a pure electron correlation effect. High level, expensive treatment of electron correlation coupled with large basis sets (typically CCSD(T)/aug-cc-pVQZ) are required to evaluate such interactions accurately.^{271–274} These methods are computationally very expensive and are applicable only to benchmark studies of small systems.

GGA, hybrid GGA, and meta-GGA are much less expensive than CCSD(T) and MP2 methods. Such functionals can at best provide an estimate of the bonding between weakly overlapped densities but fail to reproduce the long-range part of the vdW interaction, which tends to $-C_6/R^6$ as $R \rightarrow \infty$. The computed GGA or meta-GGA interaction energy arising from overlapping electron densities decays exponentially,²⁷⁵ which results in a serious underestimation of the long-range part of the interaction.^{105,276–279} A typical example is the sandwich and T-shaped configurations of the benzene dimer, which is dispersion-bound at the CCSD(T) level²⁷⁴ but essentially unbound in a PBE GGA computation.²⁷⁵ For shorter-range weak interactions characteristic in rare-gas dimers^{17,18,21,275,280–282} and other noncovalently bound diatomics,^{283–287} the performance of GGA,^{17,18,21,275,283–287} hybrid GGA,^{280,282} and TPSS or TPSSh meta-GGA^{275,281} functionals varies. While the B88 GGA¹⁵⁴ exchange functional tends to underbind (or not bind at all),^{14,15,275} LSDA seriously overbinds.^{275,281} In contrast, PBE and TPSS often give reasonable binding energies.^{17,18,275,280,281} The partial success of PBE and TPSS was attributed predominantly to the large gradient behavior (satisfaction of the Lieb-Oxford bound lower bound on the exchange-correlation energy for all possible electron densities).²⁷⁵ In some rare-gas diatomics, however, the PBE, TPSS, and TPSSh density functionals overcorrect the serious overbinding tendency of LSDA^{275,281} resulting in too long bond lengths and reduced binding energies. This deficiency suggests the need for some attractive shorter-range correction. In other words, a consistent description of the weak attractive interactions by a GGA or meta-GGA requires a full treatment of the long-range behavior^{109,141,276} along with an improved treatment of the shorter-range part. These results also show that including rare gas diatomics (short-range interactions) into the training sets for empirically fitted density functionals does not guarantee an improvement for larger stacking complexes (long-range interactions) of chemical or biological interest.

Fully nonlocal functionals^{109,141,276} or generalizations of the random phase approximation¹⁰⁵ that capture the long-range correlation effects are more promising and also computationally more demanding for the description of the dispersion effects. Further possibilities are the following: the optimized potential method within KS perturbation theory,^{288,289} empirically calibrating dispersion corrected atom centered potentials,^{254,256} or fitting the exchange-correlation enhancement function (using a large number of empirical parameters) to a data set that contains weakly bonded compounds.²⁹⁰ Although the resulting M06-2X hybrid meta-GGA functional shows good overall performance for treating weak interactions, its highly fitted nature does not guarantee the correct asymptotic behavior and leads to failures.²⁹¹ Similarly, the so-called double hybrid functionals¹⁶³ (which scale roughly as MP2) are only partially successful and also need a long-range attractive energy correction for a more general description of weak interactions.⁸⁵

3.2 Computational Methods

An efficient solution to improve the performance of density functionals for weak interactions is to add a damped attractive atom pairwise dispersion energy correction^{38,39,269} to the GGA, hybrid GGA, or meta-GGA energy

$$E_{\text{disp}} = - \sum_{i=2}^{N_{\text{at}}} \sum_{j=1}^{i-1} d(R_{ij}) \quad (3.1)$$

The summation is over all atom pairs ij in the N_{at} atomic system, and the $d(R_{ij})$ attractive function is properly damped at short internuclear separations R_{ij} . We suggest the following double-damped formula for $d(R_{ij})$

$$d_{\text{dD10}} = F_{\text{F}}(a, R_{ij}) \sum_{n=3}^5 f_{2n}(bR_{ij}) \frac{C_{2n}^{ij}}{R_{ij}^{2n}} \quad (3.2)$$

where

$$F_{\text{F}}(a, R_{ij}) = \frac{1}{1 + e^{-46 \left(\frac{R_{ij}}{aR_{ij}^{\text{vdW}}} - 1 \right)}} \quad (3.3)$$

In eq 3.2, $F_{\text{F}}(a, R_{ij})$ is a Fermi damping function³⁸ given in eq 3.3, that is used to switch off the first damping (i.e., $f_{2n}(bR_{ij})$) at short internuclear separation. $f_{2n}(bR_{ij})$ are damping functions specific to a given dispersion coefficient (*vide infra*), a and b are empirical damping parameters, and the C_{2n}^{ij} are the dispersion coefficients.

The steepness factor in eq 3.3 (i.e., 46) was chosen such as to minimize the effect of the Fermi function on the damping function $f_{2n}(bR_{ij})$ at larger internuclear separations by imposing $F_{\text{F}}(a, 1.1 \cdot a \cdot R_{ij}^{\text{vdW}}) \leq 0.99$. R_{ij}^{vdW} is the vdW distance of the atom pair, and a is the parameter that scales the vdW radii to improve the flexibility in the parametrization scheme.²⁵¹ The summation in eq 3.2 goes up to 5 to include damped C_6 , C_8 , and C_{10} terms leading to the resulting dD6, dD8, and dD10 formulas (the latter contains all terms up to C_{10}). The f_{2n} damping functions are used in the following form

$$f_{2n}(x) = 1 - \exp(-x) \sum_{k=0}^{2n} \frac{x^k}{k!} \quad (3.4)$$

where $x = bR_{ij}$, with b being the damping (due to overlapping densities) parameter.⁷³ These general damping function terms were proposed by Tang and Toennies⁷³ (TT), and successfully used for dispersion interaction of several noble-gas and metal atom pairs.^{73,292,293} In the original TT model, the long-range attractive potential, which is computed from the damped dispersion series, is added to a short-range purely repulsive Born-Mayer potential with b being the range parameter. The importance of the C_8 and C_{10} terms is emphasized in ref 79. As standard functionals are able to treat short-range correlation accurately, regions of strongly overlapping densities do not need to be corrected, which justifies the use of the

second damping (Fermi) function. The hybridization state dependent³⁸ C_6 dispersion coefficients are averaged and combined according to the rule proposed by Grimme:²⁶⁹ $C_6^{ij} = 2 \frac{C_6^i C_6^j}{C_6^i + C_6^j}$. Other atomic coefficients³⁹ or combination rules^{39,294} give similar but slightly less consistent results after refitting. C_8 and C_{10} coefficients were estimated based on the average C_6 dispersion coefficients and empirical rules as established in refs 295 and 22: i.e. $C_8/C_6 = 45.9$ and $C_6 C_{10}/C_8^2 = 1.21$ (in atomic units). An alternative that is going to be investigated in subsequent chapters would be to use Becke-Johnson exchange hole dipole model.^{75,77,78,80}

Bondi's²⁹⁶ vdW radii were used and combined according to a "cubic mean" combination rule put forward by Halgren:²⁹⁴ $R_{ij}^{\text{vdW}} = \frac{R_{i,\text{vdW}}^3 + R_{j,\text{vdW}}^3}{R_{i,\text{vdW}}^2 + R_{j,\text{vdW}}^2}$.

The motivation for the use of a damped dispersion series along with a Fermi formula such as in eq 3.2 is the removal of the systematic errors for the treatments of short-range weak interactions, while preserving good performance for more typical long-range vdW interactions. Recently, several studies pointed to large errors in the description of the nonbonded intramolecular interaction in alkanes.^{68–71,297} Corminboeuf and coworkers⁷² showed that the atom pairwise dispersion correction containing only $\sim R^{-6}$ terms and optimized for reproducing intermolecular energies (PBE-inter, *vide infra*)²⁷⁰ only slightly improve the description of intramolecular interactions. In contrast, the reparametrized PBE-intra (i.e., parametrized for intramolecular interactions) performs considerably better for isodesmic (i.e., the number of formal bond types is conserved) bond separation equation (BSE) reaction energies^{82,83} of hydrocarbons but seriously overbinds the T-shaped benzene dimer. While the PBE-inter T-shaped dimer dissociation curve is considerably better than that of the PBE-intra, it has a much higher curvature than the corresponding CCSD(T) curve (*vide infra*). The dispersion energy formula suggested in eq 3.2 should preserve the description of both interactions.

The two empirical parameters, a and b , contained in eq 3.2 are obtained from two prototypes of reaction energies that are the Pople's isodesmic bond energy separation reaction of propane (eq 3.5 with $m = 1$) and the hydrogenation reaction of [2.2]paracyclophane to p-xylene



Correcting eq 3.5 accounts for the intramolecular (short-range) error. Note that the bond lengths do not change considerably along reaction 3.5. The reaction is therefore not suited for determining the value of the parameter a that describes the distance where to switch off the correction. On the other hand, obtaining an accurate energy for the challenging hydrogenation reaction of [2.2]paracyclophane to p-xylene (3.6)^{85,298} necessitates a correct description of the long-range interactions between the two benzene rings of paracyclophane as well as the reaction energy for converting a H–H and two C–C bonds into two C–H bonds



The first-principle GGA functionals are very efficient computationally and provide reasonable results for a wide range of problems (molecular geometry, vibration, reaction energies, lattice

constants, bulk moduli, cohesive energies, surface energies). Several nonempirical functionals that use the PBE form were selected for this study. PBE itself¹⁵⁶ is generally used in chemistry and physics. Its failure to improve the solid lattice constants, bulk moduli, and surface energies upon LSDA motivated the development of the recent PBEsol first-principles GGA functional²⁶⁶ that is based on the exact second order gradient expansion of the exchange energy (the PBE functional is also a first principles GGA functional that satisfies other exact constraints as second order gradient expansion for correlation and LSDA-like linear density response of a uniform electron gas). PBEsol gives excellent lattice constants and surface energies but poorer atomization energies than PBE. An attempt to develop a simple GGA that unites the good properties of PBE and PBEsol led to the second regularized gradient expansion (RGE2). For further details the interested readers turn to refs 156, 266 and 268.

Because of the different energy range of the two prototype reactions ($2.8 \text{ kcal mol}^{-1}$ for the propane BSE and $-58.5 \text{ kcal mol}^{-1}$ for the hydrogenation of [2.2]paracyclophane), a straight-forward least-squares minimization of the combined error is not suited. The error criterion for the hydrogenation reaction was therefore chosen to be 2 kcal mol^{-1} ("chemical accuracy"). From all combinations fulfilling this requirement, the one with the lowest error for the propane BSE was selected. Parameter a is 1.45 for all functionals. b is 0.88, 1.03, and 1.00 for PBEsol, PBE, and RGE2, respectively.

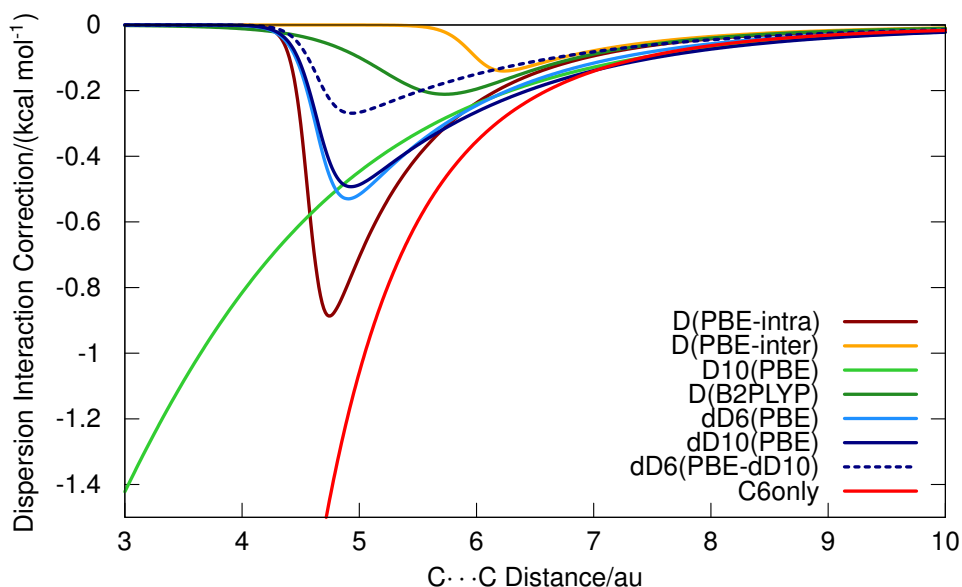


Figure 3.1: Dispersion energy correction curve for C...C dispersion interaction vs the C...C distance. Parameters of eq 3.2 are $a = 1.45$ PBE-dD10: $b = 1.03$; PBE-dD6: $b = 1.34$. The broken line gives the C_6/R^6 contribution to PBE-dD10 ($b = 1.03$). For PBE-D10 without Fermi damping $b = 1.0001$.

Figure 3.1 shows the R_{ij} dependence of the dD10 formula of eq 3.2 using the a and b parameters obtained for PBE vs C...C internuclear separation. The dD10 correction balances between the inter- (i.e., long-range) and intra- (short-range) molecular dispersion corrections. Figure 3.1 also demonstrates that obtaining good BSE energies requires a dispersion energy

correction up to relatively short 4.5 au internuclear separations. At short distances the dispersion energy coming from PBE-inter vanishes and is absolutely ineffective. On the other hand, PBE-intra is steeper and larger in magnitude as compared to PBE-dD10 resulting in inaccurate energies for intermolecular interactions. The double-damped dispersion series with up to C_{10} terms (i.e dD10) easily resolves this dilemma. For comparison, D10, which is a dispersion correction free of the Fermi damping function (that “turns off” the correction at covalent bond distance), is given as well.

The performance of the dD10 energy correction is tested on five test sets. Three of the sets assess Pople’s isodesmic bond separation equation reactions (BSE, eq 3.5) of saturated hydrocarbons (chains, rings, and cages in H, R, and C sets, respectively, Figure 3.2).⁷² The fourth set that reflects “intramolecular dispersion interactions in hydrocarbons” (IDHC)⁸⁵ contains two isomerization reactions, two folding reactions of large hydrocarbon chains, the dimerization of anthracene, and the hydrogenation reaction of [2.2]paracyclophane (Figure 3.3). The fifth set corresponds to the common benchmark for noncovalent complexes (S22)²⁹⁹ and includes the benzene dimers.

Geometries of the H, R, and C sets were optimized at the B3LYP/6-311+G** level using Gaussian 03.³⁰⁰ Unscaled zero point and thermal corrections to the enthalpy are computed in the harmonic approximation at the same level. Experimental heats of formation (NIST)³⁰¹ at 298 K are used as reference. Geometries and reference values for the IDHC set were taken from ref 85. Our results are compared to LSDA (SWVN5),^{131,149} TPSS,¹⁵⁸ M06-2X,²¹⁴ B3LYP,^{161,162} B97-D,³⁹ B2PLYP,¹⁶³ and B2PLYP-D.⁸⁵ Benzene dimers were derived from the equilibrium structures of ref 274 and the monomers³⁰² kept frozen. The geometries and reference values (CCSD(T)/CBS) for the S22 set were obtained from the BEGDB database.³⁰³

Given the size of the molecules in our test sets, the cc-pVTZ basis set was chosen for the single point energy computations. This basis set contains small exponent functions and gives only a small artificial binding error for weakly bond complexes.²⁵¹ The energy differences between the cc-pVTZ and the aug-cc-pVTZ basis set computed with the PBE GGA are 0.006 kcal mol⁻¹ (0.4%) for the propane BSE (eq 3.5), 2 kcal mol⁻¹ (2.8%) for the hydrogenation reaction energy of [2.2]paracyclophane to p-xylene (eq 3.6), and 0.25 kcal mol⁻¹ for the *n*-octane isomerization problem (*vide infra*). This latter difference is negligible compared to the 7.6 kcal mol⁻¹ error with respect to the experimental energy for octane isomerization. The cc-pVTZ basis set performs considerably better than the diffuse 6-311+G(2d,2p) basis set used earlier³⁰⁴ for the octane isomerization. The 0.26 kcal mol⁻¹ difference between the PBE/cc-pVTZ and PBE/aug-cc-pVTZ energies for the anthracene dimer dissociation energy is also negligible compared to the 23.6 kcal mol⁻¹ error of the PBE (the reaction energy is 14.6 kcal mol⁻¹ with the cc-pVTZ basis set) against the best experimental estimate (-9 kcal mol⁻¹ in ref 305). Note that the S22 test set contains several hydrogen bonded complexes for which a larger basis set is required to reach convergence.³⁰⁶ For this set, computations at the aug-cc-pVTZ level are also provided and discussed.

A modified version of deMon-2K 2.3³⁰⁷ was used for all computations with the new dispersion correction. B2PLYP computations were performed with Turbomole 5.1.^{308,309} M06-2X computations were performed with NWChem 5.1^{310,311} using the ‘xfine’ grid.

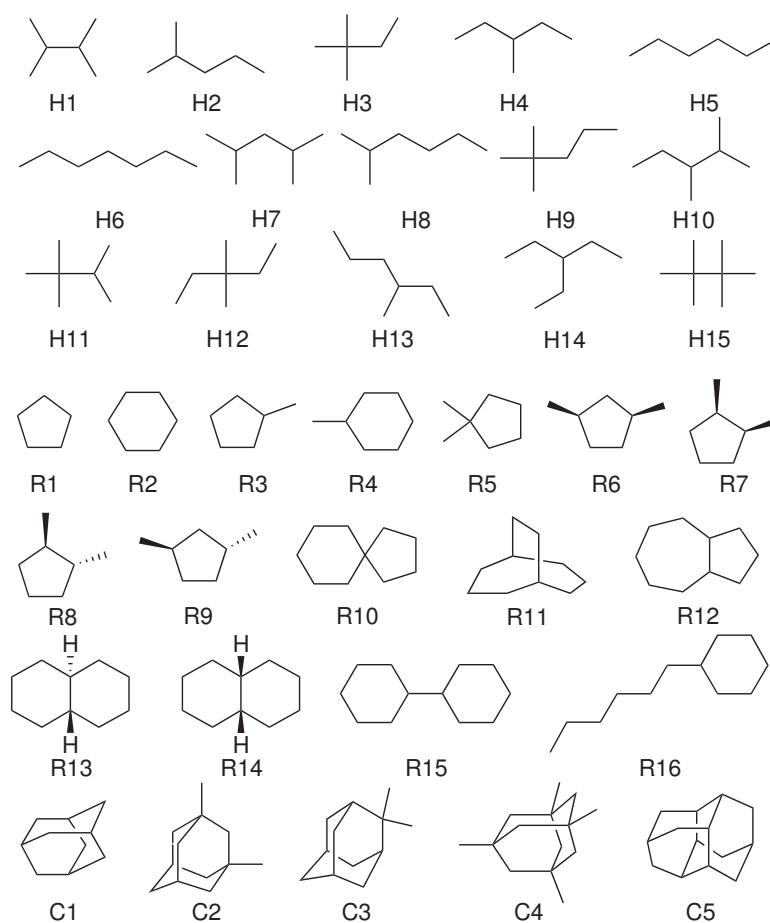


Figure 3.2: Schematic representation of the 36 saturated hydrocarbons in the H, C, and R sets.

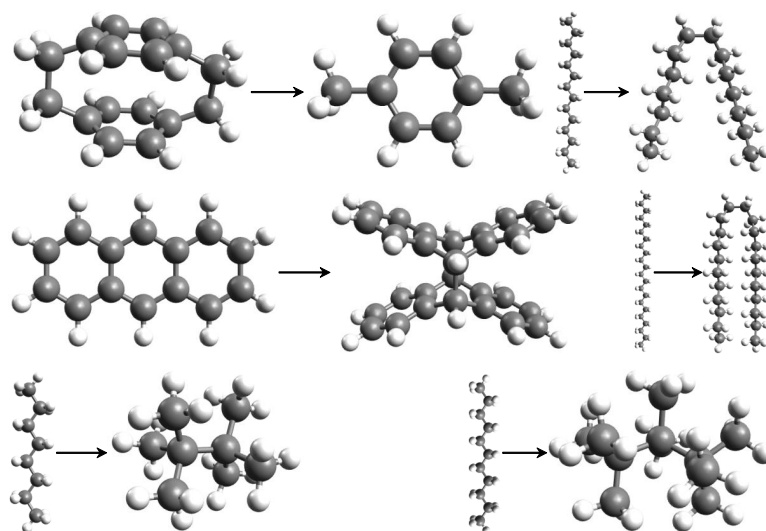


Figure 3.3: The six reactions of the IDHC test set

Table 3.1: MAD (in kcal mol⁻¹) Comparison for All Functionals Tested

	H	R	C	IDHC	S22 ^a	weighted average ^a
B3LYP	9.73	11.60	25.99	16.45	3.20	9.85
TPSS	10.33	11.64	25.67	14.66	3.01	9.75
PBE	7.99	9.59	22.52	12.52	2.24 (2.55)	7.97 (8.08)
RGE2	8.27	8.52	19.14	12.41	2.97 (3.51)	7.75 (7.93)
B2PLYP	6.05	7.02	14.41	9.19	1.41 (1.20) ^b	5.64 (5.57)
PBEsol	5.16	6.68	15.41	6.10	2.09 (1.89)	5.37 (5.31)
PBEsol-PBE	5.40	6.31	14.20	6.19	2.21	5.29
PBEsol-D6	2.48	3.06	9.06	9.09	3.24 (2.56)	4.02 (3.79)
M06-2X	3.60	6.02	13.45	2.23	0.51	3.78
SVWN5	0.78	3.97	10.21	2.01	2.85	3.14
B97-D	2.06	3.37	7.59	3.48	0.52 (0.36)	2.42 (2.37)
PBE-D10	2.50	2.59	4.84	1.69	1.06 (0.48)	2.14 (1.94)
B2PLYP-D	1.60	2.82	4.66	1.60	1.02 (0.44) ^b	1.95(1.75)
RGE2-D10	2.78	1.60	2.49	3.30	1.06 (0.90)	1.92 (1.86)
PBEsol-D10	0.42	0.98	2.29	5.76	2.40 (1.72)	1.89 (1.65)
PBEsol-dD10	1.32	1.92	3.21	2.27	1.48 (0.92)	1.76 (1.57)
PBEsol-dD6	1.16	1.76	2.67	2.34	1.43 (0.95)	1.63 (1.47)
RGE2-dD10	2.02	1.21	1.70	2.53	0.97 (0.89)	1.48 (1.45)
PBE-D6	0.31	1.05	2.19	2.94	1.90 (1.17)	1.44 (1.18)
PBE-dD10	1.01	1.33	1.69	1.50	1.16 (0.45)	1.24 (1.00)
PBE-dD6	0.82	1.17	1.58	2.01	0.95 (0.55)	1.12 (0.99)

^a Values in parentheses refers to aug-cc-pVTZ computations for the S22 test set.

^b The B2PLYP(-D) number in parentheses refer to noncounterpoise corrected energies taken from ref 85 for an optimized value of $s = 0.35$.

3.3 Results and Discussion

Figure 3.4 and Table 3.1 summarize the mean absolute deviation (MAD) for the functionals tested. The proposed dD10 energy correction reduces the errors of PBE drastically (MAD for chains/cages of 8.0/22.5 and 1.0/1.7 kcal mol⁻¹ for PBE and PBE-dD10, respectively). Only the dD10 correction reduces the systematic increase in MAD going from chains to rings to cages. Similar improvements are obtained while correcting PBEsol and RGE2.

Remarkably, for the subtle intramolecular interactions, Perdew’s “Jacobs-ladder”¹⁶⁸ is reversed! Ascending toward more sophisticated (and expectedly more robust³¹²) functionals corresponds to a significant increase in error (e.g., MAD over alkane chains increases from 0.8, to 8.0 and 10.3 kcal mol⁻¹ for LSDA, PBE, and TPSS, respectively). PBEsol (constructed to recover the exact second order gradient expansion for the exchange energy at the sacrifice of accuracy for atoms³¹³) shows the best uncorrected performance. This is best understood recalling that PBEsol exchange enhancement function $F_x(s)$ does not correct LSDA as much as the PBE functional for wide range of the reduced gradient, s , and that LSDA performs well for these reactions. Note also that the combination of the PBEsol exchange with PBE

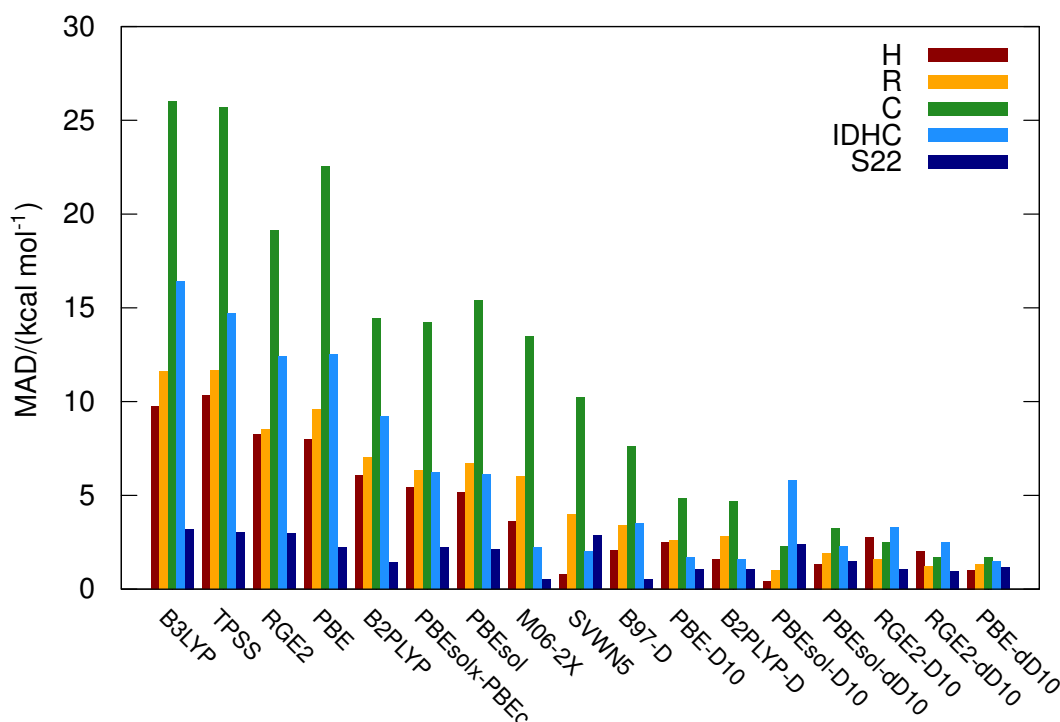


Figure 3.4: Mean absolute deviations for bond separation energies over hydrocarbon chains (H set), rings (R set), and cages (C set); for reaction energies of the test set “intramolecular dispersion in hydrocarbons” (IDHC) and the common benchmark for noncovalent complexes (S22) using the cc-pVTZ basis set.

correlation gives lower MAD than the PBE functional (Figure 3.4). This result demonstrates that the origin of the improvement arises from the modified PBEsol exchange.²⁶⁶ RGE2 is also designed to recover the second order gradient expansion for exchange over a wide range of s (typically important for correct description of solids), but it is more similar to PBE in the large density gradient region (important for free atoms) than to PBEsol. While RGE2 is built to be more satisfying from the point of view of general applicability, it performs only slightly better than PBE for the reactions tested. However, PBE-dD10 slightly outperforms RGE2-dD10 and gives the best overall results. Interestingly, the overall performance of the double hybrid B2PLYP is less satisfactory unless an attractive dispersion correction is added. Similarly, the empirical M06-2X meta-GGA results are better than those of all the noncorrected GGA but still far from the PBE-dD10 for the test sets investigated herein. The relevance of the double-damping, that is the necessity of switching off the D10 correction at short internuclear separations (<4.5 au for carbon), is illustrated by the significantly larger total MAD ($2.14 \text{ kcal mol}^{-1}$ vs $1.24 \text{ kcal mol}^{-1}$) obtained with the singly damped D10 correction to PBE (i.e., PBE-D10 in Figure 3.4). The dispersion correction discussed in this chapter works well also in the D6 form as shown by the results obtained with the damped dispersion series including the C_6 terms only (Table 3.1). PBE-D6 performs better than PBE-D10 for the alkanes series but has a significantly larger MAD for both the IDHC and S22 sets (mean error larger by 1.25 and $0.69 \text{ kcal mol}^{-1}$, respectively). While PBE-dD10 is best overall, excellent results are obtained with

Table 3.2: Computed Relative Enthalpies (ZPE and Thermal Corrected to 298 K, in kcal mol⁻¹) for Selected Alkanes Isomerization Reactions in the H and R Sets^a(97)

	H3→H5	H11→H6	H12→H6	R5→R6	MAD
Exp ^b	4.39	4.07	3.28	1.12	
B3LYP	-0.26	-2.56	-2.62	-1.07	4.84
PBE	0.28	-1.48	-1.74	-0.93	4.18
PBEsol	1.34	-0.04	-0.65	-0.34	3.14
B2PLYP	1.67	0.75	0.09	-0.33	2.67
M06-2X	3.03	2.64	1.58	0.69	1.23
B97-D	3.19	3.23	2.22	0.63	0.90
PBE-dD10	3.26	3.34	2.14	0.54	0.90
B2PLYP-D	3.51	3.52	2.29	0.73	0.70
SVWN5	3.69	3.88	2.63	0.43	0.56

^a Note that the computed energies are based on single most stable conformers and not on the Boltzmann distribution of conformers. For those small selected alkanes, it is reasonable to assume that the other conformers have a negligible contribution to the experimental result.

^b Reference 301.

the simpler PBE-dD6 variant. For the H, R, C and S22 test sets, the performance of PBE-dD6 is marginally better (by 0.1 kcal mol⁻¹ on average) than that of PBE-dD10, but the latter is better by 0.5 kcal mol⁻¹ for the IDHC test set. Since the dD6 curve mimics the position and the depth of the minima of the dD10 correction curve, these results demonstrate that the small difference between the two dispersion corrections in the longer distances does not influence the results considerably. Another illustrative example of common DFT errorsⁱ is the relative stability of isomers. As shown in Table 3.2, the errors in the alkane isomerization energies also suffer dramatically from the systematic GGA error. Apart from LDA and M06-2X, none of the (uncorrected) density functional gives an acceptable correlation with respect to the experimental heat of formations.³⁰¹ In contrast, the three empirically dispersion-corrected functionals, B97-D, PBE-dD10, and in particular B2PLYP-D, lead to a considerable improvement and describe the more compact structures (e.g., H3, H11, H12) as reasonably more stable (>2 kcal mol⁻¹) than their linear counterparts (e.g., H5, H6).

The benzene dimers serve as prototypical examples for evaluating the detailed performance of the dD10 correction on typical intermolecular interactions (Figure 3.5). For the stacked dimer, the equilibrium distance at the PBE-dD10 level is the same as with the CCSD(T) reference curve, but the dissociation energy is overestimated (by 0.59 kcal mol⁻¹, 35%). For the T-shaped dimer, the dD10 correction leads to a considerable improvement as compared to the intramolecular alternative (i.e., PBE-intra). PBE-dD10 gives a slightly larger dissociation energy than CCSD(T) (by 0.35 kcal mol⁻¹, 13%) but matches the curvature of the reference potential better than that of the dispersion correction parametrized for intermolecular in-

ⁱ“DFT error” (or “DFT failure”) refers to the errors obtained when applying density functional approximations instead of the exact density functional.

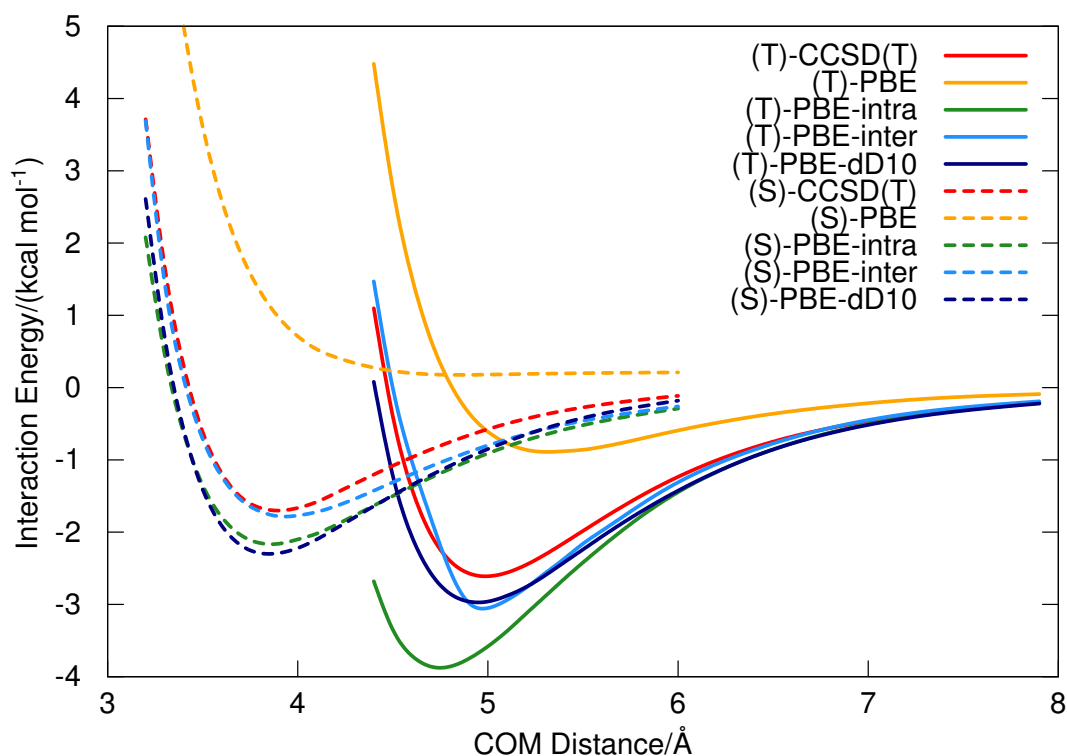


Figure 3.5: Stacked (broken lines) and T-shaped (solid lines) benzene dimer interaction energies against the center of mass distance (COM). CCSD(T) reference curve taken from ref 274, PBE-inter and PBE-intra from ref 72.

interactions (PBE-inter).^{72,270} The PBE-inter curve indeed exhibits a sudden repulsive change below 5 Å (light blue line in Figure 3.5). For the benzene dimers as well as the full S22 set, the agreement between PBE-dD10 and CCSD(T)/CBS can be considerably improved by using the larger aug-cc-pVTZ basis set (*vide infra*).

The results on the full S22 set confirm the good overall performance of dD10 on common weakly bound complexes. Unlike the DFT-D methods, which use the S22 test set to obtain parameters for the dispersion correction,^{39,85} the S22 test set was not used in the parametrization of PBE-dD10. With a MAD of 0.45 kcal mol⁻¹ using the aug-cc-pVTZ basis set (Table 3.1), PBE-dD10 gives binding energies comparable to those obtained with B2PLYP-D/aug-cc-pVTZ (0.44 kcal mol⁻¹) given in ref 85 and B97-D/aug-cc-pVTZ (0.36 kcal mol⁻¹). Note that counterpoise corrected results for B2PLYP-D can be better (MAD = 0.25 kcal mol⁻¹).⁸⁵ However, such counterpoise corrections are not straightforward for intramolecular situations, can be expensive and have not been applied here.

The general applicability of PBE-dD10 is further illustrated by the assessment of two challenging reaction energies: the dimerization reaction of anthracene and the isomerization reaction of *n*-octane into tetramethylbutane (Figure 3.3). The anthracene dimer is connected by two covalent C–C bonds resulting from a [4 + 4] cycloaddition reaction. The conversion of C–C π double bonds into two C–C σ bonds upon dimerization results in considerable change in the

energetic properties. Similar large energy difference can be observed between protobranch *n*-octane and the highly branched tetramethylbutane. PBE-dD10 performs once again nearly perfectly for both these difficult cases (Figure 3.6), while none of the other functionals are fully satisfactory. PBE-dD10 also leads to very accurate results for the entire IDHC set (MAD 1.5 kcal mol⁻¹, Figure 3.4) outperforming the other methods tested. For these two reactions and the IDHC set in general, the singly damped PBE-D10 performs almost as well as PBE-dD10.

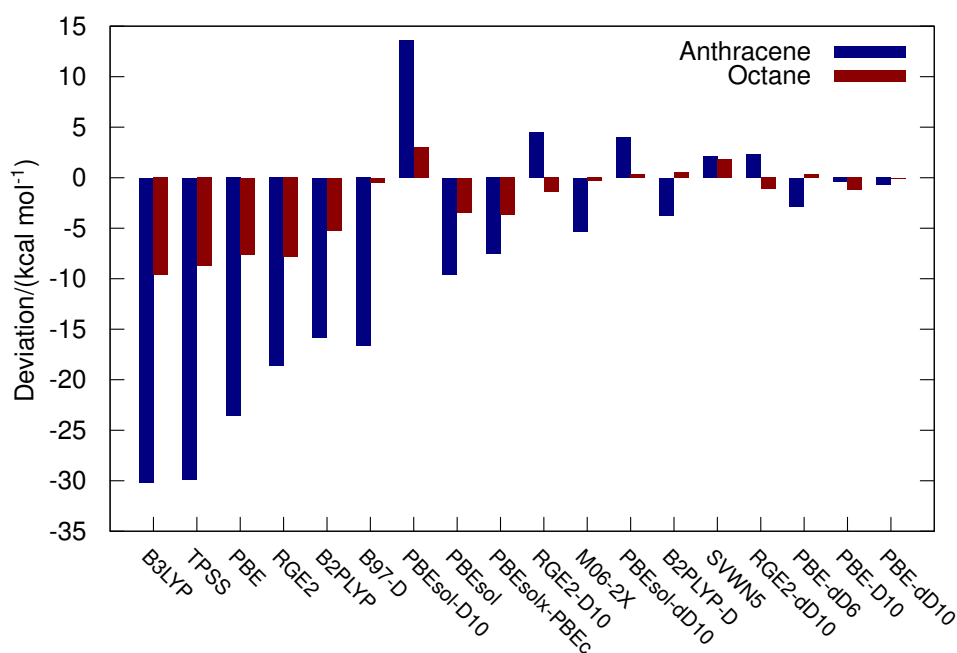


Figure 3.6: Errors associated with the two examples of reaction energies ($E_{\text{exp}} - E_{\text{theory}}$) the IDHC set: the anthracene dimerization and the octane isomerization. Details of the right-hand side are given as an inset.

Overall, PBE-dD10 gives the most robust results and the lowest MAD for a series of prototypical and challenging reaction and binding energies. With a total MAD of only 1.00 kcal mol⁻¹ for the five sets of Figure 3.4, PBE-dD10 outperforms both uncorrected and corrected functionals. For the S22 test set, the aug-cc-pVTZ basis set is necessary to obtain converged results. The smaller cc-pVTZ basis set gives converged energies for the other test sets. The success of the dispersion correction is attributed to the inclusion of an adequate damping function. In addition, the necessity of switching off the correction at short internuclear separations (<4.5 au for carbon), is illustrated by a 1 kcal mol⁻¹ higher total MAD (1.94 kcal mol⁻¹) obtained with the singly damped D10 correction to PBE (Figure 3.4).

3.4 Conclusions

We have presented a unified empirical dispersion energy correction for first principle GGA functionals. The Lennard-Jones potential $\sim R^{-6}$ dependence is augmented with higher-order correction terms (R^{-8} and R^{-10} dependent) through the use of the universal damping function of Tang and Toennies.⁷³ For general applicability, a second damping function is employed to turn off the correction at short distances. Among the three first-principal GGAs tested (PBE, PBEsol, and RGE2), PBE-dD10 give the most robust results, closely followed by PBE-dD6 and RGE2-dD10. With only two empirical parameters and one prefactor, PBE-dD10 outperforms the computationally more demanding B2PLYP-(D) and the most recent functionals such as M06-2X, which contain more empirical parameters. PBE-dD10 considerably reduces common errors for a set of 64 illustrative reaction energies, successfully balancing intra- (short-range) and inter- (long-range) molecular interactions. The dispersion corrections introduced here do not deteriorate the performance for equilibrium geometries, atomization energies, and reaction barriers.

4 A System-Dependent Density-Based Dispersion Correction

4.1 Introduction

Kohn-Sham density functional theory (DFT)¹¹ offers a powerful and robust methodology for investigating electronic structures of many-body systems, providing a practical balance of accuracy and computational cost unmatched by other methods. Despite this success, the commonly used semilocal approximations have difficulties in properly describing attractive dispersion interactions that decay with R^{-6} at large intermolecular distances. Even in the short to medium-range, most semilocal density functionals fail to give an accurate description of weak interactions.^{22,240,241}

Accurate treatment of weakly interacting systems is crucial, especially in the field of biomolecules (stacking of DNA,⁷ protein folding⁸), host-guest chemistry, surface chemistry, and condensed phases of organic molecules. Yet, even seemingly innocuous looking reactions such as alkane isomerization energies and Pople's isodesmic bond separation equations (BSEs),^{82,83} where formal bond types are preserved, suffer from errors at standard DFT levels.^{68–71}

SAPT(DFT)^{314–316} gives highly accurate interaction energies for two or three interacting closed-shell subsystems, but the method is not applicable to intramolecular interactions. Around the equilibrium distance, dispersion corrected atom centered potentials (DCAPs)^{254–257,317–319} or specifically fitted density functionals^{164,208,214,278,290,320} have led to satisfactory results. Nevertheless, both approaches lack the ability to recover the long-range $\sim R^{-6}$ attractive form. Conceptually, the simplest remedy is to correct for the missing interaction *a posteriori* by adding an attractive energy term summed over all atom pairs in the system. The strategy was originally proposed to improve Hartree-Fock energies (known as HF-D)^{37,237–239} and was later applied to DFT.^{22,38,240,241} With parameters for most elements in the periodic table, Grimme's parametrization³⁹ is the best known DFT-D variant. Since then, there has been considerable interest in finding an optimal parametrization.^{39,42,44,45,49,51,72,74,77,251,253,269,270,321–326} DFT-D is generally accurate for the treatment of intermolecular interactions, but proper description of weak intramolecular interactions is trickier.^{68,305,327} Specific fitting to a suitable training set⁷² decreases the “intramolecular” error, albeit we have recently shown that the two parametrizations can be unified using a physically motivated damping function called dD10.⁷⁴

Our dD10 correction⁷⁴ is, however, restricted to only a few elements (H, C, N, O) and, like most DFT-D schemes, employs system-independent dispersion coefficients. The present work overcomes these limitations by combining the efficiency of a new damping criterion with the attractiveness of deriving system-dependent dispersion coefficients. Akin to our former dispersion correction,⁷⁴ two damping functions are used jointly to treat both intra- and intermolecular weak interactions consistently. System-dependent dispersion coefficients are computed on the basis of the analytical approximation of the Becke and Johnson^{76–80,187,328} (BJ) exchange hole dipole moment (XDM) formalism.^{87,329} Iterative Hirshfeld weights³³⁰ are used to partition the dispersion coefficients among the atoms.^{49,331} A genuine and universal damping criterion based on iterative Hirshfeld weights is introduced for the first time. Our approach has the additional advantage of easily incorporating higher-order dispersion coefficients absent in, for instance, the related C₆-only scheme of Tkatchenko and Scheffler.⁴⁴ With only two fit parameters, this new dDXDM correction solves difficulties arising from elements positioned in different chemical environments (i.e., selecting a dispersion coefficient^{38,39,269}) and is easily applicable to every element of the periodic table.

The next sections give details on the implementation and computations. The performance of dDXDM, on test sets featuring both intra- and intermolecular weak interactions, is then compared with the interaction energies of (un)corrected popular functionals (BP86,^{151,154,332} BLYP,^{154,155} BHLYP,³³³ B3LYP,^{161,162} PBE,¹⁵⁶ and PBE0^{217,280}) and established DFT-methods designed to better describe weak interactions (B97-D,³⁹ B2PLYP-D,^{85,163} and M06-2X²¹⁴).

4.2 Theory

The basic form of our dispersion correction is the Tang and Toennies (TT) damping function⁷³

$$E_{\text{disp}} = - \sum_{i=2}^{N_{\text{at}}} \sum_{j=1}^{i-1} \sum_{n=3}^5 f_{2n}(bR_{ij}) \frac{C_{2n}^{ij}}{R_{ij}^{2n}} \quad (4.1)$$

where N_{at} is the number of atoms in the system and b is the TT-damping factor (*vide infra*). The dispersion correction is called dDXDM6 if only the first term is retained in the multipole expansion ($n = 3$, corresponding to C₆) and is called dDXDM otherwise ($n = 5$, up to C₁₀). $f_{2n}(bR_{ij})$ represents the “universal damping functions”⁷³ that are specific to each dispersion coefficient and that serve to attenuate the correction at short internuclear distances to account for overlapping densities.

$$f_{2n}(x) = 1 - \exp(-x) \sum_{k=0}^{2n} \frac{x^k}{k!} \quad (4.2)$$

This coming section describes the procedure employed for the determination of the two nontrivial arguments of eq 4.1: (i) the dispersion coefficients and (ii) the damping factor b .

4.2.1 Dispersion Coefficients

Dispersion coefficients are computed according to Becke and Johnson's XDM^{76–80,187,328} formalism, as efficiently implemented in Q-Chem by Kong and coworkers.^{87,329}

The XDM formalism is motivated by the second order perturbation interaction energy⁸⁰

$$E^{(2)} = -\frac{\langle V_{\text{pert}}^2 \rangle}{\Delta E_{\text{av}}} \quad (4.3)$$

where ΔE_{av} is the average excitation energy, rooted in the “Unsöld” or “closure” approximation.³³⁴

Expanding V_{pert} in terms of multipoles, the induced dipole – induced dipole (C_6^{ij}) term is obtained as

$$C_6^{ij} = \frac{2}{3} \frac{\langle M_1^2 \rangle_i \langle M_1^2 \rangle_j}{\Delta E_{\text{av}}} \quad (4.4)$$

ΔE_{av} is then assumed to be the sum of the individual atoms, i.e., $\Delta E_{\text{av}} = \Delta E_{\text{av}}^i + \Delta E_{\text{av}}^j$. The atomic polarizabilities α_i in turn define the individual average excitation energies

$$\Delta E_{\text{av}}^i = \frac{2}{3} \langle M_1^2 \rangle_i \alpha_i \quad (4.5)$$

which are fully compatible with the second order and multipole expansion applied to the dispersion coefficients.

Combining eq 4.4 with 4.5, the C_6^{ij} coefficients between atoms i and j are obtained according to

$$C_6^{ij} = \frac{\alpha_i \alpha_j \langle M_1^2 \rangle_i \langle M_1^2 \rangle_j}{\alpha_j \langle M_1^2 \rangle_i + \alpha_i \langle M_1^2 \rangle_j} \quad (4.6)$$

Along the same lines, higher-order dispersion coefficients (C_8^{ij} and C_{10}^{ij}) are obtained

$$C_8^{ij} = \frac{3}{2} \frac{\alpha_i \alpha_j (\langle M_1^2 \rangle_i \langle M_2^2 \rangle_j + \langle M_2^2 \rangle_i \langle M_1^2 \rangle_j)}{\alpha_j \langle M_1^2 \rangle_i + \alpha_i \langle M_1^2 \rangle_j} \quad (4.7)$$

$$C_{10}^{ij} = 2 \frac{\alpha_i \alpha_j (\langle M_1^2 \rangle_i \langle M_3^2 \rangle_j + \langle M_3^2 \rangle_i \langle M_1^2 \rangle_j)}{\alpha_j \langle M_1^2 \rangle_i + \alpha_i \langle M_1^2 \rangle_j} + \frac{21}{5} \frac{\alpha_i \alpha_j \langle M_2^2 \rangle_i \langle M_2^2 \rangle_j}{\alpha_j \langle M_1^2 \rangle_i + \alpha_i \langle M_1^2 \rangle_j} \quad (4.8)$$

The original idea of Becke and Johnson is that the multipole moments $\langle M_l^2 \rangle$ ($l = 1, 2, 3$ for dipoles, quadrupoles, and octupoles, respectively) can be approximated as atomic expectation values over the dipole $d_{X\sigma}$ between the positively charged exchange hole and its negatively

charged reference electron

$$\langle M_l^2 \rangle_i = \sum_{\sigma} \int w_i(\mathbf{r}) \rho_{\sigma}(\mathbf{r}) [\mathbf{r}_i^l - (\mathbf{r}_i - d_{X\sigma})^l]^2 d^3\mathbf{r} \quad (4.9)$$

where $\rho_{\sigma}(\mathbf{r})$ is the σ -spin density and $w_i(\mathbf{r})$ represents atomic partitioning weights. The exact expression for the exchange hole dipole moment $d_{X\sigma}$ is given by

$$d_{X\sigma}(\mathbf{r}_1) = \left[\frac{1}{\rho_{\sigma}(\mathbf{r}_1)} \sum_{ij} \psi_{i\sigma}(\mathbf{r}_1) \psi_{j\sigma}(\mathbf{r}_1) \int \mathbf{r}_2 \psi_{i\sigma}(\mathbf{r}_2) \psi_{j\sigma}(\mathbf{r}_2) d^3\mathbf{r}_2 \right] \quad (4.10)$$

However, eq 4.10 is both computationally more expensive and turns out to be less accurate than the XDM computed from the Becke-Roussel (BR)¹⁶⁰ model exchange hole.³²⁶

Becke and Roussel's model exchange hole is given by a spherically symmetric exponential function $-Ae^{-ar}$ at a distance b from the reference electron. The three parameters (A , a and b) are determined nonempirically at each point in space: the second order Taylor expansion of the spherically averaged exchange hole is required to match between the BR and the exact exchange hole. Together with the exchange hole normalization, a nonlinear equation is obtained. The solution of this equation was originally done numerically. However, Kong and coworkers introduced an analytic function fitting the solution with high accuracy.^{87,329} In Chapter 6 we will introduce a simple approximation for b , which directly characterizes the XDM in the BR model.

4.2.2 Atomic Partitioning Weights

Becke and Johnson⁷⁶ used classical Hirshfeld weightings³³⁵ in eq 4.9

$$w_{i,\text{HC}}(\mathbf{r}) = \frac{\rho_i^{\text{at}}(\mathbf{r})}{\sum_n \rho_n^{\text{at}}(\mathbf{r})} \quad (4.11)$$

where ρ_i^{at} is the sphericalized free atomic density of atom i , weighted by the superposition of all ρ_i^{at} with all atoms n positioned as in the real molecule. The classical Hirshfeld scheme depends on the (arbitrary) choice of the atomic reference densities. Molecules with large ionic character, such as LiF, offer a clear illustration of this dependence. If one uses the typical superposition of neutral atomic densities (i.e., Li^0 and F^0), the atomic charges have an absolute value of 0.57. However, a value of 0.98 is obtained when Li^+ and F^- densities are considered.³³⁰ This arbitrariness can be overcome by using the iterative version of the Hirshfeld partitioning procedure, called Hirshfeld-I.³³⁰ In the k^{th} iteration, the weight for atom i is given by

$$w_{i,\text{HI}}^k(\mathbf{r}) = \frac{\rho_i^{k-1}(\mathbf{r})}{\sum_n \rho_n^{k-1}(\mathbf{r})} \quad (4.12)$$

Conveniently, the first iteration can use neutral atomic densities, leading to the classical Hirshfeld charges. Of course, the electronic populations, $N_i = \int w_i(\mathbf{r}) \rho(\mathbf{r}) d\mathbf{r}$, are usually

fractional numbers, and the corresponding densities are thus computed according to³³⁶

$$\rho_i^k = \rho_i^{N_i} = \rho_i^{n+x} = x \cdot \rho_i^{n+1} + (1-x) \cdot \rho_i^n \quad (4.13)$$

where n is the integer part of N_i and $x = N_i - n$. The partitioning is converged if the electronic populations do not change significantly between two iterations (the convergence criterion was set to a root-mean-square deviation of 0.0005 au). Compared to the rest of the dispersion correction, the iterative scheme is computationally demanding, as integration over the entire grid is necessary for each iteration.¹ For this reason, we also report values based on the classical Hirshfeld partitioning. Note, that all the corrections are applied *a posteriori* and therefore do not influence the electron density, but only the total energy.

Finally, the determination of the dispersion coefficients from eqs 4.6-4.8 also depends on atomic polarizabilities. We herein follow Becke and Johnson's proposal to exploit the proportionality³³⁷ between polarizability and volume to estimate the effective atom in molecule (AIM) polarizabilities from tabulated free atomic polarizabilities³³⁸

$$\alpha_i = \frac{\langle r^3 \rangle_i}{\langle r^3 \rangle_{i,\text{free}}} \alpha_{i,\text{free}} = \frac{\int r^3 w_i(\mathbf{r}) \rho(\mathbf{r}) d^3\mathbf{r}}{\int r^3 \rho_{i,\text{free}}(\mathbf{r}) d^3\mathbf{r}} \alpha_{i,\text{free}} = \frac{V_{i,\text{AIM}}}{V_{i,\text{free}}} \alpha_{i,\text{free}} \quad (4.14)$$

4.2.3 The Damping

A key component of dDXDM is the damping factor b . We showed previously⁷⁴ that the performance of the TT-damping function is improved by the introduction of a second damping function to prevent dispersion corrections at covalent distances. In the full TT model,⁷³ the attractive potential should give relatively strong contribution at short distances in order to soften the repulsive Born-Mayer potential. In contrast, a dispersion correction to density functional approximations necessitates additional damping as density functionals better describe the region of strong density overlap (short-range). We herein introduce a variable, damped b , in which the second damping is intrinsically absorbed as an alternative to our previous model using a Fermi damping function.⁷⁴ In Tang and Toennies' seminal work,⁷³ the damping parameter b is also the range parameter of the repulsive Born-Mayer potential and thus depends on the two interacting atoms. Later, the same authors converted b from a constant into a function:³³⁹ for an arbitrary repulsive potential $V(\mathbf{r})$

$$b(\mathbf{r}) = -\frac{d \ln V(\mathbf{r})}{d\mathbf{r}} \quad (4.15)$$

Here, we replace the distance dependence by the following form

$$b(x) = F(x) \cdot b_{ij,\text{asym}} \quad (4.16)$$

¹Lowering the convergence threshold and using an improved guess would decrease the number of iterations. The improved guess is expected to be especially efficient for geometry optimization, where partial charges do not vary a lot between two steps.

Chapter 4. A System-Dependent Density-Based Dispersion Correction

x and $F(x)$ are respectively the damping argument and the function for $b_{ij,\text{asym}}$, the TT-damping factor associated with two separated atoms. $b_{ij,\text{asym}}$ is computed according to the combination rule^{293,340}

$$b_{ij,\text{asym}} = 2 \frac{b_{ii,\text{asym}} \cdot b_{jj,\text{asym}}}{b_{ii,\text{asym}} + b_{jj,\text{asym}}} \quad (4.17)$$

The $b_{ii,\text{asym}}$ values are estimated^{341,342} by the square root of the atomic ionization energy $\sqrt{I_i}$ taken from the literature.³⁴³ Inspired by the approach of Tkatchenko and coworkers,^{44,120} the atom in molecule character is taken into account through a cubic root scaling of the ratio between the free atom and the AIM volume. After introduction of the parameter b_0 , which determines the strength of the dispersion correction in the medium-range, we arrive at

$$b_{ii,\text{asym}} = b_0 \cdot \sqrt{2I_i} \cdot \sqrt[3]{\frac{V_{i,\text{free}}}{V_{i,\text{AIM}}}} \quad (4.18)$$

The most robust form for the damping functionⁱⁱ proved to be

$$F(x) = 1 - \frac{2\arctan(a_0 \cdot x)}{\pi} \quad (4.19)$$

where the fitted parameter a_0 adjusts the short-range behavior.

The last element of the dispersion correction is the damping argument x

$$x = \text{abs} \left(q_{ij} + q_{ji} - \frac{(Z_i - N_i) \cdot (Z_j - N_j)}{r_{ij}} \right) \frac{N_i + N_j}{N_i \cdot N_j} \quad (4.20)$$

where Z_i and N_i are the nuclear charge and Hirshfeld population of atom i (*vide supra*), respectively. The overlap population³⁴⁴ $q_{ij} = \int w_i(\mathbf{r}) w_j(\mathbf{r}) \rho(\mathbf{r}) d\mathbf{r}$ is a covalent bond index, and the fraction term in the parentheses is an ionic bond index.³⁴⁵ The multiplicative factor, $(N_i + N_j)/(N_i \cdot N_j)$, serves to attenuate the damping of $b_{ij,\text{asym}}$ for heavier atoms (containing more electrons). Note that the damping function has an adequate form (i.e., $F(0) = 1$ and $F(\infty) = 0$), given that x is large for close atoms pairs and vanishes with increasing distance r_{ij} . This is the first example for which the damping of an atom pairwise dispersion correction depends on Hirshfeld (overlap) populations rather than on “critical” or “van der Waals” radii. Our approach is, however, similar in spirit to Slipchenko and Gordon’s³⁴⁶ overlap-matrix-based formula employed within the framework of the effective fragment potential method.

To summarize, the presented dDXDM correction uses electronic structure information to determine dispersion coefficients and two fitted damping parameters that are the strength of the TT-damping (b_0) and the steepness factor (a_0).

ⁱⁱ Different functionals, different order of multipole expansion, classical/iterative Hirshfeld partitioning.

4.3 Determination of the Adjustable Parameters

In line with our former work,^{72,74} the chosen fitting procedure ensures a successful treatment of both weak intra- (short-range) and inter- (long- range) molecular interactions. From a theoretical perspective, typical weakly bound systems, such as rare gas dimers, seem the appropriate choice as a training set. However, the description of rare gas dimers by standard density functionals is not consistent; for instance, PBE overbinds the helium dimer and underbinds the argon dimer. Such behavior is not easily improved by a dispersion correction and highlights that inclusion of rare gas dimers into the training set does not necessarily guarantee a generally improved treatment of weak intra- and intermolecular interactions.^{31,299} In contrast, we and others demonstrated that the large errors in the description of alkane intramolecular interactions (e.g., isomerization energies) are systematic^{68,69} and conveniently reduced by a dispersion correction.^{72,85,347–349} Our recent work, introducing a flexible TT-based dispersion energy correction,⁷⁴ demonstrated that using alkane reaction energies as a training set results in a highly transferable correction, which outperforms others, even for systems well outside the range of the training set (e.g., intermolecular complexes).⁷⁴ Akin to our former fitting procedure, the two parameters (a_0 and b_0) are fitted for each functional as to minimize the mean absolute deviation (MAD) over five reaction energies that are the Pople’s isodesmic bond energy separation reaction of *n*-hexane and cyclohexane



the folding energy of $\text{C}_{22}\text{H}_{46}$, and the isomerization energy of *n*-octane and *n*-undecane to 2,2,3,3-tetramethylbutane and 2,2,3,3,4,4-hexamethylpentane, respectively.

Best fit parameters are determined for dDXDM (i.e., iterative Hirshfeld weights and terms up to C_{10}), dDXDMc (using classical Hirshfeld weights), dDXDM6 (iterative Hirshfeld weights, only up to C_6), and dDXDM6c (classical Hirshfeld weights and only up to C_6). Short form parenthetical notations that are used in the text refer to the two levels of dispersion correction with or without the parentheses (e.g., dDXDM6(c) refers to dDXDM6 and dDXDM6c). For the models including terms up to C_{10} , best fit a_0 and b_0 correlate well with each other. There is also a good correlation between each of the fitted parameters and the repulsive character of the functional,ⁱⁱⁱ as represented by the error in the methane dimer interaction energy.³⁶ In contrast, the C_6 -based energy corrections show poor (dDXDM6) or even no (dDXDM6c) correlation between a_0 and b_0 . The missing higher-order dispersion terms in dDXDM6c are compensated by relatively higher b_0 values.²⁹² The a_0 parameters adjust accordingly following the repulsive character of the functional to prevent a too strong energy correction in the short-range. These results emphasize the physical relevance of including higher dispersion terms to achieve a more consistent correction.

ⁱⁱⁱA detailed analysis of a correlation of errors for reaction energies with failures in the short-range potential energy will be reported Chapter 5.

4.4 Test Sets

The robustness of the dDXDM correction is tested on seven illustrative sets featuring both intra- and intermolecular weak interactions, as described hereafter.

Three of the sets assess Pople's isodesmic bond separation equation reactions^{82,83} of saturated hydrocarbons (H, R, and C for chains, rings, and cages, respectively, see Figure 3.2 on page 27). As in ref 74, B3LYP/6-311+G** geometries and thermal corrections are included, and reference values are derived from experimental heats of formation.³⁰¹

The "intramolecular dispersion interactions in hydrocarbons" (IDHC)⁸⁵ set contains two isomerization reactions (*n*-octane and *n*-undecane to the fully branched isomer), two folding reactions of large hydrocarbon chains (C₁₄H₃₀ and C₂₂H₄₆), the dimerization of anthracene, and the hydrogenation reaction of [2.2]paracyclophane to p-xylene. Geometries and reference values are taken from ref 85.

The S22²⁹⁹ set validates the performance of the dispersion correction on noncovalent complexes, while the P76 set test probes peptide conformational energies.³⁵⁰ P76 contains 76 conformations of five small peptides having aromatic side chains (FGG, GFA, GGF, WG, and WGG). For these two sets, geometries and reference values (estimated CCSD(T)/CBS) are taken from the literature.^{303,351}

The last test set (EX3) exclusively features weak interactions involving heavy atoms in the dimers of pnictogen trihalides (NF₃, NCl₃, PCl₃, PBr₃, and AsBr₃).³⁵² Geometries (counterpoise corrected df-MP2/aug-cc-pVTZ) were taken from ref 352. Reference values (estimated CCSD(T)/CBS) were computed at the counterpoise corrected level³⁵³ according to

$$E(\text{CCSD(T)/CBS}) = \text{HF/AVQZ} + \text{CCSD-F12b/CBS(AVTZ/AVQZ)} + (\text{T})/\text{CBS(AVDZ/AVTZ)} \quad (4.22)$$

where aug-cc-pVDZ, aug-cc-pVTZ, and aug-cc-pVQZ are abbreviated by AVDZ, AVTZ, and AVQZ, respectively. These computations were performed with Molpro2009.1³⁵⁴ at the F12 level,³⁵⁵ with the HF energy containing the CABS single correction and the triples being based on F12 amplitudes. The g functions are omitted in all aug-cc-pVQZ computations, except for the heaviest dimer (i.e., (AsBr₃)₂). The extrapolation functional proposed by Helgaker and coworkers^{356,357} ($E_n^{\text{corr}} = E_{\text{CBS}}^{\text{corr}} + AX^{-3}$ with $X = 2, 3$, and 4 for AVDZ, AVTZ, and AVQZ, respectively) is applied *a posteriori* to the CCSD-F12b and (T) correlation energies.³⁵⁸ The T1 diagnostic was below 0.02 and the D1 diagnostic³⁵⁹ around 0.04, except for NCl₃, where D1 \approx 0.065 (monomer and dimer) is indicative of a multireference character. The NBr₃ dimer was discarded from the test set due to its D1 \approx 0.085 and an unreliable basis-set convergence.

The performance of the dDXDM correction was further examined on four potential energy profiles: (a) the stacked benzene dimer (geometry and reference values taken from refs 274 and 360, respectively), (b) a propane dimer conformation (geometry based on the experimental geometry³⁶¹ and arranged like in ref 362), (c) a benzene-H₂S complex (geometry and reference from ref 360), and (d) a benzene-H₂O complex (orientation analogous to the benzene-H₂S conformation, with the same benzene geometry³⁰² and the experimental water geometry).³⁶¹

For b and c, reference values were computed at the counterpoise corrected level³⁵³

$$E(\text{CCSD(T)}/\text{CBS}) = \text{df-MP2}/\text{CBS}(\text{AVDZ}, \text{AVTZ}) + \Delta\text{CCSD(T}^*)\text{-F12b}/\text{AVDZ} \quad (4.23)$$

where $\Delta\text{CCSD(T}^*)\text{-F12b}/\text{AVDZ}$ is the difference between df-MP2-F12 and CCSD(T^{*})-F12b evaluated with the aug-cc-pVDZ basis set, and (T^{*}) stands for the perturbative triple corrections improved by scaling by the ratio of df-MP2-F12/df-MP2.¹²¹

4.5 Computational Methods

B97-D and B2PLYP-D computations with the cc-pVTZ basis set^{363–365} were performed with Turbomole 5.10^{308,309} using the resolution of identity (RI-MP2)³⁶⁶ with matching auxiliary basis functions³⁶⁷ to speed up B2PLYP. M06-2X energies were computed with NWChem 5.1^{310,311} using the “xfine” grid. All of the other computations were performed with a developmental version of Q-Chem 3.2.³⁶⁸ The cc-pVTZ basis set^{363–365} was used except for the potential energy curves, for which the larger aug-cc-pVTZ basis set was employed. The energy differences between cc-pVTZ and the larger aug-cc-pVTZ basis set were found to be negligible compared to the error of the method against the reference value³⁶⁹ (e.g., the averaged total MAD for PBE/cc-pVTZ, 4.27 kcal mol⁻¹, differs by only 2%, 0.08 kcal mol⁻¹, from PBE/aug-cc-pVTZ, 4.20 kcal mol⁻¹).

To ensure a consistent treatment between intra- and intermolecular interaction, no basis set superposition correction was applied (e.g., P76 contains peptide conformations with intramolecular interactions resembling closely those of intermolecular complexes in the S22 test set). XDM-based dispersion corrections were done post-SCF. The iterative Hirshfeld partitioning was implemented using sphericalized restricted-open atomic densities computed on the fly (i.e., functional specific) with a 99/590 Euler-Maclaurin-Lebedev^{370,371} grid. The energy profiles were computed with a 99/302 Euler-Maclaurin-Lebedev grid. Otherwise, the SG1 grid³⁷² was used.

4.6 Results and Discussion

Figure 4.1 summarizes the mean absolute deviation for established methods tested on the seven sets described above. The difference between “standard” and “recent” functionals (M06-2X, B97-D, and B2PLYP-D) is significant for all of the test sets (averaged total MAD 5.0 vs 1.5 kcal mol⁻¹). As noted previously,⁷⁴ the performance of the recent functionals on hydrocarbon reaction energies (H, R, C, and IDHC) is significantly better than that of the standard ones (MAD of 3.8 and 12.9 kcal mol⁻¹, respectively), although chemical accuracy has yet to be obtained.

The MADs for the best performing variant of the dispersion correction (-dDXDM i.e., iterative Hirshfeld weights and terms up to C₁₀) are shown in Figure 4.2a. Note that (un)corrected B2LYP (0.47 B88 + 0.53 HF + 0.73 LYP, same functional contributions as in B2PLYP¹⁶³) is not

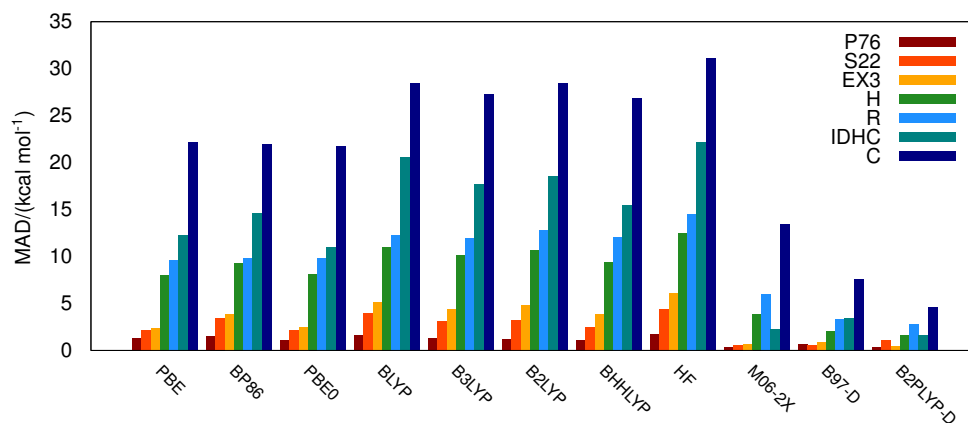


Figure 4.1: Performance for commonly used functionals: Mean absolute deviations for binding energies for noncovalent complexes (S22 and EX3); relative conformational energies of five small peptides (P76); and bond separation energies over hydrocarbon chains (H), rings (R), and cages (C) and for reaction energies of the test set “intramolecular dispersion interactions” (IDHC) using the cc-pVTZ basis set.

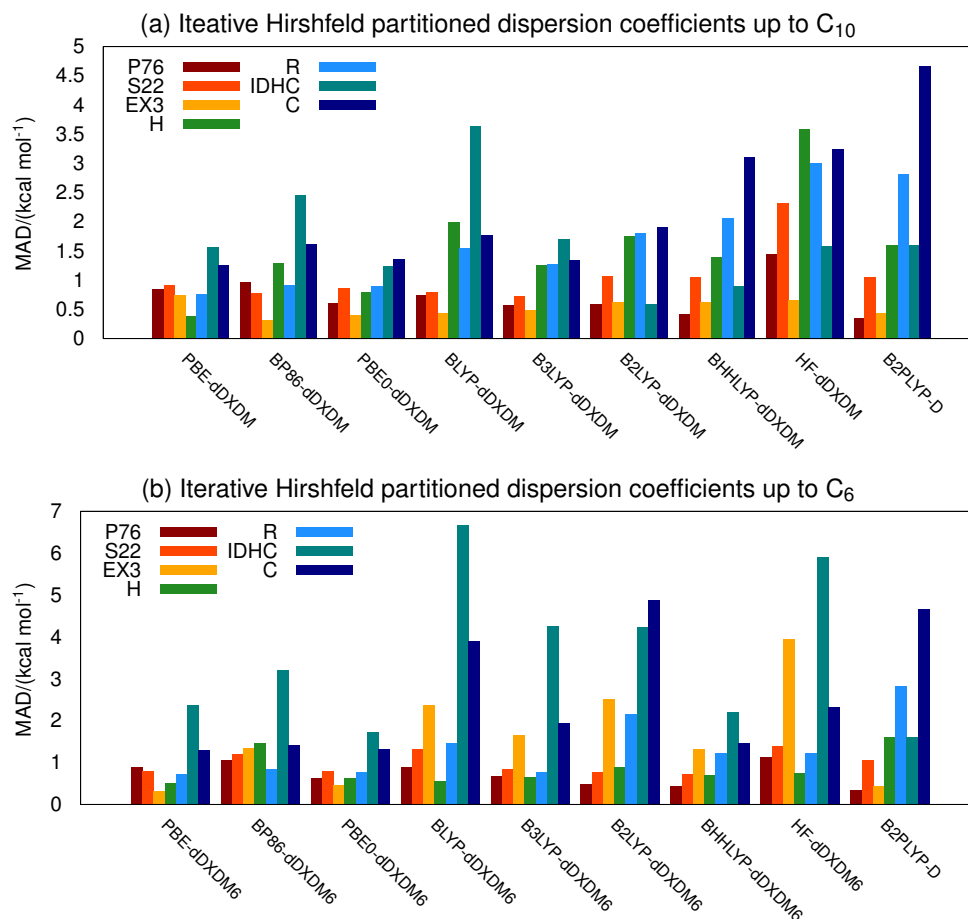


Figure 4.2: Performance for the iterative Hirshfeld-distributed dispersion coefficients up to C_{10} (a) and up to C_6 (b): Mean absolute deviations for binding energies for noncovalent complexes (S22 and EX3); relative conformational energies of five small peptides (P76); and bond separation energies over hydrocarbon chains (H), rings (R), and cages (C) and for reaction energies of the test set “intramolecular dispersion interactions” (IDHC) using the cc-pVTZ basis set. B2PLYP-D serves as an “internal standard”.

intended for “real world” applications but provides insight into the good performance of B2PLYP-D. Overall, dDXDM largely improves the parent functionals, yielding low errors. Over the seven dispersion corrected functionals tested, the averaged total MAD (TMAD) is 0.9 kcal mol⁻¹ (min 0.74 (PBE0-dDXDM); max 1.11 (BLYP-dDXDM)), significantly lower than for the recent M06-2X, B97-D, and B2PLYP-D (1.5 kcal mol⁻¹, min 1.06 (B2PLYP-D)). The dispersion correction improves the IDHC energies for both PBE and HF (MAD of 12.3 and 22.2 kcal mol⁻¹, respectively) to a respectable mean absolute deviation of 1.6 kcal mol⁻¹. B2LYP- and BHHLYP-dDXDM give remarkably low MADs of 0.6 and 0.9 kcal mol⁻¹ (B2PLYP-D gives 1.6 kcal mol⁻¹), while BLYP-dDXDM performs less convincingly (MAD of 3.6 kcal mol⁻¹) for this set. The robustness and range of applicability of dDXDM combined with various functionals is further illustrated by the consistent improvement of alkane BSE reaction energies and weak intermolecular interactions: averaged MADs for the HRC, P76 (relative conformational energies of small peptides), and S22 (intermolecular weak interactions) sets are 1.4, 0.7, and 0.9 kcal mol⁻¹, respectively, corresponding to roughly 10, 50, and 30% of the deviations of the uncorrected values (12.9, 1.3, and 3.2 kcal mol⁻¹). The 0.5 kcal mol⁻¹ averaged MAD for the pure inorganic test set (EX3; vs an uncorrected 3.9 kcal mol⁻¹) is also rewarding. PBE0-dDXDM is the most accurate combination presented herein (TMAD of 0.74 kcal mol⁻¹) but dDXDM with the popular B3LYP functional is, as well, very satisfactory (TMAD of 0.82 kcal mol⁻¹). The best dispersion corrected GGA, PBE-dDXDM, performs nearly as well as PBE0-dDXDM with a TMAD of 0.84 kcal mol⁻¹. Such a performance is of interest for applications to large systems (or even bulk materials), where hybrid functionals are computationally considerably more demanding. Nevertheless, hybrid functionals, which generally outperform the GGA in many thermochemistry applications, provide the best dDXDM corrected results.

4.6.1 Classical Hirshfeld Partitioning and C₆-Only Dispersion Corrections

The reliability of simpler variants of the dispersion correction, i.e., including only terms up to C₆ or using Hirshfeld classical instead of iterative weights, has also been evaluated. The use of the classical Hirshfeld weights is of practical interest, as it is significantly less computationally demanding than the iterative version. In the BJ formalism, C₈/R⁻⁸ and C₁₀/R⁻¹⁰ terms are relatively inexpensive but have non-negligible contributions to the interaction energy at short internuclear separations.^{45,79,292} A comparison with the C₆ truncation is thus of theoretical relevance.

Figure 4.2a (dDXDM) and 4.2b (dDXDM6) reveal that the BSE of alkane cages, the IDHC, and the EX3 test sets are most affected by the truncation. Whereas the first two sets are characterized by a high number of short-range interactions, the effect in the EX3 interaction energies is more difficult to interpret. Overall, only the combinations of dDXDM6 with PBE, PBE0, and BHHLYP match the dDXDM results closely.

For the higher-order multipole expansion, classical Hirshfeld weights result in larger errors than the iterative procedure (Figure 4.3). With an increase in averaged MAD from 0.9 (dDXDM) to 1.5 kcal mol⁻¹ (dDXDMc), the S22 test set is the most representative of the classical partitioning limitation (underestimation of ionic characters).³⁷³ As an example, the C₆(PBE)

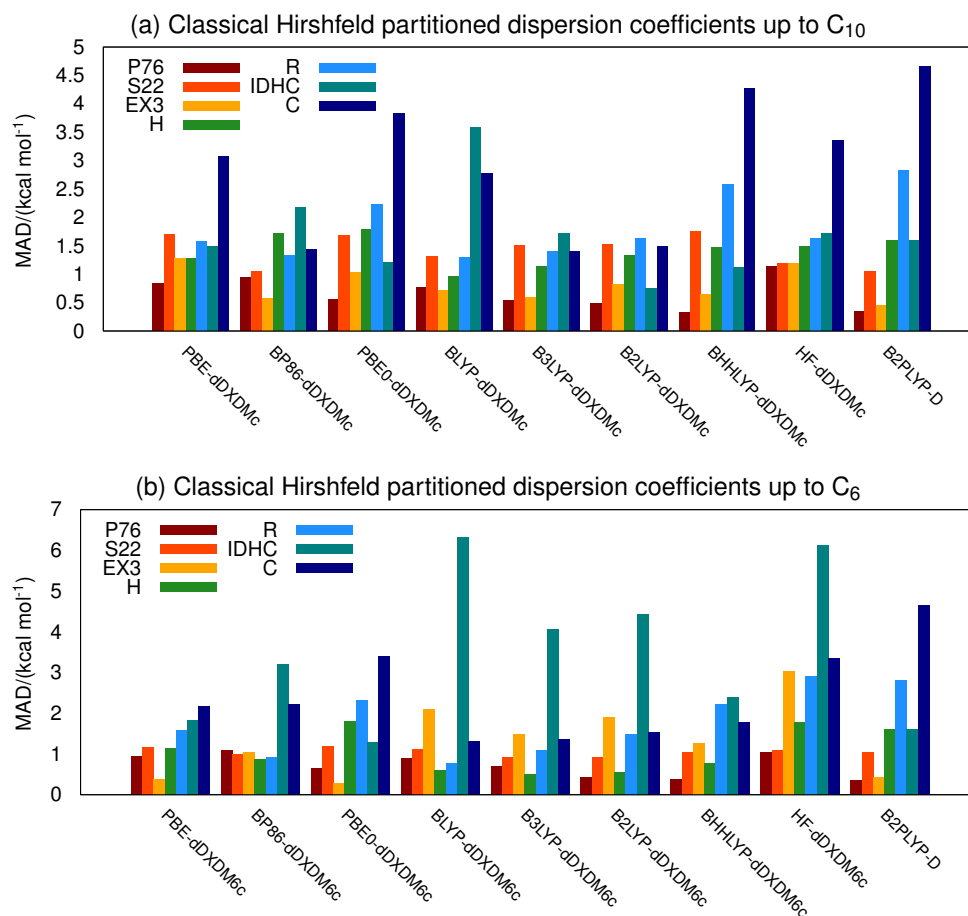


Figure 4.3: Performance for the classical Hirshfeld distributed dispersion coefficients up to C₁₀ (a) and up to C₆ (b): Mean absolute deviations for binding energies for noncovalent complexes (S22 and EX3); relative conformational energies of five small peptides (P76); and bond separation energies over hydrocarbon chains (H), rings (R), and cages (C) and for reaction energies of the test set “intramolecular dispersion interactions” (IDHC) using the cc-pVTZ basis. B2PLYP-D serves as an “internal standard”.

O \cdots O/H \cdots H dispersion coefficients for the water dimer are 12.6/2.5 with classical Hirshfeld weights, compared to 21.2/0.9 with the iterative procedure. The key difference arises from the ionic bond index appearing in eq 4.20. The index for the O \cdots O atom pair is 0.014 while using atomic densities (classical partitioning) and 0.15 after the iterative scheme. This difference translates into a strong/weak damping when iterative/classical Hirshfeld charges are used. As DFT approximations correctly account for interaction energy between strongly polarized fragments (e.g., H bonds), higher iterative Hirshfeld charges (i.e., strong damping, small dispersion corrections) are better suited. In contrast, HF that systematically neglects correlations benefits from the larger dispersion corrections associated with the use of classical Hirshfeld weights. It is thus not surprising that Hartree-Fock gives its best results when combined with dDXDMc (TMAD of 1.3 kcal mol⁻¹, MAD(S22) = 1.18 kcal mol⁻¹) and that HF-dDXDM is the least accurate variant (TMAD of 2.01 kcal mol⁻¹, MAD(S22) = 2.32 kcal mol⁻¹). HF-dDXDMc could thus be a general alternative to the recent refined HF-D approach, which has been proven to be successful for intermolecular interactions.³²⁴

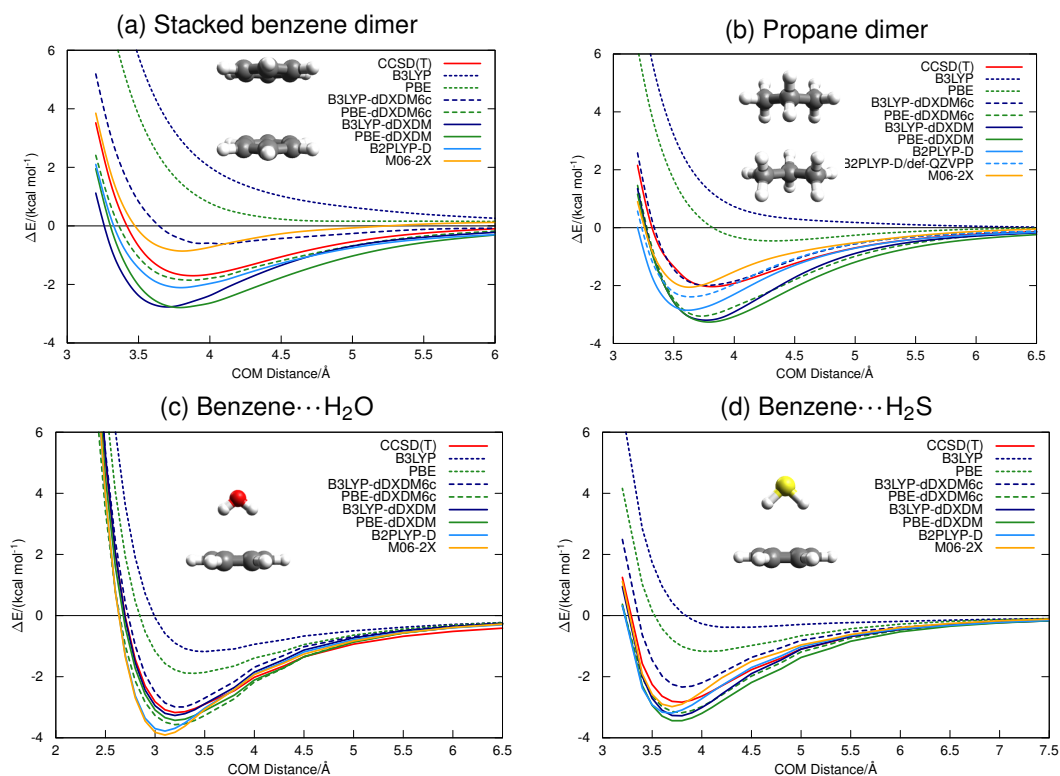


Figure 4.4: Interaction energy (ΔE) profiles for the (a) stacked benzene dimer, (b) propane dimer, (c) benzene- H_2O complex, and (d) benzene- H_2S complex. CCSD(T) references for a and d are taken from ref 360, while b and d are computed (see Test Sets). If not stated otherwise, density functional computations were performed with the aug-cc-pVTZ basis set.

For the reasons given above, the classical Hirshfeld partitioning performs better on the S22 set when terms only up to C_6 are included (see Figure 4.3b): excluding higher dispersion terms attenuates the overcorrections of polar interactions. With TMADs below $1.0 \text{ kcal mol}^{-1}$, B3LYP-dDXDM6c and BHHLYP-dDXDM6c represent attractive alternatives to avoid the iterative scheme. As for the GGAs, PBE-dDXDM6c and BP86-dDXDM6c are the most consistent over the seven sets tested (TMAD of 1.12 and $1.14 \text{ kcal mol}^{-1}$, respectively). Comparisons of B2LYP-dDXDM6(c) to B2PLYP-D and B2LYP-dDXDM demonstrate that the C_6/R^6 -dispersion terms are not sufficient to correct B2LYP errors in the EX3 and IDHC sets. Including either higher dispersion terms semiempirically as in B2LYP-dDXDM(c) or adding a fraction of PT2 energy to give B2PLYP-D is crucial for these two test sets. Apart from those, B2LYP-dDXDM6(c) performs similarly to B2PLYP-D, even improving alkane BSE energies. Corrected B2LYP and B3LYP also tend to perform the same. The similarity relies on the fitting procedure used to determine the empirical parameters of both, B3LYP and B2PLYP.

4.6.2 Interaction Energy Profiles

Figure 4.4 shows potential energy curves of complexes typically underbound at the (hybrid-) GGA levels: stacked benzene dimer (a), propane dimer (b), and the benzene complex with wa-

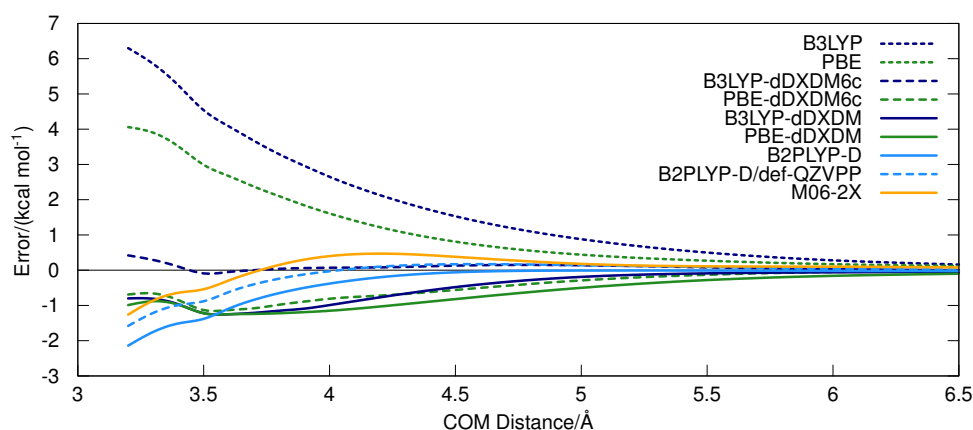


Figure 4.5: Errors (with respect to estimated CCSD(T)/CBS) in DFT interaction energies for the propane dimer.

ter (c) and hydrogen sulfide (d). The hybrid-meta-GGA M06-2X offers substantial improvement for the benzene-H₂S complex but under- and overbinds the stacked benzene dimer conformation and the water-benzene complex, respectively. PBE-dDXDM, B3LYP-dDXDM, and, to a lesser extent, B2PLYP-D overbind all four complexes, while the dDXDM6c correction provides significantly better results for these weakly bound complexes (*vide infra*). Since B2PLYP-D suffers greatly from basis set superposition and incompleteness errors,^{85,163} both B2PLYP-D/aug-cc-pVTZ and B2PLYP-D/def-QZVPP energy curves are reported for the propane dimer. As expected, the accuracy of the energy curve is drastically improved with the large def-QZVPP basis set.

The MAD and mean absolute relative deviation over all 67 points associated with the four potential energy curves are given in Table 4.1. Figure 4.5, on the other hand, displays the error in the propane dimer interaction energy. With the exception of PBE-dDXDM, all dispersion corrected methods have MADs between 0.4 and 0.5 kcal mol⁻¹. PBE-dDXDM6c is the most accurate combination (MAD 0.39 kcal mol⁻¹). The distinctive performance of the current dispersion corrections is further emphasized by the remarkably low error in both the short (i.e., repulsive wall) and long-range of Figure 4.5. Overall, the error range spans between 55% (B3LYP-dDXDM) and 70% (PBE-dDXDM), thereby outperforming M06-2X (75%) and B2PLYP-D (80%) (Table 4.1).

Table 4.1: MAD (in kcal mol⁻¹) and Mean Absolute Relative Deviation (MARD) (in percent) over All 67 Points of Figure 4.4

	MAD	MARD
B3LYP	2.67	357.2
PBE	1.69	222.0
B3LYP-dDXDM6c	0.45	56.8
PBE-dDXDM6c	0.39	58.6
B3LYP-dDXDM	0.49	54.9
PBE-dDXDM	0.59	69.9
B2PLYP-D	0.47	81.8
M06-2X	0.41	75.2

4.7 Conclusions

We have presented an improved scheme for computing system-dependent dispersion coefficients and damping parameters for a dispersion correction to density functional approximations. The dispersion coefficients are evaluated exploiting the XDM formalism of Becke and Johnson^{76–80,187,328} and are distributed among the atoms according to a(n) (iterative)³³⁰ Hirshfeld³³⁵ partitioning. The universal damping function of Tang and Toennies⁷³ is used with a damping factor depending on Hirshfeld (overlap) populations and charges as well as on two adjustable parameters. In addition to the fitted parameters and the density-based information, only free atomic polarizabilities and ionization energies are needed. Hence, the dDXDM correction is applicable to all elements of the periodic table and is easily combined with every density functional. This flexibility permits choosing a functional on the basis of its performance for properties not dominated by weak interactions (e.g., spin states and barrier heights), while still correcting any failures for weak interaction energies. The analysis of 30 (dispersion corrected) density functionals on 145 systems reveals that dDXDM(6c) largely reduces the error of the parent functionals for both inter- and intramolecular interactions. PBE0-dDXDM and PBE-dDXDM are the best performing hybrid-GGA and GGA, respectively, outperforming M06-2X and B2PLYP-D. The use of B3LYP-dDXDM is recommended as well, and it gives the second best overall performance.

5 Overcoming Systematic DFT Errors for Hydrocarbon Reaction Energies

5.1 Introduction

Kohn-Sham density functional theory (DFT)¹¹ is a powerful framework for many aspects of electronic structure theory and has become the preferred method for modeling the energy and structural properties of large molecules. Despite overwhelming popularity, common semilocal and hybrid density functional approximations are affected by well-known deficiencies. In addition to the inability of the most popular exchange-correlation functionals to accurately model long-range (dispersion) interactions in van der Waals complexes,^{13–22} recent studies have also noted failures to describe intramolecular energies in seemingly simple hydrocarbons.^{68,69,71,374}

Alkanes represent the simplest examples of organic molecules for which the energetic description remains challenging for density functional approximations. The accuracy for alkane energies is generally benchmarked through computed heats of formation^{62,375–378} or reaction energies.^{82–84} Disturbing failures have, for instance, been noted for the evaluation of isodesmic bond separation reactions^{82–84} of *n*-alkanes (eq 5.1; Figure 5.1), which are commonly used to determine the total sum of the (de)stabilizing interactions within molecules. In the bond separation equation (BSE) procedure, all bonds between heavy (non-hydrogen) atoms are split into their simplest (or parent) molecular fragments preserving the heavy atom bond types. Reactions are balanced by inclusion of the necessary number of simple hydrides (methane, ammonia, water, etc.). The BSE of propane (eq 5.1) has been used to quantify the 1,3-methyl-methyl stabilizing interaction, 2.83 kcal mol⁻¹, termed protobranching by Schleyer and coworkers.²⁹⁷ Most functionals systematically underestimate the BSE of propane and larger alkanes (Figure 5.1).^{69,347,349}



While the physical origin of the branching stabilization remains uncertain, its roots trace to both Allen's^{379,380} and Pitzer's^{381,382} 1950s studies of alkane stability, where van der Waals type (London dispersion⁹⁸) interactions were invoked to explain the enhanced stability of

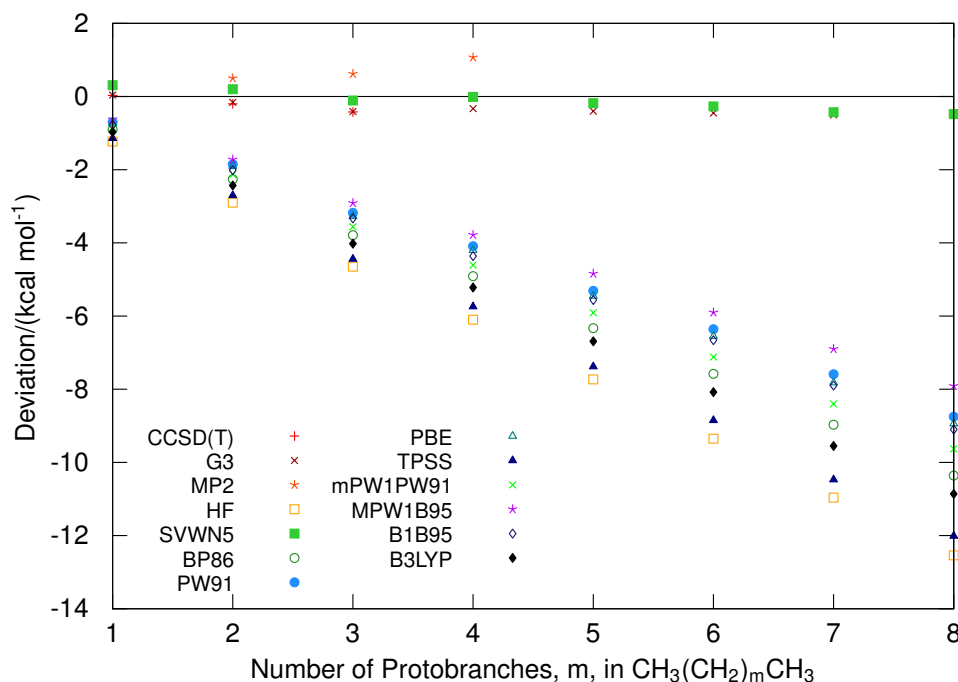


Figure 5.1: Deviations of various DFT functionals from experimental (0K) protobranching stabilization energies. Negative values denote underestimation. Stabilization energies are based on eq 5.1. CCSD(T) and MP2 refer to CCSD(T)/aug-cc-pVTZ//MP2/6-311+G(d,p) and MP2/aug-cc-pVTZ//MP2/6-311+G(d,p), respectively, and include MP2/6-311+G(d,p) zero-point energy corrections. All other computations employed the 6-311+G(d,p) basis set. Data taken from ref 69.

branched over linear species. For this reason, the poor treatment of nonbonded intramolecular interactions between 1,3-disposed methyl/methylene groups has been proposed to explain the failure of standard density functionals.^{72,74,81,85,348,349,383,384}

Numerous related problems have been reported for the computation of hydrocarbon bond energies.^{64–66,385–387} Redfern et al. noted large per bond B3LYP deviations for alkane heats of formation, which grew with increasing alkane size.⁶² Grimme's analysis of the alkane isomerization reactions showed that many density functionals do not reproduce the correct ordering for heats of formation, preferring *n*-alkanes over their more highly branched (and more stable) counterparts.⁶⁸ Feng et al. first noted considerable underestimation of C–C bond energies using B3LYP.⁶⁴ Later, Check and Gilbert showed increasing errors in C–C bond energies as the peripheral hydrogen atoms were replaced with methyl groups, resulting in an error of over 20 kcal mol^{–1} for cleavage of the central C–C in tetramethylbutane.⁶⁵ Note that the cleavage of these C–C bonds necessarily involves changes in the number of 1,3-alkyl-alkyl (protobranching) interactions, thus, similar shortcomings are observed for bond cleavage energies as for alkane BSEs.

Organic systems possessing structural features other than C–C and C–H single bonds are also susceptible to DFT failures. Schreiner and coworkers showed that gradient corrected functionals overstabilize cummulene structures when examining cummulene/acetylene energy differences in small organic compounds.⁶³ Different functionals yielded widely varying energy

differences for sets of hydrocarbon structural isomers (over 40 kcal mol⁻¹ for C₁₂H₁₂).⁶⁷ For the same set of compounds, bond separation reactions give generally smaller errors that increase with the system size.⁷⁰

Over the past decades, the shortcomings of standard semilocal and hybrid density functionals have motivated developments “beyond” the realm of traditional DFT approximations. These more sophisticated and/or more accurate formalisms generally aim at (i) improving the treatment of long-range dispersive interactions, which, by construction, is missing in semilocal density functionals and (ii) reducing the intrinsic self-interaction error,^{24,181,388} generalized to “delocalization error” in many electron systems.^{28,30,190,389} In this chapter, we discuss the current state of density functional approximations for describing energies associated with weak intramolecular interactions present in four test sets featuring hydrocarbons. Our primary focus is to evaluate the performance of the most recent but not widely used DFT methods and test their ability to overcome known deficiencies. The latest functionals are often implemented in developmental versions of codes, frequently unavailable to users. A comprehensive benchmarking of “modern” functionals on the reactions energies of hydrocarbons will not only enable straightforward comparisons of their performance, but also serve to supplement the debate regarding the origin of the DFT errors.^{68,349,390,391} Our classification and applications of “modern” density functionals distinguish “pure” from atom pairwise dispersion corrected density functionals. The “pure” class includes vdW-density functionals (e.g., vdW-DF04¹⁴¹ and VV09^{47,236}), long-range corrected exchange (LC-) functionals (e.g., LC-BLYP,^{349,392} LC-PBE,³⁴⁹ LC- ω PBE,^{393,394} LC- ω PBEh³⁹⁴), and functionals designed specifically to minimize the delocalization errors (e.g., MCY3).¹⁸⁹ For comparisons, this category also includes the increasingly popular highly parameterized hybrid Minnesota functional, M06-2X.²¹⁴ The second class of methods considers Grimme’s B97-D³⁹ and B2PLYP-D,^{85,163} along with our recent density-dependent dispersion correction dDXDM,⁸¹ in which an explicit atom pairwise dispersion correction is added *a posteriori*.

5.2 Computational Methods

5.2.1 Test Sets

The performance of a series of recent functionals (described below) is compared with traditional semilocal and hybrid functionals for four test sets representative of the intramolecular weak interactions in hydrocarbons (Figure 3.2 and 3.3 on page 27). Three of these test sets assess Pople’s isodesmic bond separation equation reactions^{82–84} of alkanes (chains, rings and cages, see Figure 3.2). The geometries and thermal corrections are taken at the B3LYP/6-311+G** level from ref 74,81 except for R14, which has been updated. Reference values are derived from experimental heats of formation.³⁰¹ Whereas the use of these experimental reference data has been disputed,³⁹⁵ our recent density-dependent dispersion correction (dDXDM)⁸¹ was fit to experimental energy differences, which compared well with composite approaches. Note that the general trends and analysis discussed in this work, however,

remain unaffected by the choice of reference values (experimental vs. CCSD(T)/CBS). The “intramolecular dispersion interactions in hydrocarbons” (IDHC)⁸⁵ set contains two isomerization reactions (*n*-octane and *n*-undecane to the fully branched isomer), two folding reactions of large hydrocarbon chains (C₁₄H₃₀ and C₂₂H₄₆), the dimerization of anthracene, and the hydrogenation reaction of [2.2]paracyclophane to p-xylene (Figure 3.3). Geometries and reference values are taken from ref 85. Finally, the geometries and CCSD(T*)-F12a/aug-cc-pVTZ^{121,355} reference values for the methane dimer, used as a model system, are taken from reference 81 and the interaction energy profile completed at the same level using Molpro2009.1.³⁵⁴ SAPT0 computations⁹³ were performed with the aug-cc-pVTZ basis set³⁶³ in Molpro2009.1.

5.2.2 Functionals

The energy data for HF, PBE,¹⁵⁶ PBE0,^{217,280} BP86,^{151,154,332} BLYP,^{154,155} B3LYP,^{161,162} B2LYP, and their dDXDM⁸¹ corrected versions as well as M06-2X,²¹⁴ B2PLYP-D,^{85,163} and B97-D³⁹ are taken from ref 81. Data for SVWN5^{131,149} are taken from ref 74.

LC-BLYP,^{349,392} LC-PBE,³⁴⁹ LC- ω PBE,^{393,394} LC- ω PBEh,³⁹⁴ HFLYP, HFPBE, S,¹³¹ rPW86,^{151,396} B88,¹⁵⁴ PBEx,¹⁵⁶ VV09,^{47,236} and vdW-DF04¹⁴¹ energies are computed with a developmental version of Q-Chem 3.2.³⁶⁸ HSE06^{397,398} computations were performed in Gaussian 09,³⁹⁹ while CAMB3LYP,⁴⁰⁰ rCAMB3LYP,¹⁸⁹ LC-BLYP(0.33), MCY2,¹⁸⁶ and MCY3¹⁸⁹ were computed with a version of CADPAC 6.5,⁴⁰¹ⁱ kindly provided by Aron Cohen. The cc-pVTZ³⁶³ basis set was used for all test sets, but interaction energies for the methane dimer were computed with the aug-cc-pVTZ basis set.

The specificities of the “modern” functionals listed above are briefly summarized below. M06-2X²¹⁴ is a fitted hybrid meta-GGA functional (about 30 parameters), designed to describe main group elements and weak interactions accurately. B97-D³⁹ is a GGA fitted together with the dispersion correction in order to minimize the double-counting of DFT correlation and the empirical dispersion term. The double hybrid B2PLYP-D^{85,163} contains 27% MBPT2 correlation energy, 53% “exact” exchange, and an *a posteriori* dispersion correction. vdW-DF04¹⁴¹ and VV09^{47,236} are two fully nonlocal vdW-density functionals that are supplemented by an exchange and a local correlation functional. There is some freedom in the choice of the exchange component, but functionals that bind van der Waals complexes are obviously unsuitable (revPBE⁴⁰² and recently PW86 refits^{151,396} are popular options). The PW92¹⁵⁰ parameterization is usually chosen for the local correlation.

LC-BLYP, LC-PBE, LC- ω PBE, and LC- ω PBEh are long-range corrected exchange functionals (labeled LC or LCR): the long-range is described by “exact” exchange and the short-range by semilocal DFT exchange (eq 5.2). In the range-separation scheme, pioneered by Savin et al. for combining multi-determinantal methods with DFT approaches,^{193,194} the electron repulsion operator $\frac{1}{r_{12}}$ is partitioned into two ranges (long and short) with the most common choice

ⁱif functions were omitted in CADPAC computations of the anthracene dimerization and the folding of C₂₂H₄₆ for technical reasons.

being an Ewald-style partition based on the error function

$$\frac{1}{r_{12}} = \underbrace{\frac{\text{erfc}(\mu r_{12})}{r_{12}}}_{\text{SR}} + \underbrace{\frac{\text{erf}(\mu r_{12})}{r_{12}}}_{\text{LR}} \quad (5.2)$$

where the μ parameter is selected empirically and controls the definition of the two ranges (for other forms of eq 5.2 see ref 193,403–406). The LC scheme is motivated by the incorrectly decaying potential of standard DFT functionals (the xc potential of semilocal functionals decays exponentially along with the density, while the asymptotic form of the exact potential is $-1/r$). Applying the range separation and introducing HF exchange for the long-range corrects this error. The “long-range” is considered especially important in the asymptotic region (i.e., surface) of molecules. Given a GGA or hybrid functional, the corresponding LRC functional is

$$E_{xc}^{\text{LRC}} = E_c + (1 - C_{\text{HF}})E_{x,\text{GGA}}^{\text{SR}} + C_{\text{HF}}E_{x,\text{HF}}^{\text{SR}} + E_{x,\text{HF}}^{\text{LR}} \quad (5.3)$$

The components labeled “LR” and “SR” are evaluated using the long- and short-range Coulomb potential, respectively, while C_{HF} denotes the coefficient of the HF exchange present in the original functional ($E_{x,\text{HF}}$). Hybrid LRC functionals therefore contain some fraction of short-range HF exchange, but all LRC (CAMB3LYP excluded) functionals contain full HF exchange in the long-range limit (eq 5.3). The construction of the short-range exchange functional ($E_{x,\text{GGA}}^{\text{SR}}$) requires an expression for the exchange hole, which is readily available for LDA, but not immediately accessible for most semilocal GGAs. The LC schemes thus mostly vary by the construction of the short-range functional. An illustrative example is PBE, for which four short-range parameterizations exist in the literature ranging from using a pseudo-LDA exchange hole⁴⁰⁷ (LC-PBE), applying the range separation to the enhancement factor (sr-PBE or μ -PBE),⁴⁰⁸ taking the model PBE exchange hole⁴⁰⁹ (LC- ω PBE)⁴¹⁰ or using a more general exchange hole³⁹³ parameterized to reproduce PBE-results (called LC- ω PBE as well or LC- ω PBE08 to distinguish the two).³¹³ HSE06,^{397,398} which has been motivated mainly for use in solid state computations, is a screened hybrid that is the inverse of a long-range corrected exchange functional: the short-range is described by “exact” exchange and the long-range by semilocal DFT exchange, which avoids the computationally expensive full-range “exact” exchange. CAMB3LYP⁴⁰⁰ uses a different partitioning than eq 5.3, but can be seen as an extension of LC-BLYP (similar to the B3LYP extension to BLYP) fitted to atomization energies, ionization potentials, and total atomic energies, by varying the fraction of global and long-range “exact” exchange. rCAMB3LYP¹⁸⁹ is a re-parameterization of CAMB3LYP containing about twice the amount of the long-range corrected exchange and aims to improve the fractional charge behavior of a carbon atom. MCY2¹⁸⁶ was constructed to be one-electron self-interaction free and to give good thermochemistry and reaction barriers, while MCY3¹⁸⁹ uses long-range corrected exchange components and has been, akin to rCAMB3LYP, fitted to improve the fractional charge behavior. Finally, LC-S-vdW-DF04 and LC-S-VV09⁴⁷ pair the long-range corrected Slater exchange with the fully nonlocal vdW-density functionals with (i.e., VV09⁴⁷) or without (i.e., vdW-DF04¹⁴¹) refitting the long-range separation parameter.

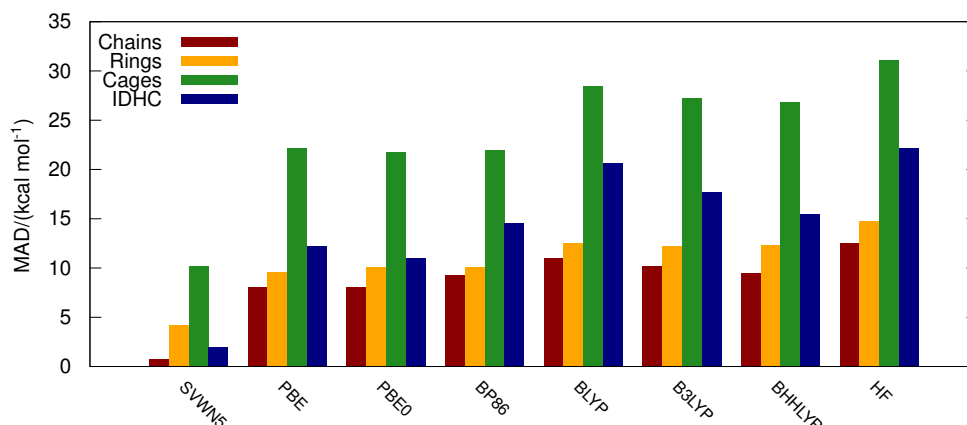


Figure 5.2: Performance for standard functionals: Mean absolute deviations for bond separation energies over hydrocarbon chains, rings and cages, and for reaction energies of the test set “intramolecular dispersion interactions” (IDHC) using the cc-pVTZ basis set

Very recently we introduced a dispersion correction⁸¹ that combines Becke and Johnson’s exchange hole dipole moment (XDM) formalism^{76–80,187,328} with an extended Tang and Toennies damping function,⁷³ in which the damping parameter depends on atomic (overlap) populations. For details, we refer to Chapter 4.

5.3 Results and Discussions

5.3.1 General Performance

Simple (closed shell molecules) hydrocarbon reactions such as Pople’s bond separation equations (BSEs) of linear alkanes (chains), cycloalkanes (rings), or cages (such as adamantane) show highly characteristic and systematic DFT errors⁶⁹ (see Figure 5.2) of the same magnitude as HF (except for SVWN5). SVWN5 outperforms all the others common density functionals for alkane reaction energies (*vide infra*).

With the exception of SVWN5 (LDA), the contrast between “standard” (Figure 5.2) and “modern” density functionals (Figure 5.3) is striking, with the average mean absolute deviation (MAD) over the four test sets being 40% lower for the latter ($\text{MAD}(\text{standard}) = 13.3 \text{ kcal mol}^{-1}$, $\text{MAD}(\text{modern}) = 7.7 \text{ kcal mol}^{-1}$). Two general tendencies emerge from the comparisons between Figure 5.2 and 5.3: (i) the inclusion of long-range corrected exchange energy terms improves the general performance, while the incorporation of a fraction of global exchange does not and (ii) the accurate treatment of weak interactions is essential. The most illustrative examples are the superior performance of LC-BLYP0.33 ($\text{MAD} = 5.5 \text{ kcal mol}^{-1}$) and of the VV09-based functionals, rPW86-VV09 and LC-S-VV09 (MAD of 5.8 and 3.6 kcal mol^{-1} , respectively). On the other hand, the remarkable performance of the hybrid meta-GGA, M06-2X ($\text{MAD} = 5.6 \text{ kcal mol}^{-1}$) highlights the valuable success of semiempirical fitting for improving the performance of standard DFT approximations.

Inconveniently, the approaches that are best for general thermochemistry (i.e., atomization

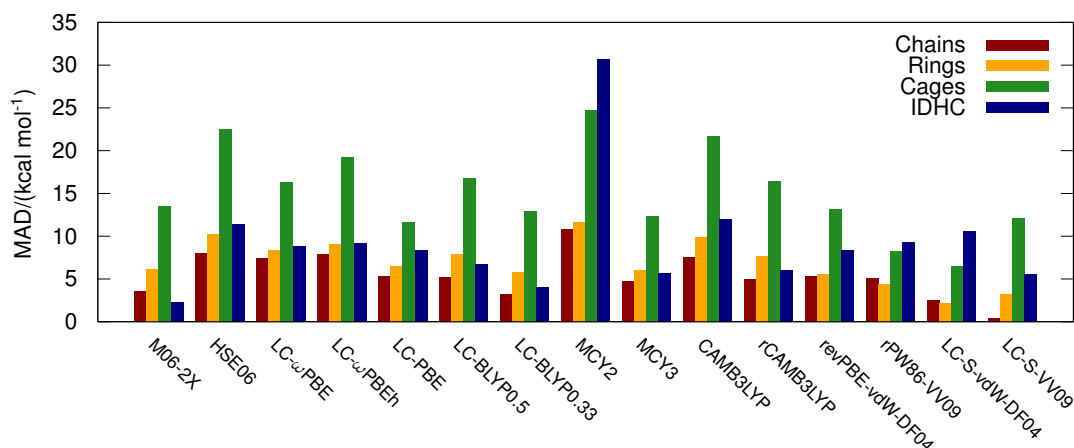


Figure 5.3: Performance for “modern” functionals: Mean absolute deviations for bond separation energies over hydrocarbon chains, rings and cages, and for reaction energies of the test set “intramolecular dispersion interactions” (IDHC) using the cc-pVTZ basis set

energies and barrier heights) tend to perform worst for the weak intramolecular interactions discussed herein, and *vice versa*. For instance, the inclusion of global HF exchange in conjunction with the long-range exchange correction (i.e., (r)CAMB3LYP and LC-ωPBEh) increases the MADs for each of our individual sets when compared to the “pure” long-range corrected exchange functional (e.g., MAD = 9.9 and 9.0 kcal mol⁻¹ for LC-ωPBEh and LC-ωPBE, respectively). These results contrast with other thermochemical properties for which the additional empirical parameter associated with the fraction of “exact” exchange improves the functional performance.^{394,400} Similarly, the LC-BLYP long-range separation parameter optimized for atomization energies (0.5),^{349,411} is significantly less accurate (MAD(0.5) = 7.8 kcal mol⁻¹) than LC-BLYP0.33 (MAD(0.33) = 5.5 kcal mol⁻¹),³⁹² which has been shown to give considerably lower delocalization errors,^{28,189} but poor atomization energies.⁴⁰⁰ MCY3 (MAD = 6.3 kcal mol⁻¹), which has been designed to minimize the delocalization error and benefits from the inclusion of long-range corrected exchange energy terms and from the same parameterization as rCAMB3LYP¹⁸⁹ also performs very well for our test sets, but less satisfactory for general thermochemistry.¹⁸⁹ This performance contrasts with MCY2 (MAD = 15.6 kcal mol⁻¹, full-range “exact” exchange, one-electron self-interaction free), which has been parameterized against “general” thermochemistry and gives poor results for weak intramolecular interactions. Screened hybrid density functionals, which perform similar to PBE0 for thermochemistry,⁴¹² also do not outperform the LC-functionals in the presently studied cases (e.g., MAD HSE06 = 11.0 kcal/mol). The sets tested herein seemingly benefit from a later switching to the long-range interactions in exchange, but at this stage, no simple rationalization is possible as it is not unequivocally clear from where the improvement arises. In a recent study, Tsuneda and coworkers claimed that the lack of long-range interactions in exchange functionals is the major cause for the underestimation of alkane isodesmic reaction energies,³⁴⁹ but this on-going question^{68,349,390,391} will be thoroughly discussed in the next section.

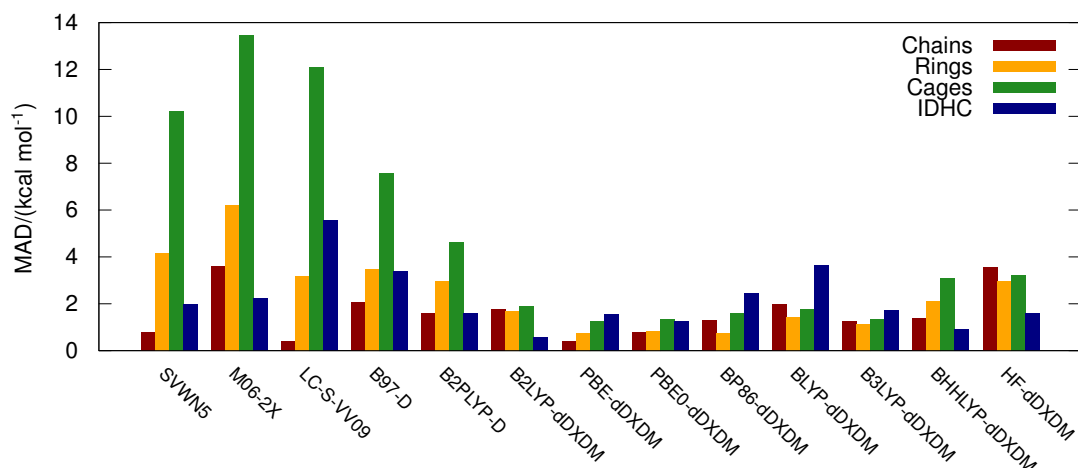


Figure 5.4: Performance for dispersion corrected functionals: Mean absolute deviations for bond separation energies over hydrocarbon chains, rings and cages, and for reaction energies of the test set “intramolecular dispersion interactions” (IDHC) using the cc-pVTZ basis set. SVWN5, M06-2X, and LC-S-VV09 are shown for comparison with Figure 5.2 and 5.3

A much less debated origin for these DFT errors is the absence of nonlocal correlation effects to account for long-range intramolecular interactions such as dispersion.⁴¹³ This dependency is demonstrated by the good performance of the vdW-density functionals such as revPBE-vdW-DF04 and rPW86-VV09 (MAD = 6.8 and 5.8 kcal mol⁻¹, respectively). Combining VV09 with a LC-functional, as suggested in ref 47, further stabilizes the hydrocarbons (MAD = 3.6 kcal mol⁻¹). LC-S-vdW-DF04 performs similarly (MAD = 4.0 kcal mol⁻¹). The relevance of such combinations has also been demonstrated for rare-gas dimers and other systems.^{227,228,414–417} An alternate and computationally cheaper solution to the intramolecular dispersion problem is to add a damped, atom pairwise energy correction to the standard DFT energy as originally proposed by Wu and Yang³⁸ and others.^{22,240,241} Our recently introduced system-dependent dispersion correction (dDXDM), based on Becke and Johnson’s exchange hole dipole moment formalism, has been shown to reduce both these “intramolecular errors” as well as the errors on typical (intermolecular) van der Waals complexes.⁸¹ Figure 5.4 illustrates the performance of dDXDM along with that of the popular B97-D and B2PLYP-D.^{39,85} Note that Grimme’s latest DFT-D3 correction⁴² is not considered herein, but its performance on isodesmic reactions for linear alkane chains has been demonstrated in ref 391. The success of dDXDM is due to a flexible, density-dependent, damping function that adapts well to a given functional (*vide infra*) together with accurate, density-dependent dispersion coefficients. To enable comparisons with Figure 5.3, the best performing “standard” and “modern” functionals (SVWN5, MAD = 3.4 kcal mol⁻¹, M06-2X, MAD = 5.6 kcal mol⁻¹ and LC-S-VV09, MAD = 3.6 kcal mol⁻¹) are included in Figure 5.4.

The explicitly dispersion corrected functionals outperform the best functionals tested in Figure 5.3, LC-BLYP0.33 and LC-S-VV09. In particular, PBE-dDXDM and PBE0-dDXDM (MAD = 0.8 and 0.9 kcal mol⁻¹, respectively) give the best results with respect to experiment. The dDXDM correction also lowers the error, which generally increases considerably going from chains, to

rings, to cages. B2LYP-dDXDM (same functional contributions as in B2PLYP, but without PT2 correlation energy) is not intended for real world applications, but provides insights into the good performance of B2PLYP-D. dDXDM alone is able to reproduce the combined role of the PT2 energy and the empirical dispersion correction for the present test sets.

The main outcome resulting from this preliminary investigation of the general performance of various functionals is (i) accounting for dispersion interactions is indispensable, (ii) the improved treatment of “medium-range correlation” decreases the errors significantly (e.g., M06-2X), and (iii) a long-range corrected exchange improves performance. Whereas (i) can be efficiently solved by the use of a dispersion correction that offers an attractive alternative to the computationally more expensive nonlocal vdW functionals, the importance of the exchange is uncertain.^{68,349,390,391} In the next section, we analyze the errors for these simple systems in greater detail to shed greater light on the origin of the DFT failures.

5.3.2 Detailed Analysis of the Functional Performance

Our recent dispersion corrections, which are calibrated on alkane reaction energies,^{72,74} aimed at accounting for “intramolecular errors” efficiently, without deteriorating the long-range dispersion interactions. Interestingly, our empirical dispersion energy corrections^{72,74} show a minimum between 2.3 and 2.6 Å for the carbon···carbon interaction (see Figure 3.1 on page 25), a distance that corresponds roughly to the 1,3 C···C distance in propane (2.536 Å).³⁶¹ This distance range is also similar to the compressed methane dimer as originally chosen by Yang and coworkers¹⁹⁰ as a model for probing delocalization errors^{28,190,389} in Diels-Alder reaction energies. Comparisons between the errors in our test sets with those of the methane dimer interactions at the highly repulsive distance of 2.4 Å and at the equilibrium distance²⁹⁹ is instructive, as a correlation would be indicative of a common source of error.

The correlation of MADs is vastly superior with the error in the repulsive methane interaction (Figure 5.5b) than with the error at the equilibrium distance (Figure 5.5a). The poorer correlation between the errors in our test sets and the methane interaction at the equilibrium distance is in line with the strongly varying results given by the density functionals for describing vdW-interactions.^{17,205,418} The treatment of long-range dispersion is missing, and the various performances strongly depend on the high-reduced density gradient $s \propto \frac{|\nabla\rho|}{\rho^{4/3}}$ (low density, high gradient) behavior of the exchange functional. As demonstrated hereafter, the situation differs drastically in the repulsive range, which is more adapted to the description of branching in alkanes and compact hydrocarbons (e.g., anthracene dimer). M06-2X gives small errors for both the methane interaction and the IDHC test set. The errors are the largest for the BSE of the alkane cages, which result in a large y-axis intercept for this series. We suggest that the non-zero intercept is due to the missing long-range dispersion that can, by no means, be recovered by a local functional (not even by extensive fitting like in M06-2X) and that increases with system size. Figures 5.7 and 5.6 give valuable insights on the improved performance of PBE0 when compared to its parent ingredients, HF and PBE, which both overestimate the repulsion of the compressed methane dimer. PBEx is considerably more repulsive than HF in the highly repulsive region modeled by the compressed methane dimer (Figure 5.7)!

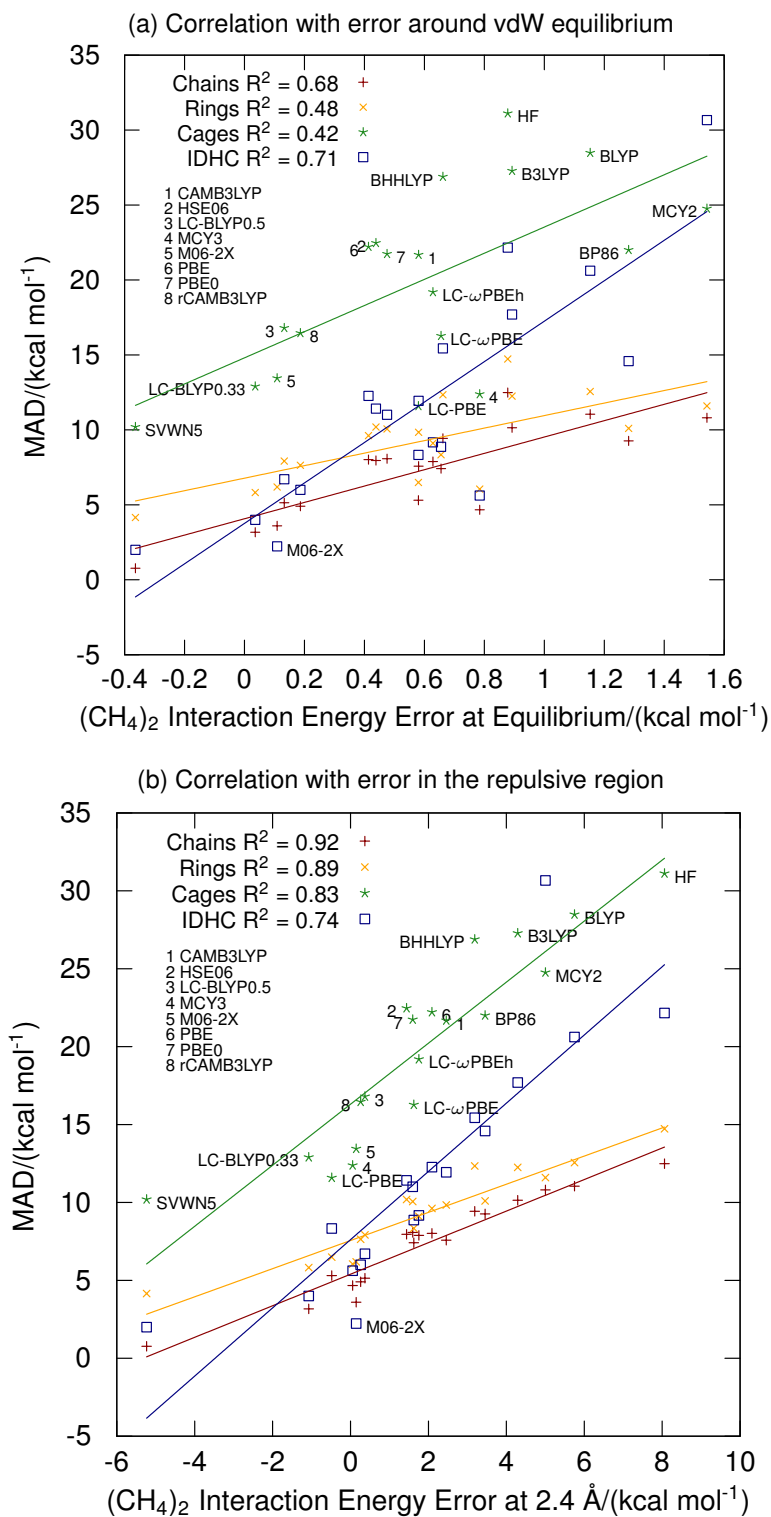


Figure 5.5: Correlations of “standard” and “modern” functionals between the methane interaction energy and the mean absolute deviations for, bond separation energies over hydrocarbon chains, rings and cages, and for reaction energies of the test set “intramolecular dispersion interactions” (IDHC)

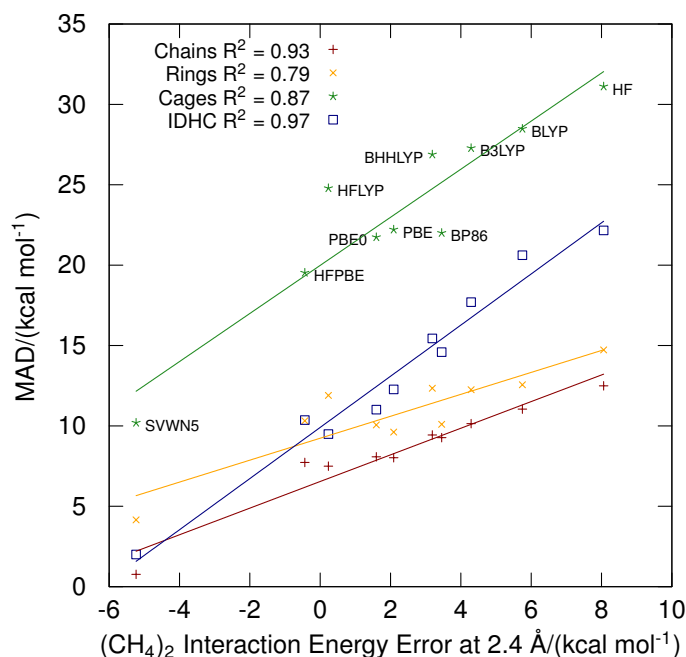


Figure 5.6: Correlations of “standard” semilocal and hybrid density functionals between the methane interaction energy and the mean absolute deviations for, bond separation energies over hydrocarbon chains, rings and cages, and for reaction energies of the test set “intramolecular dispersion interactions” (IDHC)

Whereas density functionals do not reproduce the repulsive wall of rare-gas dimers, most studies have focused on the slightly repulsive region, where exchange-only computations give various trends from too soft (e.g., PBEx) to too repulsive (e.g., B88).^{17,325,396,418} One thus argues that in the highly repulsive range, the improved performance of PBE0 compared to PBE is due to the smaller amount of overly repulsive PBE exchange (75% instead of 100%) in favor of the HF exchange. The improvement compared to HF is obviously due to the correlation functional. In line with Brittain et al.,³⁹⁰ the more accurate interactions given by HF exchange together with PBE correlation, HFPBE, corroborate this interpretation. This reasoning in terms of over-repulsive semilocal DFT exchange is, however, only valid for nonbonded interactions and not for semilocal DFT exchange treatments of covalent bonds.³²⁸ HF supplemented with semilocal correlation is, of course, not recommended for general purposes. The present interpretation of the overly repulsive nature of standard DFT exchange functionals at compressed distances are also responsible, potentially, for the “surprising and somewhat alarming” larger errors recently noticed by Hobza and coworkers⁴¹⁹ for noncovalent energy computations of the compressed S22 geometries when compared to those at equilibrium (0.9 shift when compared to the equilibrium distance). At the equilibrium, PBE exchange is, on the contrary, under-repulsive. Thus, the combination of HF exchange with standard semilocal DFT cor-

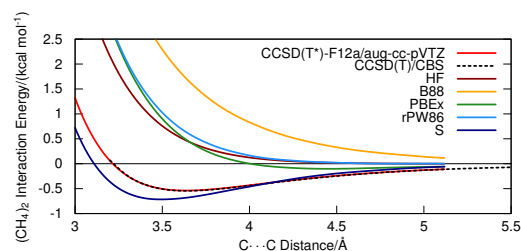


Figure 5.7: Methane dimer interaction profiles for exchange-only computations. CCSD(T*)-F12a/aug-cc-pVTZ serves as a reference for the true interaction energy. The corresponding CCSD(T)/CBS benchmark values are also shown for the region considered in ref 360

relation worsens the description of vdW-complexes²⁰ (e.g., HFPBE error at the equilibrium is in between HF and PBE). To a lesser extent, similar trends are observed for the BSE of the alkane cages and the IDHC test set (i.e., highly branched and compact system), whereas the alkane chains and rings (less branching, not as compact) remain weakly affected by the incorporation of global exchange. The improved performance of the LC-functionals for all our test sets and the compressed methane dimer illustrate, somewhat, that the description of nonbonded interactions in the increasingly repulsive range benefits more from having full HF exchange at the surface of the molecule (in the long-range) than from containing some fraction of HF exchange at all ranges or full HF exchange at the short-range (e.g., screened hybrid functionals). As demonstrated by Yang and coworkers, the overly repulsive nature of the functional at compressed distances decreases considerably if the delocalization error is reduced (e.g., MCY3).

Table 5.1: Interaction Energy Contributions for the Methane Dimer at Equilibrium (C...C Distance = 3.7 Å) and a Repulsive Distance (C...C Distance = 2.4 Å), Computed with SAPT0 Using the aug-cc-pVTZ Basis Set. CCSD(T*)-F12a/aug-cc-pVTZ is Given as a Reference. All Values in kcal mol⁻¹

	Repulsive methane dimer	Equilibrium distance
$E_{\text{pol}}^{(1)}$	-14.11	-0.14
$E_{\text{exch}}^{(1)}$	45.55	0.53
$E_{\text{ind}}^{(2)}$	-11.17	-0.06
$E_{\text{ind-exch}}^{(2)}$	9.82	0.06
$E_{\text{disp}}^{(2)}$	-13.14	-0.98
$E_{\text{disp-exch}}^{(2)}$	2.99	0.07
$E_{\text{el}} = E_{\text{pol}}^{(1)} + E_{\text{exch}}^{(1)}$	31.44	0.39
$E_{\text{ind}}^{(2)} + E_{\text{ind-exch}}^{(2)}$	-1.35	0.00
$E_{\text{disp}}^{(2)} + E_{\text{disp-exch}}^{(2)}$	-10.15	-0.91
E_{tot}	19.94	-0.52
HF (BSSE corrected)	29.21	0.37
δHF	-0.88	-0.02
CCSD(T*)-F12a	21.11	-0.53

Apart from the exchange functional, correlation and especially dispersion play a major role in these errors, as confirmed by the dramatic improvement obtained when accounting for dispersion interactions.^{72,74,81,85,348,349,383} We here distinguish long-range dispersion from “overlap” dispersion (that is shorter-range dispersion in the region of overlapping density, partially accounted for by semilocal functionals), both of which accumulate with system size. The notion of “overlap” dispersion is in line with a recent DFT study of the description of water hexamer interactions that recover a large part of the dispersion energy, dominated by the short-range.⁴²⁰ It is also closely related to Grimme’s “overlap dispersive” interactions.²⁹⁸ We, however, regard “overlap” dispersion as a particular case of medium-range correlation^{68,384} and not as an alternate terminology.⁴² The importance of dispersion interactions is directly illustrated by the Hartree-Fock error for the compressed methane dimer (8.1 kcal mol⁻¹).

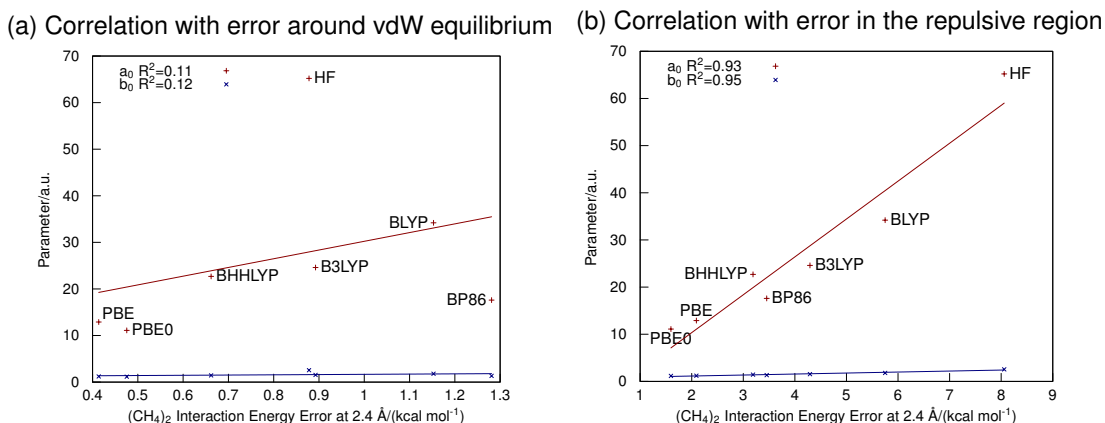


Figure 5.8: Correlation between best fit a_0 and b_0 values for dDXDM against the absolute interaction energy error for the uncorrected functional of the methane dimer at equilibrium and a compressed distance.

The individual contributions to the energy interaction of the methane dimer are analyzed in Table 5.1 by symmetry adapted perturbation theory (SAPT0).⁹³ The difference between HF and SAPT first-order interaction energies plus second order induction (-exchange) is given by δHF .^{421,422} The HF error exactly matches the second order dispersion energy. However, note that SAPT does not distinguish between “long-range” and “overlap” (i.e., shorter-range) dispersion that are, to a certain extent, captured by the DFT correlation functionals. At the highly repulsive distance, the correlation functional accounts for some “overlap” dispersion (due to overlapping density, see HFPBE and HFLYP large improvement when compared to HF in Figure 5.6), but there are severe shortcomings (over-repulsive) in the exchange functional. In line with the compressed methane dimer, the IDHC test set and the BSEs of branched alkanes (cages > rings > chains) follow the same interpretation regarding the origin of the DFT errors. The error at the equilibrium distance is, however, interpreted in terms of the missing dispersion that can be compensated by an under-repulsive semilocal DFT exchange (e.g., PBE). The good overall performance of SVWN5 for alkane BSEs is easily explained by error compensation between the short-range (overly attractive) and the missing long-range weak interactions. It has also been explained in terms of the surface energies¹⁵³ (LDA inherently favors compact over extended systems, and thereby correctly describes alkane branching).

Given that the dDXDM correction efficiently reduces the MADs of our test sets, it is reasonable to expect a correlation between the parameters adjusting the dispersion correction for a given functional and the error in the methane dimer interaction energies for the parent functional (see Figure 5.8). dDXDM contains only two fitted parameters: a_0 , which controls how fast the correction decays to zero for short interatomic distances and b_0 , which determines the strength of the correction at intermediate distances (i.e., in the medium-range).

The physical interpretation of the good correlation for b_0 in Figure 5.8b is straightforward: the higher the b_0 value, the stronger the dispersion correction at intermediate distances. At long ranges, the damping vanishes exponentially and b_0 becomes unimportant. At short ranges, the second damping function, with the steepness a_0 , dominates: $a_0 = 0$ turns off the additional

damping and restores the “conventional” Tang and Toennies damping, whereas $a_0 = \infty$ turns off the entire dispersion correction. Intermediary, the additional damping responds to b_0 . A high b_0 value means large dispersion terms at short (even covalent) internuclear distances that are prevented by increasing a_0 . For a given density overlap, a high a_0 value turns down the TT-dispersion correction more than a low a_0 . This behavior justifies the poorer performance of dDXDM when combined with highly repulsive functionals such as BLYP (or HF) when compared to softer functionals, such as PBE or even B3LYP. The high b_0 values required for correcting the medium-range increases a_0 as well, thereby diminishing the dispersion correction at distances with considerable density overlap whether the overlap is bonding or not. dDXDM is, nevertheless, a powerful dispersion correction, as even HF and BLYP are improved to an extent that they compete with M06-2X. The fact that dDXDM benefits from the “overlap dispersion” intrinsic to the DFT functional advises against combining the dDXDM with the dispersionless functional of Pernal et al.⁵¹

5.4 Conclusions

The benchmarking of “modern” density functionals for overcoming common DFT errors in hydrocarbon reaction energies provides valuable insight into the origin of the errors given by traditional semilocal and hybrid density functionals. The most illustrative example for these shortcomings is the large B3LYP energy underestimation ($\text{MAD} = 14.1 \text{ kcal mol}^{-1}$) over four test sets of hydrocarbons featuring weak intramolecular interactions. Our comprehensive analysis demonstrates that for increasingly branched alkanes and most compact hydrocarbons, the “intramolecular errors” strongly correlate with the error for the compressed methane dimer interaction energy. At these compressed distances, the shortcomings can be partially attributed to the general overly repulsive nature of semilocal exchange in the treatment of nonbonded density overlaps. The significant improvement offered by the long-range corrected exchange functionals stems from the substitution of the long-range DFT exchange by a less repulsive “exact” exchange (e.g., LC-BLYP0.33, $\text{MAD} = 5.5 \text{ kcal mol}^{-1}$). The overly repulsive nature of the semilocal DFT exchange at compressed distances sharply contrasts with the various trends (e.g., PBEx under-repulsive to B88 over-repulsive) characteristic of the near equilibrium region. Our study also emphasizes the essential role played by the correlation functional for lowering the error of these hydrocarbon reactions. At regions of nonbonded density overlap, the correlation functionals account for a non-negligible extent of “overlap dispersion” (Figure 5.6). Improving the treatment of long-range dispersive interactions leads to enhanced performances, as illustrated by both the impressive results of the nonlocal van der Waals density functionals (e.g., rPW86-VV09, $\text{MAD} = 5.8$ and LC-S-VV09, $\text{MAD} = 3.6 \text{ kcal mol}^{-1}$) and the atom pairwise density-dependent corrected PBE (e.g., PBE-dDXDM, $\text{MAD} = 0.8 \text{ kcal mol}^{-1}$). The overall repulsive nature of the functionals for treating these weak intramolecular interactions also decreases considerably if the delocalization error is reduced (e.g., MCY3, $\text{MAD} = 6.3 \text{ kcal mol}^{-1}$) or by developing improved and flexible hybrid meta functional forms coupled with careful parameter fitting (e.g., M06-2X, $\text{MAD} = 5.6 \text{ kcal mol}^{-1}$).

6 A Generalized Gradient Approximation Exchange Hole Model for Dispersion Coefficients

6.1 Introduction

The accurate computation of atomic dispersion coefficients is of fundamental importance in view of the role weak interactions play in many energetic and structural phenomena (e.g., stacking of nucleic acid in DNA, proteins folding, adsorption of molecules on surfaces). Despite being the most widely used tools for molecular properties computations, standard semilocal and hybrid density functional approximations are known to neglect long-range dispersion interactions.¹⁴ The damped atom pairwise additive London dispersion⁹⁸ expression is highly valuable for introducing weak long-range attraction in molecules and soft-matter, at minimal computational cost.^{38,39} A significant shortcoming associated with fixed empirical coefficients³⁹ is the lack of dependency on the electronic structure. In contrast, fully nonlocal (van der Waals) functional formulations^{47,109,141} contain at most one empirical coefficient, but suffer from a high computational cost. The derivation of accurate atomic dispersion coefficients dependent on the molecular environment represents an attractive alternative. The first general approach, devised by Becke and Johnson (BJ),⁷⁶ uses the exchange hole dipole moment (XDM) and free atomic polarizabilities to model dispersion coefficients. The method of Sato et al.,^{45,46} based on local response theory, eliminates the dependence on free atomic polarizabilities with a moderate increase in computational demand. The C₆-only (excluding higher terms, such as C₈ and C₁₀) scheme of Tkatchenko and Scheffler⁴⁴ relies on a simple rescaling (depending on the “size of the atoms in molecules”) of free atomic C₆ coefficients to determine accurate molecular dispersion coefficients. Grimme et al.,⁴² proposed an approximation (e.g., no dependence on the molecular charge) in which geometry-dependent dispersion coefficients are interpolated from tabulated values.

In this study, we introduce a substantial reformulation of the XDM utilized by Becke and Johnson^{75,77,78,80} that is rooted in a simple generalized gradient approximation (GGA) exchange hole model. In addition, we address the conceptual discrepancy existing between the multipole-expansion (on the basis of an atom pairwise dispersion correction⁹⁸) and the

overlapping atoms in molecules (AIMs) used in practical schemes.⁴²³ Whereas the multipole-expansion relates to a set of disjoint interacting fragments, commonly used density-dependent schemes compute atomic dispersion coefficients from partitioning functions involving overlapping AIMs (e.g., Hirshfeld³³⁵ or Mayer’s fuzzy atoms³⁴⁴). This issue was recently discussed by Angyan, who invoked electron localization domains as optimal partitions of the molecular space for the multipole-expansion (as opposed to the commonly used atomic domains).⁴²³ A more pragmatic solution, which consists of assigning each point in space to the atom carrying the highest weight, is shown herein to yield results competitive with the overlapping approach.

6.2 The Exchange Hole Model

The BJ XDM model relies on the idea that the dipole arising from an exchange hole and its reference electron is related to the fluctuating dipole moments responsible for dispersion. The original BJ implementation,^{75,78} based on the “exact” exchange hole XDM(XX), is generally both more demanding computationally and less accurate than that based on the Becke and Roussel exchange hole formulation,¹⁶⁰ i.e., XDM(BR).³²⁶

The BR-exchange hole is a rather simple and formally attractive model represented by a spherically averaged Slater-type function.¹⁶⁰ The two free parameters, the exponent a and b , the distance from the reference electron, are determined by imposing the condition that the spherical average of the Taylor expansion of the model exchange hole reproduces that of the “exact” exchange hole at each reference point up to second order. The second order term depends on both the Laplacian ($\nabla^2 \rho$) and the local kinetic density ($\tau = \sum (\nabla \psi)^2$) and is therefore responsible for the largest computational cost of XDM(BR).

Imposing that the exchange hole density at the reference point is exactly the same as the electron density (exact on-top density value) yields the following constraint on a and b for the zeroth order Taylor expansion term (applied separately to the α - and β -spin)

$$b^3 = \frac{(ab)^3 e^{-ab}}{8\pi\rho} = \frac{x^3 e^{-x}}{8\pi\rho} \quad (6.1)$$

Building a XDM model solely based on the local density and its gradient (i.e., GGA-type) can considerably reduce the numerical complexity. In the gradient expansion, the exchange hole is implicitly assumed to be spherically symmetric around the reference electron. For inhomogeneous densities, however, the true exchange hole is not spherically symmetric around this point. To overcome this deficiency and provide the possibility of yielding an exchange hole that is localized far away from the reference electron, Bahmann and Ernzerhof recently introduced an explicitly asymmetric GGA exchange hole model.⁴²⁴ Their model offers a smooth interpolation between the spherically symmetric local density approximation exchange hole and a non-centrosymmetric modified Becke-Roussel exchange hole depending on the reduced density gradient. The extent of asymmetry is determined by imposing the exact on-top density value and by ensuring that the Perdew-Burke-Ernzerhof (PBE) exchange-energy density is recovered. Whereas such an exchange hole, along with other recent GGA exchange

hole models,^{393,409,425} is aimed at deriving improved energy functionals, we here propose a pragmatic GGA-type expression to model the exchange hole dipole moment. For homogenous densities, the exchange hole has a spherical symmetry and the distance between the center of the exchange hole and the reference electron, b , has to be zero. Our ansatz makes use of the simplest possible dependence of x (in eq 6.1) on the reduced density gradient ($s = \frac{|\nabla\rho|}{2 \cdot (3\pi^2)^{1/3} \cdot \rho^{4/3}}$ which serves as a measure for the inhomogeneity of the electron density) that satisfies this constraint: $x = C \cdot s$, where C is a constant. Using the definition of the Wigner-Seitz radius ($r_s = \sqrt[3]{\frac{3}{4\pi\rho}}$) and reorganizing gives

$$\frac{b}{r_s} = \frac{C}{6^{1/3}} s \cdot e^{-\frac{1}{3}C \cdot s} \quad (6.2)$$

Equation 6.2 has the form of a non-normalized convolution of two exponentially decaying functions ($f(x) = \lambda^2 x e^{-\lambda x}$ is the corresponding normalized distribution function). C controls the sharpness of the distribution. For enhancing the flexibility of the GGA-exchange hole dipole moment, the constraint of the exact on-top density is relaxed by introducing two uncoupled parameters A and B

$$\frac{b}{r_s} = A \cdot s \cdot e^{-B \cdot s} \quad (6.3)$$

Equation 6.2 is recovered, if $A = \sqrt[3]{9/2} \approx 1.65B$. Equation 6.3 ensures, however, that the XDM is zero for the uniform electron gas. Unlike recent modified BR GGA exchange holes,^{424,425} the presented model retains the Slater exponential form.

The two empirical parameters A and B are fitted to reproduce C_6 -dispersion coefficients of rare gas homodimers (He, Ne, Ar, and Kr) (ref 426) separated by 20 Å (to avoid any dependence of the fit on the partitioning method). The resulting parameters ($A = 2.018$, $B = 0.974$) are close to integer values and are thus set to $A = 2$ and $B = 1$. The exchange hole dipole moment, b , depending only on the reduced density and its gradient, is then inserted into BJ's expressions (see Equations 4.6-4.8, page 37). Note that the deviation from the anticipated A/B ratio (1.65, *vide supra*) supports the view that eq 6.3 models an exchange-correlation rather than of an exchange hole.^{423,427}

6.3 Atomic Partitioning

We combine the proposed s -dependent dispersion coefficients (C) simplification of the BR model (sC-BR, eq 6.3) with three different partitioning schemes: the iterative Hirshfeld (HI),³³⁰ which is the rigorous extension of the classical scheme (HC)³³⁵ based on self-consistently optimized atomic charges (advantageous for ionic systems, see ref 330 for details); the iterative Hirshfeld-dominant (HID)⁴²⁸ and the classical Hirshfeld-dominant (HCD) partitioning. In line with a disjoint description of AIMS,⁴²⁸ the last two schemes analyze the Hirshfeld weights at each grid point setting the weight of the "dominant" atom to 1.0, and all others to zero.

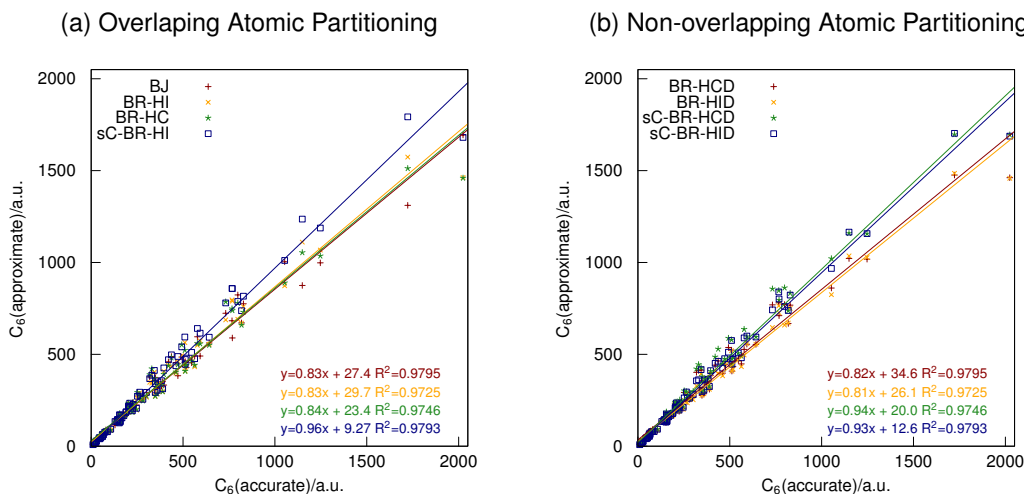


Figure 6.1: Approximate C_6 dispersion coefficients for 90 molecular complexes correlated to accurate dipole oscillator strength distribution reference values (taken from ref 76). Three different XDM schemes are tested: (a) the original BJ (= XX) data (from ref 76), Becke-Roussel along with classical (BR-HC)^{77,87,329} or iterative (BR-HI)⁸¹ Hirshfeld partitioning, and the sC-BR GGA-approximation of eq 6.3. (b) Binary weights based on the classical (HCD) or iterative Hirshfeld partitioning (HID).

6.4 Results

The sC-BR-HI, sC-BR-HID, and sC-BR-HCD variants (eq 6.3) are tested on 90 complexes built from He, Ne, Ar, Kr, H_2 , N_2 , O_2 , Cl_2 , CO_2 , CH_4 , SiH_4 , SiF_4 , CCl_4 , C_2H_2 , C_3H_8 , SF_6 , and C_6H_6 separated by roughly 20 Å. If not otherwise stated, all computations use PBE¹⁵⁶/aug-cc-pVTZ densities, a 99/590 Euler-Maclaurin-Lebedev^{370,371} integration grid, and are carried out in a developmental version of Q-Chem.³⁶⁸ The intermolecular dispersion coefficients are computed as the sum over intermolecular atom pairs.

The sC-BR model gives highly accurate C_6 dispersion coefficients for systems far beyond the training set (Figure 6.1). The linear regression and mean absolute percentage errors (Table 6.1) show that the simple GGA approximation matches or improves upon previous models. In particular, the slope and y-intersect of the linear regression are closer to the ideal values of 1.0 and 0.0, respectively. The use of disjoint in place of overlapping Hirshfeld weights (Figure 6.1b) reduces the slope slightly, without deteriorating the R^2 value. The mean absolute percentage deviations, along with the three other accuracy criteria (slope, y-intercept, R^2), illustrate the remarkable performance of sC-BR-HCD, the most cost-effective combination presented herein. Typical examples for intermolecular C_6 dispersion coefficients are given in Table 6.2.

Table 6.1: Mean Absolute Percentage Deviations (MA%D) over 90 C_6 Dispersion Coefficients.

XDM-scheme	MA%D
BJ (= XX)	9.28
BR-HC	10.03
BR-HI	9.23
sC-BR-HI	8.17
BR-HCD	10.71
BR-HID	10.16
sC-BR-HCD	9.19
sC-BR-HID	6.99

Table 6.2: Typical Examples for Intermolecular C_6 Dispersion Coefficients in Atomic Units Computed with BR-HCD and sC-BR-HCD. Values from Becke and Johnson (BJ, ref 76) Are Given for Comparison. The Reference Values Are Taken from the same Publication.

Complex	Accurate	BJ	BR-HCD	sC-BR-HCD
CH ₄ -CH ₄	129.60	115.30	135.52	134.09
CH ₄ -C ₂ H ₂	162.50	147.50	168.54	167.73
CH ₄ -C ₆ H ₆	472.10	383.50	444.19	475.57
C ₂ H ₂ -C ₂ H ₂	204.10	188.70	210.13	210.04
C ₂ H ₂ -C ₂ H ₄	247.7	225.3	246.22	249.94
C ₂ H ₂ -C ₃ H ₈	395.60	332.80	386.09	408.77
C ₂ H ₂ -C ₅ H ₁₂	622.9	514.6	604.99	653.12
C ₂ H ₂ -C ₆ H ₆	593.00	491.00	555.11	596.86
C ₂ H ₂ -C ₆ H ₁₄	734.7	606.8	713.06	774.32
C ₂ H ₄ -C ₂ H ₄	300.5	270.1	286.24	294.75
C ₂ H ₄ -C ₆ H ₆	719.5	592.2	648.71	707.1
C ₂ H ₆ -C ₂ H ₆	381.8	310.6	364.42	390.98
C ₂ H ₆ -C ₆ H ₆	810.1	633.8	732.2	814.41
C ₃ H ₈ -C ₃ H ₈	768.10	589.40	710.79	795.20
C ₃ H ₈ -C ₆ H ₆	1149.00	875.00	1021.55	1158.77
C ₄ H ₈ -C ₄ H ₈	1130	951	1024.54	1149.47
C ₆ H ₆ -C ₆ H ₆	1723.00	1311.00	1476.07	1696.86
CCl ₄ -CH ₄	512.20	438.90	433.53	474.56
CCl ₄ -C ₂ H ₂	642.40	561.70	554.47	594.62
CCl ₄ -C ₃ H ₈	1247.00	998.00	1018.10	1156.57
CCl ₄ -SiH ₄	828.60	775.40	767.85	832.67
CCl ₄ -CCl ₄	2024.00	1694.00	1461.58	1694.89
SiH ₄ -CH ₄	209.40	199.50	234.46	237.82
SiH ₄ -C ₂ H ₂	264.00	255.40	292.30	297.47
SiH ₄ -C ₃ H ₈	509.70	455.60	523.13	579.21
SiH ₄ -C ₆ H ₆	766.50	683.10	780.51	847.48
SiH ₄ -SiH ₄	343.90	356.10	414.01	427.76
SiF ₄ -CH ₄	202.30	213.30	234.45	240.37
SiF ₄ -C ₂ H ₂	251.90	273.00	292.59	302.23
SiF ₄ -C ₃ H ₈	492.70	485.20	537.56	588.05

The robustness of the presented scheme is further illustrated by the use of C_6 , C_8 , and C_{10} dispersion coefficients within our recent density-dependent dispersion correction⁸¹ (dDXDM, see Chapter 4 for details), reparameterized to the S22 test set.^{299,351}

The S22 set validates the excellent performance of the new dispersion coefficients on noncovalent complexes. The sC-BR-HCD coefficients lead to the most accurate results (MAD = 0.14, 0.21, and 0.29 kcal mol⁻¹ for BLYP, B3LYP, and PBE, respectively). Other sC-BR variants also give accurate MADs between 0.26 and 0.36 kcal mol⁻¹. For comparison, the “best” S22 MADs listed by Grimme et al.⁴² are within 0.2-0.25 kcal mol⁻¹ for ω B97X-D,²⁵² and BLYP-D3.

6.5 Conclusion

In summary, we have presented a simple GGA-based model for computing density-dependent dispersion coefficients. The sC-BR-HCD variant yields remarkably accurate results by enabling the inclusion of the missing dispersion interactions into standard density functionals at low computational cost, in addition to giving a disjoint description of AIMs. The method, which relies on both the GGA-information and the Hirshfeld-population analysis, can easily be implemented in any density functional code in a post-SCF process. The GGA-formalism is furthermore expected to dramatically simplify self-consistent implementations and benefit the evaluation of self-consistent forces.

7 Comprehensive Benchmarking of a Density-Dependent Dispersion Correction

7.1 Introduction

Many chemical phenomena are dominated by weak interactions, as exemplified by the highly ordered structures of biomolecules (stacking of DNA,⁷ protein folding⁸) and supramolecular assemblies,⁹ crystals arrangements of organic⁴²⁹ and inorganic materials,⁴³⁰ or catalysis intermediates (see, e.g., ref 431). Because of the incomparable balance of accuracy and computational cost, Kohn-Sham density functional theory¹¹ has emerged as the most widely applied methodology for investigating electronic structures and geometries of extended molecular systems. Despite this success, standard semilocal approximations do not properly describe attractive dispersion interactions that decay with R^{-6} at large intermolecular distances.^{14–17} Even at the medium-range, most semilocal density functionals fail to give an accurate description of weak interactions such as those dominating alkane isomerization energies and Pople's isodesmic bond separation equations (BSEs).^{68–71,82,83}

Near the energy minimum, dispersion corrected atom centered potentials (DCAPs)^{254–257,319} or carefully fitted density functionals^{164,208,214,278,290,320} (M06-2X²¹⁴ is certainly the most successful functional originating from this approach) give satisfactory results. Nevertheless, both approaches lack the ability to recover the correct long-range $\sim R^{-6}$ attractive form. The simplest conceptual remedy,^{22,38,240,269,321} first popularized by Grimme (motivated by HF-D)^{37,237–239,432} under the DFT-D acronym,^{39,42,269} is to correct for the missing interaction energy *a posteriori* by adding an attractive energy term summed over all of the atom pairs in the system. The quest for the optimal parametrization is, however, still an active field of research.^{42,44–46,49,51,72,74,81,251–253,270,322–326} Recent DFT-D (e.g., D2³⁹ and D3⁴²) gives an accurate description for intermolecular interactions, but the proper treatment of weak intramolecular interactions is trickier.^{42,43,68,305,327} Our group has pioneered the design of dispersion corrections which give a balanced description of both inter- and intramolecular weak interactions.^{72,74,81,86,433} Our most recent scheme combines dispersion coefficients (C) computed on the basis of an approximation to Becke and Johnson's^{75–80,328} exchange hole-

dipole moment (XDM) formalism depending on the reduced density gradient (s)⁸⁸ and a genuine density-dependent damping factor.⁸¹ The resulting density-dependent dispersion correction, called dDsC, promises substantial advantages over standard DFT computations for a broad range of applications. Following a careful validation of the dDsC scheme, we here introduce a few improvements to our original density-dependent damping factor^{81,88} and provide a comprehensive benchmarking of the density-dependent dispersion correction scheme. dDsC is tested on 18 diverse test sets featuring both intra- and intermolecular weak interaction energies together with a series of illustrative density functionals, i.e., BP86,^{151,154,332} BLYP,^{154,155} B3LYP,^{154,155,161,162} PBE,¹⁵⁶ B97²⁰⁹ and the long-range corrected exchange functional LC- ω PBELYP.^{155,313,393,394} Results for other schemes designed to better describe weak interactions are discussed as well: the local response dispersion (LRD) correction combined with LC-BOP,^{45,46} two fully nonlocal density functionals, VV10⁴⁸ and vdW-DF10,⁵³ the double hybrid functional B2PLYP-D3^{42,163} and M06-2X.²¹⁴ The benchmark is completed by a short assessment of the dDsC schemes on geometries.

7.2 Theory

The basic form of our dispersion correction is the Tang and Toennies (TT) damping function⁷³

$$E_{\text{disp}} = - \sum_{i=2}^{N_{\text{at}}} \sum_{j=1}^{i-1} \sum_{n=3}^{n=5} f_{2n}(bR_{ij}) \frac{C_{2n}^{ij}}{R_{ij}^{2n}} \quad (7.1)$$

where N_{at} is the number of atoms in the system and b is the TT-damping factor (*vide infra*). The dispersion correction is called dDsC if only the first term is retained in the multipole expansion ($n = 3$, corresponding to C_6), and dDsC10 otherwise (up to $n = 5$, i.e., up to C_{10}). Note that the effects of the higher-order terms strongly depend on the type of damping function. The TT-damping function applied herein “simulates” the missing higher-order dispersion terms by increasing the damping factor b ,²⁹² as illustrated in Figure 3.1 on page 25. $f_{2n}(bR_{ij})$ are the “universal damping functions”⁷³ that are specific to each dispersion coefficient and that serve to attenuate the correction at short internuclear distances (to account for overlapping densities).

$$f_{2n}(x) = 1 - \exp(-x) \sum_{k=0}^{2n} \frac{x^k}{k!} \quad (7.2)$$

This section describes the determination of the damping factor b in eq 7.1. The dispersion coefficients themselves are obtained as described previously in Chapter 6⁸⁸ and rely on a classical Hirshfeld dominant partitioning of the electron density among the atomic centers.

Classical Hirshfeld weightings are defined as³³⁵

$$w_i(\mathbf{r}) = \frac{\rho_i^{\text{at}}(\mathbf{r})}{\sum_n \rho_n^{\text{at}}(\mathbf{r})} \quad (7.3)$$

where ρ_i^{at} is the sphericalized free (neutral) atomic density of atom i , weighted by the superposition of all ρ_i^{at} with all atoms n positioned as in the real molecule. The classical Hirshfeld dominant partitioning w_i^D is obtained by assigning each point exclusively to the atom which has the highest weight at that particular grid point. Such a partitioning is more appealing than the classical Hirshfeld populations, as it avoids overlapping atomic regions that conflict with the multipole expansion that is at the origin of the atom pairwise London dispersion correction.⁴²³

A key component of dDsC is the damping factor b . We showed previously^{74,81} that the performance of the TT-damping function is improved by the introduction of a second damping function, which prevents the corrections at regions of strong density overlap (i.e., covalent distances) that are better described by density functionals.⁸⁶ Akin to our previous work,⁸¹ $b_{ij,\text{asym}}$, the asymptotic value of b , accounts for the short-range effect through a multiplicative function

$$b(x) = F(x)b_{ij,\text{asym}} \quad (7.4)$$

x and $F(x)$ are, respectively, the damping argument and function for $b_{ij,\text{asym}}$, the TT-damping factor associated with two separated atoms. $b_{ij,\text{asym}}$ is computed according to the combination rule^{293,340}

$$b_{ij,\text{asym}} = 2 \frac{b_{ii,\text{asym}} \cdot b_{jj,\text{asym}}}{b_{ii,\text{asym}} + b_{jj,\text{asym}}} \quad (7.5)$$

$b_{ii,\text{asym}}$ is generally estimated from the square root of (atomic) ionization energies.^{341,342,434–436} However, the ionization energy does not correlate well with the size of an atom that is a determinant characteristic for the damping of a dispersion term.^{38,39,44,120} We instead propose to compute $b_{ii,\text{asym}}$ on the basis of effective atomic polarizabilities. Note that polarizabilities as a measure of the “size” are extensively used in the closely related context of Thole’s interacting dipole moments.⁴³⁷ After introduction of the parameter b_0 , which dictates the strength of the dispersion correction in the medium-range, one obtains

$$b_{ii,\text{asym}} = b_0 \cdot \sqrt[3]{\frac{1}{\alpha_i}} = b_0 \cdot \sqrt[3]{\frac{1}{\alpha_{i,\text{free}}}} \cdot \sqrt[3]{\frac{V_{i,\text{free}}}{V_{i,\text{AIM}}}} \quad (7.6)$$

In the above definition, b_0 includes the conversion factor from \AA^3 to atomic units for α_i . The effective atom in molecule (AIM) polarizabilities are estimated from scaled free atomic

polarizabilities^{337,338}

$$\alpha_i = \frac{\langle r^3 \rangle_i}{\langle r^3 \rangle_{i,\text{free}}} \alpha_{i,\text{free}} = \frac{\int r^3 w_i^D(\mathbf{r}) \rho(\mathbf{r}) d^3 r}{\int r^3 \rho_{i,\text{free}}(\mathbf{r}) d^3 r} \alpha_{i,\text{free}} = \frac{V_{i,\text{AIM}}}{V_{i,\text{free}}} \alpha_{i,\text{free}} \quad (7.7)$$

A density cutoff of 0.002 au is applied to improve the consistency of atomic volumes between atoms at the surface and in the interior of a molecule.^{88,438} The $b_{ii,\text{asym}}$ dependency on atomic polarizabilities (instead of atomic ionization energies) mostly benefits the treatment of highly polarizable atoms as shown later (e.g., neutral alkali-metal cluster like K_8 of the ALK6 test set). A similar relationship could also be an advantage in force fields specifically designed to predict crystal structures. In such force fields, atomic polarizabilities have already been introduced, but $b_{ii,\text{asym}}$ is usually determined from the molecular ionization energy with no dependency on the specific atom pair.^{434–436} Along with the modified $b_{ii,\text{asym}}$, the secondary damping function is modified slightly and represented by a (steeper) exponential decay rather than by the previously used arctan function

$$F(x) = \frac{2}{e^{a_0 \cdot x} + 1} \quad (7.8)$$

where the fitted parameter a_0 adjusts the short-range behavior.

The last element of the correction is the damping argument x

$$x = \left(2q_{ij} + \frac{\text{abs}((Z_i - N_i^D) \cdot (Z_j - N_j^D))}{r_{ij}} \right) \frac{N_i^D + N_j^D}{N_i^D \cdot N_j^D} \quad (7.9)$$

where Z_i and N_i^D are the nuclear charge and Hirshfeld dominant population of atom i , respectively. $2q_{ij} = q_{ij} + q_{ji}$ is a covalent bond index³⁴⁴ based on the overlap of classical Hirshfeld populations $q_{ij} = \int w_i(\mathbf{r}) w_j(\mathbf{r}) \rho(\mathbf{r}) d\mathbf{r}$, and the fractional term in the parentheses is a distance-dependent ionic bond index³⁴⁵ taken as an absolute value. Classical Hirshfeld dominant charges in the damping function resolve the inconvenience of classical Hirshfeld charges that are generally too small.^{81,373,439} The multiplicative factor, $\frac{N_i^D + N_j^D}{N_i^D \cdot N_j^D}$, serves to attenuate the damping of $b_{ii,\text{asym}}$ for heavier atoms (containing more electrons). Note that the damping function $F(x)$ has the adequate form (i.e., $F(0) = 1$ and $F(\infty) = 0$), given that x is large when atoms are close to each other and goes to zero with increasing distance r_{ij} .

In the present form, approximated dDsC gradients are available: all derivatives of the (density-dependent) parameters (the damping parameter b and the dispersion coefficients) are set to zero, or in other words, kept fixed at their values corresponding to the energy of the geometry for which the gradient is being computed. The approximation is expected to introduce only small errors, similar to those engendered by the use of a smaller basis set for geometry optimization, followed by energy refinement with a larger basis set. Exact gradients are computationally more expensive (although simpler than those derived for the original Becke-Roussel exchange hole in ref 87) given that the contributions to the Fock matrix are needed at each SCF cycle.

To summarize, the presented dDsC correction employs electronic structure information to

determine dispersion coefficients and two fitted, functional dependent, damping parameters that are the strength of the TT-damping (b_0) and the steepness factor (a_0).

7.3 Determination of the Adjustable Parameters

In line with our former work,^{72,74,81} the chosen fitting procedure ensures a successful treatment of both weak intra- (medium-range) and inter- (long-range) molecular interactions. The two parameters (a_0 and b_0) are fitted for each functional so as to minimize the mean absolute deviation (MAD) over a representative set of 48 reactions, assessing inter- and intramolecular interactions. In summary, 3-6 entries are taken from the following test sets (*vide infra*): BSR36, RSE43, ISO34, NBPRC, WATER27, ACONF, CYCONF, SCONF, HEAVY28, and S22.

Figure 7.1 illustrates the dependence of the MAD over all test sets (*vide infra*) on the two fitted parameter a_0 and b_0 . Variations of $\sim 5\%$ and $\sim 10\%$ in b_0 and a_0 respectively lead to only negligible changes in the MAD. The proximity of the fitted parameters (minimum for 48 reactions) to the minimum for all test sets together (341 reactions) provides further validates the chosen training set.

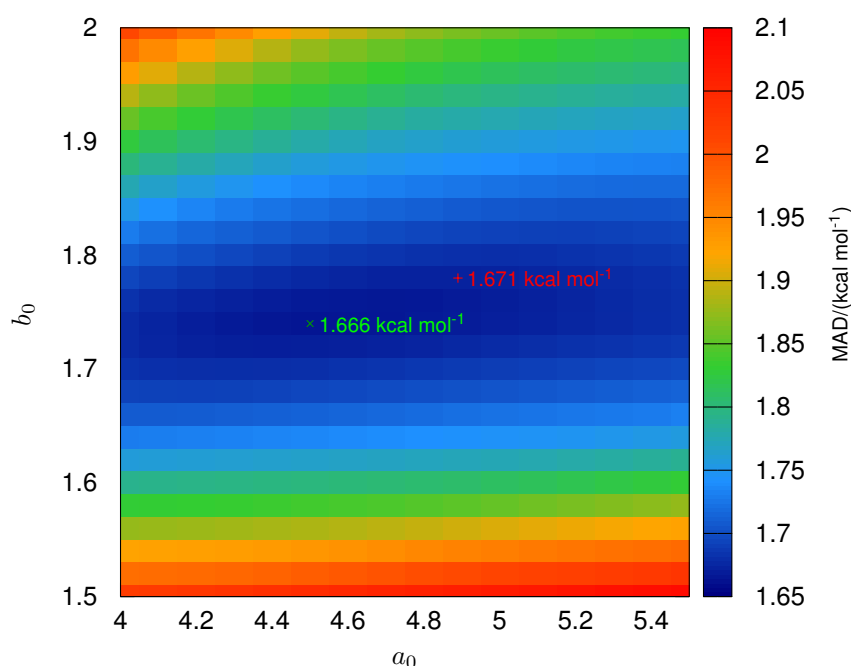


Figure 7.1: Illustration of the mean absolute deviation of B3LYP-dDsC as a function of a_0 and b_0 . The point labeled in red corresponds to the minimum according to the training set. The green label corresponds to the minimum over all test sets combined.

7.4 Test Sets

Eighteen test sets, corresponding to 341 reaction energies, were selected out of the 30 test sets from the GMTKN30 (database for general main group thermochemistry, kinetics, and noncovalent interactions) database^{225,440} from where the geometries and reference values were taken. The sets are divided into three categories:

Intramolecular interactions: 5 sets, 85 reactions: ISOL22 (isomerization energies of large organic molecules),⁴⁴¹ DARC (Diels-Alder reactions energies),³⁶ BSR36 (bond separation reactions of alkanes),^{72,395} IDISP (intramolecular dispersion interactions),^{68,85,225} and AL2X (dimerization energies of AlX_3 and AlHX_2 compounds, $\text{X} = \text{F}, \text{Cl}, \text{Br}, \text{and Me}$).³⁶

Intermolecular interactions and conformational energies: 7 sets, 108 reactions: S22 (binding energies of noncovalently bound dimers),^{299,351,442} ADIM6 (interaction energies of *n*-alkane dimers),⁴² HEAVY28 (noncovalent interaction energies between heavy element hydrides),⁴² ACONF (relative energies of alkane conformers),⁴⁴³ SCONF (relative energies of sugar conformers),^{444,445} PCONF (relative energies of PHE-GLY-GLY),⁴⁴⁶ and CYCONF (relative energies of cysteine conformers).⁴⁴⁷

Mixed category of reaction energies: 6 sets, 148 reactions: ALK6 (fragmentation and dissociation reactions of alkaline metal clusters and alkaline-cation benzene complexes),⁴² BHPERI (barrier heights of pericyclic reactions),^{383,448–450} RSE43 (radical stabilization energies),⁴⁵¹ NBPRC (oligomerizations and H_2 fragmentations of NH_3/BH_3 systems and H_2 activation reactions with PH_3/BH_3),^{444,452} ISO34 (isomerization energies of small and medium-sized organic molecules),³⁶⁹ and WATER27 (binding energies of water, $\text{H}^+(\text{H}_2\text{O})_n$ and $\text{OH}^-(\text{H}_2\text{O})_n$ clusters).⁴⁵³

7.5 Computational Methods

BLYP,^{154,155} BP86,^{151,154} PBE,¹⁵⁶ revPBE,⁴⁰² B3LYP,^{154,155,161,162} and PBE0^{156,280} computations were performed with a developmental version of ADF.^{454,455} HF, BHHLYP,³³³ Becke's hybrid B97²⁰⁹ functional (that is to be distinguished from Grimme's GGA functional B97-D³⁹), PW6B95,⁴⁵⁶ LC- ω PBE^{313,393,394} ($\omega = 0.45$), LC- ω PBELYP ($\omega = 0.45$), LC- ω PBEB95¹⁸⁵ ($\omega = 0.45$), VV10 (rPW86 exchange,³⁹⁶ PBE correlation¹⁵⁶ + nonlocal term),⁴⁸ and vdW-DF10 (rPW86³⁹⁶PW92¹⁵⁰+nonlocal term)⁵³ were performed in a local version of Q-Chem,³⁶⁸ while LC-BOP,^{154,407,411,457} LC-BOP-LRD,^{45,46} (excluding multicenter contributions to C_6 coefficients is denoted as LRD[10,0]) and TPSSm¹⁵⁷ and all geometry optimizations were run with a modified version of GAMESS.⁴⁵⁸ Due to SCF convergence problems, computations in GAMESS use the cc-pVTZ basis set^{363–365} (augmented with diffuse functions, leading to aug-cc-pVTZ in order to minimize the BSSE for the WATER27 complexes and all but the benzene-indole complexes of the S22 test set), except for potassium and the heavier elements for which the def2-QZVP(-g) basis set was used. All Q-Chem computations were done with the def2-QZVP(-g)⁴⁵⁹ basis set except for the clusters involving OH^- from the WATER27 test set, for which the

aug-cc-pVQZ basis set was used. In GAMESS and Q-Chem, the numerical integrations were performed on a fine 99/590 and 75/302 Euler-Maclaurin-Lebedev grid, respectively, with an integration threshold of 10^{-12} . In ADF, the QZ4P basis set was used for all systems except for the OH^- -containing WATER27 clusters, which were described by the ET-QZ3P-DIFFUSE basis set. All-electron computations in ADF for the HEAVY27 test set include the ZORA⁴⁶⁰ relativistic corrections. The “dependency” and “addDiffuseFit” keys were applied throughout and the integration accuracy set to 8. For the sake of clarity, only a selection of the tested functionals is included in the figures, but all of the statistics are collected in Table 7.1. Geometries and reference values for the peptide conformational energies (4) and the cyclization reaction (5) are taken from ref 441 and refs 350 and 303, respectively. The Grubbs catalysts’ (6 and 7) geometries and zero-point energies are taken from ref 461.

The dDsC corrections are applied post-SCE, using atomic fragments computed on the fly with the same method and basis set as the molecular computation. All DFT-D3⁴² and M06-2X²¹⁴ values are taken from the GMTKN30 Web page.⁴⁴⁰

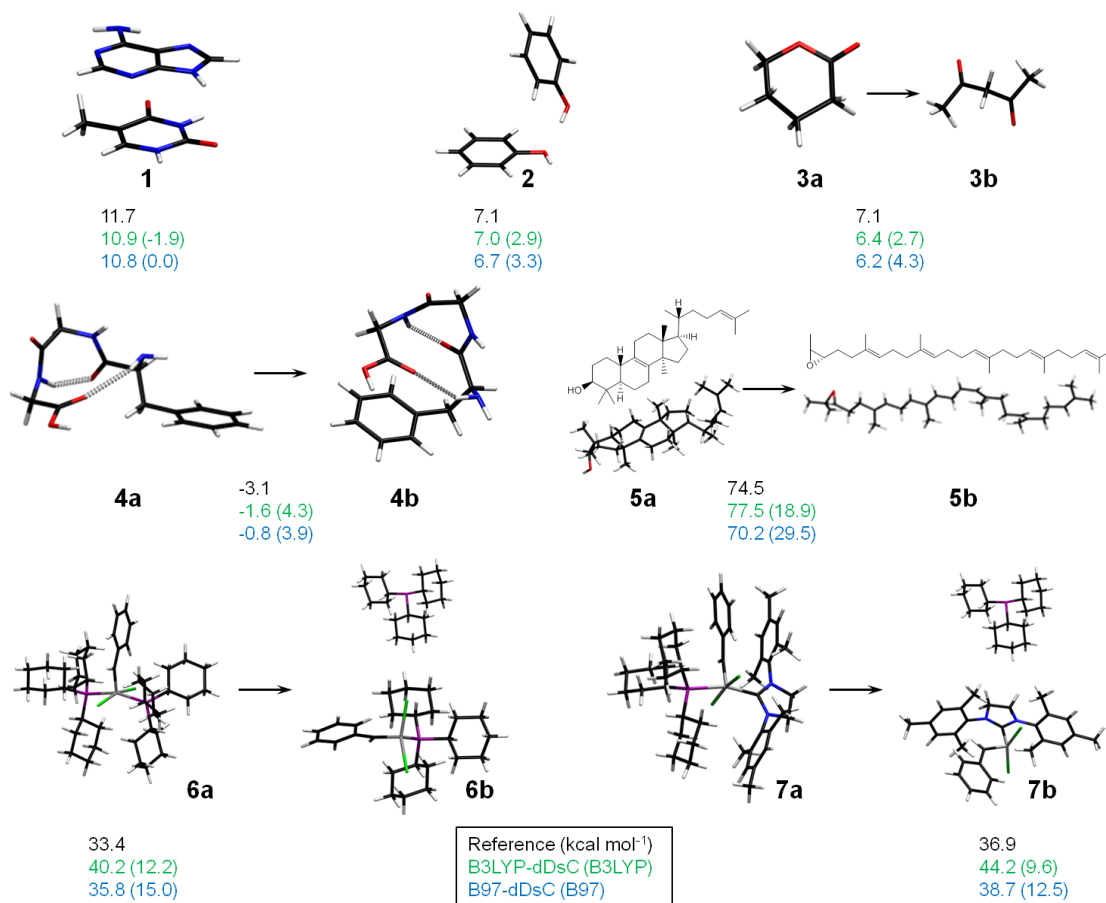


Figure 7.2: Set of illustrative examples of reactions poorly described by standard density functionals (e.g., B3LYP and B97) and corrected by dDsC. The reference values^{291,351,369,441} are computed at the CCSD(T)/CBS level, except for 5, where SCS-MP3/CBS serves as the benchmark, and for 7, experimental values are used.⁴⁶² The DFT energies for 4-7 are computed with the def2-TZVP basis set.

7.6 Results and Discussion

The performance of dDsC is at first illustrated by Figure 7.2, which collects seven typical reactions for which a dispersion correction is essential. The first two reactions are taken from the S22 test set²⁹⁹ and represent general $\pi - \pi$ -stacking interactions (adenine-thymine base pair (**1**), which is unbound at the B3LYP level) and the phenol dimer (**2**) that features a combination of hydrogen-bond and other interactions often present in organic molecules. The isomerization reaction of δ -valerolactone (**3a**) into 2,4-penandione (**3b**)³⁶⁹ is characteristic of typical organic isomerization reactions and is also in the training set. The relative conformation energies of the two FGG tripeptides (**4**) is another example in which modeling of weak interactions is crucial to identifying the lower-lying conformer.²⁹¹ The cascade reaction leading to the formation of the steroid framework **5a** from the squalene precursor **5b** is a striking case with an error of almost 50 kcal mol⁻¹ at the B3LYP level.⁴⁴¹ Finally, the experimental⁴⁶² energy difference between the bond dissociation energies of PCy₃ from Grubbs' first (**6a**) and second generation (**7a**) catalysts⁴⁶³ are qualitatively incorrect at standard density functional levels⁴⁶⁴ but well reproduced when improving the treatment of medium-range correlation⁴⁶⁵ or when using a dispersion correction.⁴⁶¹

Reaction energies associated with a considerable change in molecular size and shape are challenging cases for density functional approximations. As discussed previously,⁸⁶ the problem may be associated with over-repulsiveness in the short-range,^{36,349} but missing weak interactions in the medium and long-ranges are the largest contributors to the errors.^{72,86,374,395,441} By including reactions accounting for weak intramolecular interactions into the training set, our aim is to (i) obtain additional information regarding the proper form of the damping that is empirical in nature and (ii) devise a robust scheme that improves both reaction energies and weak intermolecular interactions that are generally the only focus of empirical dispersion energy corrections.^{38,39,44–46,252}

dDsC reduces the MAD of the parent functional for intramolecular interactions (see Figure 7.3) by a factor of 3-6, depending on the functional. The dramatically low (<1.0 kcal mol⁻¹) MAD(BSR36) results from the highly systematic error in bond separation energies^{69,72,86} along with the relatively large number (i.e., five) of such reactions included in the training set. The improvements for the intramolecular dispersion in hydrocarbons (IDISP) and the dimerizations of aluminum species (AL2X) as well as for the isomerizations of large organic molecules (ISOL22) highlight the high transferability of the density-dependent scheme using the present parametrization. Long-range corrected exchange functionals, such as LC- ω PBE, are among the best uncorrected approximations (see Table 7.1). However, the remaining error is less systematic than that of standard functionals, and their combination with dDsC often leads to overcorrection. LC- ω PBELYP-dDsC is the most accurate combination, but the variant does not present significant advantages over standard DFT-dDsC methods. The latter also clearly outperform the more sophisticated nonlocal van der Waals density functionals. The poorer performance of vdW-DF10 as compared to VV10 is most likely related to the replacement of the local PW92 by the PBE correlation in VV10: the PBE correlation functional is known to capture intramolecular interactions involving weakly interacting densities that overlap

Table 7.1: Mean Absolute Deviations for All Methods Tested, For All Test Sets (Overall), and the Three Individual Subcategories, i.e., Intramolecular Interactions (Intra), Intermolecular Interactions and Relative Conformational Energies (Inter+Conf), and the Mixed Test Sets (Mix)^a

	Overall	Intra	Inter+Conf	Mix
HF	9.05	12.62	3.10	11.34
BLYP	6.85	14.38	2.53	5.67
revPBE	6.26	11.28	2.70	5.97
B3LYP	5.70	12.22	2.20	4.50
TPSSM	4.84	10.47	1.98	3.68
vdW-DF10	4.80	11.13	0.61	4.00
BP86	4.54	9.07	2.14	3.68
B97	4.47	9.56	1.83	3.48
BHHLYP	4.40	9.10	1.77	3.63
HF-dDsC	3.74 (3.57)	5.82 (4.87)	1.25 (1.40)	4.37 (4.41)
LC- ω PBE	3.49	6.24	1.48	3.38
PBE	3.49	7.39	1.39	2.77
LC- ω PBELYP	3.35	6.14	1.26	3.26
VV10	3.34	5.50	0.43	4.22
LC-BOP	3.32	5.36	1.45	3.52
PBE0	3.11	6.55	1.44	2.34
PW6B95	3.01	6.01	0.92	2.81
B3LYP-D3	2.96	6.82	0.28	2.70
LC- ω PBEB95	2.89	4.29	0.78	3.62
LC-BOP-LRD[10,0]	2.56	3.63	0.43	3.51
LC-BOP-LRD	2.56	3.50	0.49	3.54
BLYP-dDsC	2.45 (2.65)	3.71 (4.26)	0.62 (0.63)	3.05 (3.21)
LC- ω PBEB95-dDsC	2.39 (2.39)	4.15 (4.11)	0.66 (0.67)	2.65 (2.66)
LC- ω PBE-dDsC	2.37 (2.37)	4.82 (4.87)	0.43 (0.41)	2.38 (2.37)
PBE-dDsC	2.19 (2.22)	1.94 (1.94)	0.52 (0.57)	3.56 (3.58)
LC- ω PBELYP-dDsC	2.14 (2.04)	2.35 (2.05)	0.71 (0.59)	3.06 (3.08)
revPBE-dDsC	2.12 (1.92)	1.83 (1.89)	0.70 (0.59)	3.32 (2.90)
BP86-dDsC	2.03 (2.01)	2.44 (2.47)	0.81 (0.72)	2.68 (2.69)
TPSSM-dDsC	1.96 (1.96)	2.54 (2.61)	0.65 (0.63)	2.59 (2.56)
B3LYP-dDsC	1.67 (1.86)	2.43 (2.85)	0.48 (0.58)	2.11 (2.23)
BHHLYP-dDsC	1.66 (1.73)	1.76 (1.81)	0.48 (0.53)	2.47 (2.55)
PBE0-dDsC	1.59 (1.66)	1.98 (2.04)	0.42 (0.52)	2.22 (2.28)
M06-2X	1.41	2.94	0.40	1.26
PW6B95-dDsC	1.39 (1.39)	1.70 (1.67)	0.62 (0.66)	1.78 (1.76)
B2PLYP-D3	1.37	3.41	0.16	1.08
B97-dDsC	1.30 (1.32)	1.78 (1.82)	0.48 (0.47)	1.62 (1.65)

^a Values in parentheses refer to the dispersion correction including coefficients up to C_{10} (dDsC10). All values are in kcal mol⁻¹. Results for B2PLYP-D3 and M06-2X are taken from refs 440 and 466.

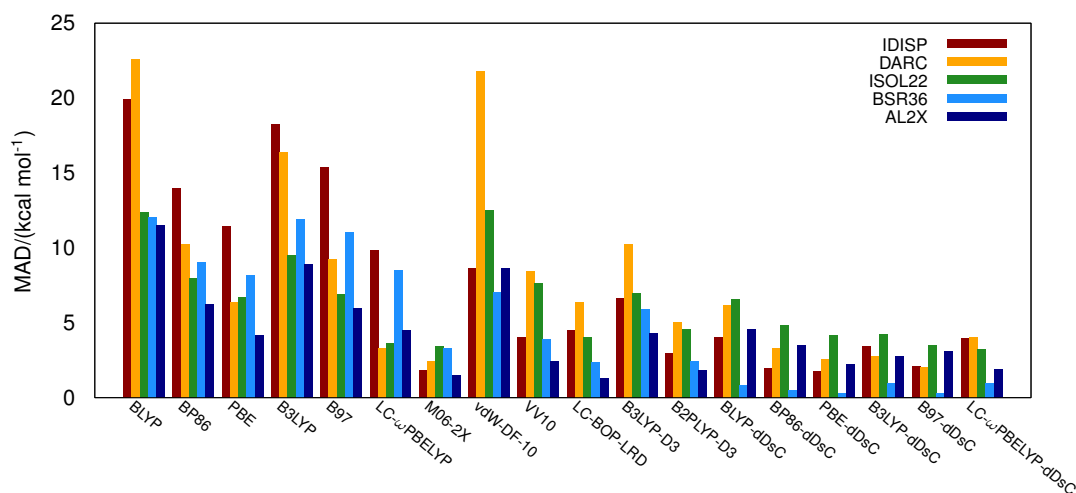


Figure 7.3: Mean absolute deviations for test sets dominated by intramolecular weak interactions.

reasonably well.⁸⁶ The changes in bond types of the AL2X, DARC, and ISOL22 test sets might be more accurate with the PBE than the PW92 correlation functional as well. LC-BOP-LRD further lowers the MAD to 3.5 kcal mol⁻¹ in this category. With a MAD of 2.9 and 3.4 kcal mol⁻¹ over the five “intramolecular” test sets, M06-2X and B2PLYP-D3, respectively, improve considerably over the standard density functionals (e.g., MAD(B3LYP) = 12.2 kcal mol⁻¹) but do not achieve the high accuracy of DFT-dDsC, where most functionals are corrected to a MAD of only about 2 kcal mol⁻¹, with a minimum of 1.7 kcal mol⁻¹ for PW6B95-dDsC.

The improved energies for systems characterized by typical weak intermolecular interactions are collected in Figure 7.4. Most atom pairwise dispersion corrections and fully nonlocal van der Waals functionals are designed to improve the treatment of those interactions. Accordingly, the performance of methods such as B2PLYP-D3 is excellent, and VV10, vdW-DF10, and LC-BOP-LRD give relatively low errors as well. The remarkable performance of M06-2X is, on the other hand, illustrative of the success of extensive fitting. With an average MAD of 0.6 kcal mol⁻¹ (over 13 density functionals, excluding HF-dDsC), DFT-dDsC also performs well for diverse types of weak intermolecular interactions and relative conformational energies (see Table 7.1). The small errors obtained for the S22 test set (assessing pure dispersion to H-bonding) along with those on the heavy atom hydrides confirm the general accuracy of the density-dependent dispersion scheme. Alkane dimers (ADIM6) are, however, overcorrected by dDsC. Our careful analysis suggests that ADIM6 is an exception rather than the result of an overfitting toward intramolecular interactions dominating the training set. Subtle changes in nonbonded interactions such as those dictating the relative conformational energies of alkanes (ACONF) are, for instance, well captured by dDsC, which shows that the strong dispersion energy correction needed for improving bond separation equations does not generally deteriorate longer-range interactions. To a much lesser extent, the D3 level also overcorrects alkane dimers, even though D3 is parametrized to perform well for these systems (see the detailed performance of D3 on the GMTKN Web site⁴⁴⁰). The peculiarity of the ADIM6 test set is further illustrated by the contrasting trend in the performance of MP2/CBS (MAD =

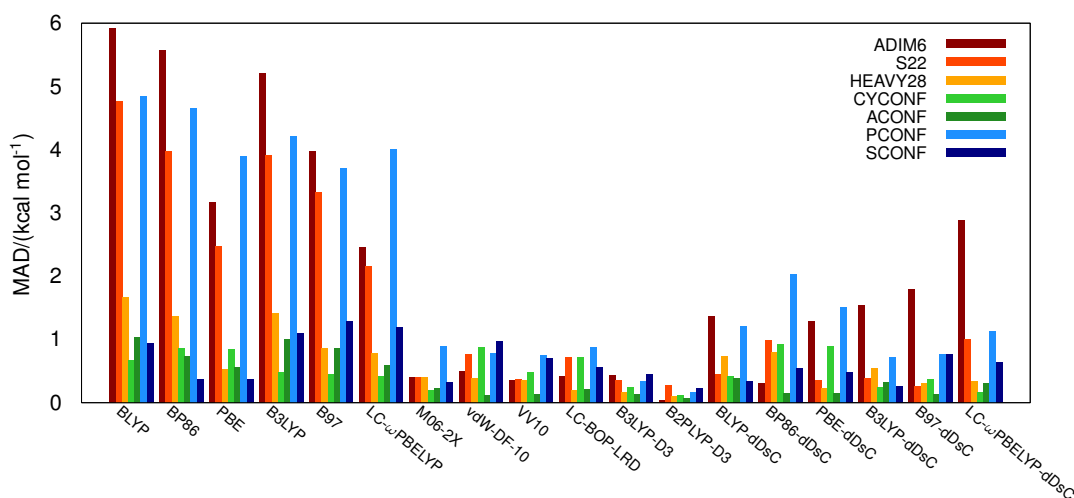


Figure 7.4: Mean absolute deviations for test sets featuring intermolecular weak interactions or relative conformational energies.

0.27 kcal mol⁻¹) and SCS-MP2/CBS (MAD = 1.05 kcal mol⁻¹), which is opposite that of the S22 test set.⁴⁶⁶ The modest performance of dDsC for the Phe-Gly-Gly-peptide conformations (PCONF) is, to a large extent, influenced by the choice of “reference” conformer used in the relative energy computations. Standard functionals indeed identify the second lowest energy conformer instead of the correct conformation (at the CCSD(T) level) as the lowest energy one. The MADs are thus lowered by up to 50%, when considering the second lowest lying (0.14 kcal/mol higher according to the CCSD(T) reference values⁴⁴⁶) as the “reference compound”. Several additional interesting features of Figure 7.4 can be better understood by considering the characteristics of the parent functional. For instance, the accurate treatment of the relative conformational energies of cysteine (CYCONF) relies on a balanced description between strong (e.g., OH⋯N) intramolecular hydrogen bonds (that dominate some of the conformers) and weaker interactions (e.g., NH⋯S present in other conformers). The good description of OH⋯N and NH⋯O hydrogen bonds by PBE and BP86 versus their underestimation of weak interactions bias the relative conformational energies and result in the poorer performance of PBE(-dDsC) and BP86(-dDsC) for CYCONF than for SCONF. The relative energies of sugar conformers, which are all dominated by strong hydrogen bonds, are indeed better described by these levels,⁴⁴⁵ which do not benefit from the inclusion of a dispersion correction.

Figure 7.5 collects errors for the “mixed” category, regrouping six test sets, which are not all dominated by weak interactions but are nevertheless important for typical computational chemistry applications. The errors in radical stabilization energies (RSE43), isomerization energies of small molecules (ISO34), and the NBPRC test set, for instance, originate from subtle inaccuracies in, e.g., bond energies. The inaccurate treatment of barrier heights of pericyclic reactions (BHPERI) is generally attributed to the self-interaction error,^{182,467–470} and to the delocalization error³⁶ (or the error in the repulsive wall⁸⁶) that is also at the origin of the poor assessment of the related Diels-Alder reaction energies (see DARC in Figure 7.3). For “repulsive” functionals such as BLYP or B3LYP, the dispersion correction stabilizes the transition state

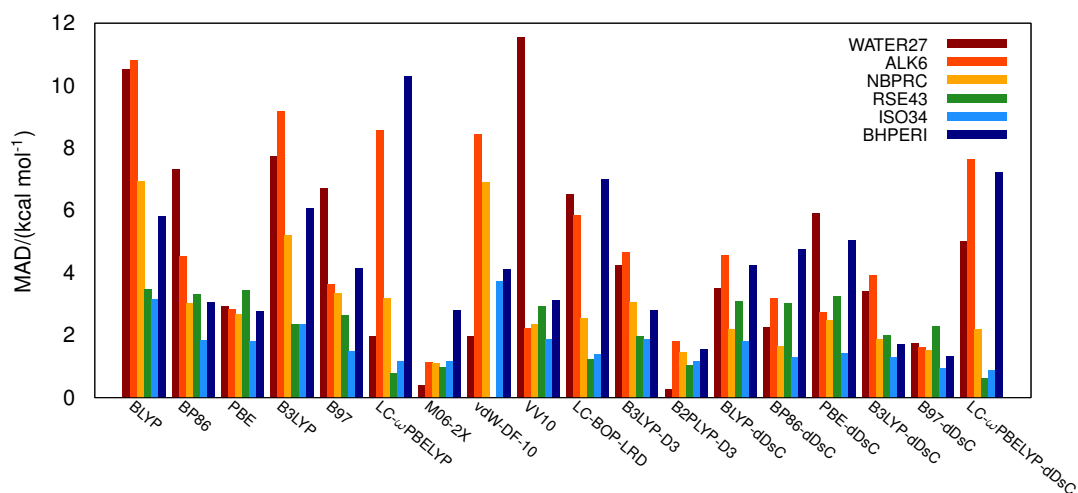


Figure 7.5: Mean absolute deviations over test sets assessing various reaction energies and barrier heights for pericyclic reactions. For vdW-DF10, the RSE43 set could not be computed since it is not defined for open-shell systems.

and leads to a clear improvement. The barrier heights are, however, overcorrected with more attractive approximation such as PBE. The unexpected poor performance of LC- ω PBELYP (LC- ω PBE and LC- ω PBEB95 perform better in this case, with a MAD of about 6.7 kcal mol⁻¹ vs 10.3 kcal mol⁻¹, but even BLYP (MAD= 5.8 kcal mol⁻¹) outperforms the long-range corrected exchange functionals) results from a strong overestimation of the barrier heights in line with that of HF (23.2 kcal mol⁻¹ and 10.6 kcal mol⁻¹ with HF-dDsC). The high error for BHPERI along with the general difficulty of systematically improving the LC- ω PBE functional group by a dispersion correction (*vide supra*) reflects the need for a better-devised range-separation parameter ω . A system dependence^{197,199,200} could be a strategy that would, however, cause size-extensivity problems important for reaction energies. At higher computational costs, the more balanced description of range-separated local hybrids²⁰⁴ represents another alternative. Note that M06-2X, with a MAD of 2.8 kcal mol⁻¹, is also affected by the large amount of “exact” exchange (54%), while B97-dDsC (19% “exact” exchange) performs best for these barrier heights (MAD = 1.3 mol⁻¹).

ALK6 played an important role in cross-validating the proposed density-dependent dispersion correction: the three benzene-alkaline cation (Li⁺, Na⁺, K⁺) complexes are dominated by electrostatic and inductive interactions⁴⁷¹ and are thus well described by standard DFT levels. Such interactions are, however, problematic for “classical” dispersion corrections, which use dispersion coefficients and vdW radii corresponding (approximately) to the free (neutral) atoms, and not to the cations.⁴² The other three systems in the test set are the decomposition of Li₈, Na₈, and K₈, into their respective dimers. In our scheme, these clusters are characterized by relatively large dispersion coefficients and are almost as polarizable as free alkaline atoms. While most functionals underbind these clusters, our genuine damping factor, $b_{ij,asym}$, successfully avoids overcorrection due to its dependence on polarizability.

The overall description of test sets collected in the “mixed” category depends generally more strongly on the functional itself, than on the accuracy of the dispersion correction. For in-

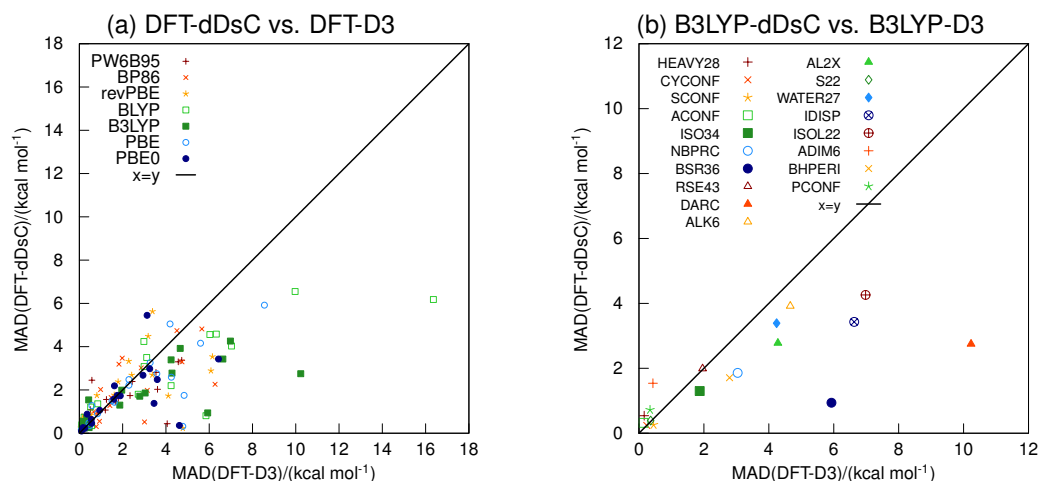


Figure 7.6: (a) Performance of DFT-dDsC versus DFT-D3 for seven functionals and the 18 selected test sets from the GMTKN30 database and (b) B3LYP-dDsC versus B3LYP-D3 with each test set as one point.

stance, the better performance of B2PLYP-D3 as compared to the dDsC corrected variants is due to B2PLYP, rather than to D3, as clearly illustrated by the comparison of B3LYP-D3 and B3LYP-dDsC (MADs of 2.7 and 2.1 kcal mol⁻¹, respectively). Similarly, even though the LRD scheme (independently from the use of multicenter contributions, i.e., LRD[10,0] or LRD) improves the overall performance on the 18 test sets (3.32 vs 2.56 kcal mol⁻¹), LC-BOP and LC-BOP-LRD, have almost the same MAD for these “mixed” test sets (3.52 and 3.54 kcal mol⁻¹, respectively). The relatively large error of PBE-dDsC originates from the overcorrected PBE energies for WATER27 and BHPERI. A similar overcorrection is at the origin of the relatively poor performance of VV10 (total MAD of 4.2 kcal mol⁻¹). PBE-dDsC gives lower MAD than PBE-D3 for two reasons: (i) the ionic term in the damping function (eq 7.9) attenuates the dispersion correction for the strong and highly polarized hydrogen bonds of WATER27, and (ii) the polarizability-dependent damping factor prevents the energy overcorrection for the alkaline metal clusters (ALK6). Overall, B97-dDsC and PW6B95-dDsC achieve MADs below 2.0 kcal mol⁻¹, which illustrate that dDsC leads to improvements for this most challenging mixed category, albeit less impressive than for inter- and especially intramolecular (weak) interactions.

Figure 7.6 provides a detailed comparison of the MADs obtained with dDsC and the geometry-dependent D3 correction for seven functionals (Figure 7.6a) and the individual test sets (Figure 7.6b). DFT-D3 performs better than DFT-dDsC in cases for which the latter has a tendency to overcorrect (e.g., ADIM6 or BHPERI with PBE) or for which the former scheme uses quasi-exact dispersion coefficients (HEAVY28). As expected, D3 also performs well for its targeted interactions (weak interactions between neutral molecules and relative conformational energies are in the training set⁴²). On the other hand, dDsC adjusts better to a given functional and provides a more robust performance, when considering both inter- and intramolecular interactions including challenging reaction energies (e.g., ISOL22, DARC, BSR36, IDISP, and AL2X).

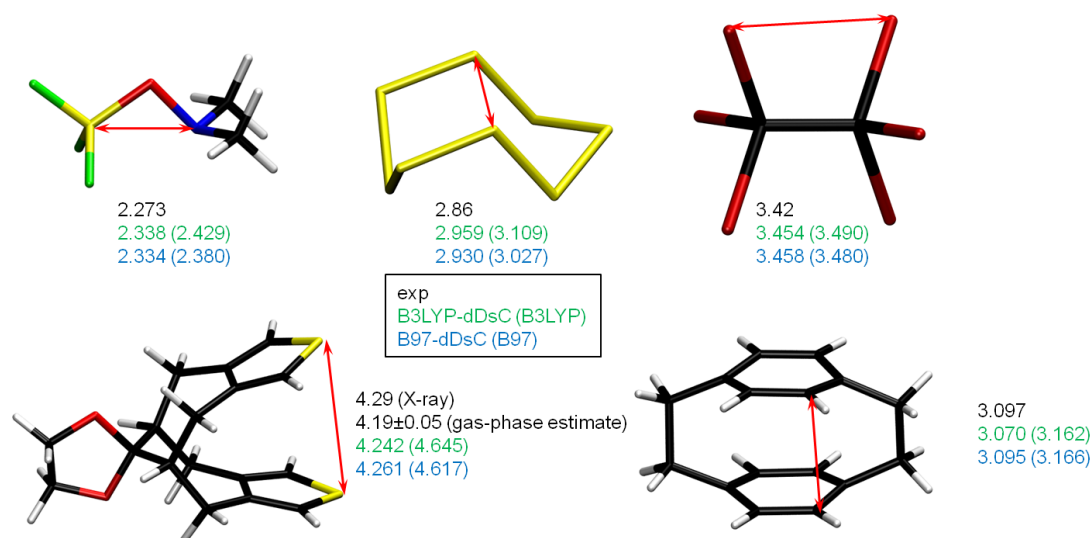


Figure 7.7: Geometrical structures of $(\text{CH}_3)_2\text{NOSiF}_3$,⁴⁷⁵ S_8^{2+} ,⁴⁷⁴ C_2Br_6 (first row),⁴⁷³ RESVAN,^{476,477} and [2.2]paracyclophane²⁶⁹ (second row) with key nonbonded distances (in Ångström) indicated.

The effect of dispersion corrections on thermochemistry has been thoroughly investigated. Geometries are usually less sensitive to the level of theory applied, but intramolecular nonbonded interactions are critical in certain cases. We thus compare the performance of two (un)corrected functionals, B3LYP and B97, for reproducing the geometry of five challenging molecules^{43,472} for which experimental structures are available: C_2Br_6 ,⁴⁷³ S_8^{2+} ,⁴⁷⁴ $(\text{CH}_3)_2\text{NOSiF}_3$,⁴⁷⁵ [2.2]paracyclophane,²⁹⁸ and a bisthieno-fused molecule known under its CSD entry name RESVAN (see Figure 7.7).^{472,476–478} B3LYP and B97 are overly repulsive for these intramolecular nonbonded contacts. The use of dDsC improves the geometries significantly, especially for the bisthieno-fused compound (RESVAN), mimicking stacked thiophene oligomers.

7.7 Conclusions

The final parametrization and refinement of the density-dependent dispersion correction, dDsC, introducing a simple atomic partitioning, computationally efficient dispersion coefficients, and advanced damping functions, considerably improves the performance of standard density functionals for various reaction energies and weakly interacting systems. With a MAD of 1.3 kcal mol⁻¹ over the 18 test investigated sets, B97-dDsC performs slightly better than M06-2X and B2PLYP-D3 (MAD = 1.4 kcal mol⁻¹ for both) but at a lower computational cost. The performance of B97-dDsC is especially impressive for the five intramolecular test sets (MAD = 1.8 kcal mol⁻¹) for which M06-2X and B2PLYP-D3 are less satisfactory (MAD of 2.9 and 3.4 kcal mol⁻¹, respectively).

The dispersion correction is available for all elements of the periodic table. Due to its robust performance and general accuracy for various interactions, ranging from hydrocarbon

reaction energies to heavy-atom hydride weak interaction energies, as well as for geometry optimization, we anticipate broad application of the dDsC scheme in diverse fields of computational chemistry (e.g., organocatalysis, QM/MM hybrid schemes, prediction of crystal structures). The density dependence of both the dispersion coefficients and the damping function has been shown to be especially valuable for modeling oxygen reduction reactions by organic reducing agents,⁴⁷⁹ the splitting of water by metallocenes,⁴⁸⁰ as well as for the molecular receptors,⁴⁸¹ which all involve charged species.

8 Why are the Interaction Energies of Charge-Transfer Complexes Challenging for DFT?

8.1 Introduction

Charge-transfer (CT) complexes, as introduced by Mulliken, are species characterized by low-lying excited states (e.g., benzene \cdots I₂).⁴⁸² Since its introduction, Mulliken's original term has been extended beyond its original definition to generally designate donor-acceptor complexes of either ground or excited states. The ground state of reactive complexes between alkenes and dihalogens (e.g., C₂H₄ \cdots F₂) are illustrative examples of the broader use of the term.⁴⁸³ Currently, charge-transfer complexes span the field of organic electronics (e.g., organic solar cells or light-emitting diodes),^{484,485} making them of considerable interest.

The origin of the binding interaction in ground state charge-transfer complexes is controversial. Orbital interactions have been commonly invoked to explain the energies associated with CT complexes.⁴⁸² Although the importance of CT has been questioned,^{486,487} it is still considered to be the primary source of binding – perhaps because CT is easily rationalized and visualized in terms of orbital interactions. The importance of van der Waals (vdW, especially London dispersion) forces in providing the correct qualitative descriptions of charge-transfer complexes has been known for some time^{488,489} but remains largely overlooked. Alternatively, electrostatic interactions have also been suggested as the dominant forces in the formation of CT complexes.⁴⁹⁰ Such complexes often show a strong dependence on the relative orientation of the monomers, a characteristic typically associated with orbital interactions. However, Hobza and coworkers⁴⁹¹ recently found that dispersion forces between nonspherical molecules have a stronger dependence on the relative orientation than hydrogen-bonded complexes. These findings question the use of orientation dependence for discriminating between interaction energy types.

The investigation of the ground state of CT complexes with approximate density functionals is very challenging. Note that “strong charge-transfer complex” refers herein to complexes affected by “strong” self-interaction (or the related delocalization) errors with common density functional approximations (charge-transfer excitation energies are highly problematic

as well^{392,400,492–494} but are not discussed herein; similarly, strong multireference electron-donor acceptor complexes such as TCNQ-TTF-TCNQ in an electric field⁴⁹⁵ are also not the focus here). On one hand, “pure” density functionals (local density approximation, LDA, and generalized gradient approximation, GGA) tend to overestimate the binding energy of strong charge-transfer complexes,^{32,33} while on the other hand, semilocal and hybrid functionals are unable to describe long-range dispersion interactions.^{14–17} The overestimation of charge-transfer might somehow compensate for the neglect of dispersion energy, but the error cancellation is subtle: a given functional might be reasonably accurate for one system but quite wrong for another (e.g., F₂ is much more problematic in terms of CT, while I₂ is more problematic in terms of neglected dispersion energy). In addition, error cancellation breaks down at longer intermolecular distances, as CT should fall off exponentially with distance, while dispersion decays as R⁻⁶. Adding a sufficient amount of “exact” exchange suppresses the spurious charge transfer, while the dispersion energy can be recovered by explicitly adding the correct R⁻⁶ attractive form. On a more fundamental level, relying on error cancellation is always dangerous, as it could lead to a wrong qualitative interpretation of the origin of the binding energy. An intriguing example is the organic CT complex investigated by Bredas and coworkers, for which standard density functionals were found to transfer more electron density than MP2, even though the complex is bound less strongly with DFT than with (SCS-)MP2.⁴⁹⁶ An alternative study examines the inaccurate treatment of the interaction energy between a Lewis acid and a bulky transition metal complex. The authors attribute the error of standard DFT approximations to the missing long-range exchange prior to recommending higher percentages of “exact” exchange for the description of the dative bond between Pt and Al.⁴⁹⁷ In both cases, M06-2X performs well with respect to CCSD(T). These studies, however, did not address the apparent contradiction between the actual underbinding and the expected overbinding by semilocal density functional approximations. In fact, the performance does not correlate with the percentage of “exact” exchange, which is noted only in passing and without making a link to the importance of weak interactions.⁴⁹⁶ The very good performance of M06-2X can indeed be attributed to the improved description of weak interactions²¹⁴ rather than to the large amount of nonlocal exchange (*vide infra*).

In a previous study,⁸⁶ we demonstrated that the errors of standard density functionals for relative energies of saturated hydrocarbons are due to a combination of over-repulsiveness in the short-range and the ubiquitous missing dispersion interactions. Adding *a posteriori* an atom pairwise energy correction term to standard density functionals not only conveniently accounts for weak interactions^{39,42,81,89} for intermolecular complexes but also dramatically improves the performance for various reaction and interaction energies involving saturated hydrocarbons.^{39,72,89,466} The recently developed density-dependent dispersion correction dDsC^{81,88,89} is pertinent for systems for which density rearrangements (charge transfer, polarization) might influence the interaction energy.

In the present work, the comparison of uncorrelated (HF) and correlated *ab initio* computations suggests that the interaction energy of closed-shell neutral charge-transfer complexes is dominated by weak electron correlation (i.e., vdW interactions) and not by the charge-transfer interaction energy itself. In line with these realizations, dispersion corrected HF and density

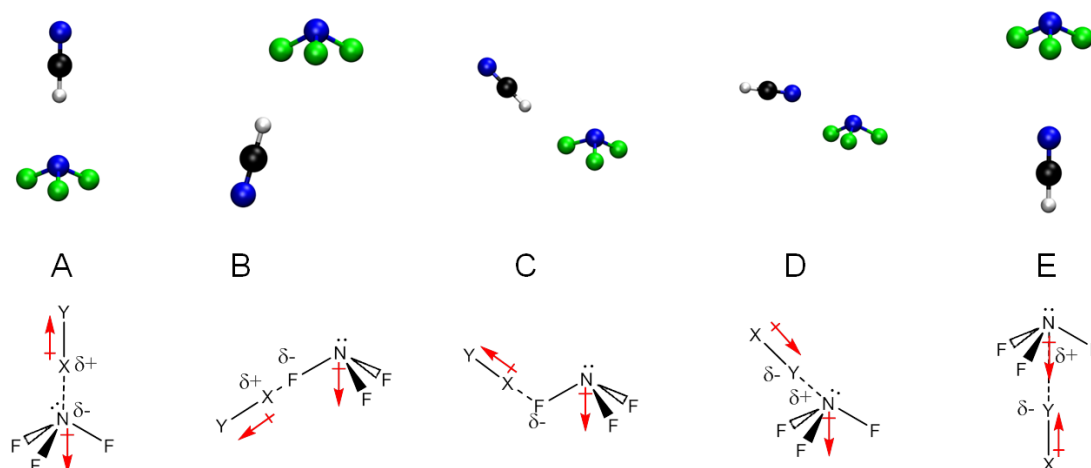


Figure 8.1: Representations of the five binding modes for the example of $\text{NF}_3 \cdots \text{HCN}$, and the general scheme is shown below. Color code: white, hydrogen; black, carbon; blue, nitrogen; and green, fluorine. In the general interaction pattern: $\text{Y} = \text{F}, \text{F}, \text{C}$, and N for ClF , HF , HNC , and HCN , respectively. The red arrows represent the direction of the monomer molecular dipoles.

functional approximations are shown to describe interaction energies substantially better than their standard counterparts. Further analysis based on energy decompositions indicates that the challenge for density functional approximations resides mostly in the description of the monomers (i.e., the self-interaction errors introduced by semilocal approximations, which affect the monomer, can lead to dramatic failures in the presence of a second molecule) and less in the strength of the actual charge-transfer interaction. We further demonstrate that only specific functionals achieve a consistent binding energy curve for typical vdW and charge-transfer complexes by providing an adequate description of the monomers, including a sufficient amount of “exact” exchange (to avoid over-repulsiveness at short and spurious charge transfers at long intermolecular distances) and accounting for weak interactions. The performance of various density functionals and the role of CT are evaluated on an illustrative series of four small ambidentate molecules (HCN , HNC , HF , and ClF) bound together with NF_3 . Five different geometries are considered for each of the small molecules (see Figure 8.1).⁴⁹⁸ These systems are particularly well suited for our purpose: depending on the orientation and relatively small electronic changes (e.g., HCN vs HNC), the binding energy and the relative importance of different components is substantially different. The broad range of interactions characterizing this series of small molecular complexes is representative of conventional applications involving charge-transfer complexes and thus valuable for gaining insight into larger related complexes that are typically targeted in chemical applications. In this respect, the crucial role of dispersion interactions, determined by these small model compounds, is further established on a typical cofacial organic complex of tetrathiafulvalene-tetracyanoquinodimethane (TTF-TCNQ).⁴⁹⁶

8.2 Theoretical Background, Methods, and Computational Details

Studies on typical strong CT complexes^{32,33} (e.g., $\text{C}_2\text{H}_4 \cdots \text{F}_2$) demonstrate that semilocal DFT exchange suffers from failures (i.e., overbinding), which can be reduced by increasing the amount of nonlocal “exact” exchange. In particular, BHHLYP has been recurrently qualified as the best performing standard functional for geometries, interaction energies, and properties of charge-transfer complexes in general.^{33,279,499–501} The need for “exact” exchange is often rationalized by invoking the wrong asymptotic potential in semilocal density functionals, which is corrected in global hybrid variants according to the percentage of “exact” exchange. Since the asymptotic potential is only partially corrected in global hybrid functionals, systems with a relatively small HOMO-LUMO gap (e.g., NaCl at long interatomic distances²⁷ as well as TTF-TCNQ, *vide infra*) can still be affected by spurious charge transfer. Alternatively, long-range corrected exchange (LC-) functionals^{193,407} possess the correct form in the asymptotic region. Two particular flavors (ω B97X-D²⁵² and LC-BOP-LRD^{45,46}) are tested here. The asymptotic potential, which is the central quantity improved by the LC-functionals, is most relevant to better describe charge-transfer at large distances, where overlap effects are negligible and qualitative (and relative) errors of semilocal functionals are therefore most pronounced (*vide infra*). For most systems of chemical interest, however, the charge-transfer in the ground state vanishes at long intermolecular distances. Thus, we argue that when standard functionals underbind, instead of overbind, improving the treatment of weak van der Waals interactions is more critical than increasing the amount of “exact” exchange. Around equilibrium, the overestimation of CT interaction with semilocal functionals can be “damped” by admixing a suitable amount of (mainly repulsive) HF exchange, resulting in seemingly accurate intermolecular distances and interaction energies. Nevertheless, the improvement originates from labile error cancellation between the (overestimated) CT and missing^{14–17} dispersion (*vide infra*).

The importance of charge transfer for interaction energies is generally assessed on the basis of energy decomposition analysis (EDA). Akin to other useful chemical concepts (e.g., atomic charge and aromaticity), interaction energy components (e.g., charge-transfer, dispersion) are, nevertheless, noumena, i.e., unobservables. Thus, they can be quantified by computational means – but not in a unique manner.ⁱ Although conceptually arbitrary, energy decomposition analysis is a powerful method for a quantitative interpretation, which is not accessible from total interaction energies. In particular, such analysis provides valuable insight into the “inner workings” of density functional approximations. Ultimately, EDA may help in further understanding functional performance and guide development aimed to go beyond or improve error cancellation. Perturbation theory can be considered as the most ambitious approach, as the interaction energy is computed directly, i.e., without any self-consistent treatment of the dimer.^{93,502–504} Interaction energies based on natural bond orbitals (NBO) extract the charge-transfer interaction from the density matrix of the dimer.⁵⁰⁵ The best known family of EDAs based on a combination of monomer and dimer computations is related to the en-

ⁱThe molecular Hamiltonian only contains the kinetic energy and the electrostatic attraction (electron–nuclei) and repulsion (electron–electron, nuclei–nuclei), which are, moreover, connected by the virial theorem.

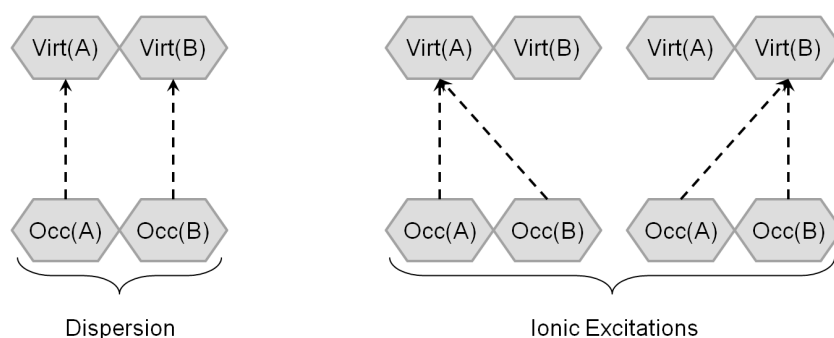


Figure 8.2: Relevant Terms Associated with the Double Excitation Classification in LMP2.

Each arrow indicates the excitation of one electron. Dispersion interactions are excitations of one electron of monomer A into one of its virtual orbitals coupled to a corresponding excitation in monomer B (“induced dipole...induced dipole” interaction). “Ionic” excitations are excitations from monomer B into the virtual space of monomer A coupled with an excitation of one electron of A into its virtual space (and the ones with A and B flipped around).

ergy decomposition of Morokuma⁵⁰⁶ and to its numerous refinements.^{507–510} The separation between charge-transfer and polarization is generally challenging, as it tends to vanish in the complete basis set (CBS) limit and is even undefined in the perturbation approach.^{487,502} The scheme based on the block localized wave function (BLW) from Mo and coworkers^{511,512} provides a well-behaved and insightful energy decomposition analysis including the separation between polarization and CT.^{513,514} Closely related alternatives have advised a real-space partitioning⁵¹⁵ or abandoning the separation altogether.⁵¹⁶ The localized orbitals variant of MP2 (LMP2) represents a special case of an EDA that splits the correlation energy into dispersion interactions and ionic contributions (see Figure 8.2).⁵¹⁷

With the goal of gaining insight into the origin of the failure of standard density functionals to describe binding energies, four energy decomposition schemes are applied herein: symmetry adapted perturbation theory (SAPT);⁹³ BLW,⁵¹³ which distinguishes polarization from charge-transfer; the scheme of Su and Li,⁵¹⁶ which separates terms arising from the exchange and the correlation functional; as well as LMP2, which is used to distinguish ionic from dispersion-type interactions.⁵¹⁷

The following subsections give a qualitative overview of each of these EDA schemes along with the details of the computational settings. As we do not provide the (mathematical/-physical) definitions associated with each scheme, the interested reader is referred to original works and reviews for BLW,^{513,518,519} LMOEDA,⁵¹⁶ SAPT,⁹³ and LMP2.^{517,520} Note that NBO,⁵⁰⁵ which emphasizes charge-transfer, turned out to be completely inadequate for the complexes studied herein: first, stronger charge-transfer interactions are found for HF than for LDA, in disagreement with previous, independent assessments, and second, the charge transfer is too long-ranged for ClF-A (e.g., 1 kcal mol⁻¹ at a distance of 5 Å, where the interaction energy is about 0.1 kcal mol⁻¹).

The geometries for the NF₃ complexes correspond to minima at the MP2/aug-cc-pVTZ level and are taken from ref 498. The geometry of TTF-TCNQ was optimized at the B97-dDsC/def2-TZVP level of theory. Nonequilibrium geometries are constructed from equilibrium structures by varying the intermolecular distance (i.e., “unrelaxed” potential energy profiles).

BLW

The BLW formalism^{512,513} (also known in Q-Chem as “absolutely localized molecular orbitals”, ALMO⁵¹⁴), which serves to separate the polarization energy from the charge-transfer interaction, can be seen as the simplest variant of valence bond theory. The distinction between polarization and charge-transfer energy is stable with respect to the basis set, provided that only a few diffuse functions are used: in the CBS limit, the polarization includes all CT terms already.

With BLW-EDA, the interaction energy is defined as

$$E_{\text{int}} = \Delta E_{\text{FRZ}}^{\text{BLW}} + \Delta E_{\text{pol}}^{\text{BLW}} + \Delta E_{\text{CT}}^{\text{BLW}} \quad (8.1)$$

Akin to the other schemes, the interaction energy is computed with respect to the monomers in the geometry they adopt in the dimer, i.e., excluding the deformation energy. The first term, $\Delta E_{\text{FRZ}}^{\text{BLW}}$, sometimes denoted Heitler-London (HL; especially in the context of BLW at the HF level⁵²¹) or “steric” energy ΔE_s ,⁵¹⁸ corresponds to the energy difference between the monomers and the dimer composed of (frozen) monomer densities. In line with Head-Gordon and coworkers,⁵¹⁴ we refer to this term as the “frozen energy”, $\Delta E_{\text{FRZ}}^{\text{BLW}}$. The frozen energy contains both the electrostatic energy and the Pauli repulsion (due to the antisymmetrization of the product of monomer wave functions). The density-dependent dispersion correction dDsC⁸⁹ essentially alters this term.⁵¹⁸ The polarization energy $\Delta E_{\text{pol}}^{\text{BLW}}$ is the difference between the energy of the “frozen” monomers and the variationally optimized localized state (i.e., the BLW state). Finally, $\Delta E_{\text{CT}}^{\text{BLW}}$ accounts for all of the delocalization energy between the monomers. The delocalization energy is affected by the basis set superposition error and is therefore BSSE corrected. The sum of polarization and charge transfer is denoted as $\Delta E_{\text{POLCT}}^{\text{BLW}}$. BLW-EDA computations, applying the algorithm of Gianinetti et al.,⁵²² were performed in a development version of Q-Chem³⁶⁸ using the 6-311+G** basis set and tight convergence criteria (max DIIS error $< 10^{-8}$), integral thresholds (10^{-12}), and grid settings (99/590 Euler-Maclaurin-Lebedev^{370,371}). The BSSE correction was computed without the dispersion correction. Identical settings were applied for ω B97X-D computations.

LMOEDA

The EDA scheme of Su and Li⁵¹⁶ is implemented under the acronym LMOEDA in GAMESS⁴⁵⁸ (but does not rely on localized molecular orbitals) and decomposes the DFT interaction energy as follows

$$E_{\text{int}} = \Delta E_{\text{ele}}^{\text{LMO}} + \Delta E_{\text{ex}}^{\text{LMO}} + \Delta E_{\text{rep}}^{\text{LMO}} + \Delta E_{\text{pol}}^{\text{LMO}} + \Delta E_{\text{disp}}^{\text{LMO}} \quad (8.2)$$

where “LMO” is used herein to distinguish the energy contributions of the LMOEDA scheme from those of the other EDAs.

Together, $\Delta E_{\text{ele}}^{\text{LMO}} + \Delta E_{\text{ex}}^{\text{LMO}} + \Delta E_{\text{rep}}^{\text{LMO}}$ is closely related to $\Delta E_{\text{FRZ}}^{\text{BLW}}$ but differs in that only the contributions from the exchange functional are included. The “polarization” energy, $\Delta E_{\text{pol}}^{\text{LMO}}$,

contains the exchange functional contributions to the energy difference between the dimer and the (antisymmetrized) product of the monomer wave functions. When compared to BLW-EDA, $\Delta E_{\text{pol}}^{\text{LMO}}$ corresponds to $\Delta E_{\text{POLCT}}^{\text{BLW}}$ minus all contributions associated with the correlation functional. The contributions rooted in the correlation functional (i.e., the difference in “correlation energy” between the monomer and the dimer) are collected into $\Delta E_{\text{disp}}^{\text{LMO}}$.

LMOEDA computations are performed in GAMESS,⁴⁵⁸ using the 6-311+G** basis set and an ultrafine Euler-MacLaurin³⁷⁰/Lebedev³⁷¹ integration grid of 99/590 and 150/1202 for the M06 family of functionals and tight (10^{-12}) integration thresholds. In agreement with earlier reports,⁵²³ the finer integration grid for the M06 family is needed for smooth energy profiles. Identical settings were adopted for LC-BOP-LRD^{45,46} computations.

SAPT

SAPT⁹³ is an *ab initio* method that computes the interaction energy between molecules based on perturbation theory. To facilitate the discussion, we divide the various interaction energy terms into three main classes (frozen energy, polarization/charge-transfer in analogy to the BLW energy decomposition, and dispersion energy, the most interesting component at the SAPT level) and two correlation corrections (one for the frozen energy and one for the polarization/charge-transfer)

$$E_{\text{int}}^{\text{SAPT}} = E_{\text{FRZ}}^{\text{SAPT}} + \epsilon_{\text{FRZ}} + E_{\text{POLCT}}^{\text{SAPT}} + \epsilon_{\text{POLCT}} + E_{\text{DISP}}^{\text{SAPT}} \quad (8.3)$$

The difference between HF and SAPT first-order interaction ($E_{\text{elst}}^{(10)} + E_{\text{exch}}^{(10)} = E_{\text{FRZ}}^{\text{SAPT}}$) plus second order induction(-exchange) ($E_{\text{ind,resp}}^{(20)} + E_{\text{exch-ind,resp}}^{(20)}$) energies is given by δHF .^{421,422} The consideration of $E_{\text{FRZ}}^{\text{SAPT}}$ rather than that of the individual electrostatic and exchange terms seems preferable to us, given that the exchange accounts for the antisymmetrization of the wave function, which is neglected when computing the electrostatic energy. We define $E_{\text{POLCT}}^{\text{SAPT}}$ as the sum of the second order induction(-exchange) energy and δHF , the latter being dominated by corrections to the induction energy. Our notation also emphasizes that polarization and charge-transfer are not separable within SAPT. The dispersion interaction ($E_{\text{DISP}}^{\text{SAPT}}$) is given by the sum of second order dispersion(-exchange) ($E_{\text{disp}}^{(20)} + E_{\text{disp-exch}}^{(20)}$) and the higher-order correction terms ($E_{\text{disp}}^{(21)} + E_{\text{disp}}^{(22)}$). The intramolecular correlation corrections to the first-order interaction energy (ϵ_{FRZ}) are obtained from the sum of the exchange correction $\epsilon_{\text{exch}}^{(1)}$ (CCSD) with that for the electrostatics, $E_{\text{elst,resp}}^{(12)} + E_{\text{elst,resp}}^{(13)}$. Finally, the correction to the induction energy due to the intramolecular correlation ϵ_{POLCT} is given by ${}^t E_{\text{ind}}^{(22)} + {}^t E_{\text{exch-ind}}^{(22)}$. SAPT computations are performed with SAPT 2008.2,⁵²⁴ interfaced to GAMESS,⁴⁵⁸ using the dimer centered aug-cc-pVTZ³⁶³ basis set and frozen core orbitals.

8.2.1 Benchmark Values

Reference binding energies are obtained at the BSSE corrected CCSD(T)-F12b/VTZ-F12^{355,525} level of theory in Molpro2010.1,⁵²⁶ where the df-LMP2⁵¹⁷/VTZ-F12 and BCCD/VTZ-F12 computations are also performed. Note that the basis set will not be indicated further and the F12b will be dropped for clarity.

The reference interaction energies for the larger TTF-TCNQ complex are computed according to

$$\Delta E(\text{CCSD(T)}^*) = \Delta E(\text{HF/AVQZ}) + \Delta E(\text{df-MP2/CBS}) + \delta\text{CCSD(T)}/6\text{-}31\text{G}^*(0.25)$$

The complete basis set extrapolation is carried out with aug-cc-pVTZ and aug-cc-pVQZ (AVTZ and AVQZ, respectively) according to the Helgaker scheme,³⁵⁶ and the higher-order correlation correction $\delta\text{CCSD(T)}/6\text{-}31\text{G}^*(0.25)$ corresponds to the difference between MP2 and CCSD(T) in the 6-31G*(0.25) basis set.^{527,528} Similarly, MP2.5*,⁵²⁹ which is computationally less expensive than CCSD(T)* and therefore applicable to larger systems, refers to MP2/CBS + 0.5(MP3-MP2)/6-31G*(0.25). The asterisk is used to indicate that the composite approach is used to obtain the CBS estimate.

All computations used the Molpro2010.1 defaults for auxiliary basis sets and technical parameters.

8.3 Results and Discussion

The following discussion is divided into five sections aimed at deciphering the physical origin of the interaction energies in CT complexes and assessing the performance of various density functional approximations. Robust *ab initio* and SAPT computations first serve to determine the nature of the interaction energy for 20 NF₃-based complexes and to benchmark DFT methods. The second section contains a detailed analysis of the interaction energy profiles of two representative complexes connecting the source of the binding energy to the DFT performance. The third section provides further insights into the error cancellation by interpreting the individual terms derived from the energy decomposition schemes at both the DFT and *ab initio* levels. The excellent performance of M06-2X is finally scrutinized prior to validating the overall conclusions on a prototypical organic charge-transfer complex, TTF-TCNQ.

8.3.1 General Trends

At the CCSD(T) level of theory, arrangement A (Figure 8.1) is the lowest lying minimum for three out of the four amphiphile molecules (ClF, HF, and HNC) with ClF forming the strongest complex among the series (see Figure 8.3a). HCN binds NF₃ not only the weakest but also with a different preferred arrangement (i.e., D). Both the most strongly bound complex (i.e., ClF-A) and the weakly bound lowest-lying minima (i.e., HCN-D) will be extensively analyzed throughout this study. Whereas half of the complexes are unbound at the HF level, MP2 is

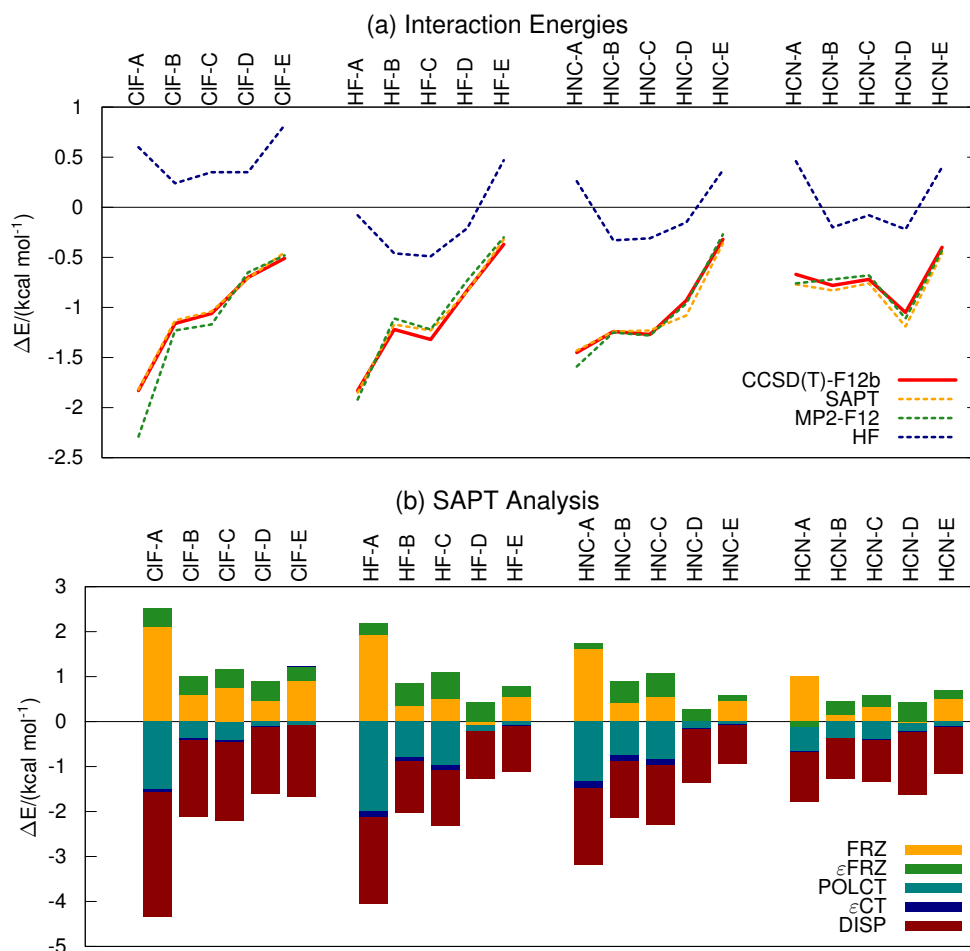


Figure 8.3: (a) Total interaction energy for the 20 complexes studied for wave function methods. (b) SAPT energy decomposition analysis for the complexes.

in a close agreement with CCSD(T) ($\text{MAD} = 0.08 \text{ kcal mol}^{-1}$), indicating that higher-order correlations are of minor importance. MP2 has an appreciable error only for the strongest charge-transfer complex (ClF-A). For these complexes, spin-component scaled MP2¹¹⁸ gives a higher MAD ($0.24 \text{ kcal mol}^{-1}$) than regular MP2. The SAPT level provides an *ab initio* energy decomposition, including some higher-order correlations. The sum of the interaction components agrees remarkably well with CCSD(T) ($\text{MAD} = 0.05 \text{ kcal mol}^{-1}$). SAPT identifies arrangement A as most favorable for charge-transfer ($E_{\text{POLCT}}^{\text{SAPT}}$). According to Figure 8.3b, the contributions of electron correlation to electrostatics and exchange (ϵ_{FRZ}) are small and the correction to polarization (ϵ_{POLCT}) even smaller. Electrostatic interactions ($E_{\text{FRZ}}^{\text{SAPT}}$, mainly dipole-dipole interactions) are most important in arrangement D, which is in line with the picture of the two interacting dipoles (see Figure 8.1). The correlation correction ϵ_{FRZ} is, however, positive, and overall the dipole-dipole interactions are unable to overcome the Pauli repulsion. The major difference between HF and CCSD(T) is thus related to dispersion, confirming that HF adequately describes charge transfer. The arrangements for which HF

Chapter 8. Why are Charge-Transfer Complexes Challenging for DFT?

Table 8.1: Description of Density Functionals, Their Mean Absolute Deviation (MAD) and Mean Signed Deviation (MSD) from CCSD(T)-F12b/VTZ-F12 for the 20 NF₃ Complexes

type	functional name	% “exact” exchange	MAD (MSD)/(kcal mol ⁻¹)
LDA	SVWN5	0.0	0.98 (-0.98)
GGA	PBE	0.0	0.34 (0.22)
	BLYP		0.88 (0.88)
meta-GGA	M06-L	0.0	0.29 (0.21)
hybrid-GGA	B97	19.43	0.52 (0.52)
	B3LYP	20	0.66 (0.66)
	PBE0	25	0.38 (0.38)
	BHHLYP	50	0.41 (0.41)
hybrid-	M06	27	0.43 (0.43)
meta-GGA	M06-2X	54	0.16 (0.09)
	M06-HF	100	0.38 (0.31)
long-range	LC-BOP-LRD	depends on	0.13 (-0.09)
corrected	ω B97X-D	interelectronic distance	0.38 (0.38)

captures some binding (e.g., HF-C or HNC-B) do not correspond to the most strongly bound complexes at the CCSD(T) level, revealing the dramatic failure of HF in correctly predicting trends. The failure is due to the dominance of $E_{\text{DISP}}^{\text{SAPT}}$ over $E_{\text{FRZ}}^{\text{SAPT}} + E_{\text{POLCT}}^{\text{SAPT}}$, even in the case of the strongest CT complex (i.e., ClF-A).

The mean absolute deviations (MAD) for the DFT approximations are given in Figure 8.4. The systematic overbinding of LDA is coincidentally on the same order of magnitude as the underbinding at the HF level (MAD of 0.98 kcal mol⁻¹ and 1.05 kcal mol⁻¹, respectively). As can be seen, the rest of the density functionals perform better than these two extremes, but their performance does not necessarily correlate with the amount of “exact” exchange admixture (e.g., the MAD varies more between two GGAs, i.e., BLYP and PBE, than between a GGA and a hybrid-GGA, i.e., PBE and PBE0, see Table 8.1). In contrast, the density-dependent dispersion correction^{88,89} systematically improves all of the methods tested, lowering the MADs to the range between 0.32 kcal mol⁻¹ (BLYP-dDsC) and 0.07 kcal mol⁻¹ (B97-dDsC). Surprisingly, the long-range corrected functional ω B97X-D²⁵² does not outperform PBE0 or BHHLYP for the NF₃ complexes. However, LC-BOP-LRD^{45,46} and the highly parametrized hybrid-meta GGA functional M06-2X²¹⁴ give excellent results (MAD = 0.13 and 0.16 kcal mol⁻¹, respectively). Dispersion clearly has a major influence on the interaction energies of the studied complexes, rationalizing the poor performance of both HF and standard density functionals. According to SAPT, the charge-transfer plays an obvious role for the most strongly bound complex arrangements (e.g., A).

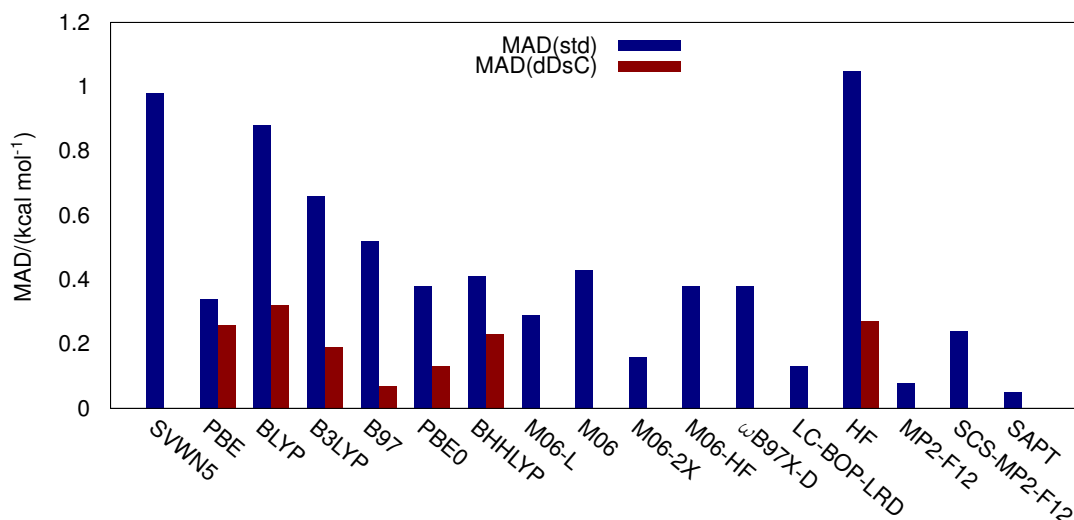


Figure 8.4: Mean absolute deviation (MAD) over the 20 complexes studied. Benchmark values are obtained at the CCSD(T)-F12b/VTZ-F12 level. “dDsC” denotes the use of the dDsC dispersion correction to the corresponding functional.

8.3.2 Relationship between the Nature of Binding Energies and DFT Performance

Interaction energy profiles for the two extreme examples, ClF-A (the most strongly bound NF_3 complex investigated herein) and HCN-D (the minimum energy arrangement for HCN), provide insights into both the origin of the binding energy and the relative functional performance.

The comparison of the rather flat HF profile of ClF-A with the $E_{\text{FRZ}}^{\text{SAPT}}$ curve (corresponding to HF without polarization/CT) indicates that the charge-transfer reduces the molecular repulsion, without actually providing any binding. Hence, for ClF-A, adding a fraction “exact” exchange does not improve the interaction energy (see B3LYP and BHHLYP as compared to BLYP). In such a case, the typical overestimation of the binding energy by the semilocal functionals is only visible when the dispersion interactions are accounted for. Adding a high amount of “exact” exchange indeed offers a significant improvement for BHHLYP-dDsC as compared to B3LYP-dDsC and BLYP-dDsC, which overestimate the binding significantly. Thus, the achievement of an accurate description is highly challenging. Interestingly, the difference between the performances of three functionals is amplified after the inclusion a dispersion correction (dDsC and other schemes).ⁱⁱ It is, however, beyond the scope of *a posteriori* dispersion corrections to overcome the underlying inadequacies of typical functionals to account for charge-transfer. As is well-known, BLYP is more repulsive than BHHLYP for vdW complexes and needs a stronger correction for dispersion in these systems. In contrast, the pure GGA functional is too attractive for charge-transfer complexes and thus should be corrected less in the medium-range. The bottom line is that standard GGA should clearly not be used, as only more sophisticated and well-balanced functionals, such as B97-dDsC, PBE0-dDsC, M06-2X, and LC-BOP-LRD, are sufficiently robust to provide a consistent treatment for these

ⁱⁱThe same amplification is found with D3 and especially with the D3(BJ) dispersion correction

different types of interactions and deliver a good overall performance. Note that we call “well-balanced” functionals those that provide a nearly optimal, yet subtle, interplay between (i) self-interaction error, (ii) over-repulsiveness in the short-range, and (iii) dispersion. ClF-A is, nevertheless, an example for which any kind of error compensation is very difficult, even around the equilibrium distance.

In contrast to the strong charge-transfer complex (i.e., ClF \cdots A), HCN \cdots D is bound even at the Hartree-Fock level, which stresses the importance of dipole-dipole interactions in the arrangement of this complex (see Figure 8.1). On the other hand, BLYP (which is known to be repulsive for van der Waals complexes) underbinds HCN-D significantly when compared to CCSD(T), corroborating that weak interactions play a role as well (see Figure 8.3). While the few complexes in which CT is most important might be overly stabilized at the standard DFT-dDsC level (e.g., ClF-A with BLYP-dDsC, Figure 8.5), the dispersion correction is fundamentally important as it lowers the overall MAD of DFT-dDsC when compared with uncorrected DFT for all other complexes. M06-2X gives an energy profile in close agreement with that of CCSD(T), indicating that the monomer density overlap is non-negligible in the probed region and provides a reasonable description if a suitable parametrization is chosen. The physical reason for the performance of M06-2X is, however, difficult to assess at this stage due to its complex functional form (see more details later). In contrast, the influence of dispersion interactions in B97-dDsC can be evaluated directly. In line with our recent benchmarking over a broad variety of reaction energies,⁸⁹ B97-dDsC shows excellent performance, even in these contrasting and challenging cases.

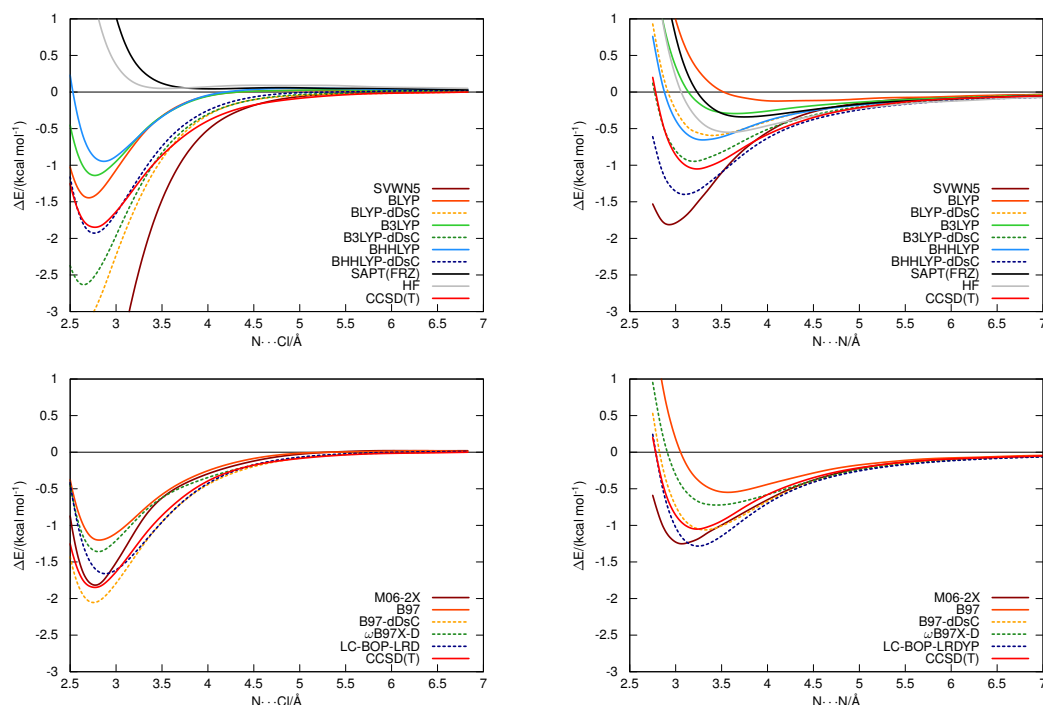


Figure 8.5: Total interaction energy profiles and $E_{\text{SAPT}}^{\text{FRZ}}$ for ClF-A (left) and HCN-D (right). Top: standard functionals. Bottom: modern functionals.

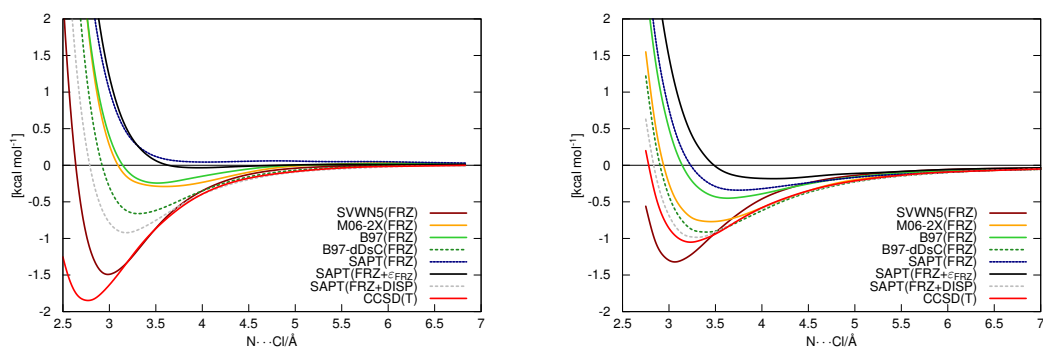


Figure 8.6: Interaction energy contributions for ClF-A (left) and HCN-D (right). For density functionals, $\Delta E_{\text{FRZ}}^{\text{BLW}}$ is shown. For SAPT, three partial sums are shown: $E_{\text{FRZ}}^{\text{SAPT}}$, $E_{\text{FRZ}}^{\text{SAPT}} + \epsilon_{\text{FRZ}}$, and $E_{\text{FRZ}}^{\text{SAPT}} + E_{\text{DISP}}^{\text{SAPT}}$. CCSD(T)-F12b/VTZ-F12 is given as the reference total interaction energy profile.

8.3.3 The Energy Decomposition

The Frozen Term

The electrostatic attraction (described as the most important interaction in related complexes⁵³⁰) is in most cases dominated by the exchange-repulsion ($E_{\text{FRZ}}^{\text{SAPT}} = E_{\text{elst}}^{(10)} + E_{\text{exch}}^{(10)}$) is thus mostly positive in Figures 8.3b and 8.6). $E_{\text{FRZ}}^{\text{SAPT}}$ is therefore of minor importance for the overall stabilizing interaction energy around the equilibrium. Intramolecular correlation influences the electrostatics and exchange only to a minor extent ($E_{\text{FRZ}}^{\text{SAPT}}$ is very similar to $E_{\text{FRZ}}^{\text{SAPT}} + \epsilon_{\text{FRZ}}$). One might expect $E_{\text{FRZ}}^{\text{SAPT}}$ to be similar to the DFT frozen-density interaction energy counterparts, but the latter generally give more attractive profiles. As suggested in ref 518, the dispersion interaction in (dispersion corrected) semilocal DFT approaches is best assigned to the frozen density (Heitler-London or “steric”) term (see refs 531 and 532 for a similar discussion addressing hydrogen bonded systems). Surprisingly, LDA is overly attractive even when compared to the combination of $E_{\text{FRZ}}^{\text{SAPT}}$ with the dispersion energy, $E_{\text{DISP}}^{\text{SAPT}}$! Given the absence of charge transfer in the frozen term, the explanation for the strong binding at the LDA level is not trivial. After correcting the asymptotic region of the LDA exchange correlation potential with the LB94 model¹⁹⁶ (the energy is evaluated with the SPW92 functional), it becomes evident that the incorrect form of long-range potential already affects the frozen term or in other words the density of the superimposed monomers (e.g., $\Delta E_{\text{FRZ}}^{\text{BLW}} = -0.82$ and 0.37 kcal mol⁻¹ for LDA and LDA//LB94 respectively at the equilibrium structure for ClF-A). LDA leads to substantial attractive energy contributions when adding the two monomer densities together. The fluorine atoms, which carry many electrons in a small volume, are affected by a large self-interaction error and characterized by a diffuse density. The association of two excessively diffuse densities, i.e., LDA monomers, is therefore at the origin of the too attractive LDA energy. The error in the exchange-correlation potential does not only affect CT interactions but clearly causes qualitatively incorrect behaviors for monomers and their superposition: the frozen term of most density functionals represents only about 60% of that of SAPT ($E_{\text{FRZ}}^{\text{SAPT}}$). In fact, this “lack of repulsiveness” has been overlooked in the literature as it is partially compensated by the missing dispersion energy in standard density functionals and

might result in relatively reasonable total interaction energies.ⁱⁱⁱ

The difficulties of standard density functionals for describing the interaction between two frozen monomer densities are partly due to the imperfect description of the individual monomer densities (i.e., self-interaction error) along with the approximated energy expression, which might account for (overlap) dispersion interactions. Thus, we expect weakly interacting systems characterized by significant self-interaction (halogenated molecules and dihalogens) to be more problematic than typical vdW complexes for dispersion corrected density functionals.

The CT Terms

For ClF-A, only about 50% of the full binding energy is lost when CT is excluded (see Figure 8.6). The minimum of $E_{\text{FRZ}}^{\text{SAPT}} + E_{\text{DISP}}^{\text{SAPT}}$ is rather flat and located at an increased intermolecular distance compared to CCSD(T). Such a profile indicates that the two monomers approach more closely due to the charge transfer (already seen in Figure 8.5 for the Hartree-Fock interaction energy) with the dispersion energy providing more stability. In contrast, the minimum for HCN-D is dominated by dispersion.

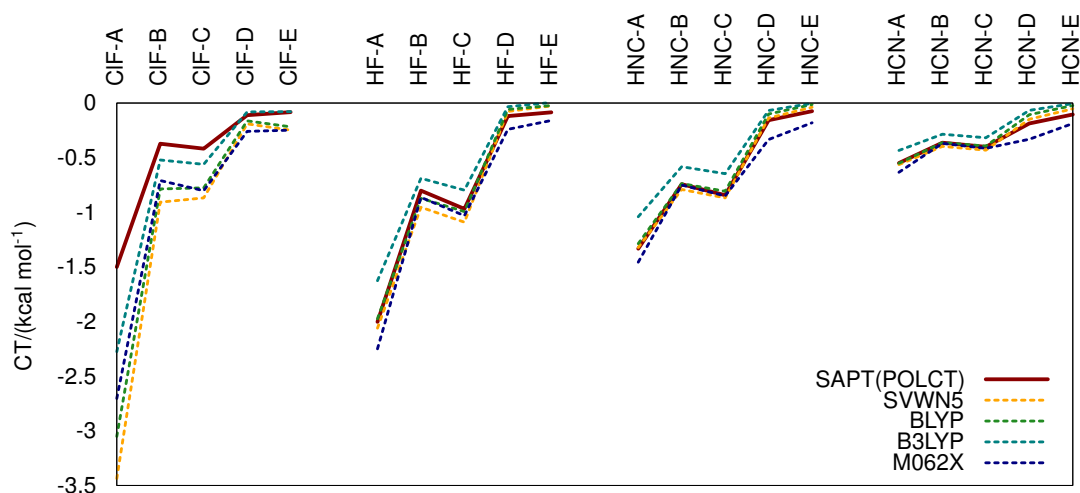


Figure 8.7: Charge-transfer terms from BLW $\Delta E_{\text{CT}}^{\text{BLW}}$ for selected functionals compared to SAPT ($E_{\text{POLCT}}^{\text{SAPT}}$).

According to SAPT, there is less CT in ClF-A than in HF-A (1.5 and 2.0 kcal mol⁻¹, respectively); however, all density functionals tested herein show the opposite trend (see Figure 8.7). In other words, the difficulties with treating CT complexes do not exclusively correlate with the extent of charge transfer, as a stronger CT is not systematically overestimated to a greater extent. $\Delta E_{\text{CT}}^{\text{BLW}}$ is higher for ClF-A than for HF-A but respectively over- and underestimated when compared to the $E_{\text{POLCT}}^{\text{SAPT}}$ value. The charge transfer in other ClF arrangements is overestimated, while for the other complexes the $\Delta E_{\text{CT}}^{\text{BLW}}$ compares well to $E_{\text{POLCT}}^{\text{SAPT}}$. Among the entire series, the description of the ClF complexes is clearly most tricky: the $\Delta E_{\text{CT}}^{\text{BLW}}$ values are

ⁱⁱⁱ A related effect occurs with LC-BLYP when a small/modest value of $\mu \sim 0.33$ bohr⁻¹ is applied.

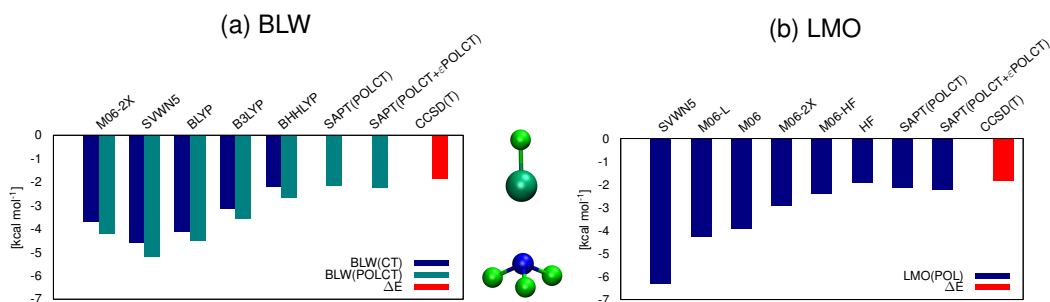


Figure 8.8: Polarization and charge-transfer terms for ClF-A from BLW (left) and $\Delta E_{\text{pol}}^{\text{LMO}}$ (right), compared among different functionals and to SAPT ($E_{\text{POLCT}}^{\text{SAPT}}$ and $E_{\text{POLCT}}^{\text{SAPT}} + \epsilon_{\text{POLCT}}$). For BLW, $\Delta E_{\text{CT}}^{\text{BLW}}$ and $\Delta E_{\text{POLCT}}^{\text{BLW}}$ are shown; CCSD(T)-F12b/VTZ-F12 is given to indicate the (total) interaction strength at the chosen (equilibrium) distance.

substantially larger than those of other complexes and that of $E_{\text{POLCT}}^{\text{SAPT}}$ (see Figure 8.8). This ClF peculiarity highlights the importance of the self-interaction errors occurring between nonbonded halogen atoms that are considerably smaller in the other complexes.

8.3.4 The Particular Case of M06-2X

The charge-transfer term of M06-2X is surprisingly large and much closer to LDA than to BHHLYP (e.g., Figures 8.7 and 8.8, for ClF-A), even though CT is expected to correlate with the amount of “exact” exchange ($\sim 50\%$ for BHHLYP and M06-2X but zero for LDA). The LMOEDA analysis of the M06 functional family delivers a term (i.e., $\Delta E_{\text{pol}}^{\text{LMO}}$) closely related to $\Delta E_{\text{POLCT}}^{\text{BLW}}$ (the energy difference between the frozen monomers and the optimized dimer density) but that depends only on the exchange functional. Unlike $\Delta E_{\text{POLCT}}^{\text{BLW}}$, $\Delta E_{\text{pol}}^{\text{LMO}}$ displays the expected behavior: LDA exhibits the larger $\Delta E_{\text{pol}}^{\text{LMO}}$, which is increasingly reduced at the M06-L, M06-2X, and M06-HF levels, respectively. Knowing that (i) the “dispersion-like” interactions proper to M06-2X do not transpire in the frozen energy (see Figure 8.6, the frozen energy for M06-2X is small compared to $E_{\text{FRZ}}^{\text{SAPT}} + E_{\text{DISP}}^{\text{SAPT}}$) but that (ii) the total interaction energy is reasonably accurate, the missing interaction energy must be recovered in polarization/charge-transfer terms. From comparing the BLW and LMOEDA interaction energy components, it follows that M06-2X compensates the repulsion introduced by “exact” exchange by a correlation functional that gives rise to terms that resemble charge transfer (errors) in standard density functionals. Around equilibrium, the depiction of M06-2X is relatively reasonable: $\sim 40\%$ (and $\sim 20\%$) of $E_{\text{DISP}}^{\text{SAPT}}$ for ClF-A (and HCN-D) originates from the ionic terms^{iv} according to LMP2 (see Figure 8.9). While resembling charge transfer,^v the ionic contributions should be interpreted as the “non-dispersive” component of the “mysterious” medium-range correlation.³⁸⁴ The LMP2 decomposition shows that the dispersion energy of SAPT is equivalent to two components (see also ref 520): one, which is the typical $\sim R^{-6}$ dependent long-range dispersion, and a shorter

^{iv}These percentages are about $\pm 10\%$ accurate, as they depend on the basis set and localization procedure.

^vThe “true” charge-transfer is associated with single-electron excitations, while the ionic terms correspond to two-electron excitations and not to the “correlation corrections” for the single-excitations. Evidence for the distinction between “ionic” and CT is provided by the BCCD reference (which includes all charge-transfer contributions of a correlated wave function) that gives even less interaction energy compared to HF.

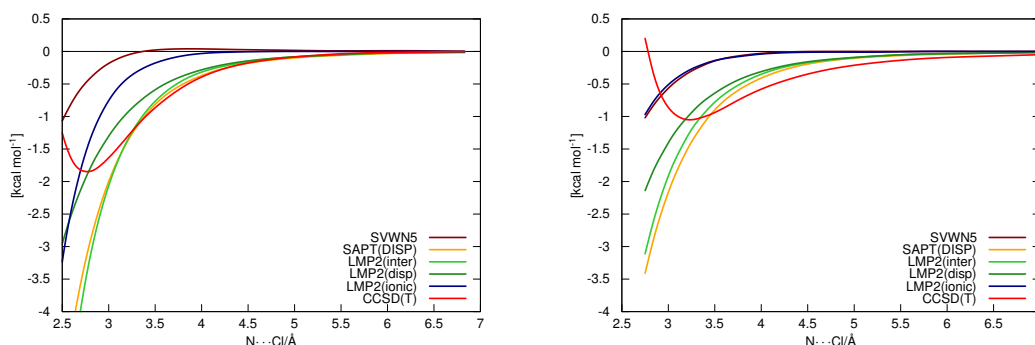


Figure 8.9: $\Delta E_{\text{disp}}^{\text{LMO}}$ from LDA compared to $E_{\text{DISP}}^{\text{SAPT}}$ and the dispersion contribution in LMP2. CCSD(T)-F12b/VTZ-F12 is given to indicate the interaction strength.

range component that should decay exponentially. The exponential decay could in principle be recovered by suitably parametrized functionals, which rationalizes the good performance of M06-2X.

In summary, the treatment of CT by standard density functionals is highly problematic when two diffuse densities interact (e.g., halogens...halogens, halogens...alkenes). The success of M06-2X relies on a significant fraction of medium-range correlation that adjusts itself to the interaction type. On the other hand, properly balanced combinations such as B97-dDsC, PBE0-dDsC, and LC-BOP-LRD represent a very reliable alternative to high parametrization.

8.3.5 A Prototype Organic Charge-Transfer Complex

As mentioned earlier, the role played by vdW interactions in the stabilization of the prototype organic charge-transfer complex, TTF-TCNQ, has not yet been discussed (see ref 496). Akin to the NF_3 complexes considered throughout this study and to the terthiophene-TCNQ assembly (see ref 533), the charge-transfer energy for TTF-TCNQ is surely overestimated by standard DFT methods, even though the minimum is too shallow. Our present analysis suggests that standard hybrid density functionals with a dispersion correction would provide the most reasonable results for interaction energies. Figure 8.11 confirms that the three standard hybrid density functionals tested (B3LYP, PBE0, and B97) together with dDsC lead to interaction energies that agree closely with reference values. Long-range and dispersion corrected functionals (ω B97X-D and LC-BOP-LRD) also perform well for this organic charge-transfer complex. M06-2X correctly describes the region around the equilibrium, but at longer distances the interaction energy falls off too quickly, illustrating that the correct long-range physics are missing. In such cases, the inclusion of a dispersion correction can improve M06-2X as well.⁵³⁴ In contrast to the NF_3 complexes, SCS-MP2 gives closer agreement with higher-level correlation methods than standard MP2 for TTF-TCNQ. Note that the apparent overbinding obtained for M06-2X and ω B97X-D in ref 496 is slightly biased, due to the too small basis set employed in the reference SCS-MP2 interaction profile.

While interaction energies do not clearly correlate with the fraction of “exact” exchange, the

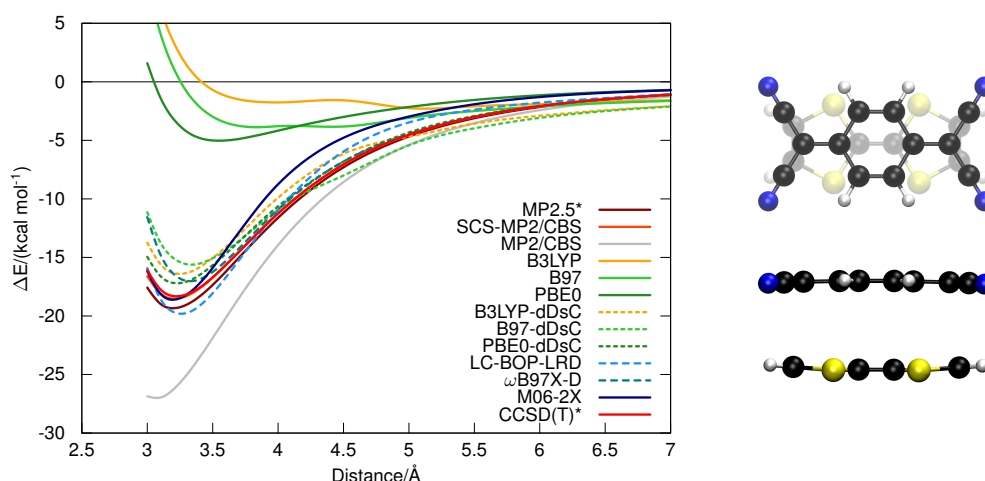


Figure 8.10: Interaction energy of cofacial TTF-TCNQ computed at various levels of theory. Top and side views of the complex are given on the right-hand side.

overestimation of charge-transfer and related properties (such as dipole moments) increase monotonically with decreasing the percentage of “exact” exchange (see Figure 8.11a). From the point of view of interaction energy (Figure 8.10) B3LYP-dDsC and B97-dDsC seem reasonable choices. In contrast, the analysis of dipole moments (which are not affected by the dispersion correction in the current implementation) reveals a serious break down of these functionals at longer (>4.0 Å) distances (Figure 8.11b), a feature which is nearly invisible in the interaction energy profile. At these larger intermolecular distances, the B3LYP and B97 HOMO-LUMO gap collapses, resulting in a spurious charge transfer. This unphysical behavior is strongly dependent on the intermolecular distance and on the planarity of the monomers’ geometry. The more pronounced orbital overlap at shorter distances or, alternatively, the inclusion of a larger amount of nonlocal exchange (e.g., PBE0) prevents this unphysical behavior. Interestingly, the limiting amount of “exact” exchange is roughly the same (20%) as that necessary for a successful geometry optimization of alkynyl radicals.⁵³⁵ The change of sign in the profile of the molecular dipole moment (Figure 8.11b) can be rationalized by the gradual decrease of the charge transfer with increasing intermolecular distance, which goes in the opposite direction as the sum of the molecular dipole moments that are aligned and amount to ~ 0.6 D in the z direction (from TCNQ to TTF) at the BCCD/6-31G*(0.25) level.

The challenge for common DFT approximations to describe charge-transfer complexes is connected to both the lack of dispersion interactions resulting in inaccurate binding energies and the overestimated charge transfer, which, depending on the percentage of “exact” exchange and the intermolecular distances, can lead to erroneous values for density-based properties (e.g., dipole moments). Stressing the role of dispersion interactions in CT complexes, of course, does not imply that electrostatics and/or charge-transfer interactions are unimportant for the description of binding energy. As mentioned above, dispersion bound complexes show a strong dependence on the relative orientation.⁴⁹¹ This dependence might reflect not only the loss of contact area but also the enhancement of dispersion through electrostatic and

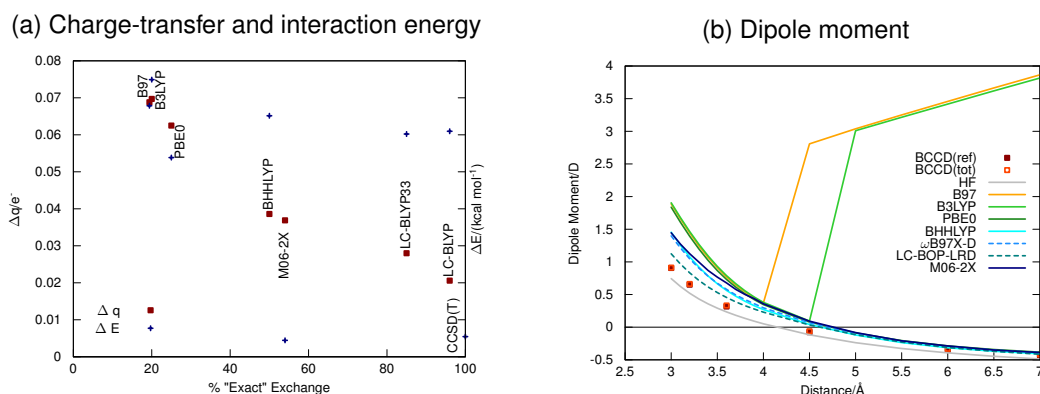


Figure 8.11: (a) Charge-transfer (according to BLW/ALMO; red diamonds, referring to the left axis) and interaction energy (blue squares, referring to the right axis) at the equilibrium distance (3.2 Å) of TTF-TCNQ. (b) Molecular dipole moment in z direction of TTF-TCNQ as a function of the distance. The z axis points from TCNQ to TTF. Due to the computational expense, only a few points at the BCCD/6-31G*(0.25) reference level are included. Note that these are closed-shell singlet computations. The spurious charge-transfer of B3LYP and B97 at longer distances can lead to a lower lying open-shell singlet solution, which enhances the charge transfer even further.

charge-transfer interactions, which may allow the monomers to approach one another more closely in one binding mode as opposed to another. In many cases, dispersion interactions are, however, responsible for most of the stabilization energy, and the use of noncorrected standard density functionals is therefore precluded, as they might lead to erroneous conclusions about the nature of the binding. The inclusion of *a posteriori* dispersion corrections such as dDsC represents an inexpensive and broadly applicable method (as compared to LMP2 and SAPT) to appropriately describe charge-transfer complexes and to provide qualitative insight into the ubiquitous importance of dispersion interactions.

8.4 Conclusions

The description of charge-transfer complexes is highly challenging for standard density functionals. On the basis of an illustrative series of NF_3 -based complexes, we have demonstrated that the stabilization of most CT complexes arises essentially from dispersion interactions, with relative orientations and intermolecular distances being dictated by electrostatics and charge-transfer interactions. Despite the illustrative overestimation of the charge-transfer interactions by common density functionals, the use of a dispersion correction is crucial in providing an accurate description of interaction energies. Highly parametrized functionals such as M06-2X also describe such systems well, due to the substantial density overlap in the intermolecular distances of interest. However, because of the lack of an explicit dispersion term, individual interaction energy components (e.g., charge-transfer) cannot be easily interpreted. Due to the subtle interplay of monomer description, overestimation of charge transfer, and neglect of dispersion interactions, only certain well balanced dispersion corrected density functionals provide excellent results; in particular, LC-BOP-LRD and PBE0-dDsC are confirmed to be broadly applicable. The validity of these observations for rationalizing the DFT binding energy of “real-world” charge-transfer complexes has been verified on a typical

cofacial TTF-TCNQ organic complex. Importantly, the description of the density at distances longer than equilibrium necessitates, even in the ground state, more than 20% of “exact” exchange to prevent spurious charge transfer, a failure that is not directly noticeable in the interaction energy profile itself.

9 Exploring the Limits of DFT for Interaction Energies of Molecular Precursors to Organic Electronics

9.1 Introduction

The rapidly growing field of organic electronics is dominated by π -conjugated molecules, which, because of their attractive properties, represent ideal functional units in molecular wires, organic solar cells, organic light-emitting diodes, and organic field-effect transistors.^{484,485,536} Similarly, molecular switches, motors and artificial muscles typically rely on π -functional frameworks for converting an optical or electrochemical signal into a mechanical response.^{537–541} Electronic structure computations provide routes to valuable information regarding the nature of the intermolecular interactions within molecular precursors to organic electronics, where neutral dimers model the resting state and charged radical π -dimers represent typical charge-carriers, i.e., the ultimate functional units.

Kohn-Sham density functional theory¹¹ (DFT) is the most popular electronic structure method for describing structures and properties of relatively large systems, including π -functional molecules and materials. Despite their ability to provide computationally efficient access to many ground state properties with reasonable accuracy, standard DFT approximations do not perform well in describing the interaction energies of π -conjugated molecules. The most obvious failures arise in assembled neutral monomers (e.g., dimers), where van der Waals interactions contribute substantially to the total binding energy. However, the most used semilocal (hybrid) functionals are intrinsically unable to accurately describe these nonlocal dispersion forces.^{14–17} Fortunately, the neglected interactions can be conveniently accounted for by *a posteriori* atom pairwise dispersion energy corrections.^{38,39,42,44,45,79,89} Our recently introduced density-dependent dispersion correction, dDsC,^{81,88,89} improves the performance of standard density functionals dramatically for describing both intermolecular interactions and reaction energies.^{86,89} Hybrid functionals, when combined with dDsC, also succeed in describing the ground state interaction energy of charge-transfer complexes, as illustrated by the prototypical tetrathiafulvalene-tetracyanoquinodimethane (TTF-TCNQ) complex.⁹⁰ In this chapter, our primary focus is placed on the investigation of binding energies of π -dimer

radical cations, e.g., (thiophene) $_2^{\cdot+}$, which are formally mixed valence dimers. Standard density functionals fail to properly handle systems with fractional charges: at large intermolecular distances the delocalization (or self-interaction) error artificially stabilizes one positive charge delocalized over two molecules in comparison to a situation with one positively charged and one neutral molecule.^{26,28,29,190} Around equilibrium, the errors are smaller, but the description of mixed valence states remains subtle. Doubly charged π -dimers (e.g., tetracyanoethylene, (TCNE) $_2^{2-}$)⁵⁴² present yet another issue, that is the static correlation error.¹⁷⁸ In this case, the dissociation of singlet (TCNE) $_2^{2-}$ is not possible without breaking spin symmetry. Such dimers are difficult to describe even around equilibrium due to an important degree of multi-reference character.^{543–545} In addition, doubly charged dimers tend to be unstable in gas-phase due to Coulomb repulsion and are therefore excluded from this study.

Taken together, the failures of standard density functionals for dispersion interactions, mixed-valence states and multi-reference character, the prospects for investigating π -functional molecules with standard DFT approximations appears rather discouraging. However, the size of the materials of practical interest precludes the application of generally robust, highly accurate *ab initio* methods to compute binding energies (e.g., CASPT2 or multi-reference coupled cluster). Herein we present a benchmarking study to identify the best available modern functionals that are applicable to reproducing interaction energies of “real world” systems. Since the typical test sets representative of noncovalent interactions are dominated by bio-related model compounds, we introduce two benchmark sets of interaction energies: Orel26rad and Pi29n. Orel26rad features 26 radical cation model compounds for charge-carriers in organic electronics, while the underrepresentation of neutral sulfur containing heterocycles (e.g., thiophene⁵⁴⁶) and naphthalene complexes^{547,548} in common test sets (e.g., S22²⁹⁹) prompted the introduction of an additional set of 29 binding energies of neutral intermolecular complexes (Pi29n). The new databases allow for a thorough assessment of the capabilities of density functionals to describe the interaction energies relevant for organic electronic precursors.

9.2 Methods and Computational Details

9.2.1 Construction of the test set

All monomers are optimized at the B3LYP/6-31G* level^{154,155,161,162} in Gaussian 09,³⁹⁹ except for TTF-TCNQ, which is our previously published equilibrium geometry.⁹⁰ The optimized geometries of the neutral and cationic monomers are used to construct the test sets without further relaxation: the radical dimer cations are built from the geometry of one neutral and one cationic monomer. Intermolecular distances and relative orientations were either taken from the literature (thiophene dimers,⁵⁴⁶ naphthalene dimers⁵⁴⁷ and naphthalene...benzene complexes⁵⁴⁸) or obtained from scans (steps of 0.1 Å) at the counterpoise corrected df-MP2/6-31G*(0.25) level of theory. In general, the monomer centers are superimposed and only the intermolecular distance is optimized. Exceptions are the parallel thiophene...benzene (T-Bz_P), the (anti)-parallel thiophene...pyridine complexes (T-Py_P and T-Py_AP) and the second anti-parallel thiophene dimer radical cation (T₂_AP2 $^{\cdot+}$) for which the relative dis-

Table 9.1: Abbreviations for Monomers and their Relative Orientation Used to Identify Dimers Included in the Two Test Sets Orel26rad and Pi29n

F : furan	S : slipped
T : thiophene	P : parallel
bz : benzene	AP : anti-parallel
Py : pyridine	X : cross
Pyr : pyrrole	T : T-shape (heteroatom down)
bF : bifuran	T' : T-shape (heteroatom up)
bT : bithiophene	·⁺ : radical cation
TT : thienothiophene	
TTF : tetrathiafulvalene	
TCNQ : tetracyanoquinodimethane	

placement was optimized as well (see Table 9.1 for the explanations of the abbreviations).

9.2.2 Benchmark Computations

The highest computational level uniformly applicable for all dimers studied herein, is an estimated CCSD(T)/CBS interaction energy, which we denote by CCSD(T)*. The MP2 interaction energy is extrapolated to the CBS limit exploiting the efficiency of density-fitting (df)⁵⁴⁹ and corrected by the δ CCSD(T) term from a much smaller basis set

$$\Delta E(\text{CCSD(T)*}) = \Delta E(\text{HF/AVQZ}) + \Delta E(\text{df-MP2/CBS}) + \delta\text{CCSD(T)}/6\text{-}31\text{G}^*(0.25) \quad (9.1)$$

The complete basis set extrapolation is carried out with aug-cc-pVTZ and aug-cc-pVQZ (AVTZ and AVQZ, respectively) employing the Helgaker scheme³⁵⁶ and the higher-order correlation correction δ CCSD(T)/6-31G*(0.25) corresponds to the difference between MP2 and CCSD(T) in the 6-31G*(0.25) basis set, where (0.25) indicates the exponent of the set of d-orbitals added to the 6-31G basis set for all atoms except hydrogen.^{527,528} All components are corrected for the basis set superposition error (BSSE) according to the Boys-Bernardi procedure.³⁵³ *Ab initio* computations used the Molpro2010.1⁵²⁶ defaults for auxiliary basis sets and technical parameters. For df-MP2/6-31G*(0.25) the auxiliary basis set of aug-cc-pVDZ has been applied. Equation of motion for ionization potentials (EOM-IP) coupled cluster methods are specifically designed to describe neutral and ionized species at a comparable level of accuracy. In order to validate the use of single reference CCSD(T)* as a benchmark level, the interaction energy of the benzene dimer cation was computed with CCSD(T), EOM-IP-CCSD^{550,551} and EOM-IP-CCSD(2,3)⁵⁵² in the small 6-31G*(0.25) basis set. The results at the three levels do not differ by more than about 1 kcal mol⁻¹, suggesting good accuracy of CCSD(T) for the radical cations. Note, that spin-contamination is largely avoided given that open-shell systems are treated in the RMP2⁵⁵³ and ROHF-UCCSD(T)^{554,555} framework. A breakdown of the single-reference treatment was observed for (pyridine)₂^{·+} complex, which is described as unbound and has

therefore been dropped from the test set.

9.2.3 Symmetry Adapted Perturbation Theory

Symmetry adapted perturbation theory (SAPT)⁹³ is an *ab initio* method that decomposes the interaction energy between molecules based on perturbation theory. At the SAPT0 level, 6 terms contribute to the interaction energy: classical electrostatics $E_{\text{elst}}^{(10)}$ (electron-electron and nuclei-nuclei repulsion, counterbalanced by electron-nuclei attraction), exchange $E_{\text{exch}}^{(10)}$ (arising from satisfying the Pauli-exclusion principle), induction $E_{\text{ind}}^{(20)}$ (equivalent to polarization or charge-transfer in other terminologies), exchange-induction $E_{\text{exch-ind}}^{(20)}$ (the correction for keeping the wave function antisymmetric) and finally dispersion and exchange-dispersion $E_{\text{disp}}^{(20)} + E_{\text{disp-exch}}^{(20)}$, accounting for the correlated motion of electrons between the two monomers.

$$E_{\text{int}}^{\text{SAPT0}} = E_{\text{elst}}^{(10)} + E_{\text{exch}}^{(10)} + E_{\text{ind}}^{(20)} + E_{\text{exch-ind}}^{(20)} + E_{\text{disp}}^{(20)} + E_{\text{disp-exch}}^{(20)} \quad (9.2)$$

For strongly interacting fragments, the δHF term^{421,422}

$$\delta^{\text{HF}} = \Delta E^{\text{HF}} - E_{\text{elst}}^{(10)} - E_{\text{exch}}^{(10)} - E_{\text{ind}}^{(20)} - E_{\text{exch-ind}}^{(20)} \quad (9.3)$$

which is the difference between the (counterpoise corrected) HF interaction energy and the electrostatics, exchange and (exchange-)induction is often necessary to achieve agreement with supermolecular approaches. $E_{\text{int}}^{\text{SAPT0}} + \delta^{\text{HF}}$ corresponds to Hartree-Fock plus the SAPT0 (exchange-)dispersion and is denoted by HF+Disp herein

$$E_{\text{int}}^{\text{HF+Disp}} = \Delta E^{\text{HF}} + E_{\text{disp}}^{(20)} + E_{\text{disp-exch}}^{(20)} \quad (9.4)$$

Open-shell SAPT0⁵⁵⁶ computations were performed in SAPT 2008,⁵²⁴ interfaced with Dalton 2.0,⁵⁵⁷ using the 6-31G*(0.25) basis set.⁵²⁷ Akin to MP2, SAPT0 is known to provide more accurate results in modest basis sets than at the complete basis set limit for neutral complexes of π -conjugated systems.^{558,559} Since MP2/6-31G*(0.25) is accurate for the radical cations studied herein (*vide infra*), SAPT0 in the same, small basis set is expected to yield reasonable results as well. Note that we use SAPT0 with uncoupled response functions (“MP2-like”), as the coupled induction and dispersion energies do not benefit from the invoked error cancellation. For example, the dispersion energy is given by

$$E_{\text{disp}}^{(20)} = -4 \sum_{ia,jb} \frac{|(i^A a^A | j^B b^B)|^2}{\epsilon_a^A - \epsilon_i^A + \epsilon_b^B - \epsilon_j^B} \quad (9.5)$$

where i, j and a, b are occupied and unoccupied orbitals, respectively, $(ia|jb)$ is the two-electron repulsion integral in chemist's notation and ϵ_i is the i^{th} orbital energy, while A and B labels the two monomers.

9.2.4 Density Functionals Tested

In addition to the standard generalized gradient approximations (GGA) BLYP and PBE and four hybrid density functionals (B3LYP,^{154,155,161,162} B97,²⁰⁹ PBE0^{217,280} and PW6B95,⁴⁵⁶ which contain 20, 19.43, 25 and 28 % “exact” exchange), several “modern” functionals are included in the benchmark:

The double hybrid B2PLYP¹⁶³ contains 53% “exact” exchange and 27% MBPT2 correlation energy, partially accounting for weak interactions. Nevertheless, for general applications *a posteriori* dispersion corrections have been recommended, denoted by appending -D (=D2),⁸⁵ -D3⁴² and -D3(BJ).⁴³

The long-range corrected (LC) exchange functionals are motivated by the incorrect decay of the potential of standard DFT functionals (the xc potential of semilocal functionals decays exponentially along with the density, while the asymptotic form of the exact potential is $-1/r$). The too rapid decay is held responsible for the delocalization error, causing the overstabilization of fractionally charged fragments.⁵⁶⁰ LC functionals lead to the correct asymptotic potential and have been shown to reduce the delocalization error significantly.^{28,189}

The long-range correction to exchange is introduced through the range-separation scheme, pioneered by Savin et al.^{193,194} and popularized by Hirao and coworkers.⁴⁰⁷ For more details see section 2.2.2 on page 13. LC-BOP,^{392,407} and LC- ω PBE^{393,394} (also known as LC- ω PBE08) are long-range corrected exchange functionals tested herein: the long-range is described by “exact” exchange and the short-range by semilocal DFT exchange.

M06-2X²¹⁴ is a flexible, carefully fitted highly empirical hybrid-meta-GGA functional (54% “exact” exchange and about 30 parameters), designed to describe main group elements and weak interactions accurately. The more recent Minnesota functional M11⁵⁶¹ follows the same spirit, but includes 100% long-range and 42.8% short-range “exact” exchange.

Dispersion is a nonlocal phenomenon, absent from standard density functionals.^{14–17} Accounting for the nonlocal nature is computationally expensive, but reasonably practical schemes have been developed recently, e.g., the herein tested VV10 functional.⁴⁸ Alternatively, *a posteriori* atom pairwise dispersion energy corrections have been shown to capture the essence of the dispersion interaction energies.^{38,39,42,44,45,79,81,89} The general formula for such corrections is given by

$$E_{\text{disp}} = - \sum_{i=2}^{N_{\text{at}}} \sum_{j=1}^{i-1} f_d(R_{ij}; i, j) \frac{C_6^{ij}}{R_{ij}^6} \quad (9.6)$$

where N_{at} is the number of atoms, C_6^{ij} the dispersion coefficient between atom i and j and $f_d(R_{ij}; i, j)$ the damping function, which has to remove the divergence at zero internuclear distance R_{ij} . Furthermore, f_d adapts the correction to a given functional. In “classical” dispersion corrections, the dispersion coefficients are fixed parameters and the damping function depends on tabulated van der Waals radii.^{38,39} To improve the accuracy, dependence on the geometry⁴² or, even more general, on the electron density have been developed.^{44,45,79,89} Two density-dependent variants are tested: our recently introduced dispersion correction

dDsC^{81,88,89} and the local response dispersion (LRD) scheme of Sato and Nakai.^{45,46} Note that both density dependent dispersion energy corrections are applied *a posteriori*, i.e., they do not influence the electron density.

Combining a LC-functional with a dispersion correction is expected to lead to generally robust functionals, even though some combinations are known to be problematic.^{89,90,414} Herein, we test LC- ω PBE($\omega = 0.45$ bohr⁻¹)^{393,394} together with dDsC and either PBE, LYP¹⁵⁵ or B95¹⁸⁵ correlation, leading to LC- ω PBE-dDsC, LC- ω PBELYP-dDsC and LC- ω PBEB95-dDsC. PBE correlation is the “natural” choice, but LYP and B95 are one-electron self-interaction free and might therefore offer some further reduction of the delocalization error. Alternatively to dDsC, LC- ω PBE is combined with Vydrov and Van Voorhis’ fully nonlocal correlation functional, denoted by LC-VV10.^{48,562} Similarly, LC-BOP-LRD corrects LC-BOP with the local response dispersion (LRD) method.^{45,46} Finally, ω B97X-D combines a highly fitted, long-range corrected exchange functional with a “classical” dispersion correction.²⁵²

In summary, five different variants of LC-functionals that should also account for weak interactions are assessed: an empirical, but specifically adapted exchange and correlation functional (M11),⁵⁶¹ an empirical exchange-correlation functional fitted together with an “classical” dispersion correction (ω B97X-D)²⁵² and three different density-dependent dispersion corrections applied to LC-functionals that have not been specifically refitted (dDsC,⁸⁹ LRD^{45,46} and VV10⁴⁸).

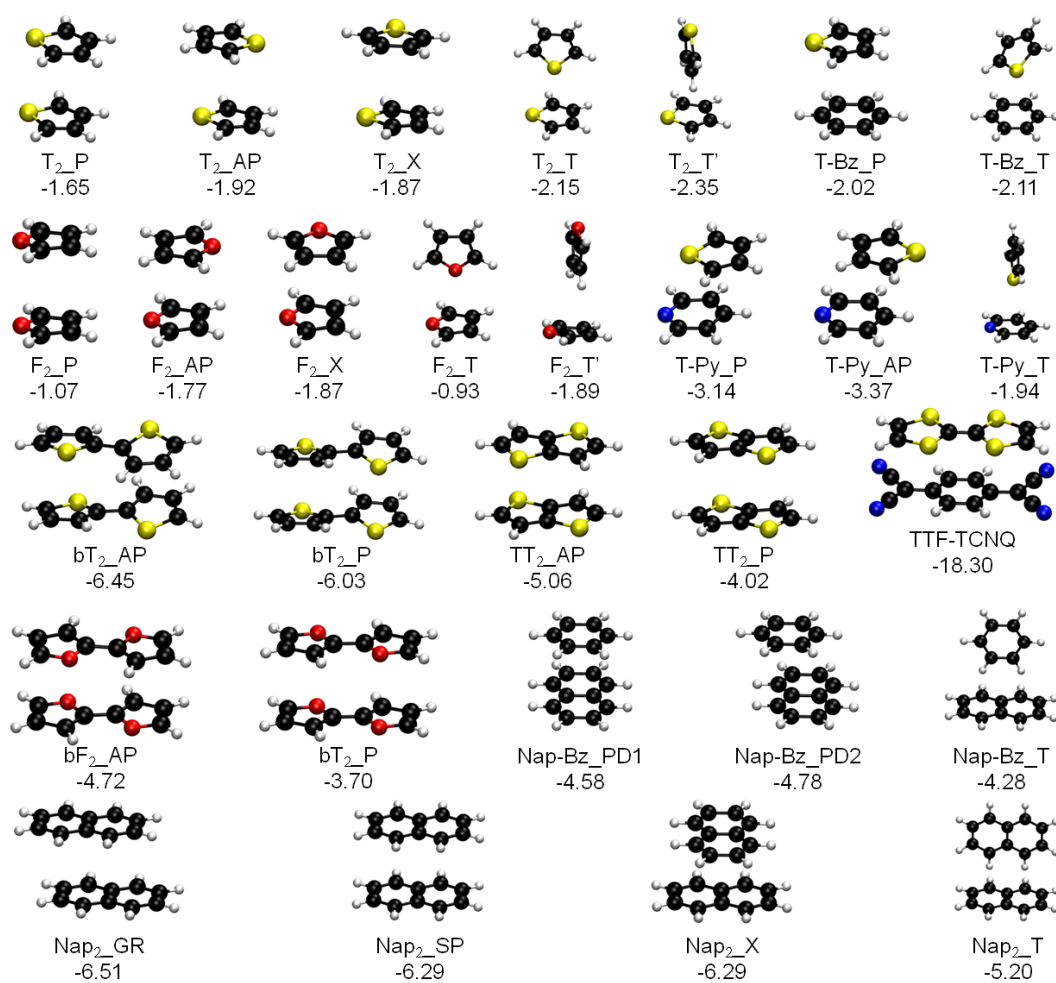
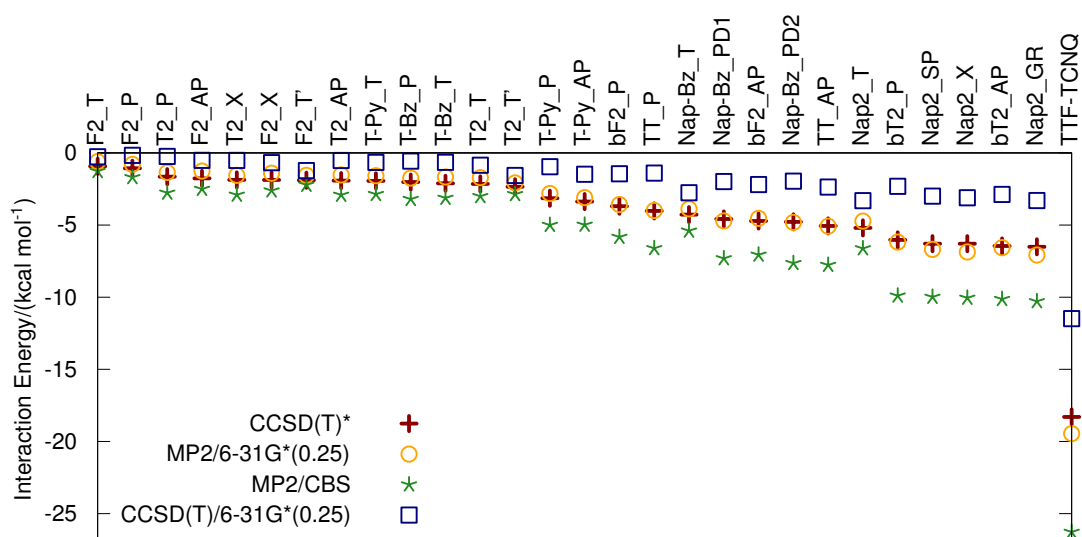
All DFT computations are run in a development version of Q-Chem,³⁶⁸ except LC-BOP-LRD,^{45,46} which is performed in GAMESS.⁴⁵⁸ LC-BOP-LRD[10,0] refers to LC-BOP-LRD without the multi-center corrections to the C_6 coefficients introduced in ref 46. For benchmarking purposes, the large def2-QZVP(-g)⁴⁵⁹ basis set has been applied. For testing a level more likely to be used in “real life” applications, selected data is also provided with the small 6-31G* and medium sized 6-311+G** basis sets. The integral threshold was set to 10^{-12} and a 75/305 Euler-Maclaurin-Lebedev^{370,371} grid was used for most computations, but for M06-2X²¹⁴ and M11⁵⁶¹ the finer 99/590 grid was adopted in order to account for their higher dependence on the integration grid accuracy.⁵²³ The nonlocal part of the VV10⁴⁸ functional and all 6-31G* computations exploited the efficient SG-1 grid.³⁷² B2PLYP¹⁶³ computations were accelerated by the resolution of identity with the auxiliary basis set of aug-cc-pVTZ. DFT computations are not corrected for the BSSE and open-shell systems were treated in the unrestricted formalism. For several of the radical cation π -dimers identifying the lowest energy SCF solution was difficult for long-range corrected exchange functionals, even around equilibrium.

9.3 Results and Discussion

9.3.1 The Test Sets

This subsection introduces the test sets and discusses general trends based on the reference interaction energies (estimated CCSD(T)/CBS).

The Pi29n test set consists of a selection of weakly polar, neutral stacked and T-shaped π -dimers including 15 sulfur-containing complexes (i.e., thiophene, thienothiophene and bithio-

Figure 9.1: Pi29n test set with estimated CCSD(T)/CBS interaction energies in kcal mol⁻¹.Figure 9.2: *Ab initio* interaction energies in kcal mol⁻¹ for the Pi29n test set. CCSD(T)* denotes the estimated CCSD(T)/CBS values serving as the benchmark.

phene). Pi29n is representative of the “resting state” of organic electronics, not well represented in other test sets (e.g., PPS5/05⁴⁵⁶ and S22²⁹⁹). The test set also contains two weak (thiophene...pyridine) and one strong (TTF-TCNQ) donor-acceptor complexes. Instead of the typical benzene dimer included in several test sets (e.g., PPS5/05⁴⁵⁶ and S22²⁹⁹), the interactions between unsaturated hydrocarbons are here illustrated by the benzene...naphthalene and naphthalene dimers. The dimers are illustrated in Figure 9.1 with their abbreviations explained in Table 9.1. Due to the absence of hydrogen bonds, the interaction energies probed by Pi29n are dominated by dispersion. Nevertheless, electrostatic (e.g., dipole-dipole) and charge-transfer (donor-acceptor) interactions modulate the strength of the dispersion interactions by influencing the intermolecular separation (*vide infra*).

In line with the benzene dimer, the T-shaped thiophene dimer is more favorable (by about 0.4 kcal mol⁻¹) than the sandwich conformation, independently from the alignment of the molecular dipoles (parallel vs. anti-parallel), which was already noted by Tsuzuki et al.⁵⁴⁶ The interaction energies of the furan dimers follow the same trends, with the exception of F₂_T, which is the least stable orientation, presumably due to the lower polarizability of the oxygen atom as compared to sulfur. The stacked thiophene...benzene dimer has essentially the same interaction energy as the anti-parallel stacked thiophene dimer (~2 kcal mol⁻¹, slightly larger than the 1.7 kcal mol⁻¹ for stacked benzene dimer³⁶⁰). The thiophene...pyridine interaction energy is substantially higher (~3 kcal mol⁻¹) also when compared to the parallel displaced benzene dimer (~2.7 kcal mol⁻¹).³⁶⁰ The increasing interaction energy going from the thiophene dimer to thiophene...pyridine can be easily rationalized by the weak donor-acceptor ability of the electron rich thiophene and the electron poor pyridine. This charge-transfer interaction reduces the intermolecular distance from ~4.0 to 3.5 Å and concurrently leads to an augmentation of the dispersion interactions in the complex similar to TTF-TCNQ.⁹⁰

Complexes involving larger monomers such as bifurane, thienothiophene, bithiophene and naphthalene are bound more strongly due to the increase in dispersion interactions. The largest interaction energy of 6.5 kcal mol⁻¹ is achieved for the anti-parallel bithiophene dimer (bT₂_AP) and the graphite like naphthalene dimer (Nap₂_GR). The less polarizable bifuran dimers are bound less strongly (4.7 kcal mol⁻¹ for bF₂_AP). Alternatively, the T-shaped dimers are destabilized with respect to parallel displaced geometries when increasing the monomer size: the two types of benzene dimers are essentially isoenergetic (2.7 kcal mol⁻¹),³⁶⁰ the parallel displaced benzene...naphthalene is slightly favored over the T-shaped (4.8 vs. 4.3 kcal mol⁻¹), whereas the energy difference is larger than 1 kcal mol⁻¹ (5.2 vs. 6.5 kcal mol⁻¹) for naphthalene dimers. The prototypical charge-transfer complex TTF-TCNQ has, by far, the largest interaction energy ($\Delta E=18.2$ kcal mol⁻¹).

This study's largest emphasis is placed on the radical cationic π -dimers (see Figure 9.4). In contrast to the neutral Pi29n complexes, the dimer radical cations are not only bound by dispersion but characterized by significant electrostatic, polarization and charge-resonance (similar to the charge-transfer in case of the neutral monomers and also sometimes referred to as “covalent-like”) interactions typical of ion...neutral complexes. The relative orientation of the two monomers is determinant for the charge-resonance: the better the orbital overlap of the HOMO/SOMO, the more stabilized is the complex.

To span a representative range of monomers commonly employed in p-doped organic polymers, we selected a set of homo- and heterodimers of pyrrole, furan and thiophene. The benzene dimer radical cation represents the most investigated species of its kind^{563–569} and is also included in the test set. The larger bithiophene, bifuran, thienothiophene and TTF mixed valence dimers provide more realistic models of organic electronics precursors.

The anti-parallel pyrrole and furan dimer radical cations ($\text{Pyr}_2\text{AP}^{+\cdot}$ and $\text{F}_2\text{AP}^{+\cdot}$) are the most strongly bound complexes (about 20 kcal mol^{-1}) of Orel26rad. This strong interaction energy is best explained by the optimum monomer orbital alignment (along the C=C double bonds) that leads to the bonding SOMOs in the dimer radical cations. The interaction energies of these “special” dimers ($\text{Pyr}_2\text{AP}^{+\cdot}$ and $\text{F}_2\text{AP}^{+\cdot}$) are matched closely only by the significantly larger TTF dimer radical cations (17 and 18 kcal mol^{-1} for the cross and parallel orientation, respectively). The anti-

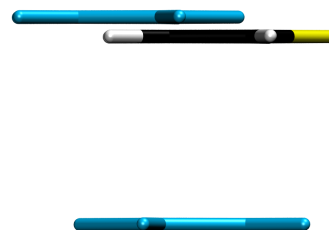


Figure 9.3: Comparison of $\text{T}_2\text{AP}^{+\cdot}$ in cyan and $\text{AP}_2^{+\cdot}$.

parallel thiophene radical cation dimer ($\text{T}_2\text{AP}^{+\cdot}$) is bound by about 14 kcal mol^{-1} , which is $2.5 \text{ kcal mol}^{-1}$ less than the benzene dimer radical cation and significantly less than $\text{Pyr}_2\text{AP}^{+\cdot}$ and $\text{F}_2\text{AP}^{+\cdot}$. It is worthwhile noting that since sulfur is larger than oxygen, the intermolecular distance is increased in $\text{T}_2\text{AP}^{+\cdot}$ relative to $\text{F}_2\text{AP}^{+\cdot}$ (3.2 vs 2.9 \AA). The amount of Pauli repulsion is reduced in the lateral displaced arrangement as the sulfur lies above the “empty” region between the two hydrogen atoms ($\text{T}_2\text{AP}_2^{+\cdot}$ in Figure 9.3). In the latter arrangement, the two thiophene monomers are closer to each other (2.9 \AA), resulting in an increase in interaction energy from 14.2 to $17.6 \text{ kcal mol}^{-1}$ for $\text{T}_2\text{AP}^{+\cdot}$ and $\text{T}_2\text{AP}_2^{+\cdot}$, respectively.

The larger anti-parallel bithiophene radical cation dimers, $\text{bT}_2\text{AP}^{+\cdot}$, is bound by only 14 kcal mol^{-1} , as the bonding orbital is delocalized over more atomic centers and, therefore, less stabilizing. Apparently, the increase in dispersion interactions is slower than the loss in charge-resonance energy when increasing the monomer size. Thus, for the relatively small dimer radical cations studied herein, variation in charge-resonance dominates over the change in dispersion interactions. For larger monomers (e.g., oligothiophenes), however, we expect that dispersion will eventually become more important for the total interaction energy, with charge-resonance contribution playing a diminishing role.

The T-shaped radical cation dimers do not benefit from significant orbital overlap (i.e. “covalent” interactions) and thus have smaller interaction energies of $\sim 9 \text{ kcal mol}^{-1}$. This energy range is only slightly below that of stacked complexes for which the charge resonance is weak (11 – 14 kcal mol^{-1}), either because of the different ionization energies of the two monomers (e.g., thiophene-pyrrole) or because of the nonbonding SOMO (e.g., the cross conformation of the pyrrole dimer, $\text{Pyr}_2\text{X}^{+\cdot}$). The interaction energy is, however, much weaker (only $\sim 2 \text{ kcal mol}^{-1}$), when the heteroatom is pointing away from the second monomer (T' orientation), similar to that of the neutral T-shaped complexes, which indicates that the pure electrostatic interaction ($\text{ion} \cdots \text{neutral}$) and charge resonance are of minor importance in T' .

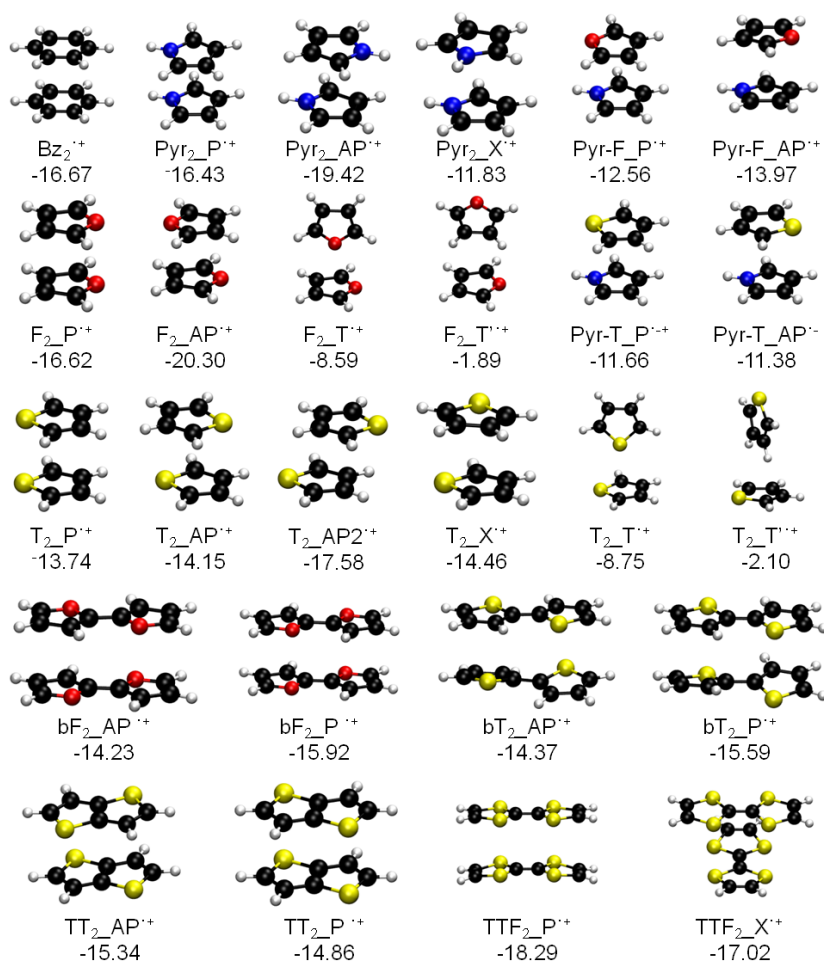


Figure 9.4: Orel26rad test set with estimated CCSD(T)/CBS interaction energies in kcal mol⁻¹.

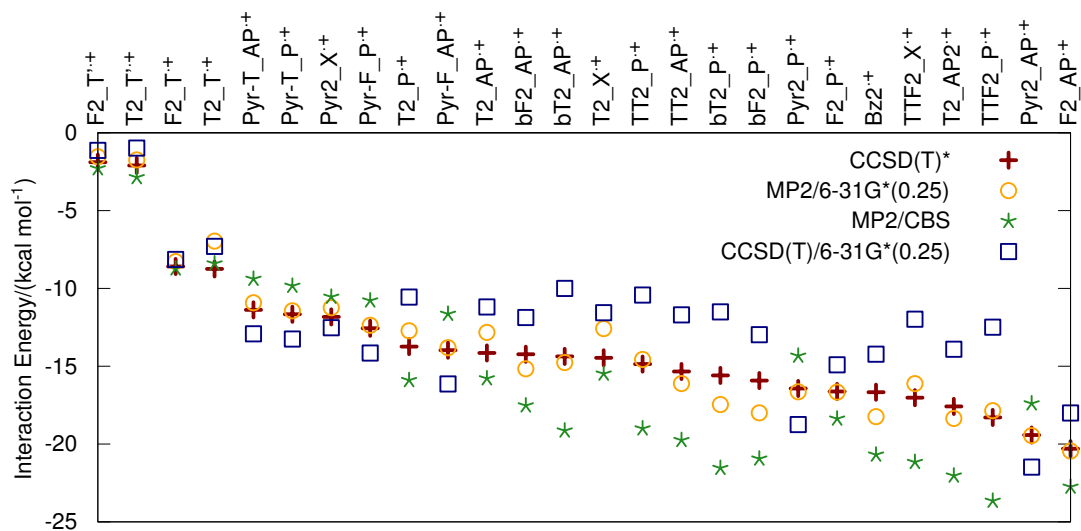


Figure 9.5: *Ab initio* interaction energies in kcal mol⁻¹ for the Orel26rad test set. CCSD(T)* denotes the estimated CCSD(T)/CBS values and serves as the benchmark.

Table 9.2: Performance of Various Methods for the Two Individual Test Sets and The average MAD.
All Energies are in kcal mol⁻¹.

	Orel26rad	Pi29n	average MAD
HF	17.31	7.79	12.29
LC-BOP	9.94	5.31	7.50
LC- ω PBE	9.14	4.92	6.92
LC- ω PBELYP	9.33	4.33	6.69
BLYP	5.67	7.56	6.67
B3LYP	5.91	6.62	6.28
B97	4.79	5.50	5.16
PBE	4.58	4.82	4.70
LC- ω PBEB95	6.06	2.83	4.36
PBE0	3.78	4.87	4.36
PBE-dDsC	7.52	0.51	3.82
VV10	7.86	0.14	3.79
BLYP-dDsC	6.28	1.25	3.63
HF-dDsC	5.16	1.70	3.34
PW6B95	2.93	3.50	3.23
M11	3.36	1.82	2.55
B2PLYP	1.79	3.20	2.54
LC- ω PBE-dDsC	4.26	0.97	2.53
CCSD(T)/6-31G*(0.25)	2.60	2.13	2.35
MP2/CBS	2.68	2.02	2.33
PW6B95-dDsC	4.16	0.60	2.28
B3LYP-dDsC	4.01	0.55	2.19
B97-dDsC	3.94	0.43	2.09
LC- ω PBELYP-dDsC	3.76	0.41	1.99
LC- ω PBEB95-dDsC	3.27	0.59	1.86
PBE0-dDsC	3.40	0.39	1.81
B2PLYP-D3(BJ)	3.26	0.42	1.76
LC-VV10	3.12	0.39	1.68
LC-BOP-LRD[10,0]	3.17	0.21	1.61
LC-BOP-LRD	2.85	0.30	1.51
B2PLYP-D	2.74	0.35	1.48
LC- ω PBEB95-dDsC/6-31G*	1.90	0.92	1.38
B2PLYP-D3	2.61	0.21	1.35
LC- ω PBEB95-dDsC/6-311+G**	1.78	0.82	1.27
M06-2X	1.08	1.25	1.16
ω B97X-D	1.41	0.41	0.88
MP2/6-31G*(0.25)	0.74	0.33	0.52

9.3.2 Performance of Standard Wave Function Methods

Interaction energies for the two test sets, Pi29n and Orel26rad, are given in Figure 9.2 and Figure 9.5 at standard *ab initio* levels (see Table 9.2 for mean absolute deviations, MADs): MP2 at the complete basis set limit together with MP2 and CCSD(T) in the small basis set, 6-31G*(0.25). With a MAD of 0.3 kcal mol⁻¹ MP2/6-31G*(0.25) clearly outperforms MP2/CBS and CCSD(T)/6-31G*(0.25) (MADs of 2.0 and 2.1 kcal mol⁻¹, respectively) for the neutral π -dimers of the Pi29n test set. The relative performance is very similar for the more challenging Orel26rad test set with a MAD of 0.7 kcal mol⁻¹ for MP2/6-31G*(0.25) compared to MADs of 2.7 and 2.6 kcal mol⁻¹ for the two much more demanding wave function methods. The remarkable performance of MP2/6-31G*(0.25) is in line with previous studies reporting the reliable accuracy of this cost effective combination^{528,570,571} due to error cancellation: MP2/CBS tends to overestimate interactions between π -conjugated molecules, while smaller basis sets limit the flexibility of the wave function and therefore lead to less binding. However, such an error cancellation does not hold for more accurate theories (e.g., CCSD(T)) for which weak interactions are underestimated in small basis sets.

With an overall MAD of 0.5 kcal mol⁻¹, MP2/6-31G*(0.25) emerges as the most accurate approximate level of theory discussed herein, outperforming all tested density functionals.

9.3.3 Performance of Density Functional Approximations

Despite the remarkable success of MP2/6-31G*(0.25), the performance of density functional approximations (see Figure 9.6) is of considerable interest for general applications and for understanding the limitations of the current approaches.

Simple PBE-dDsC achieves an impressive MAD of only 0.5 kcal mol⁻¹ for Pi29n with many other dispersion corrected functionals providing an excellent accuracy, as illustrated by the performance of VV10 (MAD=0.1 kcal mol⁻¹). The success of dispersion corrected functionals for Pi29n indicates good transferability from the smaller complexes dominating most training sets for weak interactions (e.g., S22) to the larger and sulfur containing complexes of Pi29n. In other words, as long as dispersion is accounted for, neutral model complexes of organic electronics are not problematic. The description of Orel26rad is more delicate. GGA functionals (BLYP and PBE) are among the worst methods tested (averaged MAD of 6.7 and 4.7 kcal mol⁻¹) but have a lower MAD for Orel26rad than for Pi29n due to error cancellation between overestimated charge-delocalization and missing dispersion. Adding a dispersion energy correction to a GGA functional (i.e., BLYP-dDsC, PBE-dDsC), deteriorates the performance for Orel26rad of these functionals even further. The fully nonlocal VV10 functional is not better than PBE-dDsC and is therefore not recommended either.

Standard hybrid density functionals such as B3LYP or PBE0 show a slight improvement over GGAs (averaged MAD of 6.3 and 4.4 kcal mol⁻¹ for B3LYP and PBE0, respectively). With an average MAD of 1.8 kcal mol⁻¹, PBE0-dDsC, is the best performing functional among the “simple” approaches. The other dispersion corrected hybrid functionals perform slightly worse, with average MADs of about 2.2 kcal mol⁻¹. These results demonstrate that the real benefit of

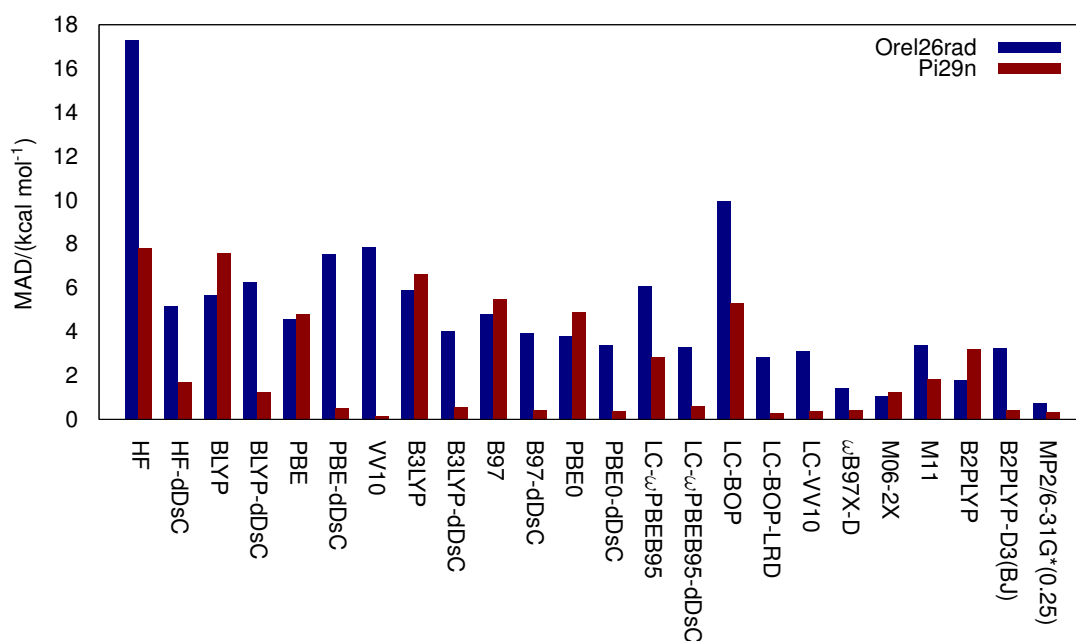


Figure 9.6: Performance of density functional approximations for radical cations (Orel26rad) and neutral π -dimers (Pi29n).

including a fraction of “exact” exchange is only visible in combination with a dispersion energy correction. Alternatively, the highly empirical global hybrid meta-GGA functional M06-2X achieves an overall MAD of $1.2 \text{ kcal mol}^{-1}$, providing a balanced description of Orel26rad and Pi29n (MADs of 1.1 and $1.3 \text{ kcal mol}^{-1}$, respectively).

Similar to global hybrids, LC- variants of standard functionals (e.g., LC- ω PBE or LC-BOP) do not perform well for either Pi29n or Orel26rad (MADs $> 7 \text{ kcal mol}^{-1}$), illustrating again the importance of weak interactions for achieving quantitative agreement with benchmark data. The modest performance of M11 (MAD_{Orel26rad} = $3.4 \text{ kcal mol}^{-1}$) indicates that the reduction of the delocalization error alters the error cancellation at the origin of the successful description of weak interactions by M06-2X (the global-hybrid predecessor of M11). In other words, long-range corrected exchange necessitates the explicit treatment of dispersion interactions for achieving accurate energetics. Orel26rad benefits the most from simultaneously accounting for weak interaction and reducing the delocalization energy. However, only ω B97X-D (MAD of $1.4 \text{ kcal mol}^{-1}$) reaches chemical accuracy (2 kcal mol^{-1}). In other words, the addition of a dispersion correction (dDsC, VV10 or LRD) to a standard LC- functional is not fully satisfactory and a better performance is achieved when fitting empirically the exchange-correlation functional together with the dispersion correction. LC-BOP-LRD is the best amongst the less empirical functionals, but the MAD of $2.9 \text{ kcal mol}^{-1}$ indicates that improvement is still possible.ⁱ

ⁱComparing the two LRD variants tested (with and without nonlocal contributions to the C_6 coefficients), suggests that Orel26rad benefits from these nonlocal contributions, which lower the MAD by $0.3 \text{ kcal mol}^{-1}$. Similarly, LC-VV10, which is fully nonlocal, slightly outperforms the best LC-dDsC variant (LC- ω PBEB95-dDsC), in which no explicitly nonlocal terms are considered.

The most popular double hybrid functional, B2PLYP¹⁶³ has been combined with the three successively recommended dispersion corrections: D (=D2),⁸⁵ D3⁴² and D3(BJ).⁴³ With a MAD of 1.8 and 3.2 kcal mol⁻¹ for Orel26rad and Pi29n, respectively, plain B2PLYP satisfies the chemical accuracy criterion for Orel26rad, but not for the neutral complexes. Adding a dispersion correction improves the performance for Pi29n significantly (MAD of 0.2-0.4 kcal mol⁻¹), but the accuracy for the other test set is clearly affected, e.g., the MAD for B2PLYP-D3 is 2.6 kcal mol⁻¹ for Orel26rad.

With average MADs of 1.2 and 0.9 kcal mol⁻¹, the best performing M06-2X and ω B97X-D rival with the accuracy of MP2/6-31G*(0.25) (MAD=0.6 kcal mol⁻¹). As compared to MP2, M06-2X has more difficulties describing the dispersion-dominated complexes (MADPi29n=1.3 vs. 0.3 kcal mol⁻¹, for M06-2X and MP2, respectively), whereas Orel26rad is trickier for ω B97X-D (MAD=1.4 and 0.7 kcal mol⁻¹ for ω B97X-D and MP2, respectively).

To summarize, interaction energies of radical cation π -dimers as illustrated by the Orel26rad test set are especially challenging: the electronic structure is more complicated than for the neutral dimers of Pi29n and dispersion interactions are still important. The carefully fitted M06-2X, which performs very well, exploits the error cancelation between the missing dispersion and the delocalization error. Without relying on such delicate error cancellations, only ω B97X-D adequately describes interaction energies of both neutral and radical cations. The reduction of the delocalization error in ω B97X-D is, however, associated with the fitting of the (exchange-correlation) functional augmented by an explicit dispersion correction.

The MAD is a good indicator of the overall accuracy, but capturing trends is sometimes more relevant than reproducing absolute binding energies. In particular, achieving the correct relative interactions between a series of complexes is of primary interest for identifying potential next-generation molecular precursors to organic electronics. The extent to which these trends are reproduced is analyzed on a subset of Orel26rad given in Figure 9.7. In contrast to Pi29n, for which the correlation between dispersion corrected functionals and CCSD(T)* is rather good (not shown), Orel26rad is more problematic. Neither B2PLYP (which neglects ~50% of the dispersion) nor dispersion corrected density functionals clearly discriminate between the two TTF₂^{•+} complexes and the parallel thiophene cation dimer (T₂_P⁺). Only B2PLYP-D3(BJ), which systematically overbinds the series, reproduces the 4.6 kcal mol⁻¹ energy spread between the parallel TTF (TTF₂_P⁺) and T₂_P⁺. The improvement of B2PLYP-D3(BJ) upon B2PLYP is rationalized by the proper treatment of dispersion interactions dominating the binding energy of the larger dimers.

The negative slope of PBE indicates that the delocalization error affects smaller systems more than extended ones: in larger monomers, the charge is more delocalized so that further spreading is not as advantageous. The “artificially” good performance of PBE for the smaller dimers (due to the larger delocalization error and less missing dispersion) is, therefore, not effective for the larger systems, which are significantly underbound in the absence of a dispersion correction.

In line with the MADs discussed above, the reduction of the delocalization error together with the description of dispersion interactions leads to a dramatic improvement going from PBE to PBE0-dDsC or ω B97X-D. Nevertheless, given that neither HF (the slope of the linear regression

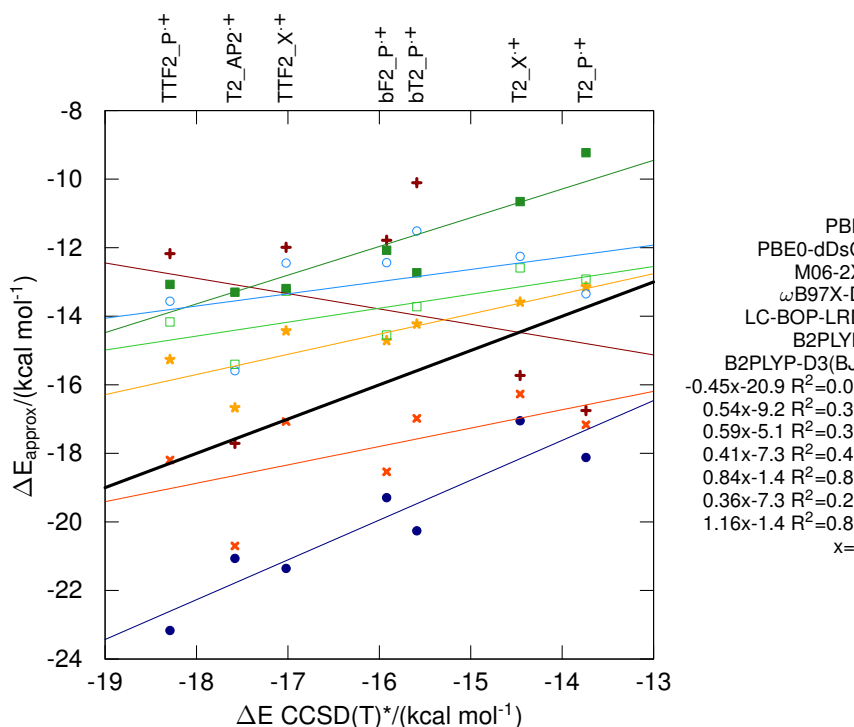


Figure 9.7: Correlation between DFT and estimated CCSD(T)/CBS interaction energies for a parallel and crossed TTF, bithiophene, bifuran dimers from Orel26rad test set.

is zero, not shown) nor pure GGAs (negative slope e.g., PBE) contain the right physics to stabilize the larger systems more than the smaller ones, their linear combination (i.e., global hybrids) is not an ideal basis for a dispersion correction. Long-range corrected exchange together with an explicit treatment of dispersion can provide more reasonable slopes, but the trends are not necessarily consistent (e.g., ω B97X-D vs. LC-BOP-LRD). B2PLYP performs somewhat better, because the negative slope of the GGA component is counterbalanced by the fraction correlation energy from perturbation theory.

Overall, achieving the correct balance between the decrease of charge resonance and the gain in dispersion interactions in larger dimers is highly challenging. In particular, the approximations giving the most accurate binding energies (e.g., ω B97X-D and M06-2X) do not accurately reproduce the relative strength of a series of dimers.

9.3.4 Interaction Energy Profiles

The reproduction of interaction energy profiles certainly represents the most rigorous validation for identifying robust methods. Non-equilibrium geometries are especially relevant in the context of molecular dynamics simulations. Interaction energy profiles are computed for the anti-parallel furan and thiophene dimer radical cations ($F_2_AP^{+}$ and $T_2_AP^{+}$), two prototypical examples of organic charge-carriers. The comparison of the two profiles is convenient because despite their similar structures their interaction energy differs by about 6 kcal mol⁻¹.

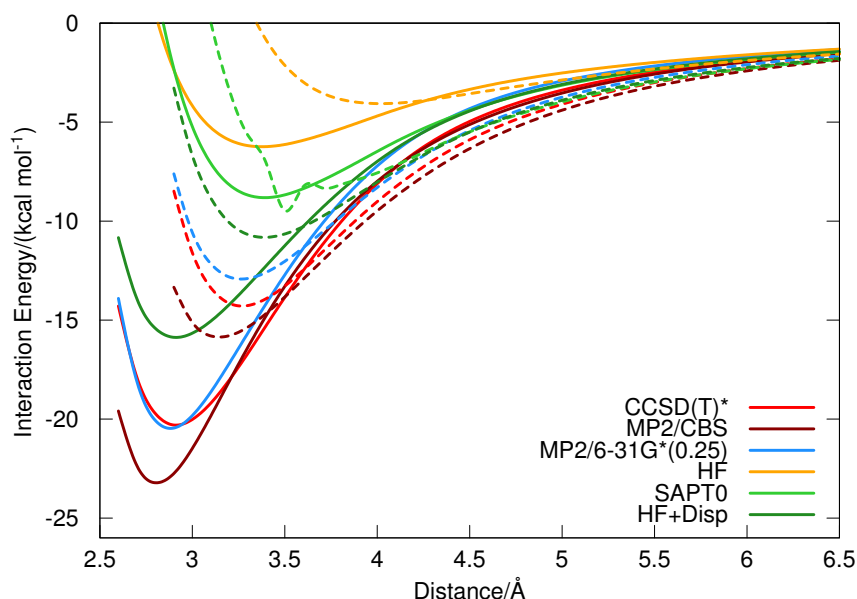


Figure 9.8: Interaction energy profiles for the radical cation dimers of furan (solid line) and thiophene (broken lines) at various levels of theory. SAPT0 is performed in the small 6-31G*(0.25) basis set and HF+Disp refers to the Hartree-Fock interaction energy augmented by the SAPT0 dispersion energy. The “discontinuous” point of SAPT0 for the thiophene dimer corresponds to the maximum net stabilization due to induction. It is probably an artifact from the perturbative treatment (e.g. eq 9.5); note that at this intermolecular distance, electrostatic attraction is still dominated by exchange repulsion.

The interaction energy profiles are computed based on the respective dimers of the Orel26rad test set ($F_2\text{-AP}^{++}$ and $T_2\text{-AP}^{++}$), i.e., one monomer corresponds to the optimized neutral and the other one to the radical cation geometry at the B3LYP/6-31G* level. The asymmetric nature of the dimers aims at improving the dissociation of the dimers: density functional approximations are more accurate for integer than for fractional numbers of electrons. Charge-localization induced by a geometrical bias is expected to disfavor the symmetric solution with two monomers charged +0.5.

Symmetry adapted perturbation theory,⁹³ allows in principle to identify the origin of the interaction energies. Unfortunately, SAPT is far less developed for open-shell than for closed-shell complexes. Therefore, only the simplest variant, SAPT0, is applied herein in which the monomers are treated at the (RO)HF level and electron correlation is neglected except for the dispersion energy.

Akin to the equilibrium interaction energies, MP2/6-31G*(0.25) is in excellent agreement with CCSD(T)/CBS, whereas MP2/CBS overbinds the radical cation dimers of furan and thiophene (see Figure 9.8). In contrast, SAPT0 accounts for only ~50% of the CCSD(T)* interaction energy. More importantly, the difference between furan and thiophene is not reproduced. This qualitative failure is not surprising, considering that charge-resonance is important in these dimers and that SAPT is based on one charged and one neutral monomer. Adding the δHF term to SAPT0, which corresponds to Hartree-Fock supplemented by the SAPT dispersion energy (HF+Disp), leads to a qualitative improvement. However, the remaining errors of $\sim 4 \text{ kcal mol}^{-1}$ around equilibrium, indicates that HF+Disp is not in quantitative agreement

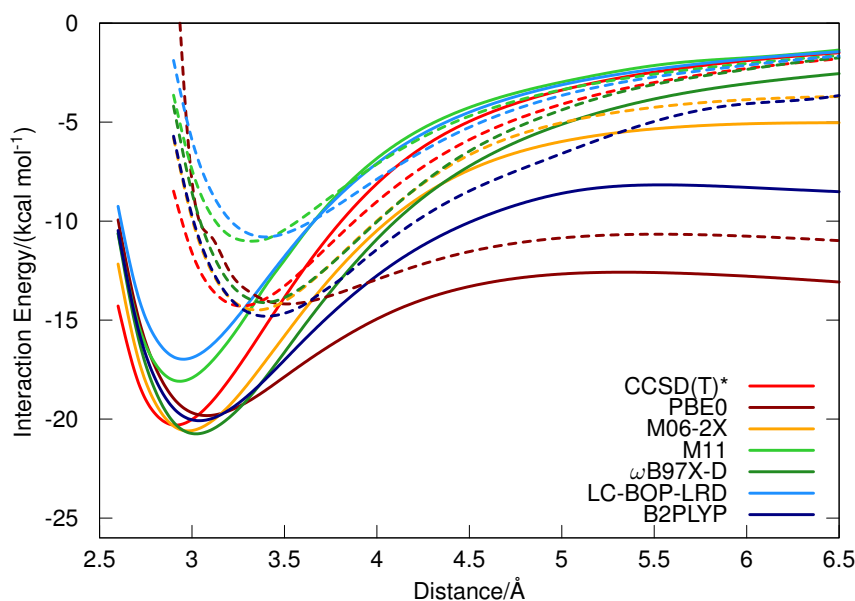


Figure 9.9: Interaction energy profiles for the radical cation dimers of furan (solid line) and thiophene (broken lines) at various DFT levels compared to estimated CCSD(T)/CBS.

with either CCSD(T)* or MP2/6-31G*(0.25).ⁱⁱ In summary, the SAPT0 analysis confirms the importance of charge-resonance (i.e., δ HF is essential for the qualitative agreement) and dispersion interactions. However, correlation contributions beyond “simple” monomer-based dispersion (e.g., induction-dispersion) are expected to be non-negligible for these strongly interacting monomers: the monomer densities at the basis of the SAPT0 treatment are only a very rough approximation to the dimer densities.

The overall performance of the DFT approximations is rather poor (Figure 9.9): the qualitative difference between the furan and thiophene dimer radical cations is adequately reproduced, but only ω B97X-D provides both accurate binding energies and correct dissociation behavior. The other LC-functionals perform very similarly to each other and underestimate the interaction energy by about 3 kcal mol⁻¹ (as apparent in their MAD for Orel26rad). The equilibrium distance is nevertheless accurate to within ± 0.1 Å for all the LC- functionals. Finally, the wrong dissociation behavior of M06-2X contrasts with the low MAD for Orel26rad (1.1 kcal mol⁻¹). However, the high amount of “exact” exchange in M06-2X reduces the delocalization error sufficiently to remove the spurious barriers towards dissociation obtained with other functionals (e.g., furane dimer radical cation with PBE0 and B2PLYP).

ⁱⁱFor the equilibrium geometry of the neutral anti-parallel thiophene dimer (T2_AP) excellent agreement is obtained between HF+Disp ($\Delta E = 1.55$ kcal mol⁻¹ and MP2/6-31G*(0.25) ($\Delta E = 1.53$ kcal mol⁻¹).

9.3.5 Basis Set Dependence

Large basis sets are necessary to assess the “true” functional performance but quadruple zeta basis sets are not realistic for routine applications. We here compare the performance of two standard, economic basis sets with that of def2-QZVP(-g) using the best dDsC corrected variant, i.e., the long-range corrected exchange functional, LC- ω PBEB95-dDsC (Figure 9.10). The average MADs over all the interaction energies are 1.4, 1.3 and 1.9 kcal mol⁻¹ for 6-31G*, 6-311+G** and def2-QZVP(-g) respectively. The use of the LC- ω PBEB95-dDsC/6-31G* combination, in future application, is justified by the small difference between 6-31G* and 6-311+G** and by the highly reasonable accuracy of the most cost-efficient variant tested herein. In fact, the average MAD is lower when using the small basis sets: the underbinding of LC- ω PBEB95-dDsC is compensated by the basis set superposition error (average MADs of 1.4 and 1.9 kcal mol⁻¹ for 6-31G* and def2-QZVP(-g), respectively).

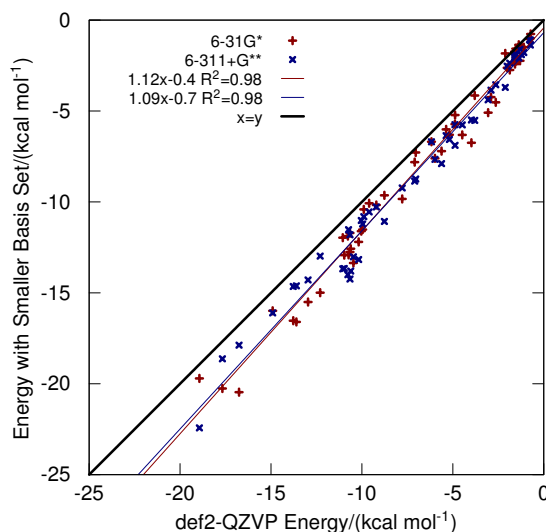


Figure 9.10: Correlation between interaction energies in smaller basis sets (6-31G* and 6-311+G**) and def2-QZVP(-g) values for the LC- ω PBEB95-dDsC density functional.

9.4 Conclusions

The accurate computational description of molecular precursors to organic electronics may promote our ability to address the most relevant questions in the field. With the aim of assessing the performance of the most accessible electronic structure methods for relevant interaction energies, we have introduced two test sets composed of neutral and radical dimer complexes, which best represent the resting (Pi29n) and charge-carrier states (Orel26rad) of organic functional units. The description of the interaction energies of neutral complexes (Pi29n) is straightforward, so long as dispersion interactions are properly taken into account: the best performing combinations are MP2/6-31G*(0.25), B2PLYP-D3, LC-BOP-LRD and VV10, as well as the less demanding PBE0-dDsC. In contrast, these approaches give results greatly exceeding chemical accuracy for the Orel26rad test set, with the exception of MP2/6-31G*(0.25), which clearly outperforms all other tested schemes. Achieving interplay between reducing charge delocalization and accounting for dispersion interactions in π -dimer radical cations is highly challenging for density functional approximations. For equilibrium geometries, M06-2X and ω B97X-D best reproduce the binding energies of the charged radical complexes (MAD of 1.1 and 1.4 kcal mol⁻¹, respectively). The inclusion of long-range corrected exchange requires explicit treatment of dispersion interactions yet, with the exception of ω B97X-D, the perfor-

mance of the LC- family of functionals is disappointing due to the systematic underestimation of the binding energy. The advantage of the long-range corrected exchange is nevertheless significant, particularly when energy profiles are considered. The correct dissociation behavior of a dimer into one charged and one neutral monomer is achieved only with functionals possessing the correct form in the asymptotic region. In addition, the underestimation of interaction energies at the equilibrium distance can be compensated by the basis set superposition error when using small, more practical basis sets.

Overall, the dilemma between reproducing absolute binding energies, relative energy trends, and dissociation behavior indicates that MP2/6-31G*(0.25) is the best approximation. When dealing with “real-world” applications involving larger systems, our findings indicate that the use of dispersion corrected long-range “exact” exchange functionals together with a small double-zeta basis set (e.g., LC- ω PBEB95-dDsC/6-31G*) represent the most cost-effective and promising alternative. The challenging Orel26rad database can function as a valuable test set to develop or validate improved schemes.

10 General Conclusions and Outlook

Density functional approximations promise high accuracy at low computational cost for the description of the electronic structure of extended systems. However, the neglect of long-range dispersion limits the reliability of standard methods. To extend the scope of approximations to Kohn-Sham density functional theory, this thesis has introduced original descriptions of dispersion interactions. These prevalent attractive forces govern myriad of chemical phenomena such as the $\pi - \pi$ stacking in DNA, the existence of condensed phases of non-polar molecules and the stability of self-assembled materials in organic electronics. The comprehensive analysis of challenging test cases, including alkane chemistry, charge-transfer complexes and radical cationic π -dimers, illustrates the importance of dispersion both for achieving quantitative agreement with highly accurate values and for identifying the key factors at the origin of the errors of standard functional approximations.

The first objective of this thesis was to achieve good accuracy for inter- and intramolecular dispersion interactions. The proposed “classical” dD10 correction incorporates higher-order terms in the multipole-expansion (i.e., C_8/R^8 and C_{10}/R^{10}) along with the physically motivated Tang and Toennies damping function that is modified at covalent bond distances to minimize double counting effects. The combination of nonempirical density functional approximations, e.g., PBE, with dD10 leads to excellent results simultaneously for difficult reactions involving hydrocarbons and for typical weak intermolecular complexes.

The subsequent dDXDM correction depends on the density and is applicable to all the elements of the Periodic Table. The nonempirical dispersion coefficients are computed based on Becke and Johnson’s exchange hole dipole moment (XDM) formalism. The iterative Hirshfeld scheme provides an accurate estimate of the (intramolecular) polarization, and achieves a realistic distribution of the dispersion coefficients among the atoms. Hirshfeld atomic overlaps and charges serve to identify the overlapping regions in the extended Tang and Toennies damping function. Density functionals augmented by the dispersion energy correction outperform standard approaches (e.g., M06-2X) for hydrocarbon chemistry and largely decrease the errors of the parent functionals for both inter- and intramolecular interactions.

Chapter 6 introduced a semi-empirical GGA-like formalism, which reduces considerably

the complexity of the exchange hole dipole moment that is used to model the dispersion coefficients. The developed dispersion correction based on the reformulated XDM requires less computational effort than the original XDM formalism of Becke and Johnson. We also propose to replace the spatial partition functions involving overlapping atoms by a set of disjoint Hirshfeld-dominant atoms to address the conceptual discrepancy between multipole expansion and the overlapping atoms in molecules used in most schemes.

The final density-dependent dispersion correction, dDsC, arises from the use of the simplified dispersion coefficients and the disjoint atomic partitioning. Only the leading term (C_6) is sufficient to provide high accuracy, because the flexible, extended Tang and Toennies damping function mimicks the effect of higher-order dispersion coefficients conveniently by increasing the value of the empirical parameter that adapts the dispersion correction to the given density functional approximation. In line with the preceding variants, hydrocarbon chemistry, including Diels-Alder reactions, benefits dramatically from the improved treatment of intramolecular dispersion without deteriorating the description of weak intermolecular interactions. The robust performance of dDsC is demonstrated through the comprehensive benchmarking of 340 diverse reaction energies featuring illustrative chemical problems ranging from heavy atom hydride weak interactions to ligand dissociation energies of Grubbs' first and second generation catalysts. In addition, optimized geometries of molecules containing nonbonded contacts in close proximity, e.g., [2.2]-paracyclophane, are in good agreement with experiment. The success of DFT-dDsC is already demonstrated through its broad applications, which include the modeling of oxygen reductions by an organic electron donor, the splitting of water by metallocenes, as well as the design of molecular receptors. Furthermore, we have implemented dDsC in three mainstream quantum chemistry programs, i.e., ADF, GAMESS-US and Q-Chem and the dispersion correction is therefore available to the computational community.

The devised schemes serve as a primary tool to tackle a second aspect of this thesis that is the identification of the key factors responsible for errors of standard density functional approximations. Seemingly simple hydrocarbon reaction energies are representative examples for which semilocal (hybrid) density functionals fail. These "intramolecular errors" associated with the increasing branching in alkanes correlate strongly with the error in the interaction energy of the compressed methane dimer. We demonstrate that the overly repulsive semilocal DFT exchange is partially responsible for the severe underestimation of branching interactions. As a result, the substitution of long-range GGA exchange by the less repulsive "exact" exchange represents a reasonable refinement. Most of the remaining error arises from the missing long-range dispersion interactions. Carefully designed dispersion corrections overcome both flaws: they include dispersion interactions in the long-range, while at short distances, the appropriate damping function reduces the over-repulsiveness of the parent functional. All our dispersion corrections lead to an impressive improvement for these hydrocarbon reaction energies.

The last two chapters focus on the interaction energies of charge-transfer (CT) complexes and radical cationic π -dimers, which are both highly challenging for density functional approximations. The performance of density functional approximations is governed by the

interplay between the delocalization error and the neglect of dispersion. We demonstrate that the physical origin of the stabilization of charge-transfer complexes is dominated by dispersion interactions, while the relative orientations and intermolecular distances are dictated by electrostatics and charge-transfer. Thus, dispersion corrections are crucial for providing an accurate description of CT-complexes. In addition, a relatively high fraction of “exact” exchange is necessary to prevent the overestimation of charge transfer and avoid spurious dissociation into fractionally charged monomers. Indeed, few well-balanced functionals provide reliable results. Our novel database modeling charge-carrier states of organic electronics reveals then that the interactions within π -dimer radical cations are even more subtle than that of charge-transfer complexes: the inclusion of long-range “exact” exchange is mandatory to achieve a qualitatively correct dissociation behavior, yet the treatment of dispersion needs to be incorporated at all ranges. Unfortunately, long-range corrected exchange functionals tend to underestimate the interaction energies at the equilibrium distance even after correction for dispersion. The most valuable and cost-effective option involves the combination of dDsC with a long-range corrected exchange functional and a small basis set.

In summary, the atom pairwise dispersion corrections developed within this thesis are powerful methods to systematically enhance the performance of standard density functional approximations and elucidate the source of their failures. In particular, we are confident that the latest density-dependent scheme, dDsC, which offers a highly robust performance, will continue to deliver reliable energies and geometries when used to address myriad chemical questions. Despite this bright perspective, open questions remain:

- *How could the “optimal” density functional to pair with the dispersion correction be designed?*

In comparison with standard parameterizations, a specifically devised functional would have the advantage of exploiting the density information twice: once for the dispersion correction and once for the improved description of all other exchange and correlation effects. Such a functional could lead to an improved treatment of transition states, spin state splittings and other issues related to near-degeneracies that are tricky for standard approximations. The disadvantage is the lack of a clear-cut physical distinction between “overlap dispersion”, captured by empirical functionals (e.g., M06-2X) and the strongly damped regions of the dispersion corrections. Thus, such a method is necessarily empirical and requires a careful design and fitting procedure to cope with the linear dependencies in the parameter space.

- *Do current formulations capture subtle dispersion energy enhancements in low band-gap molecular systems?*

The second order formula predicts increased dispersion interactions for systems with low-lying excited states characteristic for delocalized electrons, e.g., charge-transfer complexes. However, current density-dependent dispersion corrections depend mostly on local ground state information. It is therefore not obvious how do these schemes respond to the presence of remarkably low-lying excited states. The analysis is certainly feasible at large intermolecular distances, yet the most interesting regions are close to

equilibrium, where complications stem from the approximated density functional, the empirical form of the damping function and the accuracy of the dispersion coefficients.

- *How important are beyond dDsC dispersion effects for general thermochemistry?*

Firstly, dDsC provides an isotropic long-range dispersion energy, while anisotropy should be included in general. However, the short-range anisotropy is assumed to be more important and might be captured by a combination of the damping function and the density functional performance. Detailed studies are necessary to clarify these points. Secondly, since dDsC approximates the second order dispersion energy, it suffers from the same shortcoming as most other schemes: pairwise additivity, meaning that many-body effects (including long-range screening interactions) are missing in the formalism. Many-body effects becomes more important with increasing system size and might therefore become the accuracy limiting factor for large molecular assemblies and condensed phases.

- *How are the dispersion corrections adapted to (low-lying) excited states?*

Compared to ground state molecules, two competing physical effects are expected: excited states are assumed to have higher polarizabilities than ground states, but at the same time negative contributions to dispersion are predicted. The importance of the negative terms is not yet fully established. However, all current density-dependent dispersion corrections are probably unable to capture the fundamental difference in the physics of dispersion interactions between ground- and excited states. Furthermore, not all excited states are equally well described by standard time-dependent DFT. Hence, for a typical photo-chemical processes one might wonder, which error will dominate: the intrinsic errors of TD-DFT, the neglect of dispersion or the application of a dispersion correction missing the proper physics of excited states? Excited states promise a fascinating diversity of challenges.

Preconceptions about the “negligibly weak” van der Waals interactions need to be revised: dispersion is vital for (metal-)organic chemistry and has to be explicitly accounted for within density functional approximations. The development of post-HF techniques based on localized orbitals or the divide and conquer philosophy is promising for treating large molecular systems at systematic *ab initio* levels. However, even efficient post-HF methods are no substitute for density functional approximations: DFT will be applied to even larger systems and, concomitantly, the dispersion corrections will continue to gain in pertinence.

Bibliography

- [1] Siegbahn, P. E. M.; Blomberg, M. R. A. *Annu. Rev. Phys. Chem.* **1999**, *50*, 221.
- [2] Chermette, H. *Coord. Chem. Rev.* **1998**, *178-180*, 699.
- [3] Hu, H.; Yang, W. *Annu. Rev. Phys. Chem.* **2008**, *59*, 573.
- [4] Frank, N. *Coord. Chem. Rev.* **2009**, *253*, 526.
- [5] Cramer, C. J.; Truhlar, D. G. *Phys. Chem. Chem. Phys.* **2009**, *11*, 10757.
- [6] Norskov, J. K.; Bligaard, T.; Rossmeisl, J.; Christensen, C. H. *Nat. Chem.* **2009**, *1*, 37.
- [7] Dabkowska, I.; Gonzalez, H. V.; Jurecka, P.; Hobza, P. *J. Phys. Chem. A* **2005**, *109*, 1131.
- [8] Bashford, D.; Chothia, C.; Lesk, A. M. *J. Mol. Biol.* **1987**, *196*, 199.
- [9] Hollingsworth, M. D. *Science* **2002**, *295*, 2410.
- [10] Hohenberg, P.; Kohn, W. *Phys. Rev.* **1964**, *136*, B864.
- [11] Kohn, W.; Sham, L. J. *Phys. Rev.* **1965**, *140*, A1133.
- [12] Senn, H. M.; Thiel, W. *Angew. Chem., Int. Ed.* **2009**, *48*, 1198.
- [13] Jones, R. O.; Gunnarsson, O. *Rev. Mod. Phys.* **1989**, *61*, 689.
- [14] Kristyan, S.; Pulay, P. *Chem. Phys. Lett.* **1994**, *229*, 175.
- [15] Perez-Jorda, J. M.; Becke, A. D. *Chem. Phys. Lett.* **1995**, *233*, 134.
- [16] Hobza, P.; Sponer, J.; Reschel, T. *J. Comput. Chem.* **1995**, *16*, 1315.
- [17] Zhang, Y.; Pan, W.; Yang, W. *J. Chem. Phys.* **1997**, *107*, 7921.
- [18] Patton, D. C.; Pederson, M. R. *Phys. Rev. A* **1997**, *56*, R2495.
- [19] Milet, A.; Korona, T.; Moszynski, R.; Kochanski, E. *J. Chem. Phys.* **1999**, *111*, 7727.
- [20] Perez-Jorda, J. M.; San-Fabian, E.; Perez-Jimenez, A. J. *J. Chem. Phys.* **1999**, *110*, 1916.
- [21] Tsuzuki, S.; Luthi, H. P. *J. Chem. Phys.* **2001**, *114*, 3949.
- [22] Wu, X.; Vargas, M. C.; Nayak, S.; Lotrich, V.; Scoles, G. *J. Chem. Phys.* **2001**, *115*, 8748.
- [23] Allen, M. J.; Tozer, D. J. *J. Chem. Phys.* **2002**, *117*, 11113.
- [24] Perdew, J. P.; Zunger, A. *Phys. Rev. B* **1981**, *23*, 5048.

Bibliography

- [25] Perdew, J. P.; Parr, R. G.; Levy, M.; Balduz, J., Jose L. *Phys. Rev. Lett.* **1982**, 49, 1691.
- [26] Zhang, Y.; Yang, W. *J. Chem. Phys.* **1998**, 109, 2604.
- [27] Dutoi, A. D.; Head-Gordon, M. *Chem. Phys. Lett.* **2006**, 422, 230.
- [28] Mori-Sanchez, P.; Cohen, A. J.; Yang, W. *J. Chem. Phys.* **2006**, 125, 201102.
- [29] Ruzsinszky, A.; Perdew, J. P.; Csonka, G. I.; Vydrov, O. A.; Scuseria, G. E. *J. Chem. Phys.* **2006**, 125, 194112.
- [30] Cohen, A. J.; Mori-Sanchez, P.; Yang, W. *Science* **2008**, 321, 792.
- [31] Cerny, J.; Hobza, P. *Phys. Chem. Chem. Phys.* **2005**, 7, 1624.
- [32] Ruiz, E.; Salahub, D. R.; Vela, A. *J. Am. Chem. Soc.* **1995**, 117, 1141.
- [33] Ruiz, E.; Salahub, D. R.; Vela, A. *J. Phys. Chem.* **1996**, 100, 12265.
- [34] Cohen, A. J.; Mori-Sachez, P.; Yang, W. *Chem. Rev.* **2012**, 112, 289.
- [35] Heaton-Burgess, T.; Yang, W. *J. Chem. Phys.* **2010**, 132, 234113.
- [36] Johnson, E. R.; Mori-Sanchez, P.; Cohen, A. J.; Yang, W. *J. Chem. Phys.* **2008**, 129, 204112.
- [37] Ahlrichs, R.; Penco, R.; Scoles, G. *Chem. Phys.* **1977**, 19, 119.
- [38] Wu, Q.; Yang, W. *J. Chem. Phys.* **2002**, 116, 515.
- [39] Grimme, S. *J. Comput. Chem.* **2006**, 27, 1787.
- [40] Burns, L. A.; Mayagoitia, A. V.; Sumpter, B. G.; Sherrill, C. D. *J. Chem. Phys.* **2011**, 134, 084107.
- [41] Gould, T.; Dobson, J. F. *Phys. Rev. B* **2011**, 84, 241108.
- [42] Grimme, S.; Antony, J.; Ehrlich, S.; Krieg, H. *J. Chem. Phys.* **2010**, 132, 154104.
- [43] Grimme, S.; Ehrlich, S.; Goerigk, L. *J. Comput. Chem.* **2011**, 32, 1456.
- [44] Tkatchenko, A.; Scheffler, M. *Phys. Rev. Lett.* **2009**, 102, 073005.
- [45] Sato, T.; Nakai, H. *J. Chem. Phys.* **2009**, 131, 224104.
- [46] Sato, T.; Nakai, H. *J. Chem. Phys.* **2010**, 133, 194101.
- [47] Vydrov, O. A.; Van Voorhis, T. *Phys. Rev. Lett.* **2009**, 103, 063004.
- [48] Vydrov, O. A.; Van Voorhis, T. *J. Chem. Phys.* **2010**, 133, 244103.
- [49] Krishtal, A.; Vanommeslaeghe, K.; Olasz, A.; Veszpremi, T.; Alsenoy, C. V.; Geerlings, P. *J. Chem. Phys.* **2009**, 130, 174101.
- [50] Hesselmann, A. *J. Chem. Phys.* **2009**, 130, 084104.
- [51] Pernal, K.; Podeszwa, R.; Patkowski, K.; Szalewicz, K. *Phys. Rev. Lett.* **2009**, 103, 4.
- [52] Klimes, J.; Bowler, D. R.; Michaelides, A. *J. Phys.: Condens. Matter* **2010**, 22, 022201.
- [53] Lee, K.; Murray, E. D.; Kong, L.; Lundqvist, B. I.; Langreth, D. C. *Phys. Rev. B* **2010**, 82, 081101.

- [54] Liu, Y.; Goddard, W. A. *J. Phys. Chem. Lett.* **2010**, *1*, 2550.
- [55] Mackie, I. D.; DiLabio, G. A. *Phys. Chem. Chem. Phys.* **2009**, *12*, 6092.
- [56] Torres, E.; DiLabio, G. A. *J. Phys. Chem. Lett.* **2012**, *3*, 1738.
- [57] Krishtal, A.; Geldof, D.; Vanommeslaeghe, K.; Alsenoy, C. V.; Geerlings, P. *J. Chem. Theory Comput.* **2012**, *8*, 125.
- [58] Kim, H.; Choi, J.-M.; Goddard, W. A. *J. Phys. Chem. Lett.* **2012**, *3*, 360.
- [59] Deligkaris, C.; Rodriguez, J. H. *Phys. Chem. Chem. Phys.* **2012**, *14*, 3414.
- [60] Schneebeli, S. T.; Bochevarov, A. D.; Friesner, R. A. *J. Chem. Theory Comput.* **2011**, *7*, 658.
- [61] Hesselmann, A. *J. Chem. Phys.* **2012**, *136*, 014104.
- [62] Redfern, P. C.; Zapol, P.; Curtiss, L. A.; Raghavachari, K. *J. Phys. Chem. A* **2000**, *104*, 5850.
- [63] Woodcock, H. L.; Schaefer, H. F.; Schreiner, P. R. *J. Phys. Chem. A* **2002**, *106*, 11923.
- [64] Feng, Y.; Liu, L.; Wang, J.-T.; Huang, H.; Guo, Q.-X. *J. Chem. Inf. Comput. Sci.* **2003**, *43*, 2005.
- [65] Check, C. E.; Gilbert, T. M. *J. Org. Chem.* **2005**, *70*, 9828.
- [66] Izgorodina, E. I.; Coote, M. L.; Radom, L. *J. Phys. Chem. A* **2005**, *109*, 7558.
- [67] Schreiner, P. R.; Fokin, A. A.; Pascal, R. A.; de Meijere, A. *Org. Lett.* **2006**, *8*, 3635.
- [68] Grimme, S. *Angew. Chem., Int. Ed.* **2006**, *45*, 4460.
- [69] Wodrich, M. D.; Corminboeuf, C.; Schleyer, P. v. R. *Org. Lett.* **2006**, *8*, 3631.
- [70] Wodrich, M. D.; Corminboeuf, C.; Schreiner, P. R.; Fokin, A. A.; Schleyer, P. v. R. *Org. Lett.* **2007**, *9*, 1851.
- [71] Schreiner, P. R. *Angew. Chem., Int. Ed.* **2007**, *46*, 4217.
- [72] Wodrich, M. D.; Jana, D. F.; Schleyer, P. v. R.; Corminboeuf, C. *J. Phys. Chem. A* **2008**, *112*, 11495.
- [73] Tang, K. T.; Toennies, J. P. *J. Chem. Phys.* **1984**, *80*, 3726.
- [74] Steinmann, S. N.; Csonka, G.; Corminboeuf, C. *J. Chem. Theory Comput.* **2009**, *5*, 2950.
- [75] Becke, A. D.; Johnson, E. R. *J. Chem. Phys.* **2005**, *122*, 154104.
- [76] Johnson, E. R.; Becke, A. D. *J. Chem. Phys.* **2005**, *123*, 024101.
- [77] Becke, A. D.; Johnson, E. R. *J. Chem. Phys.* **2005**, *123*, 154101.
- [78] Becke, A. D.; Johnson, E. R. *J. Chem. Phys.* **2006**, *124*, 014104.
- [79] Johnson, E. R.; Becke, A. D. *J. Chem. Phys.* **2006**, *124*, 174104.
- [80] Becke, A. D.; Johnson, E. R. *J. Chem. Phys.* **2007**, *127*, 154108.
- [81] Steinmann, S. N.; Corminboeuf, C. *J. Chem. Theory Comput.* **2010**, *6*, 1990.
- [82] Hehre, W. J.; Ditchfield, R.; Radom, L.; Pople, J. A. *J. Am. Chem. Soc.* **1970**, *92*, 4796.

Bibliography

- [83] Pople, J. A.; Radom, L.; Hehre, W. J. *J. Am. Chem. Soc.* **1971**, 93, 289.
- [84] Hehre, W.; Radom, L.; P. v. R., S.; Pople, J. *Ab initio molecular orbital theory*; Wiley, New York, 1986.
- [85] Schwabe, T.; Grimme, S. *Phys. Chem. Chem. Phys.* **2007**, 9, 3397.
- [86] Steinmann, S. N.; Wodrich, M.; Corminboeuf, C. *Theor. Chem. Acc.* **2010**, 127, 429.
- [87] Kong, J.; Gan, Z.; Proynov, E.; Freindorf, M.; Furlani, T. R. *Phys. Rev. A* **2009**, 79, 042510.
- [88] Steinmann, S. N.; Corminboeuf, C. *J. Chem. Phys.* **2011**, 134, 044117.
- [89] Steinmann, S. N.; Corminboeuf, C. *J. Chem. Theory Comput.* **2011**, 7, 3567.
- [90] Steinmann, S. N.; Piemontesi, C.; Delachat, A.; Corminboeuf, C. *J. Chem. Theory Comput.* **2012**, 8, 1629.
- [91] Møller, C.; Plesset, M. S. *Phys. Rev.* **1934**, 46, 618.
- [92] Purvis, I.; George D.; Bartlett, R. J. *J. Chem. Phys.* **1982**, 76, 1910.
- [93] Jeziorski, B.; Moszynski, R.; Szalewicz, K. *Chem. Rev.* **1994**, 94, 1887.
- [94] Korff, S. A.; Breit, G. *Rev. Mod. Phys.* **1932**, 4, 471.
- [95] Van der Waals, J. D. *Over de Continuïteit van den Gas- en Vloeistofoestand*; A. W. Sijthoff: Leiden, 1873.
- [96] Eisenschitz, R.; London, F. Z. *Phys. A* **1930**, 60, 491.
- [97] London, F. Z. *Phys. A* **1930**, 63, 245.
- [98] London, F. *Trans. Faraday Soc.* **1937**, 33, 8b.
- [99] Axilrod, B. M.; Teller, E. *J. Chem. Phys.* **1943**, 11, 299.
- [100] Muto, Y. *Proc. Phys. Math. Soc. Jpn.* **1943**, 17, 629.
- [101] Bade, W. L.; Kirkwood, J. G. *J. Chem. Phys.* **1957**, 27, 1284.
- [102] Cao, J.; Berne, B. J. *J. Chem. Phys.* **1992**, 97, 8628.
- [103] Cole, M. W.; Velegol, D.; Kim, H.-Y.; Lucas, A. A. *Mol. Simul.* **2009**, 35, 849.
- [104] Donchev, A. G. *J. Chem. Phys.* **2006**, 125, 074713.
- [105] Dobson, J. F.; Wang, J.; Dinte, B. P.; McLennan, K.; Le, H. M. *Int. J. Quantum Chem.* **2005**, 101, 579.
- [106] Kim, H.-Y.; Sofo, J. O.; Velegol, D.; Cole, M. W.; Lucas, A. A. *J. Chem. Phys.* **2006**, 124, 074504.
- [107] Longuet-Higgins, H. C. *Faraday Discuss.* **1965**, 40, 7.
- [108] Zaremba, E.; Kohn, W. *Phys. Rev. B* **1976**, 13, 2270.
- [109] Andersson, Y.; Langreth, D. C.; Lundqvist, B. I. *Phys. Rev. Lett.* **1996**, 76, 102.
- [110] Dobson, J. F.; Dinte, B. P. *Phys. Rev. Lett.* **1996**, 76, 1780.

- [111] Misquitta, A. J.; Jeziorski, B.; Szalewicz, K. *Phys. Rev. Lett.* **2003**, *91*, 033201.
- [112] Pitonak, M.; Hesselmann, A. *J. Chem. Theory Comput.* **2010**, *6*, 168.
- [113] Casimir, H. B. G.; Polder, D. *Phys. Rev.* **1948**, *73*, 360.
- [114] Dobson, J. F.; White, A.; Rubio, A. *Phys. Rev. Lett.* **2006**, *96*, 073201.
- [115] Liu, R.-F.; Franzese, C. A.; Malek, R.; Zuchowski, P. S.; Angyan, J. G.; Szczesniak, M. M.; Chalasinski, G. *J. Chem. Theory Comput.* **2011**, *7*, 2399.
- [116] Dobson, J. F.; Gould, T. *J. Phys.: Condens. Matter* **2012**, *24*, 073201.
- [117] Misquitta, A. J.; Spencer, J.; Stone, A. J.; Alavi, A. *Phys. Rev. B* **2010**, *82*, 075312.
- [118] Grimme, S. *J. Chem. Phys.* **2003**, *118*, 9095.
- [119] DiStasio, R. A.; Head-Gordon, M. *Mol. Phys.* **2007**, *105*, 1073.
- [120] Tkatchenko, A.; Robert A. DiStasio, J.; Head-Gordon, M.; Scheffler, M. *J. Chem. Phys.* **2009**, *131*, 094106.
- [121] Marchetti, O.; Werner, H.-J. *J. Phys. Chem. A* **2009**, *113*, 11580.
- [122] Feynman, R. P. *Phys. Rev.* **1939**, *56*, 340.
- [123] Dwyer, A. D.; Tozer, D. J. *J. Chem. Phys.* **2011**, *135*, 164110.
- [124] Autumn, K.; Liang, Y. A.; Hsieh, S. T.; Zesch, W.; Chan, W. P.; Kenny, T. W.; Fearing, R.; Full, R. J. *Nature* **2000**, *405*, 681.
- [125] Earles, T. T. *J. Chem. Educ.* **1995**, *72*, 727.
- [126] Noble, D. *Anal. Chem.* **1995**, *67*, 435A.
- [127] DeLorenzo, R.; Kimbrough, D. R. *J. Chem. Educ.* **1998**, *75*, 1300.
- [128] Thomas, L. H. *Math. Proc. Cambridge* **1927**, *23*, 542.
- [129] Fermi, E. *Z. Phys. A* **1928**, *48*, 73.
- [130] Dirac, P. A. M. *Math. Proc. Cambridge* **1930**, *26*, 376.
- [131] Slater, J. C. *Phys. Rev.* **1951**, *81*, 385.
- [132] Teller, E. *Rev. Mod. Phys.* **1962**, *34*, 627.
- [133] Levy, M. *Int. J. Quantum Chem.* **2010**, *110*, 3140.
- [134] Kato, T. *Commun. Pure Appl. Math.* **1957**, *10*, 151.
- [135] Steiner, E. *J. Chem. Phys.* **1963**, *39*, 2365.
- [136] Levy, M. *Proc. Natl. Acad. Sci.* **1979**, *76*, 6062.
- [137] Fock, V. *Z. Phys. A* **1930**, *63*, 855.
- [138] Langreth, D.; Perdew, J. *Solid State Commun.* **1975**, *17*, 1425.
- [139] Gunnarsson, O.; Lundqvist, B. I. *Phys. Rev. B* **1976**, *13*, 4274.

Bibliography

- [140] Langreth, D. C.; Perdew, J. P. *Phys. Rev. B* **1977**, *15*, 2884.
- [141] Dion, M.; Rydberg, H.; Schröder, E.; Langreth, D. C.; Lundqvist, B. I. *Phys. Rev. Lett.* **2004**, *92*, 246401.
- [142] Eshuis, H.; Bates, J.; Furche, F. *Theor. Chem. Acc.* **2012**, *131*, 1.
- [143] Harris, J.; Griffin, A. *Phys. Rev. B* **1975**, *11*, 3669.
- [144] Hunt, K. L. C. *J. Chem. Phys.* **2002**, *116*, 5440.
- [145] Baerends, E. J.; Gritsenko, O. V. *J. Phys. Chem. A* **1997**, *101*, 5383.
- [146] Peverati, R.; Truhlar, D. G. *J. Chem. Theory Comput.* **2012**, *8*, 2310.
- [147] Ceperley, D. M.; Alder, B. J. *Phys. Rev. Lett.* **1980**, *45*, 566.
- [148] Sun, J.; Perdew, J. P.; Seidl, M. *Phys. Rev. B* **2010**, *81*, 085123.
- [149] Vosko, S. H.; Wilk, L.; Nusair, M. *Can. J. Phys.* **1980**, *58*, 1200.
- [150] Perdew, J. P.; Wang, Y. *Phys. Rev. B* **1992**, *45*, 13244.
- [151] Perdew, J. P.; Wang, Y. *Phys. Rev. B* **1986**, *33*, 8800.
- [152] Perdew, J. P.; Ruzsinszky, A.; Tao, J. M.; Staroverov, V. N.; Scuseria, G. E.; Csonka, G. I. *J. Chem. Phys.* **2005**, *123*.
- [153] Stroppa, A.; Kresse, G. *New J. Phys.* **2008**, *10*, 063020.
- [154] Becke, A. D. *Phys. Rev. A* **1988**, *38*, 3098.
- [155] Lee, C.; Yang, W.; Parr, R. G. *Phys. Rev. B* **1988**, *37*, 785.
- [156] Perdew, J. P.; Burke, K.; Ernzerhof, M. *Phys. Rev. Lett.* **1996**, *77*, 3865.
- [157] Perdew, J. P.; Ruzsinszky, A.; Tao, J.; Csonka, G. I.; Scuseria, G. E. *Phys. Rev. A: At., Mol., Opt. Phys.* **2007**, *76*, 042506.
- [158] Tao, J.; Perdew, J. P.; Staroverov, V. N.; Scuseria, G. E. *Phys. Rev. Lett.* **2003**, *91*, 146401.
- [159] Zhao, Y.; Truhlar, D. G. *J. Chem. Phys.* **2006**, *125*, 194101.
- [160] Becke, A. D.; Roussel, M. R. *Phys. Rev. A* **1989**, *39*, 3761.
- [161] Becke, A. D. *J. Chem. Phys.* **1993**, *98*, 5648.
- [162] Stephens, P. J.; Devlin, F. J.; Chabalowski, C. F.; Frisch, M. J. *J. Phys. Chem.* **1994**, *98*, 11623.
- [163] Grimme, S. *J. Chem. Phys.* **2006**, *124*, 034108.
- [164] Zhao, Y.; Truhlar, D. G. *J. Phys. Chem. A* **2004**, *108*, 6908.
- [165] Bartlett, R. J.; Grabowski, I.; Hirata, S.; Ivanov, S. *J. Chem. Phys.* **2005**, *122*, 034104.
- [166] Bartlett, R. J.; Lotrich, V. F.; Schweigert, I. V. *J. Chem. Phys.* **2005**, *123*, 062205.
- [167] Grabowski, I.; Teale, A. M.; Smiga, S.; Bartlett, R. J. *J. Chem. Phys.* **2011**, *135*, 114111.
- [168] Perdew, J. P.; Schmidt, K. *Density Functional Theory and Its Application to Materials*

- 2001**, 577, 207.
- [169] Slater, J. C. *The self-consistent field for molecules and solids*; McGraw-Hill: New York, 1974.
- [170] Perdew, J. P.; Smith, J. R. *Surf. Sci.* **1984**, 141, L295.
- [171] Reiher, M.; Salomon, O.; Sellmann, D.; Hess, B. A. *Chem.-Eur. J.* **2001**, 7, 5195.
- [172] Paulsen, H.; Trautwein, A. X. *J. Phys. Chem. Solids* **2004**, 65, 793.
- [173] Swart, M. *J. Chem. Theory Comput.* **2008**, 4, 2057.
- [174] Cramer, C. J.; Smith, B. A. *J. Phys. Chem.* **1996**, 100, 9664.
- [175] Ess, D. H.; Johnson, E. R.; Hu, X.; Yang, W. *J. Phys. Chem. A* **2011**, 115, 76.
- [176] Kurlancheek, W.; Lochan, R.; Lawler, K.; Head-Gordon, M. *J. Chem. Phys.* **2012**, 136, 054113.
- [177] Baerends, E. J. *Phys. Rev. Lett.* **2001**, 87, 133004.
- [178] Cohen, A. J.; Mori-Sanchez, P.; Yang, W. *J. Chem. Phys.* **2008**, 129, 121104.
- [179] Mori-Sanchez, P.; Cohen, A. J.; Yang, W. *Phys. Rev. Lett.* **2009**, 102, 066403.
- [180] Haunschild, R.; Henderson, T. M.; Jimenez-Hoyos, C. A.; Scuseria, G. E. *J. Chem. Phys.* **2010**, 133, 134116.
- [181] Fermi, E.; Amaldi, E. *Accad. Ital. Rome* **1934**, 6, 119.
- [182] Patchkovskii, S.; Ziegler, T. *J. Chem. Phys.* **2002**, 116, 7806.
- [183] Patchkovskii, S.; Ziegler, T. *J. Phys. Chem. A* **2002**, 106, 1088.
- [184] Vydrov, O. A.; Scuseria, G. E. *J. Chem. Phys.* **2004**, 121, 8187.
- [185] Becke, A. D. *J. Chem. Phys.* **1996**, 104, 1040.
- [186] Mori-Sanchez, P.; Cohen, A. J.; Yang, W. *J. Chem. Phys.* **2006**, 124, 091102.
- [187] Becke, A. D. *J. Chem. Phys.* **2005**, 122, 064101.
- [188] Perdew, J. P.; Staroverov, V. N.; Tao, J.; Scuseria, G. E. *Phys. Rev. A* **2008**, 78, 052513.
- [189] Cohen, A. J.; Mori-Sanchez, P.; Yang, W. *J. Chem. Phys.* **2007**, 126, 191109.
- [190] Ruzsinszky, A.; Perdew, J. P.; Csonka, G. I.; Vydrov, O. A.; Scuseria, G. E. *J. Chem. Phys.* **2007**, 126, 104102.
- [191] Kim, M.-C.; Sim, E.; Burke, K. *J. Chem. Phys.* **2011**, 134, 171103.
- [192] Jensen, F. *J. Chem. Theory Comput.* **2010**, 6, 2726.
- [193] Savin, A.; Flad, H.-J. *Int. J. Quantum Chem.* **1995**, 56, 327.
- [194] Savin, A. In *Theoretical and Computational Chemistry*; Seminario, J. M., Ed.; Elsevier: Amsterdam, 1996; Vol. Volume 4; p 327.
- [195] Almbladh, C. O.; von Barth, U. *Phys. Rev. B* **1985**, 31, 3231.

Bibliography

- [196] van Leeuwen, R.; Baerends, E. J. *Phys. Rev. A* **1994**, 49, 2421.
- [197] Livshits, E.; Baer, R. *Phys. Chem. Chem. Phys.* **2007**, 9, 2932.
- [198] Livshits, E.; Baer, R. *J. Phys. Chem. A* **2008**, 112, 12789.
- [199] Stein, T.; Kronik, L.; Baer, R. *J. Am. Chem. Soc.* **2009**, 131, 2818.
- [200] Baer, R.; Livshits, E.; Salzner, U. *Annu. Rev. Phys. Chem.* **2010**, 61, 85.
- [201] Korzdorfer, T.; Sears, J. S.; Sutton, C.; Bredas, J.-L. *J. Chem. Phys.* **2011**, 135, 204107.
- [202] Minami, T.; Nakano, M.; Castet, F. *J. Phys. Chem. Lett.* **2011**, 2, 1725.
- [203] Srebro, M.; Autschbach, J. *J. Phys. Chem. Lett.* **2012**, 3, 576.
- [204] Haunschild, R.; Scuseria, G. E. *J. Chem. Phys.* **2010**, 132, 224106.
- [205] Wesolowski, T. A.; Parisel, O.; Ellinger, Y.; Weber, J. *J. Phys. Chem. A* **1997**, 101, 7818.
- [206] Lieb, E. H.; Oxford, S. *Int. J. Quantum Chem.* **1981**, 19, 427.
- [207] Chan, G. K.-L.; Handy, N. C. *Phys. Rev. A* **1999**, 59, 3075.
- [208] Xu, X.; Goddard, W. A. *Proc. Natl. Acad. Sci.* **2004**, 101, 2673.
- [209] Becke, A. D. *J. Chem. Phys.* **1997**, 107, 8554.
- [210] Becke, A. D. *J. Chem. Phys.* **2000**, 112, 4020.
- [211] Boese, A. D.; Handy, N. C. *J. Chem. Phys.* **2002**, 116, 9559.
- [212] Boese, A. D.; Martin, J. M. L. *J. Chem. Phys.* **2004**, 121, 3405.
- [213] Zhao, Y.; Schultz, N. E.; Truhlar, D. G. *J. Chem. Theory Comput.* **2006**, 2, 364.
- [214] Zhao, Y.; Truhlar, D. *Theor. Chem. Acc.* **2008**, 120, 215.
- [215] Gorling, A.; Levy, M. *Phys. Rev. B* **1993**, 47, 13105.
- [216] Yang, W.; Ayers, P. W.; Wu, Q. *Phys. Rev. Lett.* **2004**, 92, 146404.
- [217] Perdew, J. P.; Ernzerhof, M.; Burke, K. *J. Chem. Phys.* **1996**, 105, 9982.
- [218] Sharkas, K.; Toulouse, J.; Savin, A. *J. Chem. Phys.* **2011**, 134, 064113.
- [219] Toulouse, J.; Sharkas, K.; Bremond, E.; Adamo, C. *J. Chem. Phys.* **2011**, 135, 101102.
- [220] Fromager, E. *J. Chem. Phys.* **2011**, 135, 244106.
- [221] Zhang, Y.; Xu, X.; Goddard, W. A. *Proc. Natl. Acad. Sci.* **2009**, 106, 4963.
- [222] Zhang, I. Y.; Su, N. Q.; Bremond, E. A. G.; Adamo, C.; Xu, X. *J. Chem. Phys.* **2012**, 136, 174103.
- [223] Chai, J.-D.; Head-Gordon, M. *J. Chem. Phys.* **2009**, 131, 174105.
- [224] Kozuch, S.; Martin, J. M. L. *Phys. Chem. Chem. Phys.* **2011**, 13, 20104.
- [225] Goerigk, L.; Grimme, S. *J. Chem. Theory Comput.* **2011**, 7, 291.
- [226] Kozuch, S.; Gruzman, D.; Martin, J. M. L. *J. Phys. Chem. C* **2010**, 114, 20801.

- [227] Angyan, J. G.; Gerber, I. C.; Savin, A.; Toulouse, J. *Phys. Rev. A* **2005**, 72, 012510.
- [228] Goll, E.; Werner, H. J.; Stoll, H. *Phys. Chem. Chem. Phys.* **2005**, 7, 3917.
- [229] Graham, D. C.; Menon, A. S.; Goerigk, L.; Grimme, S.; Radom, L. *J. Phys. Chem. A* **2009**, 113, 9861.
- [230] Karton, A.; Martin, J. M. L. *J. Chem. Phys.* **2011**, 135, 144119.
- [231] Eshuis, H.; Furche, F. *J. Chem. Phys.* **2012**, 136, 084105.
- [232] Burke, K.; Perdew, J. P.; Langreth, D. C. *Phys. Rev. Lett.* **1994**, 73, 1283.
- [233] Hattig, C.; Klopper, W.; Kohn, A.; Tew, D. P. *Chem. Rev.* **2012**, 112, 4.
- [234] Kong, L.; Bischoff, F. A.; Valeev, E. F. *Chem. Rev.* **2012**, 112, 75.
- [235] Roman-Perez, G.; Soler, J. M. *Phys. Rev. Lett.* **2009**, 103, 096102.
- [236] Vydrov, O. A.; Van Voorhis, T. *J. Chem. Phys.* **2010**, 132, 164113.
- [237] Conway, A.; Murrell, J. N. *Mol. Phys.* **1974**, 27, 873.
- [238] Wagner, A. F.; Das, G.; Wahl, A. C. *J. Chem. Phys.* **1974**, 60, 1885.
- [239] Hepburn, J.; Scoles, G.; Penco, R. *Chem. Phys. Lett.* **1975**, 36, 451.
- [240] Meijer, E. J.; Sprik, M. *J. Chem. Phys.* **1996**, 105, 8684.
- [241] Elstner, M.; Hobza, P.; Frauenheim, T.; Suhai, S.; Kaxiras, E. *J. Chem. Phys.* **2001**, 114, 5149.
- [242] Ikabata, Y.; Sato, T.; Nakai, H. *Int. J. Quantum Chem.* **2012**, DOI: 10.1002/qua.24092.
- [243] Thonhauser, T.; Cooper, V. R.; Li, S.; Puzder, A.; Hyldgaard, P.; Langreth, D. C. *Phys. Rev. B* **2007**, 76, 125112.
- [244] Nabok, D.; Puschnig, P.; Ambrosch-Draxl, C. *Comput. Phys. Commun.* **2011**, 182, 1657.
- [245] Hujo, W.; Grimme, S. *J. Chem. Theory Comput.* **2011**, 7, 3866.
- [246] Eldredge, C. P.; Heath, H. T.; Linder, B.; Kromhout, R. A. *J. Chem. Phys.* **1990**, 92, 6225.
- [247] Krishtal, A.; Vannomeslaeghe, K.; Geldof, D.; Van Alsenoy, C.; Geerlings, P. *Phys. Rev. A* **2011**, 83, 024501.
- [248] Tkatchenko, A.; DiStasio, J., Robert A.; Car, R.; Scheffler, M. *Phys. Rev. Lett.* **2012**, 108, 236402.
- [249] DiStasio, R. A.; von Lilienfeld, O. A.; Tkatchenko, A. *Proc. Natl. Acad. Sci.* **2012**, 109, 14791.
- [250] Koide, A. *J. Phys. B* **1976**, 9, 3173.
- [251] Jurecka, P.; Cerny, J.; Hobza, P.; Salahub, D. R. *J. Comput. Chem.* **2007**, 28, 555.
- [252] Chai, J.-D.; Head-Gordon, M. *Phys. Chem. Chem. Phys.* **2008**, 10, 6615.
- [253] Liu, Y.; Goddard, W. A. *Mater. Trans.* **2009**, 50, 1664.

Bibliography

- [254] von Lilienfeld, O. A.; Tavernelli, I.; Rothlisberger, U.; Sebastiani, D. *Phys. Rev. Lett.* **2004**, *93*, 153004.
- [255] von Lilienfeld, O. A.; Tavernelli, I.; Rothlisberger, U.; Sebastiani, D. *Phys. Rev. B* **2005**, *71*, 195119.
- [256] Lin, I.-C.; Coutinho-Neto, M. D.; Felsenheimer, C.; Lilienfeld, O. A. v.; Tavernelli, I.; Rothlisberger, U. *Phys. Rev. B: Condens. Matter Mater. Phys.* **2007**, *75*, 205131.
- [257] Mackie, I. D.; DiLabio, G. A. *J. Phys. Chem. A* **2008**, *112*, 10968.
- [258] DiLabio, G. A. *Chem. Phys. Lett.* **2008**, *455*, 348.
- [259] Troullier, N.; Martins, J. L. *Phys. Rev. B* **1991**, *43*, 1993.
- [260] Goedecker, S.; Teter, M.; Hutter, J. *Phys. Rev. B* **1996**, *54*, 1703.
- [261] Stevens, W. J.; Krauss, M.; Basch, H.; Jasien, P. G. *Can. J. Chem.* **1992**, *70*, 612.
- [262] Hay, P. J.; Wadt, W. R. *J. Chem. Phys.* **1985**, *82*, 299.
- [263] Tavernelli, I.; Lin, I. C.; Rothlisberger, U. *Phys. Rev. B* **2009**, *79*, 045106.
- [264] Ehrlich, S.; Moellmann, J.; Reckien, W.; Bredow, T.; Grimme, S. *ChemPhysChem* **2011**, *12*, 3414.
- [265] Hujo, W.; Grimme, S. *Phys. Chem. Chem. Phys.* **2011**, *13*, 13942.
- [266] Perdew, J. P.; Ruzsinszky, A.; Csonka, G. I.; Vydrov, O. A.; Scuseria, G. E.; Constantin, L. A.; Zhou, X.; Burke, K. *Phys. Rev. Lett.* **2008**, *100*, 136406.
- [267] Perdew, J. P.; Ruzsinszky, A.; Csonka, G. I.; Vydrov, O. A.; Scuseria, G. E.; Constantin, L. A.; Zhou, X.; Burke, K. *Phys. Rev. Lett.* **2009**, *102*, 039902.
- [268] Ruzsinszky, A.; Csonka, G. I.; Scuseria, G. E. *J. Chem. Theory Comput.* **2009**, *5*, 763.
- [269] Grimme, S. *J. Comput. Chem.* **2004**, *25*, 1463.
- [270] Ducere, J.-M.; Cavallo, L. *J. Phys. Chem. B* **2007**, *111*, 13124.
- [271] Chalasiński, G.; Szczesniak, M. M. *Chem. Rev.* **1994**, *94*, 1723.
- [272] Hobza, P.; Selzle, H. L.; Schlag, E. W. *J. Phys. Chem.* **1996**, *100*, 18790.
- [273] Mourik, T. V.; Wilson, A. K.; Dunning, T. H. *Mol. Phys.* **1999**, *96*, 529.
- [274] Sinnokrot, M. O.; Sherrill, C. D. *J. Phys. Chem. A* **2004**, *108*, 10200.
- [275] Ruzsinszky, A.; Perdew, J. P.; Csonka, G. I. *J. Phys. Chem. A* **2005**, *109*, 11015.
- [276] Langreth, D. C.; Dion, M.; Rydberg, H.; Schröder, E.; Hyldgaard, P.; Lundqvist, B. I. *Int. J. Quantum Chem.* **2005**, *101*, 599.
- [277] Sponer, J.; Jurecka, P.; Hobza, P. *J. Am. Chem. Soc.* **2004**, *126*, 10142.
- [278] Zhao, Y.; Truhlar, D. G. *J. Phys. Chem. A* **2005**, *109*, 4209.
- [279] Zhao, Y.; Truhlar, D. G. *J. Chem. Theory Comput.* **2005**, *1*, 415.

- [280] Adamo, C.; Barone, V. *J. Chem. Phys.* **1999**, *110*, 6158.
- [281] Tao, J.; Perdew, J. P. *J. Chem. Phys.* **2005**, *122*, 114102.
- [282] Xu, X.; Goddard, W. A. *J. Phys. Chem. A* **2004**, *108*, 8495.
- [283] Furche, F.; Perdew, J. P. *J. Chem. Phys.* **2006**, *124*, 044103.
- [284] Jellinek, J.; Acioli, P. H. *J. Phys. Chem. A* **2002**, *106*, 10919.
- [285] Kohn, A.; Weigend, F.; Ahlrichs, R. *Phys. Chem. Chem. Phys.* **2001**, *3*, 711.
- [286] Murray, C. W.; Handy, N. C.; Amos, R. D. *J. Chem. Phys.* **1993**, *98*, 7145.
- [287] Ruzsinszky, A.; Perdew, J. P.; Csonka, G. I. *J. Phys. Chem. A* **2005**, *109*, 11006.
- [288] Engel, E.; Hock, A.; Dreizler, R. M. *Phys. Rev. A* **2000**, *61*, 032502.
- [289] Kummel, S.; Kronik, L. *Rev. Mod. Phys.* **2008**, *80*, 3.
- [290] Zhao, Y.; Truhlar, D. G. *Acc. Chem. Res.* **2008**, *41*, 157.
- [291] Valdes, H.; Spiwok, V.; Rezac, J.; Reha, D.; Abo-Riziq, A.; de Vries, M.; Hobza, P. *Chem.-Eur. J.* **2008**, *14*, 4886.
- [292] Tang, K. T.; Toennies, J. P. *J. Chem. Phys.* **2003**, *118*, 4976.
- [293] Sheng, X. W.; Li, P.; Tang, K. T. *J. Chem. Phys.* **2009**, *130*, 174310.
- [294] Halgren, T. A. *J. Am. Chem. Soc.* **1992**, *114*, 7827.
- [295] Thakkar, A. J.; Hettema, H.; Wormer, P. E. S. *J. Chem. Phys.* **1992**, *97*, 3252.
- [296] Bondi, A. *J. Phys. Chem.* **1964**, *68*, 441.
- [297] Wodrich, M. D.; Wannere, C. S.; Mo, Y.; Jarowski, P. D.; Houk, K. N.; Schleyer, P. v. R. *Chem.-Eur. J.* **2007**, *13*, 7731.
- [298] Grimme, S. *Chem.-Eur. J.* **2004**, *10*, 3423.
- [299] Jurecka, P.; Sponer, J.; Cerny, J.; Hobza, P. *Phys. Chem. Chem. Phys.* **2006**, *8*, 1985.
- [300] Gaussian 03, Revision C.01; Frisch, M. J., Trucks G. W. Schlegel H. B. Scuseria G. E. Robb M. A. Cheeseman J. R. Montgomery J. A. Vreven T. Kudin K. N. Burant J. C. Millam J. M. Iyengar S. S. Tomasi J. Barone V. Mennucci B. Cossi M. Scalmani G. Rega N. Petersson G. A. Nakatsuji H. Hada M. Ehara M. Toyota K. Fukuda R. Hasegawa J. Ishida M. Nakajima T. Honda Y. Kitao O. Nakai H. Klene M. Li X. Knox J. E. Hratchian H. P. Cross J. B. Bakken V. Adamo C. Jaramillo J. Gomperts R. Stratmann R. E. Yazyev O. Austin A. J. Cammi R. Pomelli C. Ochterski J. W. Ayala P. Y. Morokuma K. Voth G. A. Salvador P. Dannenberg J. J. Zakrzewski V. G. Dapprich S. Daniels A. D. Strain M. C. Farkas O. Malick D. K. Rabuck A. D. Raghavachari K. Foresman J. B. Ortiz J. V. Cui Q. Baboul A. G. Clifford S. Cioslowski J. Stefanov B. B. Liu G. Liashenko A. Piskorz P. Komaromi I. Martin R. L. Fox D. J. Keith T. Laham A. M. A. Peng C. Y. Nanayakkara A. Challacombe M. Gill P. M. W. Johnson B. Chen W. Wong M. W. Gonzalez C. Pople J. A.; Gaussian Inc., Wallingford CT.
- [301] Afeefy, H.; Liebman, J.; Stein, S. *NIST Chemistry WebBook, NIST Standard Reference*

Bibliography

- Database Number 69*; National Institute of Standards and Technology: Gaithersburg MD, 20899.
- [302] Gauss, J.; Stanton, J. F. *J. Phys. Chem. A* **2000**, *104*, 2865.
- [303] Rezac, J.; Jurecka, P.; Riley, K. E.; Cerny, J.; Valdes, H.; Pluhackova, K.; Berka, K.; Rezac, T.; Pitonak, M.; Vondrasek, J.; Hobza, P. *Collect. Czech. Chem. Commun.* **2008**, *73*, 1261.
- [304] Csonka, G. I.; Ruzsinszky, A.; Perdew, J. P.; Grimme, S. *J. Chem. Theory Comput.* **2008**, *4*, 888.
- [305] Grimme, S.; Diedrich, C.; Korth, M. *Angew. Chem., Int. Ed.* **2006**, *45*, 625.
- [306] Csonka, G. I.; Ruzsinszky, A.; Perdew, J. P. *J. Phys. Chem. B* **2005**, *109*, 21471.
- [307] Koster, A. M.; Calaminici, P.; Casida, M. E.; Flores-Moreno, R.; Geudtner, G.; Gour-sot, A.; Heine, T.; Ipatov, A.; Janetzko, F.; Campo, J. M. d.; Patchkovskii, S.; Reveles, J. U.; Salahub, D. R.; Vela, A. *deMon2k*; deMon2k, 2006.
- [308] Ahlrichs, R.; Bar, M.; Haser, M.; Horn, H.; Kolmel, C. *Chem. Phys. Lett.* **1989**, *162*, 165.
- [309] Ahlrichs, R.; al., e. TURBOMOLE V5.10. 2008; www.turbomole.com.
- [310] Bylaska, E. J. et al. *NWChem, A Computational Chemistry Package for Parallel Computers, Version 5.1*; Pacific Northwest National Laboratory, 2007.
- [311] Kendall, R. A.; Apra, E.; Bernholdt, D. E.; Bylaska, E. J.; Dupuis, M.; Fann, G. I.; Harrison, R. J.; Ju, J.; Nichols, J. A.; Nieplocha, J.; Straatsma, T. P.; Windus, T. L.; Wong, A. T. *Comput. Phys. Commun.* **2000**, *128*, 260.
- [312] Korth, M.; Grimme, S. *J. Chem. Theory Comput.* **2009**, *5*, 993.
- [313] Weintraub, E.; Henderson, T. M.; Scuseria, G. E. *J. Chem. Theory Comput.* **2009**, *5*, 754.
- [314] Lotrich, V. F.; Szalewicz, K. *J. Chem. Phys.* **1997**, *106*, 9668.
- [315] Misquitta, A. J.; Podeszwa, R.; Jeziorski, B.; Szalewicz, K. *J. Chem. Phys.* **2005**, *123*, 214103.
- [316] Podeszwa, R.; Szalewicz, K. *J. Chem. Phys.* **2007**, *126*, 194101.
- [317] Aeberhard, P. C.; Arey, J. S.; Lin, I. C.; Rothlisberger, U. *J. Chem. Theory Comput.* **2008**, *5*, 23.
- [318] Cascella, M.; Lin, I. C.; Tavernelli, I.; Rothlisberger, U. *J. Chem. Theory Comput.* **2009**, *5*, 2930.
- [319] Nilsson Lill, S. O. *J. Phys. Chem. A* **2009**, *113*, 10321.
- [320] Zhao, Y.; Lynch, B. J.; Truhlar, D. G. *J. Phys. Chem. A* **2004**, *108*, 2715.
- [321] Zimmerli, U.; Parrinello, M.; Koumoutsakos, P. *J. Chem. Phys.* **2004**, *120*, 2693.
- [322] Olasz, A.; Vanommeslaeghe, K.; Krishtal, A.; Veszpremi, T.; Alsenoy, C. V.; Geerlings, P. *J. Chem. Phys.* **2007**, *127*, 224105.
- [323] Murdachaew, G.; de Gironcoli, S.; Scoles, G. *J. Phys. Chem. A* **2008**, *112*, 9993.

- [324] Podeszwa, R.; Pernal, K.; Patkowski, K.; Szalewicz, K. *J. Phys. Chem. Lett.* **2009**, *1*, 550.
- [325] Kannemann, F. O.; Becke, A. D. *J. Chem. Theory Comput.* **2009**, *5*, 719.
- [326] Kannemann, F. O.; Becke, A. D. *J. Chem. Theory Comput.* **2010**, *6*, 1081.
- [327] Grimme, S.; Steinmetz, M.; Korth, M. *J. Chem. Theory Comput.* **2007**, *3*, 42.
- [328] Becke, A. D.; Johnson, E. R. *J. Chem. Phys.* **2007**, *127*, 124108.
- [329] Proynov, E.; Gan, Z.; Kong, J. *Chem. Phys. Lett.* **2008**, *455*, 103.
- [330] Bultinck, P.; Alsenoy, C. V.; Ayers, P. W.; Carbo-Dorca, R. *J. Chem. Phys.* **2007**, *126*, 144111.
- [331] Krishtal, A.; Senet, P.; Van Alsenoy, C. *J. Chem. Theory Comput.* **2008**, *4*, 2122.
- [332] Perdew, J. P.; Yue, W. *Phys. Rev. B* **1989**, *40*, 3399.
- [333] Becke, A. D. *J. Chem. Phys.* **1993**, *98*, 1372.
- [334] Unsold, A. *Z. Phys. A* **1927**, *43*, 563.
- [335] Hirshfeld, F. L. *Theor. Chem. Acc.* **1977**, *44*, 129.
- [336] Yang, W.; Zhang, Y.; Ayers, P. W. *Phys. Rev. Lett.* **2000**, *84*, 5172.
- [337] Brinck, T.; Murray, J. S.; Politzer, P. *J. Chem. Phys.* **1993**, *98*, 4305.
- [338] Miller, T. M. *CRC Handbook of Chemistry and Physics*; Taylor & Francis Group, p 10.
- [339] Tang, K. T.; Toennies, J. P. *Surf. Sci.* **1992**, *279*, L203.
- [340] Bohm, H.-J.; Ahlrichs, R. *J. Chem. Phys.* **1982**, *77*, 2028.
- [341] Douketis, C.; Scoles, G.; Marchetti, S.; Zen, M.; Thakkar, A. J. *J. Chem. Phys.* **1982**, *76*, 3057.
- [342] Tang, K. T.; Toennies, J. P.; Yiu, C. L. *Phys. Rev. Lett.* **1995**, *74*, 1546.
- [343] Martin, W.; Musgrove, A.; Kotochigova, S.; Sansonetti, J. *Physical Reference Data, NIST Standard Reference Database Number 111*; National Institute of Standards and Technology: Gaithersburg MD, 20899, 2003.
- [344] Mayer, I.; Salvador, P. *Chem. Phys. Lett.* **2004**, *383*, 368.
- [345] Mulliken, R. S. *J. Chem. Phys.* **1955**, *23*, 1841.
- [346] Slipchenko, L. V.; Gordon, M. S. *Mol. Phys.* **2009**, *107*, 999.
- [347] Karton, A.; Gruzman, D.; Martin, J. M. L. *J. Phys. Chem. A* **2009**, *113*, 8434.
- [348] Shamov, G. A.; Budzelaar, P. H. M.; Schreckenbach, G. *J. Chem. Theory Comput.* **2010**, *6*, 477.
- [349] Song, J.-W.; Tsuneda, T.; Sato, T.; Hirao, K. *Org. Lett.* **2010**, *12*, 1440.
- [350] Valdes, H.; Pluhackova, K.; Pitonak, M.; Rezac, J.; Hobza, P. *Phys. Chem. Chem. Phys.* **2008**, *10*, 2747.
- [351] Takatani, T.; Hohenstein, E. G.; Malagoli, M.; Marshall, M. S.; Sherrill, C. D. *J. Chem. Phys.*

- 2010**, 132, 144104.
- [352] Moilanen, J.; Ganesamoorthy, C.; Balakrishna, M. S.; Tuononen, H. M. *Inorg. Chem.* **2009**, 48, 6740.
 - [353] Boys, S. F.; Bernardi, F. *Mol. Phys.* **1970**, 19, 553.
 - [354] Werner, H.-J. et al. MOLPRO, version 2009.1, a package of ab initio programs. 2009.
 - [355] Adler, T. B.; Knizia, G.; Werner, H.-J. *J. Chem. Phys.* **2007**, 127, 221106.
 - [356] Helgaker, T.; Klopper, W.; Koch, H.; Noga, J. *J. Chem. Phys.* **1997**, 106, 9639.
 - [357] Halkier, A.; Helgaker, T.; Jørgensen, P.; Klopper, W.; Koch, H.; Olsen, J.; Wilson, A. K. *Chem. Phys. Lett.* **1998**, 286, 243.
 - [358] Hill, J. G.; Peterson, K. A.; Knizia, G.; Werner, H.-J. *J. Chem. Phys.* **2009**, 131, 194105.
 - [359] Janssen, C. L.; Nielsen, I. M. B. *Chem. Phys. Lett.* **1998**, 290, 423.
 - [360] Sherrill, C. D.; Takatani, T.; Hohenstein, E. G. *J. Phys. Chem. A* **2009**, 113, 10146.
 - [361] Johnson III, R. D.
 - [362] Riley, K. E.; Pitonak, M.; Cerny, J.; Hobza, P. *J. Chem. Theory Comput.* **2010**, 6, 66.
 - [363] Dunning, J., Thom H. *J. Chem. Phys.* **1989**, 90, 1007.
 - [364] Woon, D. E.; Dunning, J., T. H. *J. Chem. Phys.* **1993**, 98, 1358.
 - [365] Wilson, A. K.; Woon, D. E.; Peterson, K. A.; Dunning, J., Thom H. *J. Chem. Phys.* **1999**, 110, 7667.
 - [366] Weigend, F.; Haser, M. *Theor. Chem. Acc.* **1997**, 97, 331.
 - [367] Weigend, F.; Kohn, A.; Hattig, C. *J. Chem. Phys.* **2002**, 116, 3175.
 - [368] Shao, Y. et al. *Phys. Chem. Chem. Phys.* **2006**, 8, 3172.
 - [369] Grimme, S.; Steinmetz, M.; Korth, M. *J. Org. Chem.* **2007**, 72, 2118.
 - [370] Murray, C. W.; Handy, N. C.; Laming, G. J. *Mol. Phys.* **1993**, 78, 997.
 - [371] Lebedev, V. I.; Laikov, D. N. *Dokl. Math.* **1999**, 59, 477.
 - [372] Gill, P. M. W.; Johnson, B. G.; Pople, J. A. *Chem. Phys. Lett.* **1993**, 209, 506.
 - [373] Davidson, E. R.; Chakravorty, S. *Theor. Chem. Acc.* **1992**, 83, 319.
 - [374] Gonthier, J. E.; Wodrich, M. D.; Steinmann, S. N.; Corminboeuf, C. *Org. Lett.* **2010**, 12, 3070.
 - [375] Curtiss, L. A.; Raghavachari, K.; Redfern, P. C.; Pople, J. A. *J. Chem. Phys.* **1997**, 106, 1063.
 - [376] Raghavachari, K.; Stefanov, B. B.; Curtiss, L. A. *Mol. Phys.* **1997**, 91, 555.
 - [377] Curtiss, L. A.; Raghavachari, K.; Redfern, P. C.; Pople, J. A. *J. Chem. Phys.* **2000**, 112, 7374.
 - [378] Saeys, M.; Reyniers, M. F.; Marin, G. B.; Van Speybroeck, V.; Waroquier, M. *J. Phys. Chem. A* **2003**, 107, 9147.

- [379] Allen, T. L. *J. Chem. Phys.* **1958**, 29, 951.
- [380] Allen, T. L. *J. Chem. Phys.* **1959**, 31, 1039.
- [381] Pitzer, K. S.; Catalano, E. *J. Am. Chem. Soc.* **1956**, 78, 4844.
- [382] Pitzer, K. S. *Adv. Chem. Phys.* **1959**, 2, 59.
- [383] Karton, A.; Tarnopolsky, A.; Lamere, J.-F.; Schatz, G. C.; Martin, J. M. L. *J. Phys. Chem. A* **2008**, 112, 12868.
- [384] Zhao, Y.; Truhlar, D. G. *Org. Lett.* **2006**, 8, 5753.
- [385] Yao, F.; Xiao-Yu, D.; Yi-Min, W.; Lei, L.; Qing-Xiang, G. *Chin. J. Chem.* **2005**, 23, 474.
- [386] Coote, M.; Pross, A.; Radom, L. In *Fundamental world of quantum chemistry, vol. III*; Brandas, E., Kryachko, E., Eds.; Kluwer, The Netherlands, 2004.
- [387] Zhao, Y.; Truhlar, D. G. *J. Phys. Chem. A* **2008**, 112, 1095.
- [388] Perdew, J. P. *Chem. Phys. Lett.* **1979**, 64, 127.
- [389] Mori-Sanchez, P.; Cohen, A. J.; Yang, W. *Phys. Rev. Lett.* **2008**, 100, 146401.
- [390] Brittain, D. R. B.; Lin, C. Y.; Gilbert, A. T. B.; Izgorodina, E. I.; Gill, P. M. W.; Coote, M. L. *Phys. Chem. Chem. Phys.* **2009**, 11, 1138.
- [391] Grimme, S. *Org. Lett.* **2010**, 12, 4670.
- [392] Tawada, Y.; Tsuneda, T.; Yanagisawa, S.; Yanai, T.; Hirao, K. *J. Chem. Phys.* **2004**, 120, 8425.
- [393] Henderson, T. M.; Janesko, B. G.; Scuseria, G. E. *J. Chem. Phys.* **2008**, 128, 194105.
- [394] Rohrdanz, M. A.; Martins, K. M.; Herbert, J. M. *J. Chem. Phys.* **2009**, 130, 054112.
- [395] Krieg, H.; Grimme, S. *Mol. Phys.* **2010**, 108, 2655.
- [396] Murray, E. D.; Lee, K.; Langreth, D. C. *J. Chem. Theory Comput.* **2009**, 5, 2754.
- [397] Heyd, J.; Scuseria, G. E.; Ernzerhof, M. *J. Chem. Phys.* **2003**, 118, 8207.
- [398] Heyd, J.; Scuseria, G. E.; Ernzerhof, M. *J. Chem. Phys.* **2006**, 124, 219906.
- [399] Gaussian 09, Revision A.1, M. J. Frisch, G. W. Trucks, H. B. Schlegel, G. E. Scuseria, M. A. Robb, J. R. Cheeseman, G. Scalmani, V. Barone, B. Mennucci, G. A. Petersson, H. Nakatsuji, M. Caricato, X. Li, H. P. Hratchian, A. F. Izmaylov, J. Bloino, G. Zheng, J. L. Sonnenberg, M. Hada, M. Ehara, K. Toyota, R. Fukuda, J. Hasegawa, M. Ishida, T. Nakajima, Y. Honda, O. Kitao, H. Nakai, T. Vreven, J. A. Montgomery, Jr., J. E. Peralta, F. Ogliaro, M. Bearpark, J. J. Heyd, E. Brothers, K. N. Kudin, V. N. Staroverov, R. Kobayashi, J. Normand, K. Raghavachari, A. Rendell, J. C. Burant, S. S. Iyengar, J. Tomasi, M. Cossi, N. Rega, J. M. Millam, M. Klene, J. E. Knox, J. B. Cross, V. Bakken, C. Adamo, J. Jaramillo, R. Gomperts, R. E. Stratmann, O. Yazyev, A. J. Austin, R. Cammi, C. Pomelli, J. W. Ochterski, R. L. Martin, K. Morokuma, V. G. Zakrzewski, G. A. Voth, P. Salvador, J. J. Dannenberg, S. Dapprich, A. D. Daniels, O. Farkas, J. B. Foresman, J. V. Ortiz, J. Cioslowski, and D. J. Fox,

Bibliography

- Gaussian, Inc., Wallingford CT, 2009.
- [400] Yanai, T.; Tew, D. P.; Handy, N. C. *Chem. Phys. Lett.* **2004**, 393, 51.
- [401] CADPAC, The Cambridge Analytic Derivatives Package.
- [402] Zhang, Y.; Yang, W. *Phys. Rev. Lett.* **1998**, 80, 890.
- [403] Toulouse, J.; Colonna, E.; Savin, A. *Phys. Rev. A* **2004**, 70, 062505.
- [404] Henderson, T. M.; Izmaylov, A. E.; Scuseria, G. E.; Savin, A. *J. Chem. Phys.* **2007**, 127, 221103.
- [405] Song, J.-W.; Tokura, S.; Sato, T.; Watson, M. A.; Hirao, K. *J. Chem. Phys.* **2007**, 127, 154109.
- [406] Song, J.-W.; Watson, M. A.; Hirao, K. *J. Chem. Phys.* **2009**, 131, 144108.
- [407] Iikura, H.; Tsuneda, T.; Yanai, T.; Hirao, K. *J. Chem. Phys.* **2001**, 115, 3540.
- [408] Toulouse, J.; Colonna, E.; Savin, A. *J. Chem. Phys.* **2005**, 122, 014110.
- [409] Ernzerhof, M.; Perdew, J. P. *J. Chem. Phys.* **1998**, 109, 3313.
- [410] Vydrov, O. A.; Scuseria, G. E. *J. Chem. Phys.* **2006**, 125, 234109.
- [411] Song, J.-W.; Hirose, T.; Tsuneda, T.; Hirao, K. *J. Chem. Phys.* **2007**, 126, 154105.
- [412] Vydrov, O. A.; Heyd, J.; Krukau, A. V.; Scuseria, G. E. *J. Chem. Phys.* **2006**, 125, 074106.
- [413] Zhao, Y.; Lynch, B. J.; Truhlar, D. G. *J. Phys. Chem. A* **2004**, 108, 4786.
- [414] Kamiya, M.; Tsuneda, T.; Hirao, K. *J. Chem. Phys.* **2002**, 117, 6010.
- [415] Sato, T.; Tsuneda, T.; Hirao, K. *Mol. Phys.* **2005**, 103, 1151.
- [416] Sato, T.; Tsuneda, T.; Hirao, K. *J. Chem. Phys.* **2005**, 123, 104307.
- [417] Gerber, I. C.; Angyan, J. G. *Chem. Phys. Lett.* **2005**, 416, 370.
- [418] Lacks, D. J.; Gordon, R. G. *Phys. Rev. A* **1993**, 47, 4681.
- [419] Grafova, L.; Pitonak, M.; Rezac, J.; Hobza, P. *J. Chem. Theory Comput.* **2010**, 6, 2365.
- [420] Wang, F.-F.; Jenness, G.; Al-Saidi, W. A.; Jordan, K. D. *J. Chem. Phys.* **2010**, 132, 134303.
- [421] Jeziorska, M.; Bogumil, J.; Cizek, J. *Int. J. Quantum Chem.* **1987**, 32, 149.
- [422] Moszynski, R.; Heijmen, T. G. A.; Jeziorski, B. *Mol. Phys.* **1996**, 88, 741.
- [423] Angyan, J. G. *J. Chem. Phys.* **2007**, 127, 024108.
- [424] Bahmann, H.; Ernzerhof, M. *J. Chem. Phys.* **2008**, 128, 234104.
- [425] Takahashi, H.; Kishi, R.; Nakano, M. *J. Chem. Theory Comput.* **2010**, 6, 647.
- [426] Kumar, A.; Meath, W. J. *Mol. Phys.* **1985**, 54, 823.
- [427] Ayers, P. *J. Math. Chem.* **2009**, 46, 86.
- [428] Bultinck, P.; Cooper, D. L.; Ponec, R. *J. Phys. Chem. A* **2010**, 114, 8754.
- [429] Coombes, D. S.; Price, S. L.; Willock, D. J.; Leslie, M. *J. Phys. Chem.* **1996**, 100, 7352.

- [430] Braga, D. *Dalton Trans.* **2000**, 3705.
- [431] Knowles, R. R.; Jacobsen, E. N. *Proc. Natl. Acad. Sci.* **2010**, *107*, 20678.
- [432] Clementi, E.; Corongiu, G. *J. Phys. Chem. A* **2001**, *105*, 10379.
- [433] Steinmann, S. N.; Corminboeuf, C. *Chimia* **2011**, *65*, 240.
- [434] Misquitta, A. J.; Stone, A. J. *J. Chem. Theory Comput.* **2007**, *4*, 7.
- [435] Misquitta, A. J.; Stone, A. J.; Price, S. L. *J. Chem. Theory Comput.* **2007**, *4*, 19.
- [436] Misquitta, A. J.; Stone, A. J. *Mol. Phys.* **2008**, *106*, 1631.
- [437] Thole, B. *Chem. Phys.* **1981**, *59*, 341.
- [438] Bader, R. F. W.; Carroll, M. T.; Cheeseman, J. R.; Chang, C. *J. Am. Chem. Soc.* **1987**, *109*, 7968.
- [439] Parr, R. G.; Ayers, P. W.; Nalewajski, R. F. *J. Phys. Chem. A* **2005**, *109*, 3957.
- [440] GMTKN30, <http://toc.uni-muenster.de/GMTKN/GMTKN30/GMTKN30main.html>, accessed March 23, 2011.
- [441] Huenerbein, R.; Schirmer, B.; Moellmann, J.; Grimme, S. *Phys. Chem. Chem. Phys.* **2010**, *12*, 6940.
- [442] Podeszwa, R.; Patkowski, K.; Szalewicz, K. *Phys. Chem. Chem. Phys.* **2010**, *12*, 5974.
- [443] Gruzman, D.; Karton, A.; Martin, J. M. L. *J. Phys. Chem. A* **2009**, *113*, 11974.
- [444] Goerigk, L.; Grimme, S. *J. Chem. Theory Comput.* **2010**, *6*, 107.
- [445] Csonka, G. I.; French, A. D.; Johnson, G. P.; Stortz, C. A. *J. Chem. Theory Comput.* **2009**, *5*, 679.
- [446] Reha, D.; Valdes, H.; Vondrasek, J.; Hobza, P.; Abu-Riziq, A.; Crews, B.; de Vries, M. S. *Chem.-Eur. J.* **2005**, *11*, 6803.
- [447] Wilke, J. J.; Lind, M. C.; Schaefer, H. F.; Csaszar, A. G.; Allen, W. D. *J. Chem. Theory Comput.* **2009**, *5*, 1511.
- [448] Dinadayalane, T. C.; Vijaya, R.; Smitha, A.; Sastry, G. N. *J. Phys. Chem. A* **2002**, *106*, 1627.
- [449] Guner, V.; Khuong, K. S.; Leach, A. G.; Lee, P. S.; Bartberger, M. D.; Houk, K. N. *J. Phys. Chem. A* **2003**, *107*, 11445.
- [450] Ess, D. H.; Houk, K. N. *J. Phys. Chem. A* **2005**, *109*, 9542.
- [451] Neese, F.; Schwabe, T.; Kossmann, S.; Schirmer, B.; Grimme, S. *J. Chem. Theory Comput.* **2009**, *5*, 3060.
- [452] Grimme, S.; Kruse, H.; Goerigk, L.; Erker, G. *Angew. Chem., Int. Ed.* **2010**, *49*, 1402.
- [453] Bryantsev, V. S.; Diallo, M. S.; van Duin, A. C. T.; Goddard, W. A. *J. Chem. Theory Comput.* **2009**, *5*, 1016.
- [454] ADF2010.02, SCM, Theoretical Chemistry, Vrije Universiteit, Amsterdam, The Nether-

lands, <http://www.scm.com>.

- [455] Velde, G. t.; Bickelhaupt, F. M.; Baerends, E. J.; Guerra, C. F.; Gisbergen, S. J. A. v.; Snijders, J. G.; Ziegler, T. *J. Comput. Chem.* **2001**, *22*, 931.
- [456] Zhao, Y.; Truhlar, D. G. *J. Phys. Chem. A* **2005**, *109*, 5656.
- [457] Tsuneda, T.; Suzumura, T.; Hirao, K. *J. Chem. Phys.* **1999**, *110*, 10664.
- [458] Schmidt, M. W.; Baldridge, K. K.; Boatz, J. A.; Elbert, S. T.; Gordon, M. S.; Jensen, J. H.; Koseki, S.; Matsunaga, N.; Nguyen, K. A.; Su, S.; Windus, T. L.; Dupuis, M.; Montgomery Jr, J. A. *J. Comput. Chem.* **1993**, *14*, 1347.
- [459] Weigend, F.; Ahlrichs, R. *Phys. Chem. Chem. Phys.* **2005**, *7*, 3297.
- [460] Lenthe, E. v.; Baerends, E. J.; Snijders, J. G. *J. Chem. Phys.* **1993**, *99*, 4597.
- [461] Minenkov, Y.; Occhipinti, G.; Jensen, V. R. *J. Phys. Chem. A* **2009**, *113*, 11833.
- [462] Torker, S.; Merki, D.; Chen, P. *J. Am. Chem. Soc.* **2008**, *130*, 4808.
- [463] Sanford, M. S.; Love, J. A.; Grubbs, R. H. *J. Am. Chem. Soc.* **2001**, *123*, 6543.
- [464] Tsipis, A. C.; Orpen, A. G.; Harvey, J. N. *Dalton Trans.* **2005**, 2849.
- [465] Zhao, Y.; Truhlar, D. G. *Org. Lett.* **2007**, *9*, 1967.
- [466] Goerigk, L.; Grimme, S. *Phys. Chem. Chem. Phys.* **2011**, *13*, 6670.
- [467] Stanton, R. V.; Kenneth M. Merz, J. *J. Chem. Phys.* **1994**, *100*, 434.
- [468] Zhang, Q.; Bell, R.; Truong, T. N. *J. Phys. Chem.* **1995**, *99*, 592.
- [469] Durant, J. L. *Chem. Phys. Lett.* **1996**, *256*, 595.
- [470] Baker, J.; Muir, M.; Andzelm, J. *J. Chem. Phys.* **1995**, *102*, 2063.
- [471] Marshall, M. S.; Steele, R. P.; Thanthiriwatte, K. S.; Sherrill, C. D. *J. Phys. Chem. A* **2009**, *113*, 13628.
- [472] Pluhackova, K.; Grimme, S.; Hobza, P. *J. Phys. Chem. A* **2008**, *112*, 12469.
- [473] Mandel, G.; Donohue, J. *Acta Crystallogr., Sect. B* **1972**, *28*, 1313.
- [474] Cameron, T. S.; Deeth, R. J.; Dionne, I.; Du, H.; Jenkins, H. D. B.; Krossing, I.; Passmore, J.; Roobottom, H. K. *Inorg. Chem.* **2000**, *39*, 5614.
- [475] Mitzel, N. W.; Losehand, U.; Wu, A.; Cremer, D.; Rankin, D. W. H. *J. Am. Chem. Soc.* **2000**, *122*, 4471.
- [476] Knoblock, K. M.; Silvestri, C. J.; Collard, D. M. *J. Am. Chem. Soc.* **2006**, *128*, 13680.
- [477] Moellmann, J.; Grimme, S. *Phys. Chem. Chem. Phys.* **2010**, *12*, 8500.
- [478] Sameera, W. M. C.; Maseras, F. *Phys. Chem. Chem. Phys.* **2011**, *13*, 10520.
- [479] Olaya, A. J.; Ge, P.; Gonthier, J. F.; Pechy, P.; Corminboeuf, C.; Girault, H. H. *J. Am. Chem. Soc.* **2011**, *133*, 12115.

- [480] Ge, P.; Todorova, T. K.; Patir, I. H.; Olaya, A. J.; Vrubel, H.; Mendez, M.; Hu, X.; Corminboeuf, C.; Girault, H. H. *Proc. Natl. Acad. Sci.* **2012**, *109*, 11558.
- [481] Rochat, S.; Steinmann, S. N.; Corminboeuf, C.; Severin, K. *Chem. Commun.* **2011**, *47*, 10584.
- [482] Mulliken, R. S. *J. Am. Chem. Soc.* **1952**, *74*, 811.
- [483] Dubois, J. E.; Garnier, F. *Tetrahedron Lett.* **1965**, *6*, 3961.
- [484] Gunes, S.; Neugebauer, H.; Sariciftci, N. S. *Chem. Rev.* **2007**, *107*, 1324.
- [485] Walzer, K.; Maennig, B.; Pfeiffer, M.; Leo, K. *Chem. Rev.* **2007**, *107*, 1233.
- [486] Stone, A. J.; Price, S. L. *J. Phys. Chem.* **1988**, *92*, 3325.
- [487] Stone, A. J.; Misquitta, A. J. *Chem. Phys. Lett.* **2009**, *473*, 201.
- [488] Banthorpe, D. V. *Chem. Rev.* **1970**, *70*, 295.
- [489] Prissette, J.; Seger, G.; Kochanski, E. *J. Am. Chem. Soc.* **1978**, *100*, 6941.
- [490] Karthikeyan, S.; Sedlak, R.; Hobza, P. *J. Phys. Chem. A* **2011**, *115*, 9422.
- [491] Rezac, J.; Riley, K. E.; Hobza, P. *J. Chem. Theory Comput.* **2011**, *7*, 3466.
- [492] Dreuw, A.; Weisman, J. L.; Head-Gordon, M. *J. Chem. Phys.* **2003**, *119*, 2943.
- [493] Kohn, A.; Hattig, C. *J. Am. Chem. Soc.* **2004**, *126*, 7399.
- [494] Rappoport, D.; Furche, F. *J. Am. Chem. Soc.* **2004**, *126*, 1277.
- [495] Geskin, V.; Stadler, R.; Cornil, J. *Phys. Rev. B* **2009**, *80*, 085411.
- [496] Sini, G.; Sears, J. S.; Bredas, J.-L. *J. Chem. Theory Comput.* **2011**, *7*, 602.
- [497] Tsukamoto, S.; Sakaki, S. *J. Phys. Chem. A* **2011**, *115*, 8520.
- [498] Blanco, F.; Alkorta, I.; Rozas, I.; Solimannejad, M.; Elguero, J. *Phys. Chem. Chem. Phys.* **2011**, *13*, 674.
- [499] Garcia, A.; Elorza, J. M.; Ugalde, J. M. *J. Mol. Struct.* **2000**, *501-502*, 207.
- [500] Karpfen, A. *Theor. Chem. Acc.* **2003**, *110*, 1.
- [501] Liao, M.-S.; Lu, Y.; Scheiner, S. *J. Comput. Chem.* **2003**, *24*, 623.
- [502] Murrell, J. N.; Randic, M.; Williams, D. R. *Proc. Royal Soc. London Ser. A* **1965**, *284*, 566.
- [503] Daudey, J. P.; Claverie, P.; Malrieu, J. P. *Int. J. Quantum Chem.* **1974**, *8*, 1.
- [504] Hayes, I. C.; Stone, A. J. *Mol. Phys.* **1984**, *53*, 83.
- [505] Reed, A. E.; Curtiss, L. A.; Weinhold, F. *Chem. Rev.* **1988**, *88*, 899.
- [506] Morokuma, K. *J. Chem. Phys.* **1971**, *55*, 1236.
- [507] Kitaura, K.; Morokuma, K. *Int. J. Quantum Chem.* **1976**, *10*, 325.
- [508] Ziegler, T.; Rauk, A. *Theor. Chem. Acc.* **1977**, *46*, 1.

Bibliography

- [509] Bagus, P. S.; Hermann, K.; Bauschlicher, C. W. *J. Chem. Phys.* **1984**, *80*, 4378.
- [510] Stevens, W. J.; Fink, W. H. *Chem. Phys. Lett.* **1987**, *139*, 15.
- [511] Stoll, H.; Wagenblast, G.; Preuss, H. *Theor. Chem. Acc.* **1980**, *57*, 169.
- [512] Mo, Y.; Peyerimhoff, S. D. *J. Chem. Phys.* **1998**, *109*, 1687.
- [513] Mo, Y.; Gao, J.; Peyerimhoff, S. D. *J. Chem. Phys.* **2000**, *112*, 5530.
- [514] Khaliullin, R. Z.; Cobar, E. A.; Lochan, R. C.; Bell, A. T.; Head-Gordon, M. *J. Phys. Chem. A* **2007**, *111*, 8753.
- [515] Wu, Q.; Ayers, P. W.; Zhang, Y. *J. Chem. Phys.* **2009**, *131*, 164112.
- [516] Su, P.; Li, H. *J. Chem. Phys.* **2009**, *131*, 014102.
- [517] Schuetz, M.; Rauhut, G.; Werner, H.-J. *J. Phys. Chem. A* **1998**, *102*, 5997.
- [518] Steinmann, S. N.; Corminboeuf, C.; Wu, W.; Mo, Y. *J. Phys. Chem. A* **2011**, *115*, 5467.
- [519] Mo, Y.; Song, L.; Lin, Y. *J. Phys. Chem. A* **2007**, *111*, 8291.
- [520] Langlet, J.; Caillet, J.; Bergès, J.; Reinhardt, P. *J. Chem. Phys.* **2003**, *118*, 6157.
- [521] Mo, Y.; Bao, P.; Gao, J. *Phys. Chem. Chem. Phys.* **2011**, *13*, 6760.
- [522] Gianinetti, E.; Raimondi, M.; Tornaghi, E. *Int. J. Quantum Chem.* **1996**, *60*, 157.
- [523] Wheeler, S. E.; Houk, K. N. *J. Chem. Theory Comput.* **2010**, *6*, 395.
- [524] Bukowski, R. et al. SAPT 2008.2 “An Ab Initio Program for Many-Body Symmetry-Adapted Perturbation Theory Calculations of Intermolecular Interaction Energies”.
- [525] Peterson, K. A.; Adler, T. B.; Werner, H.-J. *J. Chem. Phys.* **2008**, *128*, 084102.
- [526] Werner, H.-J. et al. MOLPRO, version 2010.1, a package of ab initio programs. 2010.
- [527] Kroon-Batenburg, L. M. J.; van Duijneveldt, F. B. *J. Mol. Struct.* **1985**, *121*, 185.
- [528] Hobza, P.; Sponer, J. *Chem. Rev.* **1999**, *99*, 3247.
- [529] Pitonak, M.; Neogrady, P.; Cerny, J.; Grimme, S.; Hobza, P. *ChemPhysChem* **2009**, *10*, 282.
- [530] Munusamy, E.; Sedlak, R.; Hobza, P. *ChemPhysChem* **2011**, *12*, 3253.
- [531] Langlet, J.; Berges, J.; Reinhardt, P. *J. Mol. Struct.* **2004**, *685*, 43.
- [532] Langlet, J.; Berges, J.; Reinhardt, P. *Chem. Phys. Lett.* **2004**, *396*, 10.
- [533] Arago, J.; Sancho-Garcia, J. C.; Orti, E.; Beljonne, D. *J. Chem. Theory Comput.* **2011**, *7*, 2068.
- [534] Marom, N.; Tkatchenko, A.; Rossi, M.; Gobre, V. V.; Hod, O.; Scheffler, M.; Kronik, L. *J. Chem. Theory Comput.* **2011**, *7*, 3944.
- [535] Oyeyemi, V. B.; Keith, J. A.; Pavone, M.; Carter, E. A. *J. Phys. Chem. Lett.* **2012**, *3*, 289.
- [536] Allard, S.; Forster, M.; Souharce, B.; Thiem, H.; Scherf, U. *Angew. Chem., Int. Ed.* **2008**, *47*, 4070.

- [537] Sauvage, J.-P. *Acc. Chem. Res.* **1998**, *31*, 611.
- [538] Joachim, C.; Gimzewski, J. K.; Aviram, A. *Nature* **2000**, *408*, 541.
- [539] Pease, A. R.; Jeppesen, J. O.; Stoddart, J. F.; Luo, Y.; Collier, C. P.; Heath, J. R. *Acc. Chem. Res.* **2001**, *34*, 433.
- [540] Kinbara, K.; Aida, T. *Chem. Rev.* **2005**, *105*, 1377.
- [541] Kay, E.; Leigh, D.; Zerbetto, F. *Angew. Chem., Int. Ed.* **2007**, *46*, 72.
- [542] Novoa, J. J.; Lafuente, P.; Del Sesto, R. E.; Miller, J. S. *Angew. Chem., Int. Ed.* **2001**, *40*, 2540.
- [543] Jakowski, J.; Simons, J. *J. Am. Chem. Soc.* **2003**, *125*, 16089.
- [544] Jung, Y.; Head-Gordon, M. *Phys. Chem. Chem. Phys.* **2004**, *6*, 2008.
- [545] Garcia-Yoldi, I.; Mota, E.; Novoa, J. J. *J. Comput. Chem.* **2007**, *28*, 326.
- [546] Tsuzuki, S.; Honda, K.; Azumi, R. *J. Am. Chem. Soc.* **2002**, *124*, 12200.
- [547] Podeszwa, R.; Szalewicz, K. *Phys. Chem. Chem. Phys.* **2008**, *10*, 2735.
- [548] Lee, N. K.; Park, S.; Kim, S. K. *J. Chem. Phys.* **2002**, *116*, 7902.
- [549] Werner, H.-J.; Manby, F. R.; Knowles, P. J. *The Journal of Chemical Physics* **2003**, *118*, 8149.
- [550] Sinha, D.; Mukhopadhyay, S. K.; Chaudhuri, R.; Mukherjee, D. *Chem. Phys. Lett.* **1989**, *154*, 544.
- [551] Stanton, J. F.; Gauss, J. *J. Chem. Phys.* **1994**, *101*, 8938.
- [552] Hirata, S.; Nooijen, M.; Bartlett, R. J. *Chem. Phys. Lett.* **2000**, *326*, 255.
- [553] Knowles, P. J.; Andrews, J. S.; Amos, R. D.; Handy, N. C.; Pople, J. A. *Chem. Phys. Lett.* **1991**, *186*, 130.
- [554] Knowles, P. J.; Hampel, C.; Werner, H.-J. *J. Chem. Phys.* **1993**, *99*, 5219.
- [555] Knowles, P. J.; Hampel, C.; Werner, H.-J. *J. Chem. Phys.* **2000**, *112*, 3106.
- [556] Zuchowski, P. S.; Podeszwa, R.; Moszynski, R.; Jeziorski, B.; Szalewicz, K. *J. Chem. Phys.* **2008**, *129*, 084101.
- [557] DALTON, a molecular electronic structure program, Release 2.0 (2005), see <http://daltonprogram.org/>.
- [558] Lee, E. C.; Kim, D.; Jurecka, P.; Tarakeshwar, P.; Hobza, P.; Kim, K. S. *J. Phys. Chem. A* **2007**, *111*, 3446.
- [559] Hohenstein, E. G.; Sherrill, C. D. *J. Chem. Phys.* **2010**, *132*, 184111.
- [560] Perdew, J. P.; Levy, M. *Phys. Rev. B* **1997**, *56*, 16021.
- [561] Peverati, R.; Truhlar, D. G. *J. Phys. Chem. Lett.* **2011**, *2*, 2810.
- [562] Vydrov, O. A.; Van Voorhis, T. *J. Chem. Theory Comput.* **2012**, *8*, 1929.

Bibliography

- [563] Meot-Ner, M.; Hamlet, P.; Hunter, E. P.; Field, F. H. *J. Am. Chem. Soc.* **1978**, *100*, 5466.
- [564] Hiraoka, K.; Fujimaki, S.; Aruga, K.; Yamabe, S. *J. Chem. Phys.* **1991**, *95*, 8413.
- [565] Miyoshi, E.; Yamamoto, N.; Sekiya, M.; Tanaka, K. *Mol. Phys.* **2003**, *101*, 227.
- [566] Pieniazek, P. A.; Krylov, A. I.; Bradforth, S. E. *J. Chem. Phys.* **2007**, *127*, 044317.
- [567] Rapacioli, M.; Spiegelman, F.; Scemama, A.; Mirtschink, A. *J. Chem. Theory Comput.* **2011**, *7*, 44.
- [568] Diri, K.; Krylov, A. I. *J. Phys. Chem. A* **2012**, *116*, 653.
- [569] Mo, Y.; Song, L.; Lin, Y.; Liu, M.; Cao, Z.; Wu, W. *J. Chem. Theory Comput.* **2012**, *8*, 800.
- [570] Hobza, P.; Sponer, J. *J. Am. Chem. Soc.* **2002**, *124*, 11802.
- [571] Jurecka, P.; Sponer, J.; Hobza, P. *J. Phys. Chem. B* **2004**, *108*, 5466.

Glossary

AIM Atom in a molecule.

B2PLYP Double hybrid density functional with 53% “exact” exchange and 27% MBPT2 correlation¹⁶³.

B3LYP Becke-3-Parameter-Lee-Yang-Parr correlation^{161,162} hybrid functional (20% “exact” exchange).

B97 Becke’s highly empirical hybrid-GGA exchange-correlation functional containing 19.43% “exact” exchange²⁰⁹.

B97-D GGA functional by Grimme,³⁹ fitted together with an empirical dispersion correction.

BHhLYP 50% “exact” exchange, 50% Becke 1988 exchange and Lee-Yang-Parr correlation³³³ hybrid functional.

BJ Becke and Johnson.

BLW Block localized wave function^{513,514}.

BLYP Becke 1988 exchange¹⁵⁴ and Lee-Yang-Parr correlation¹⁵⁵ GGA functional.

BP86 Becke 1988 exchange¹⁵⁴ and Perdew 1986 correlation^{151,332} GGA functional.

BSE Bond separation equation^{82,83}: All bonds between heavy (non-hydrogen) atoms are split into their simplest molecular fragments preserving the heavy atom bond types. Reactions are balanced by inclusion of the necessary number of simple hydrides (methane, ammonia, water, etc.).

BSSE Basis set superposition error.

CAMB3LYP Long-range corrected functional including a fraction of “global” exchange, fitted in the B3LYP spirit⁴⁰⁰.

CBS Complete basis set limit.

CCSD(T) Coupled cluster including single, double and perturbative triple excitation.

Glossary

CSD Cambridge structural database.

CT Charge-transfer.

DCACP Dispersion corrected atom centered potentials.

DFT Density functional theory.

DFT-D Density functional theory augmented by an atom pairwise dispersion correction.

DNA Deoxyribonucleic acid.

EDA Energy decomposition analysis.

“exact” exchange Non-local exchange, computed according to the formula used in Hartree-Fock theory. The exchange is exact for a non-interacting (Kohn-Sham) system.

GGA Generalized gradient approximation.

HC classical Hirshfeld method for atoms in a molecule.

HCD classical Hirshfeld dominant method for atoms in a molecule: The classical Hirshfeld weights are analyzed at each grid point and the weight of the “dominant” atom is set to 1.00 and all others to zero.

HF the electronic structure method Hartree-Fock or the substance hydrogen fluoride.

HI iterative Hirshfeld method for atoms in a molecule.

HOMO Highest occupied molecular orbital.

HSE06 Screened “exact” exchange functional from Heyd, Scuseria and Ernzerhof^{397,398}; designed for solids.

KS-DFT Kohn-Sham density functional theory¹¹.

LC Long-range corrected exchange functional.

LC-BLYP Long-range corrected Becke 1988 exchange paired with Lee-Yang-Parr correlation³⁹².

LC-BOP Long-range corrected Becke 1988 exchange paired with Hirao’s one-parameter progressive correlation functional^{154,407,457}.

LC- ω PBE Long-range corrected Perdew-Burke-Ernzerhof exchange and correlation based on a flexible exchange hole model,^{393,394} also known als LC- ω PBE08.

LC- ω PBEB95 Long-range corrected Perdew-Burke-Ernzerhof exchange based on a flexible exchange hole model,^{393,394} paired with Becke’s 1995 meta-GGA correlation functional¹⁸⁵.

- LC- ω PBEh** Like LC- ω PBE, but 20% of global “exact” exchange is included³⁹⁴.
- LC- ω PBELYP** Long-range corrected Perdew-Burke-Ernzerhof exchange based on a flexible exchange hole model,^{393,394} paired with Lee-Yang-Parr correlation¹⁵⁵.
- LDA** Local density approximation.
- LMP2** MP2 based on localized orbitals.
- LRD** Local response formalism for dispersion developed by Sato and Nakai^{45,46}.
- LSDA** Local spin density approximation.
- LUMO** Lowest unoccupied molecular orbital.
- M06-2X** Highly empirical “Minnesota” meta-GGA hybrid functional including 54% “exact” exchange²¹⁴.
- MAD** Mean absolute deviation.
- MARD** Mean absolute relative deviation.
- MBPT2** Many-body second order perturbation theory.
- MCY2** One electron self-interaction free functional from Mori-Sanchez, Cohen and Yang¹⁸⁶.
- MCY3** Long-range corrected functional in the spirit of MCY2, but reducing the delocalization error¹⁸⁹.
- MP2** Second order Møller Plesset perturbation theory.
- NBO** Natural bond orbitals⁵⁰⁵.
- PBE** Perdew-Burke-Ernzerhof GGA exchange and correlation functional¹⁵⁶ GGA functional.
- PBE0** 25% “exact” exchange, Perdew-Burke-Ernzerhof exchange and correlation^{156,217,280} hybrid functional.
- PT2** Second order perturbation theory.
- PW6B95** hybrid meta-GGA functional containing 28% “exact” exchange developed by Zhao and Truhlar⁴⁵⁶.
- rCAMB3LYP** Long-range corrected functional including a fraction of “global” exchange, fitted to minimize the delocalization error¹⁸⁹.
- revPBE** revised PBE functional to reproduce Hartree-Fock atomic exchange-energies⁴⁰².
- rPW86** Non-empirical, refitted³⁹⁶ Perdew 1986 GGA exchange¹⁵¹.

Glossary

SAPT Symmetry adapted perturbation theory⁹³.

SAPT(DFT) Symmetry adapted perturbation theory based on monomers described by DFT, the acronym DFT-SAPT is also used.

SCS Spin-component scaled (e.g., SCS-MP2)¹¹⁸.

SIC Self-interaction correction.

SIE Self-interaction error.

SOMO Singly occupied molecular orbital.

SVWN5 Local density approximation with Slater (=Dirac) exchange^{130,131} and the Vosko-Wilk-Nusair parametrization of the correlation energy¹⁴⁹.

TCNQ Tetracyanoquinodimethane.

TPSS Nonempirical meta-GGA exchange-correlation Tao-Perdew-Staroverov-Scuseria functional¹⁵⁸.

TT Tang and Toennies.

TTF Tetrathiafulvalene.

vdW van der Waals or dispersion interactions.

vdW-DF04 Fully non-local van der Waals density functional from Langreth's group¹⁴¹.

vdW-DF10 Reparametrized version of the vdW-DF04 fully non-local van der Waals density functional⁵³.

vdW-TS Tkatchenko-Scheffler van der Waals correction⁴⁴.

VV09 Fully non-local van der Waals density functional from Vydrov and van Voorhis⁴⁷.

VV10 Simplified, fully non-local van der Waals density functional from Vydrov and van Voorhis⁴⁸.

XDM Exchange hole dipole moment, exploited for a dispersion correction by Becke and Johnson^{76-80,187,328}.

Personal Data

Full name	Stephan Niklaus Steinmann
Date of birth	21 February 1985
Marital status	Single
Nationality	Swiss
Languages	German (mother tongue), English (fluent), French (fluent)

Education

Oct. 2004 - Sept. 2007	Bachelor of Science in Chemistry, University of Basel
Mar. 2008 - Sept. 2008	Master's Thesis "Investigation of Allostery and Cooperativity by Molecular Dynamics Simulation" Supervisor: Prof. Dr. M. Meuwly, University of Basel
Nov. 2008 - Sept. 2012	Ph.D. studies in the Laboratory for Computational Molecular Design (LCMD) at the Ecole Polytechnique Fédérale de Lausanne Advisor: Prof. Dr. C. Corminboeuf

Academic Honors and Awards

- Finalist of the European Young Chemist Award 2012
- 2010 SCNAT/SCS Chemistry travel award from the Swiss Academy of Sciences and the Swiss Chemical Society
- SCS Metrohm Prize for the best oral presentation in the section Computational Chemistry of the SCS Fall Meeting 2010

Publications

20. *Exploring the Limits of DFT for Interaction Energies of Molecular Precursors to Organic Electronics*
Steinmann, S. N.; Corminboeuf, C. *J. Chem. Theory Comput.* **2012**, DOI: 10.1021/ct300657h.
19. *How are small endohedral silicon clusters stabilized?*
Avaltroni, F.; Steinmann, S. N.; Corminboeuf, C. *Phys. Chem. Chem. Phys.* **2012**, DOI: 10.1039/c2cp42097j.
18. *π -Depletion as criterion to predict π -stacking ability*
Gonthier, J.; Steinmann, S. N.; Roch, L.; Ruggi, A.; Luisier, N.; Severin, K.; Corminboeuf, C. *Chem. Commun.* **2012**, 48, 9239.
17. *A ratiometric fluorescence sensor for caffeine*
Luisier, N.; Ruggi, A.; Steinmann, S. N.; Favre, L.; Gaeng, N.; Corminboeuf, C.; Severin, K. *Org. and Biomol. Chem.* **2012**, 10, 7487.

16. *Quantification of “fuzzy” chemical concepts: a computational perspective*
Gonthier, J.; Steinmann, S. N.; Wodrich, M. D. and Corminboeuf, C., *Chem. Soc. Rev.* **2012**, 41, 4671.
15. *Why are the Interaction Energies of Charge-Transfer Complexes Challenging for DFT?*
Steinmann, S. N.; Piemontesi, C.; Delachat, A. and Corminboeuf, C. *J. Chem. Theory Comput.* **2012**, 8, 1629.
14. *Role of π -acceptor effects in controlling the lability of novel monofunctional Pt(II) and Pd(II) complexes. Crystal structure of [Pt(tripyrindimethane)Cl]Cl*
Petrovic, B., Bugarcic, Z. D.; Dees, A.; Ivanovic-Burmazovic, I.; Heinemann, F. W.; Puchta, R.; Steinmann, S. N.; Corminboeuf, C.; van Eldik, R. *Inorg. Chem.* **2012**, 51, 1516.
13. *Comprehensive Benchmarking of a Density-Dependent Dispersion Correction*
Steinmann, S. N.; Corminboeuf, C. *J. Chem. Theory Comput.* **2011**, 7, 3567.
12. *Fluorescence sensing of caffeine in water with polysulfonated pyrenes*
Rochat, S.; Steinmann, S. N.; Corminboeuf, C.; Severin, K. *Chem. Commun.* **2011**, 47, 10584.
11. *How do electron localization functions describe π -electron delocalization?*
Steinmann, S. N.; Mo, Y.; Corminboeuf, C. *Phys. Chem. Chem. Phys.* **2011**, 13, 20584.
10. *Dispersion-Corrected Energy Decomposition Analysis for Intermolecular Interactions Based on the BLW and dDXDM Methods*
Steinmann, S. N.; Corminboeuf, C.; Wu, W.; Mo, Y. *J. Phys. Chem. A* **2011**, 115, 5467.
9. *A Density Dependent Dispersion Correction*
Steinmann, S. N.; Corminboeuf, C. *Chimia, Special Issue Laureates* **2011**, 65, 240.
8. *A generalized-gradient approximation exchange hole model for dispersion coefficients*
Steinmann, S. N.; Corminboeuf, C. *J. Chem. Phys.* **2011**, 134, 044117.
7. *The Norbornene Mystery Revealed*
Steinmann, S. N.; Mo, Y.; Vogel, P.; Corminboeuf, C. *Chem. Commun.* **2011**, 47, 227.
6. *Overcoming systematic DFT errors for hydrocarbon reaction energies*
Steinmann, S. N.; Wodrich, M.; Corminboeuf, C. *Theor. Chem. Acc.* **2010**, 127, 429.
5. *Branched Alkanes Have Contrasting Stabilities*
Gonthier, J.; Wodrich, M. D.; Steinmann, S. N.; Corminboeuf, C. *Org. Lett.* **2010**, 12, 3070.
4. *How Strained are Carbomeric-Cycloalkanes?*
Wodrich, M. D.; Gonthier, J.; Steinmann, S. N.; Corminboeuf, C. *J. Phys. Chem. A* **2010**, 114, 6705.
3. *System-Dependent Density Based Dispersion Correction*
Steinmann, S. N.; Corminboeuf, C. *J. Chem. Theory Comput.* **2010**, 6, 1990.
2. *Unified Intra- and Intermolecular Dispersion Correction Formula for Generalized Gradient Approximation Density Functional Theory*
Steinmann, S. N.; Csonka, G.; Corminboeuf, C. *J. Chem. Theory Comput.* **2009**, 5, 2950.
1. *Direct Assessment of Electron Delocalization on NMR Chemical Shifts*
Steinmann, S. N.; Jana, D. F.; Wu, J. I.-C.; Schleyer, P. v. R.; Mo, Y.; Corminboeuf, C. *Angew. Chem. Int. Ed.* **2009**, 48, 9828.

Contributed Talks

8. Swiss Chemical Society Fall Meeting, Sept. 2012, Zürich (Switzerland)
Exploring the Limits of Modern Density Functional Approximations for Interaction Energies
7. 4th EuCheMS Chemistry Congress, Aug. 2012, Prague (Czech Republic)
Why are the Interaction Energies of Charge-Transfer Complexes Challenging for DFT?
6. DFTM 2012, Challenges in Density Matrix and Density Functional Theory, Apr. 2012, Ghent (Belgium)
Why are the Interaction Energies of Charge-Transfer Complexes Challenging for DFT?
5. WATOC 2011, Ninth triennial congress of the World Association of Theoretical and Computational Chemists, July 2011, Santiago de Compostela (Spain)
A Generalized-Gradient Approximation Exchange Hole Model for Dispersion Coefficients
4. STC 2010, 46th Symposium on Theoretical Chemistry, Sept. 2010, Münster (Germany)
A System-Dependent Density-Based Dispersion Correction
3. Swiss Chemical Society Fall Meeting, Sept. 2010, Zürich (Switzerland)
A System-Dependent Density-Based Empirical Dispersion Correction
2. ESPA 2010, Electronic Structure: Principles and Applications, June 2010, Oviedo (Spain)
A System-Dependent Density-Based Empirical Dispersion Correction
1. Swiss Chemical Society Fall Meeting, Sept. 2009, Lausanne (Switzerland)
Universal inter- and intramolecular empirical correction formula for generalized gradient approximation density functional theory

Poster Presentations

9. Swiss Chemical Society Fall Meeting, Sept. 2012, Zürich (Switzerland)
Non-bonded Interactions in Solution: Interplay between Theory and Experiment
8. ICQC, 14th International Congress of Quantum Chemistry, June 2009, Boulder (USA)
Why are the Interaction Energies of Charge-Transfer Complexes Challenging for DFT?
7. CUSO 2011 Summer School, August 2011, Villars-sur-Ollon (Switzerland)
A Generalized-Gradient Approximation Exchange Hole Model for Dispersion Coefficients
6. Swiss Chemical Society Fall Meeting, Sept. 2011, Lausanne (Switzerland)
A Generalized-Gradient Approximation Exchange Hole Model for Dispersion Coefficients
5. Swiss Chemical Society Fall Meeting 2010, Sept. 2010, Zürich (Switzerland)
A Novel Approach Clarifying the Electronic and Magnetic Anomalies of Norbornene
4. IX Girona Seminar, July 2010, Girona (Spain)
A System-Dependent Density-Based Dispersion Correction
3. CECAM Workshop, van der Waals forces in DFT, RPA and beyond, June 2010, Lausanne (Switzerland)
A System-Dependent Density-Based Dispersion Correction
2. DFT09, 13th International Conference on the Applications of Density Functional Theory in Chemistry and Physics, Sept. 2009, Lyon (France)

Unified Inter- and Intramolecular Empirical Correction Formula for Generalized Gradient Approximation Density Functional Theory

1. ICQC, 13th International Congress of Quantum Chemistry, June 2009, Helsinki (Finland)

Universal Inter- and Intramolecular Empirical Correction for Density Functional Approximations